UNIVERSITY OF CALIFORNIA, SAN DIEGO

Defining the early steps in nuclear pore assembly:

Chromatin-associated ELYS initiates pore assembly.

A Dissertation submitted in partial satisfaction of the requirements for the degree

Doctor of Philosophy

in

Biology

by

Beth A. Rasala

Committee in charge:

Professor Douglass J. Forbes, Chair
Professor Don Cleveland
Professor Randy Hampton
Professor Maho Niwa
Professor Mike Yaffe

The Dissertation of Beth A. Rasala is approved, and it is acceptable in quality and form for publication on microfilm:

_____

_____

_____

_____

_____

_____

Chair

University of California, San Diego

2008

To my parents,

Ed and Penny Rasala.

Thank you for all your love, support, and advice.
Thank you for teaching me independence, dedication, perseverance, and laughter. All helped to guide me through this chapter of my life.

TABLE OF CONTENTS

LIST OF FIGURES AND TABLES

General Introduction:

Chapter 1: ELYS is a dual nucleoporin/kinetochore protein required for nuclear pore assembly and proper cell division

Chapter 2: Capture of AT-rich chromatin by ELYS recruits POM121 and NDC1 to initiate nuclear pore assembly

Future Directions

Appendix A: Analysis of ELYS localization

Appendix B: xNup160 C-terminus binding partners

ACKNOWLEDGEMENTS

Special thanks to Douglass for taking me on as a graduate student at the end of my third year and for being a great mentor. She has taught me many valuable lessons, not only about cell biology and how to be a successful scientist, but about life in general as well. Sincere thanks to Randy Hampton, Mike Yaffe, Maho Niwa, and Don Cleveland for the advice, ideas and direction given to me throughout my thesis work.

Very special thanks to Art Orjalo and Rene Chan who took so much of their time in training me as a cell biologist and being so kind and patient with all my questions. Also, thanks to the rest of the Forbes Lab, past and present: Valerie Delmar, my fellow classmate and friend, for helping me through the long process of graduate school, from classes and rotations, to troubleshooting experiments that were not working, to job hunting and networking, to graduating; Corinne Ramos, my officemate and collaborator, for teaching me so much, for our frequent, highly-enlightening discussions, and for brightening up my day, every day; Corine Lau, for providing me with much scientific and technical help, and for often accompanying me to the coffee cart; and Karen Resendes, for picking up my old project and skillfully taking it to exciting places, for her levity and cheerful conversations, and for the important Thursday morning analysis of the previous night's Lost episode.

Sincere thanks to Iain Cheeseman for taking the time to teach me new techniques and analyses, and to listen and offer advice concerning my project. Also, special thanks to Zhouxin Shen and Steven Briggs for performing mass spectrometry analyses on multiple experiments, many of which have led to publications.

Thanks to Susan Forsburg and the rest of the Forsburg lab, for everything they did to mold me into the scientist I am today, especially Mike Catlett and Eliana Gomez.

And thank you to my parents, my brother and his family, and to all my friends, who taught me the importance of love, friendship and happiness.

Finally, very special thanks to Nick Herrera, for being my rock, for helping in uncountable ways, for always being there, and especially, for making me laugh when I have wanted to cry.

Chapter 1, in full, is a reprint of the material as it appears in the **Proceedings of the National Academy of Sciences**: **Beth A. Rasala**, Art Orjalo, Zhouxin Shen, Steven Briggs, Douglass J Forbes. ELYS is a Dual Nucleoporin/Kinetochore Protein Required for Nuclear Pore Assembly and Proper Cell Division. PNAS, 2006 Nov 21; 103 (47): 17801-17806, by copyright permission from National Academy of Sciences, U.S.A. I was the primary investigator and author of this paper.

Chapter 2 is a modified version of a manuscript under submission for publication in **Molecular Biology of the Cell**: **Beth A. Rasala**, Corinne Ramos, Amnon Harel, and Douglass J. Forbes. Capture of AT-rich chromatin by ELYS recruits POM121 and NDC1 to initiate nuclear pore assembly. I was the primary investigator and author of this paper.

The text in Chapter 3 is a modified version of a manuscript in preparation for publication: Corinne Ramos, **Beth A. Rasala**, and Douglass J. Forbes, Structural intermediates in fusion mediated NPC assembly. I am the secondary researcher listed in this publication which forms the basis for this chapter.

The text in Chapter 4 is a modified version of a manuscript in press in **Molecular and Cellular Biology:** Resendes K, **Rasala BA,** and Forbes DF, Centrin 2 localizes to the vertebrate nuclear pore and is involved in mRNA and protein export. Mol Cell Biol. In press. I was the second author listed in this publication which forms that basis of Chapter 4.

CURRICULUM VITA

Education:

8/95-5/99	University of California, Berkeley Bachelor of Arts in Molecular and Cell Biology with an emphasis in Immunology
9/01-3/08	University of California, San Diego Doctor of Philosophy Degree in Biology

Work Experience:

9/98-5/99	Undergraduate Researcher, University of California, Berkeley
6/99-6/01	Research Assistant, The Salk Institute, La Jolla, CA

Awards:

2001	Cell, Molecular & Genetics Training Fellowship, UC San Diego
1999	MCB Honors, UC Berkeley

Publications:

Rasala BA, Ramos C, Harel, A and Forbes DJ. Capture of AT-rich chromatin by ELYS recruits POM121 and NDC1 to initiate nuclear pore assembly. Submitted to MBC, Jan. 8, 2008.

Ramos C, **Rasala BA**, and Forbes DJ. Structural intermediates in fusion-mediated nuclear pore assembly. In preparation.

Resendes K, **Rasala BA**, and Forbes DF. Centrin 2 localizes to the vertebrate nuclear pore and is involved in mRNA and protein export. Mol Cell Biol. In press.

Rasala BA, Orjalo A, Shen Z, Briggs S, Forbes, DJ. ELYS is a Dual Nucleoporin/Kinetochore Protein Required for Nuclear Pore Assembly and Proper Cell Division. PNAS, 2006 Nov 21; 103 (47): 17801-17806.

Mariani R, **Rasala BA**, Rutter G, Wiegers K, Brandt SM, Krausslich HG, Landau NR. Mouse-human heterokaryons support efficient human immunodeficiency virus type 1 assembly. J Virol. 2001 Apr; 75 (7): 3141-51.

Townson JR, Graham GJ, Landau NR, **Rasala B**, Nibbs RJ. Aminooxypentane addition to the chemokine macrophage inflammatory protein-1alpha P increases receptor affinities and HIV inhibition. J Biol Chem. 2000 Dec 15; 275 (50): 39254-61.

Abstracts:

Talk: Rasala BA, Orjalo A, Shen Z, Briggs S, Forbes, DJ. “ELYS is a dual nucleoporin/kinetochore protein required for correct nuclear pore assembly and cell division.” Dynamic Organization of Nuclear Function, Cold Spring Harbor, Sept. 2006.

Talk: Rasala BA, Orjalo A, Shen Z, Briggs S, Forbes, DJ. “ELYS is a dual nucleoporin/kinetochore protein required for correct nuclear pore assembly and cell division.” UCSD Division of Biology Annual Retreat, Sept. 2006.

Poster: Rasala BA, Orjalo A, Shen Z, Briggs S, Forbes, DJ. “A novel nuclear pore/kinetochore protein required for correct nuclear pore assembly.” The American Society for Cell Biology Meeting, December, 2006.

Teaching:

Cell Biology. Spring, 2005
University of California, San Diego

Genetics. Fall, 2003
University of California, San Diego

Microbiology Laboratory. Fall, 2002
University of California, San Diego

ABSTRACT OF THE DISSERTATION

Defining the early steps in nuclear pore assembly:

Chromatin-associated ELYS initiates pore assembly.

by

Beth A. Rasala

Doctor of Philosophy in Biology

University of California, San Diego, 2008

Professor Douglass J. Forbes, Chair

My thesis is focused upon molecularly defining the mechanism of early steps in metazoan nuclear pore assembly. Nuclear pore complexes (NPCs) are large proteinaceous structures that span the nuclear envelope and act as gated aqueous channels to regulate the transport of macromolecules between the nucleus and cytoplasm. In metazoans, the massive NPCs disassemble into soluble subunits at the beginning of mitosis and then somehow reassemble following chromosome segregation; a process that is coordinated with membrane recruitment and fusion. The mechanism and order of NPC assembly is poorly understood. In Chapter 1, I show that ELYS co-purifies with the Nup107-160 complex, the largest subunit of the NPC, in *Xenopus* egg and human cell extracts. Indeed, I demonstrate that ELYS is a dual nucleoporin/kinetochore protein required for nuclear pore assembly and proper

cell division. In Chapter 2, I focus on defining the early steps in nuclear pore assembly, including the mechanism for ELYS as the pore 'targeting' protein. In Chapter 3, I collaborated with Dr. Corinne Ramos on a study to order pore assembly with respect to inner and outer nuclear membrane fusion. Taken the data from chapters 1-3 together, I suggest a model in which NPC assembly is initiated on AT-rich chromatin through an interaction with the C-terminus of ELYS. The data also show the chromatin binding of ELYS precedes and is required for the binding of the Nup107-160 complex. Chromatin-bound ELYS and the Nup107-160 complex then recruit integral pore membrane proteins POM121- and NDC1-containing membrane vesicles. Membrane vesicle fusion takes place to form patches of continuous double nuclear membranes. Oligomerization of ELYS/Nup107-160/POM121 then acts to promote fusion between the inner and outer nuclear membranes to form a diffusion channel. Finally, the remaining soluble pore subunits are recruited to assemble the mature, functional nuclear pore. Finally, Appendix B presents data on the *Xenopus* binding partners of the C-terminus of Nup160, a member of the Nup107-160 complex, which was derived from mass spectrometry analyses. This data led to the discovery that vertebrate centrin 2 localizes to NPCs and functions in mRNA and protein export, as described in Chapter 4.

GENERAL INTRODUCTION

The nuclear envelope (NE) is a double-lipid bilayer that separates the contents of the nucleus, including the genome, from the cytoplasm. In higher eukaryotes, the NE is composed of the inner and outer nuclear membranes, the lamina, and nuclear pore complexes (NPCs). The incorporation of genetic material inside a biochemically distinct compartment allowed eukaryotic cells a much greater element of control over biological processes. However, a mechanism for transport across the nuclear envelope was needed. Nuclear pore complexes (NPCs) span the nuclear envelope and function as the gateway to the nucleus, facilitating the bidirectional transport of molecules between the nucleus and cytoplasm (Figure I.1). Although the nuclear envelope provides the advantage of enhanced regulatory control for the eukaryotic cell, it causes complications during cell division. In higher eukaryotes, the nuclear envelope, including nuclear pore complexes, must disassemble and then reassemble each cell cycle (Vasu and Forbes, 2001; Suntharalingam and Wente, 2003; Hetzer *et al.*, 2005; Margalit *et al.*, 2005). This thesis describes the advances I have made toward understanding the order and regulation of early steps in NPC assembly, including the role of chromatin and the coordination between pore assembly and membrane recruitment and fusion.

The architecture of nuclear pore complexes.

NPCs are embedded in the nuclear envelope at sites where the inner and outer nuclear membranes are fused. The NPC is a massive protein assemblage with eight-fold rotational symmetry. It consists of ~30 different proteins, termed nucleoporins or Nups, which are present in copies of eight or multiples of eight (Yang *et al.*, 1998; Rout *et al.*, 2000; Cronshaw *et al.*, 2002). Metazoan NPCs also contain three integral membrane proteins: POM121, NDC1, and gp210; however only NDC1 is conserved between yeast and higher eukaryotes (Gerace *et al.*, 1982; Wozniak *et al.*, 1989; Greber *et al.*, 1990; Hallberg *et al.*, 1993; Cotter *et al.*, 1998; Liu *et al.*, 2003; Lau *et al.*, 2006; Mansfeld *et al.*, 2006; Stavru *et al.*, 2006). Nuclear pores are asymmetrical in structure, with cytoplasmic filaments, a central domain that spans the nuclear membranes, and a nuclear basket (Figure I.1). The central domain consists of a scaffold with eight large spokes surrounding a central transporter region. Approximately one third of the Nups contain phenylalanine-glycine (FG) repeat domains, believed to be key sites for interaction with transport receptors (Ryan and Wente, 2000).

Nuclear pores disassemble and reassemble during cell division.

During metazoan cell division, the nuclear envelope breaks down in a process termed open mitosis. Nuclear pores disassemble into ~14 soluble subunits, consisting of anywhere from one to nine proteins each. In vivo, the

nuclear membranes are believed to either retract into the ER (Ellenberg *et al.*, 1997; Yang *et al.*, 1997; Daigle *et al.*, 2001) and/or vesiculate at mitosis (Cotter *et al.*, 1998; Liu *et al.*, 2003; Cotter *et al.*, 2007). Near the end of mitosis, the nuclear membranes and NPCs reassemble to form a new nuclear envelope around each daughter genome. Nuclear pore assembly involves the stepwise recruitment of the many pore subunits beginning in late anaphase and continuing through the end of telophase and early G1 (Chaudhary and Courvalin, 1993; Bodoor *et al.*, 1999; Haraguchi *et al.*, 2000; Belgareh *et al.*, 2001; Daigle *et al.*, 2001; Rabut *et al.*, 2004; Rasala *et al.*, 2006; Franz *et al.*, 2007) (Figure I.2). In vivo, this post-mitotic pore assembly is generally restricted to the chromatin periphery and is coordinated with contemporaneous nuclear membrane recruitment and fusion. Thus, nuclear envelope assembly is both spatially and temporally regulated. NPC assembly also occurs at S phase, when the NPC number doubles in preparation for later mitosis (Maul *et al.*, 1972).

The assembly of nuclear pores in S phase involves the insertion of pore complexes into the NE and thus must require the fusion of the inner and outer nuclear membranes. However, the mechanism for how pores assemble during post-mitotic nuclear pore assembly is hotly debated. Currently, there exist two prevalent models for nuclear pore assembly (Figure I.3). The first proposes that post-mitotic NPC assembly occurs in the same manner as that of S-phase; i.e. insertion into regions of continuous double membranes, and

thus is dependent on fusion of the inner and outer nuclear membranes (Figure I.3, left panel). Indeed, previous work from our lab demonstrated that nuclear pores can assemble within a continuous double membrane of reconstituted nuclei using *Xenopus* egg extracts, an in vitro system that mimics post-mitotic nuclear assembly (Macaulay and Forbes, 1996; Harel *et al.*, 2003a). Furthermore, a study using field emission in-lens scanning electron microscopy (FEISEM) to visualize the outer membrane of *Xenopus* reconstituted nuclei identified intermediate structures in NPC assembly, including slight indentations (dimples) of the fused membrane which the authors proposed to be the initial step in assembly (Goldberg *et al.*, 1997). Multiple progressive intermediates were also observed.

A second model for post-mitotic pore assembly, termed the 'pre-pore' model, suggests that nuclear pore subunits sequentially assemble on the chromatin, and at some undefined later point, membrane sheets containing the integral membrane pore proteins coalesce around the assembled pore proteins (Sheehan *et al.*, 1988; Burke and Ellenberg, 2002; Walther *et al.*, 2003a; Antonin *et al.*, 2005; Anderson and Hetzer, 2007). In this model, fusion between the inner and outer membranes would not take place (Figure I.3, right panel). This proposed mechanism of assembly could only occur in higher eukaryotes following mitosis, when the nuclear envelope is disassembled. It could not explain NPC assembly during S-phase or in yeast,

which do not break down their nuclear membranes during mitosis; in both cases, NPCs insert into pre-existing continuous double nuclear membranes.

The regulation of pore disassembly and assembly.

It is likely that phosphorylation/dephosphorylation regulates, at least in part, the timing of post-mitotic nuclear pore assembly, as specific Nups are phosphorylated in mitosis (Macaulay *et al.*, 1995; Glavy *et al.*, 2007). Importin β and its regulator, Ran-GTP, are also intimately involved in spatially regulating nuclear pore assembly. Importin β acts as a *negative* regulator of both nuclear membrane formation and nuclear pore assembly (Harel *et al.*, 2003a; Walther *et al.*, 2003b). In contrast, Ran-GTP, an importin β-binding protein, *positively* regulates nuclear envelope assembly by promoting nuclear membrane formation and nuclear pore assembly (Wozniak and Clarke, 2003; Clarke and Zhang, 2004; Harel and Forbes, 2004). Because RCC1, the GTP exchange factor for Ran, is a chromatin-bound protein, a Ran gradient forms in which a high concentration of Ran-GTP surrounds the chromatin (Bischoff and Ponstingl, 1991). Thus, current models suggest that this high concentration of Ran-GTP around the chromatin helps to specifically promote nuclear membrane formation and pore assembly at the chromatin periphery, most likely by relieving importin β inhibition (Harel *et al.*, 2003a; Walther *et al.*, 2003b; Harel and Forbes, 2004).

Pore complexes can be found in cytoplasmic stacks of ER-membranes, termed annulate lamellae.

Interestingly, pore complexes are also assembled in cytoplasmic stacks of membranes, which together are termed annulate lamellae (AL) (Kessel, 1989). AL can form in large numbers in vitro in *Xenopus* egg extracts, when neither DNA or chromatin are present (Dabauvalle *et al.*, 1991; Meier *et al.*, 1995). AL are also found in vivo at low levels in many cell types, but at enhanced levels in rapidly developing cells, such as tumor cells and oocytes (Kessel, 1989). This suggests either that pore complexes can form in the absence of high concentrations of Ran-GTP, or that local gradients of Ran-GTP can exist in the cytoplasm. Either way, this observation begs the important question: How do cells ensure that pore complexes are assembled into the nuclear envelope rather than in cytoplasmic stacks of membranes? Over the course of my thesis work, I was able to answer this question: ELYS, the pore-targeting protein, is chromatin-bound and specifically initiates pore assembly on the chromatin surface (see below).

The Nup107-160 complex plays a pivotal role in NPC assembly.

The process of nuclear pore assembly has been the subject of intense study for a number of years. Extracts of *Xenopus* eggs, which contain large stockpiles of disassembled nuclear components for later development, have proven to be a valuable tool for the study of nuclear assembly. Nuclei can be

reconstituted in vitro by the addition of chromatin or free DNA to an interphase *Xenopus* egg extract (Forbes *et al.*, 1983; Lohka and Masui, 1983; Newport, 1987). Importantly, egg extracts can be easily manipulated. The crude extract can be separated into cytosol and membrane vesicle fractions by centrifugation. Experimentally, the effects of chemical inhibitors, dominant negative protein fragments, or the removal of specific proteins on nuclear assembly can be assessed without difficulty. A major breakthrough in the field came when the Nup107-160 complex was discovered and found to be essential for nuclear pore assembly (Belgareh *et al.*, 2001; Vasu *et al.*, 2001; Harel *et al.*, 2003b; Walther *et al.*, 2003a). This, by far the largest subunit of the metazoan nuclear pore, consists of nine proteins and resides on both the nuclear and cytoplasmic face of the pore (Fontoura *et al.*, 1999; Belgareh *et al.*, 2001; Vasu *et al.*, 2001; Boehmer *et al.*, 2003; Harel *et al.*, 2003b; Loiodice *et al.*, 2004). Immunodepletion of the Nup107-160 complex from *Xenopus* egg extracts led to the assembly of nuclei containing fused double nuclear membranes completely devoid of nuclear pores, indicating that the Nup107-160 complex plays a key role in assembly and/or structure of the nuclear pore complex (Harel *et al.*, 2003b; Walther *et al.*, 2003a).

Recent evidence suggests an emerging role for chromatin in NPC assembly. The Nup107-160 complex can bind to chromatin substrates in the absence of membranes in *Xenopus* egg extracts (Walther *et al.*, 2003a; Franz *et al.*, 2007). As stated above, immunodepletion of the Nup107-160 complex

from *Xenopus* egg extracts results in pore-free nuclei. This phenotype can be partially rescued if purified Nup107-160 complex is added back, but only if added before the closure of the nuclear envelope (Walther *et al.*, 2003a). This data indicated that the Nup107-160 complex minimally needs to be on the nuclear face of the NE to facilitate NPC assembly. Indeed, the Nup107-160 complex is required on both faces of the NE for de novo pore insertion in fully formed nuclei reconstituted from *Xenopus* egg extracts, a system that mimics NPC assembly during S phase (D'Angelo *et al.*, 2006). Taking these data together, it has been speculated that the binding of the Nup107-160 complex to chromatin is an essential step in NPC assembly (Walther *et al.*, 2003a). If so, what chromatin-associated protein does the Nup107-160 complex interact with?

ELYS, the nuclear pore targeting protein.

To help in our understanding of the role for the Nup107-160 complex in pore assembly and structure, we sought to identify proteins with which it interacts. As described in Chapter 1, we immunoprecipitated the Nup107-160 complex from *Xenopus* egg extracts and performed mass spectrometry on the immunoprecipitates (Rasala *et al.*, 2006). Interestingly, one of the major Nup107-160 complex binding proteins we observed was a large 270 kDa protein, ELYS (embryonic large molecule derived from the yolk sac). Originally proposed from somewhat circumstantial evidence to be a

transcription factor involved in mouse embryonic haematopoiesis, vertebrate ELYS had no previously described link to the nuclear pore (Kimura *et al.*, 2002; Okita *et al.*, 2003; Okita *et al.*, 2004). In contrast, I found that ELYS localizes to nuclear pore complexes and is recruited early in the post-mitotic NPC assembly process. Importantly, RNAi depletion of ELYS from HeLa cells led to a decrease in pore assembly at the nuclear envelope and to a concomitant increase in pore assembly in the cytoplasm in structures reminiscent of annulate lamellae. This data suggested that ELYS is involved in the spatial regulation of nuclear pore assembly. Thus, I proposed ELYS to function in targeting pore assembly to the nuclear envelope (Rasala *et al.*, 2006). While this work was in review, two studies came out identifying the *C. elegans* homologue of ELYS, MEL-28, as a protein of the nematode nuclear envelope and important for nuclear envelope assembly (Fernandez and Piano, 2006; Galy *et al.*, 2006).

In agreement with my work, a later study demonstrated that immunodepletion of ELYS from *Xenopus* egg extracts led to the assembly of nuclei completely devoid of nuclear pores (Franz *et al.*, 2007).

Defining the early steps in nuclear pore assembly.

Intriguingly, sequence analysis previously revealed that ELYS contains a putative AT-hook DNA-binding motif (Kimura *et al.*, 2002). As described in Chapter 2, I demonstrate that ELYS binds to chromatin in the absence of

membranes and that the chromatin binding of the Nup107-160 complex is dependent on that of ELYS. Importantly, nuclear pore assembly is also dependent on *chromatin-bound* ELYS, indicating that nuclear pore assembly is indeed initiated from the chromatin. Thus, the binding of ELYS to chromatin and the recruitment of the Nup107-160 complex are early and essential steps in nuclear pore assembly (Rasala, *et al.*, submitted).

What remains unknown is how ELYS is recruited to chromatin and what happens following the chromatin-binding of ELYS and the Nup107-160 complex. Chapter 2 also describes the work in which I focused on defining the mechanism for ELYS function and the order of the early steps in pore assembly. I demonstrate by point mutation and deletion analysis that ELYS binds to chromatin through at least two domains in its C-terminus, the AT-hook motif and a second domain residing in the last 51 amino acids of the protein. AT-hook motifs mediate binding to the minor groove of DNA specifically in AT-rich regions and are found in a number of DNA-binding proteins including members of the HMGA/HMG-I(Y) family of chromatin proteins (Reeves and Nissen, 1990). Using sequence-specific DNA-binding antibiotics, Distamycin A and Chromomycin A_3, I demonstrate that pore assembly is initiated on AT-rich chromatin via the binding of ELYS and the Nup107-160 complex. I also show that the recruitment of membrane vesicles to chromatin and vesicle-vesicle fusion occurs prior to the assembly of the remaining soluble pore subunits. Furthermore, the AT-chromatin/ELYS/Nup107-160 pore platform is

required for the important and specific recruitment of two integral membrane pore proteins, POM121 and NDC1, but not for the recruitment of gp210. Finally, I show that ELYS and the Nup107-160 complex can interact with POM121. Thus, the data point us to a nuclear pore assembly order of (1) AT-rich chromatin, (2) ELYS and the Nup107-160 complex, (3) POM121 and NDC1, (4) membrane vesicle fusion, and (5) the assembly of the rest of the soluble pore subunits (Rasala, *et al.,* submitted).

In collaboration with Dr. Corinne Ramos, we were further able to order the early steps in nuclear pore assembly in terms of both protein oligomerization and inner-outer nuclear membrane fusion (see Chapter 3). I showed that ELYS oligomerization is dependent on the presence of membranes and occurs concurrently with the appearance of POM121 and the Nup107-160 complex. Furthermore, Dr. Ramos was able to biochemically isolate, for the first time, a fusion event between the inner and outer nuclear membranes, and show that recruitment of the Nup107-160 complex and POM121 to the cytoplasm side of the nuclear membrane occurs prior to this fusion event (Ramos, Rasala, and Forbes, in preparation).

Taking our data together, we believe nuclear pore assembly occurs in the following order: (1) AT-rich chromatin, (2) chromatin binding of ELYS, which recruits the Nup107-160 complex, (3) POM121 and NDC1 recruitment, along with their accompanying membrane vesicles, (4) vesicle-vesicle fusion to form continuous double membranes, (5) ELYS/Nup107-160/POM121

oligomerization, (6) an inner and outer nuclear membrane fusion event, and (7) assembly of the bulk of the pore subunits to yield a mature and functional NPC. Overall, our data strongly support the fusion-dependent model of NPC assembly.

Identifying other novel proteins associated with the nuclear pore.

In the Appendix, I describe my early work aimed toward identifying metazoan-specific functions for Nup160, a member of the Nup107-160 complex (see Appendix A). Interestingly, this led to the identification of vertebrate Centrin 2 as a nuclear-pore associated protein, and the discovery of a role for Centrin 2 in mRNA and protein export (Resendes *et al.*, 2008), as described in Chapter 4.

In summary

During the course of my thesis research, I identified the protein, ELYS/Mel-28, to be a novel component of vertebrate NPCs (Rasala *et al.*, 2006). My data, with others, show that ELYS is essential for NPC assembly and that it functions to target pore complex assembly to the nuclear envelope. It does so by binding to chromatin and recruiting the Nup107-160 complex to the chromatin periphery at the end of mitosis (Fernandez and Piano, 2006; Galy *et al.*, 2006; Rasala *et al.*, 2006; Franz *et al.*, 2007; Gillespie *et al.*, 2007). ELYS presumably plays an identical targeting role in S phase nuclei. Lastly, I

define the early steps in nuclear pore assembly, a question that has remained highly speculative until now (Rasala *et al*., submitted; Ramos, Rasala, and Forbes, in preparation).

Figures

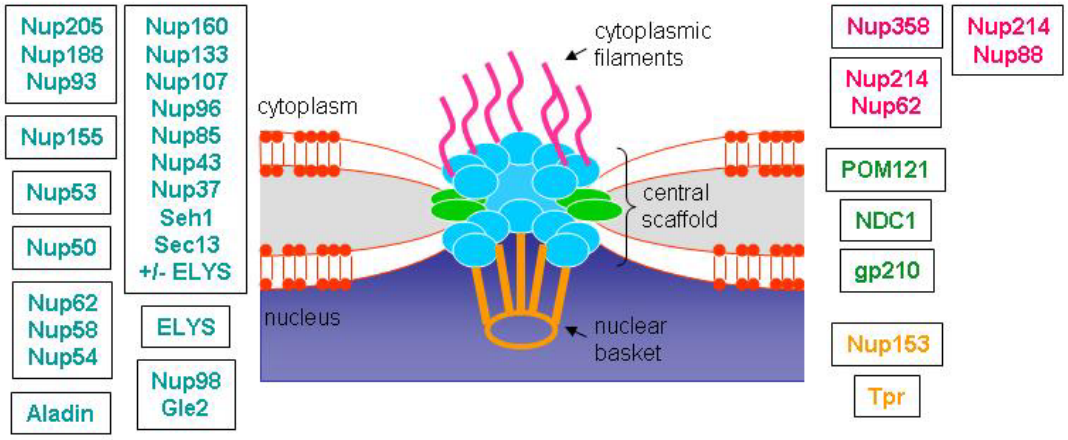

Figure I.1. The structure of the nuclear pore. Nuclear pore complexes (NPCs) are embedded in the nuclear membranes (red) at sites where the inner and outer membranes are fused. The asymmetrical structure contains cytoplasmic filaments (pink), a central scaffold (blue), and a nuclear basket (orange). NPCs are comprised of ~30 soluble nucleoporins associated in ~14 soluble subunits (boxed) and three integral pore membrane proteins (green).

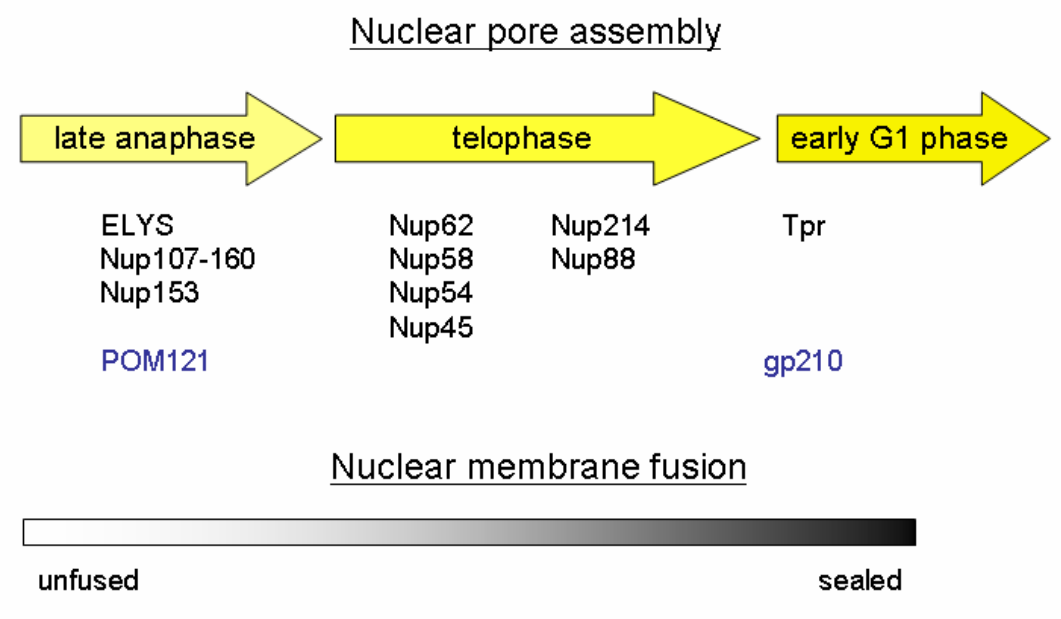

Figure I.2. Nuclear pore assembly is a stepwise process. Pore assembly has been previously examined in cultured mammalian cells for a subset of pore proteins (Chaudhary and Courvalin, 1993; Bodoor *et al.*, 1999; Haraguchi *et al.*, 2000; Belgareh *et al.*, 2001; Daigle *et al.*, 2001; Rabut *et al.*, 2004; Rasala *et al.*, 2006; Franz *et al.*, 2007). These studies showed that nuclear pore assembly begins in late anaphase and continues through telophase and early G1 phase. The soluble pore subunits (black) and integral pore membrane proteins (blue) examined assemble stepwise. Clearly pore assembly is coordinated with nuclear membrane fusion and sealing.

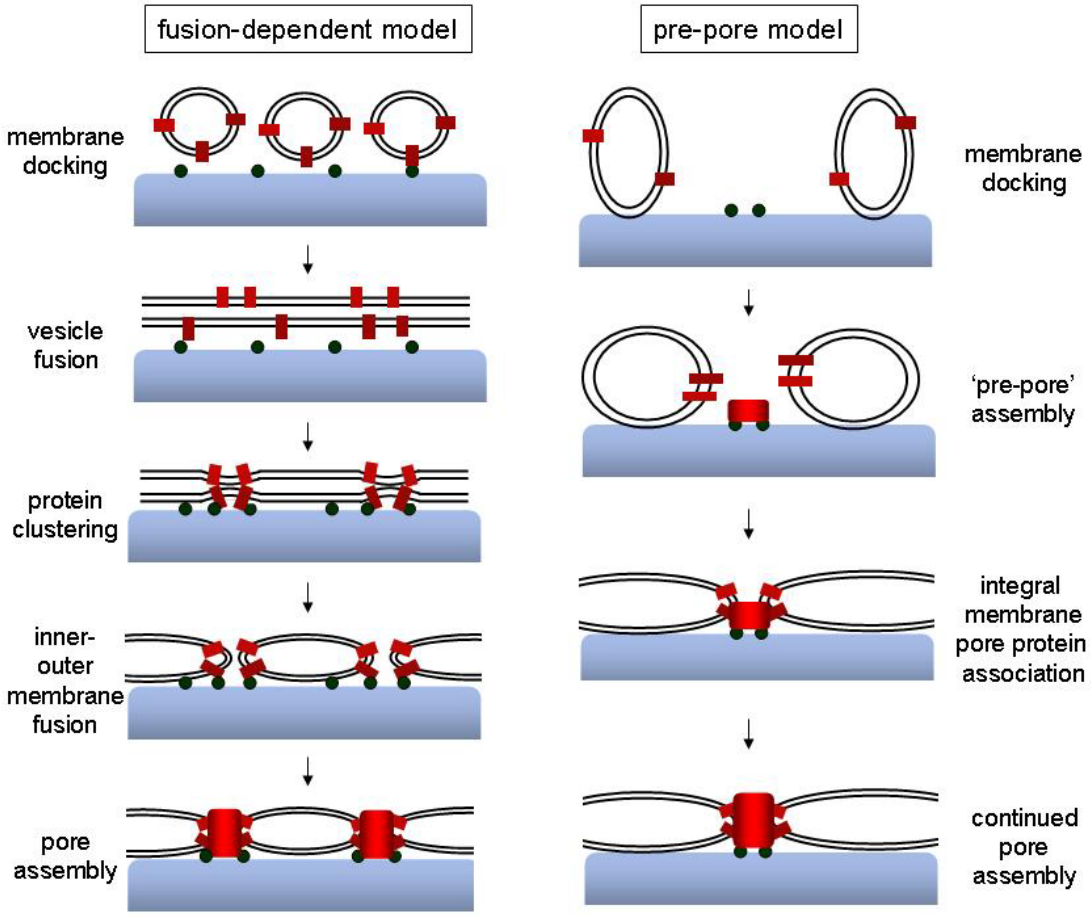

Figure I.3. Two models for nuclear pore assembly. In the fusion-dependent model (left panel), nuclear pore assembly begins with membrane vesicle/sheet/tubule docking and fusion to form areas of flattened double nuclear membranes (black lines). Nuclear pore complexes (red) then assemble by inserting into the continuous nuclear membranes. In this model, NPC assembly is dependent on fusion between the inner and outer nuclear membranes. In the pre-pore model (right panel), membrane vesicles/sheets/tubules (black lines) bind to and spread across the chromatin. Independent of these membranes, nuclear pore complexes (red) assemble on the surface of the chromatin. At some undefined point in assembly, the integral membrane pore proteins (red) associate with the pre-pores/pores and the attached membrane sheets coalesce around them. Pore assembly then continues, if necessary. Thus, inner-outer membrane fusion is *not* required; rather, the NPCs act as membrane "plugs".

References

Anderson, D.J., and Hetzer, M.W. (2007). Nuclear envelope formation by chromatin-mediated reorganization of the endoplasmic reticulum. Nat Cell Biol *9*, 1160-1166.

Antonin, W., Franz, C., Haselmann, U., Antony, C., and Mattaj, I.W. (2005). The integral membrane nucleoporin pom121 functionally links nuclear pore complex assembly and nuclear envelope formation. Mol Cell *17*, 83-92.

Belgareh, N., Rabut, G., Bai, S.W., van Overbeek, M., Beaudouin, J., Daigle, N., Zatsepina, O.V., Pasteau, F., Labas, V., Fromont-Racine, M., Ellenberg, J., and Doye, V. (2001). An evolutionarily conserved NPC subcomplex, which redistributes in part to kinetochores in mammalian cells. J Cell Biol *154*, 1147-1160.

Bischoff, F.R., and Ponstingl, H. (1991). Catalysis of guanine nucleotide exchange on Ran by the mitotic regulator RCC1. Nature *354*, 80-82.

Bodoor, K., Shaikh, S., Salina, D., Raharjo, W.H., Bastos, R., Lohka, M., and Burke, B. (1999). Sequential recruitment of NPC proteins to the nuclear periphery at the end of mitosis. J Cell Sci *112 (Pt 13)*, 2253-2264.

Boehmer, T., Enninga, J., Dales, S., Blobel, G., and Zhong, H. (2003). Depletion of a single nucleoporin, Nup107, prevents the assembly of a subset of nucleoporins into the nuclear pore complex. Proc Natl Acad Sci U S A *100*, 981-985.

Burke, B., and Ellenberg, J. (2002). Remodelling the walls of the nucleus. Nat Rev Mol Cell Biol *3*, 487-497.

Chaudhary, N., and Courvalin, J.C. (1993). Stepwise reassembly of the nuclear envelope at the end of mitosis. J Cell Biol *122*, 295-306.

Clarke, P.R., and Zhang, C. (2004). Spatial and temporal control of nuclear envelope assembly by Ran GTPase. Symp Soc Exp Biol, 193-204.

Cotter, L., Allen, T.D., Kiseleva, E., and Goldberg, M.W. (2007). Nuclear membrane disassembly and rupture. J Mol Biol *369*, 683-695.

Cotter, L.A., Goldberg, M.W., and Allen, T.D. (1998). Nuclear pore complex disassembly and nuclear envelope breakdown during mitosis may occur by both nuclear envelope vesicularisation and dispersion throughout the endoplasmic reticulum. Scanning *20*, 250-251.

Cronshaw, J.M., Krutchinsky, A.N., Zhang, W., Chait, B.T., and Matunis, M.J. (2002). Proteomic analysis of the mammalian nuclear pore complex. J Cell Biol *158*, 915-927.

Dabauvalle, M.C., Loos, K., Merkert, H., and Scheer, U. (1991). Spontaneous assembly of pore complex-containing membranes ("annulate lamellae") in Xenopus egg extract in the absence of chromatin. J Cell Biol *112*, 1073-1082.

Daigle, N., Beaudouin, J., Hartnell, L., Imreh, G., Hallberg, E., Lippincott-Schwartz, J., and Ellenberg, J. (2001). Nuclear pore complexes form immobile networks and have a very low turnover in live mammalian cells. J Cell Biol *154*, 71-84.

D'Angelo, M.A., Anderson, D.J., Richard, E., and Hetzer, M.W. (2006). Nuclear pores form de novo from both sides of the nuclear envelope. Science *312*, 440-443.

Ellenberg, J., Siggia, E.D., Moreira, J.E., Smith, C.L., Presley, J.F., Worman, H.J., and Lippincott-Schwartz, J. (1997). Nuclear membrane dynamics and reassembly in living cells: targeting of an inner nuclear membrane protein in interphase and mitosis. J Cell Biol *138*, 1193-1206.

Fernandez, A.G., and Piano, F. (2006). MEL-28 is downstream of the Ran cycle and is required for nuclear-envelope function and chromatin maintenance. Curr Biol *16*, 1757-1763.

Fontoura, B.M., Blobel, G., and Matunis, M.J. (1999). A conserved biogenesis pathway for nucleoporins: proteolytic processing of a 186-kilodalton precursor generates Nup98 and the novel nucleoporin, Nup96. J Cell Biol *144*, 1097-1112.

Forbes, D.J., Kirschner, M.W., and Newport, J.W. (1983). Spontaneous formation of nucleus-like structures around bacteriophage DNA microinjected into Xenopus eggs. Cell *34*, 13-23.

Franz, C., Walczak, R., Yavuz, S., Santarella, R., Gentzel, M., Askjaer, P., Galy, V., Hetzer, M., Mattaj, I.W., and Antonin, W. (2007). MEL-28/ELYS is required for the recruitment of nucleoporins to chromatin and postmitotic nuclear pore complex assembly. EMBO Rep *8*, 165-172.

Galy, V., Askjaer, P., Franz, C., Lopez-Iglesias, C., and Mattaj, I.W. (2006). MEL-28, a novel nuclear-envelope and kinetochore protein essential for zygotic nuclear-envelope assembly in C. elegans. Curr Biol *16*, 1748-1756.

Gerace, L., Ottaviano, Y., and Kondor-Koch, C. (1982). Identification of a major polypeptide of the nuclear pore complex. J Cell Biol *95*, 826-837.

Gillespie, P.J., Khoudoli, G.A., Stewart, G., Swedlow, J.R., and Blow, J.J. (2007). ELYS/MEL-28 chromatin association coordinates nuclear pore complex assembly and replication licensing. Curr Biol *17*, 1657-1662.

Glavy, J.S., Krutchinsky, A.N., Cristea, I.M., Berke, I.C., Boehmer, T., Blobel, G., and Chait, B.T. (2007). Cell-cycle-dependent phosphorylation of the nuclear pore Nup107-160 subcomplex. Proc Natl Acad Sci U S A *104*, 3811-3816.

Goldberg, M.W., Wiese, C., Allen, T.D., and Wilson, K.L. (1997). Dimples, pores, star-rings, and thin rings on growing nuclear envelopes: evidence for structural intermediates in nuclear pore complex assembly. J Cell Sci *110 (Pt 4)*, 409-420.

Greber, U.F., Senior, A., and Gerace, L. (1990). A major glycoprotein of the nuclear pore complex is a membrane-spanning polypeptide with a large lumenal domain and a small cytoplasmic tail. Embo J *9*, 1495-1502.

Hallberg, E., Wozniak, R.W., and Blobel, G. (1993). An integral membrane protein of the pore membrane domain of the nuclear envelope contains a nucleoporin-like region. J Cell Biol *122*, 513-521.

Haraguchi, T., Koujin, T., Hayakawa, T., Kaneda, T., Tsutsumi, C., Imamoto, N., Akazawa, C., Sukegawa, J., Yoneda, Y., and Hiraoka, Y. (2000). Live fluorescence imaging reveals early recruitment of emerin, LBR, RanBP2, and Nup153 to reforming functional nuclear envelopes. J Cell Sci *113 (Pt 5)*, 779-794.

Harel, A., Chan, R.C., Lachish-Zalait, A., Zimmerman, E., Elbaum, M., and Forbes, D.J. (2003a). Importin beta negatively regulates nuclear membrane fusion and nuclear pore complex assembly. Mol Biol Cell *14*, 4387-4396.

Harel, A., and Forbes, D.J. (2004). Importin beta: conducting a much larger cellular symphony. Mol Cell *16*, 319-330.

Harel, A., Orjalo, A.V., Vincent, T., Lachish-Zalait, A., Vasu, S., Shah, S., Zimmerman, E., Elbaum, M., and Forbes, D.J. (2003b). Removal of a single pore subcomplex results in vertebrate nuclei devoid of nuclear pores. Mol Cell *11*, 853-864.

Hetzer, M., Walther, T.C., and Mattaj, I.W. (2005). Pushing the Envelope: Structure, Function, and Dynamics of the Nuclear Periphery. Annu Rev Cell Dev Biol.

Kessel, R.G. (1989). The annulate lamellae--from obscurity to spotlight. Electron Microsc Rev *2*, 257-348.

Kimura, N., Takizawa, M., Okita, K., Natori, O., Igarashi, K., Ueno, M., Nakashima, K., Nobuhisa, I., and Taga, T. (2002). Identification of a novel transcription factor, ELYS, expressed predominantly in mouse foetal haematopoietic tissues. Genes Cells *7*, 435-446.

Lau, C.K., Delmar, V.A., and Forbes, D.J. (2006). Topology of yeast Ndc1p: predictions for the human NDC1/NET3 homologue. Anat Rec A Discov Mol Cell Evol Biol *288*, 681-694.

Liu, J., Prunuske, A.J., Fager, A.M., and Ullman, K.S. (2003). The COPI complex functions in nuclear envelope breakdown and is recruited by the nucleoporin Nup153. Dev Cell *5*, 487-498.

Lohka, M.J., and Masui, Y. (1983). Formation in vitro of sperm pronuclei and mitotic chromosomes induced by amphibian ooplasmic components. Science *220*, 719-721.

Loiodice, I., Alves, A., Rabut, G., Van Overbeek, M., Ellenberg, J., Sibarita, J.B., and Doye, V. (2004). The entire Nup107-160 complex, including three new members, is targeted as one entity to kinetochores in mitosis. Mol Biol Cell *15*, 3333-3344.

Macaulay, C., and Forbes, D.J. (1996). Assembly of the nuclear pore: biochemically distinct steps revealed with NEM, GTP gamma S, and BAPTA. J Cell Biol *132*, 5-20.

Macaulay, C., Meier, E., and Forbes, D.J. (1995). Differential mitotic phosphorylation of proteins of the nuclear pore complex. J Biol Chem *270*, 254-262.

Mansfeld, J., Guttinger, S., Hawryluk-Gara, L.A., Pante, N., Mall, M., Galy, V., Haselmann, U., Muhlhausser, P., Wozniak, R.W., Mattaj, I.W., Kutay, U., and Antonin, W. (2006). The conserved transmembrane nucleoporin NDC1

is required for nuclear pore complex assembly in vertebrate cells. Mol Cell *22*, 93-103.

Margalit, A., Vlcek, S., Gruenbaum, Y., and Foisner, R. (2005). Breaking and making of the nuclear envelope. J Cell Biochem *95*, 454-465.

Maul, G.G., Maul, H.M., Scogna, J.E., Lieberman, M.W., Stein, G.S., Hsu, B.Y., and Borun, T.W. (1972). Time sequence of nuclear pore formation in phytohemagglutinin-stimulated lymphocytes and in HeLa cells during the cell cycle. J Cell Biol *55*, 433-447.

Meier, E., Miller, B.R., and Forbes, D.J. (1995). Nuclear pore complex assembly studied with a biochemical assay for annulate lamellae formation. J Cell Biol *129*, 1459-1472.

Newport, J. (1987). Nuclear reconstitution in vitro: stages of assembly around protein-free DNA. Cell *48*, 205-217.

Okita, K., Kiyonari, H., Nobuhisa, I., Kimura, N., Aizawa, S., and Taga, T. (2004). Targeted disruption of the mouse ELYS gene results in embryonic death at peri-implantation development. Genes Cells *9*, 1083-1091.

Okita, K., Nobuhisa, I., Takizawa, M., Ueno, M., Kimura, N., and Taga, T. (2003). Genomic organization and characterization of the mouse ELYS gene. Biochem Biophys Res Commun *305*, 327-332.

Rabut, G., Doye, V., and Ellenberg, J. (2004). Mapping the dynamic organization of the nuclear pore complex inside single living cells. Nat Cell Biol *6*, 1114-1121.

Rasala, B.A., Orjalo, A.V., Shen, Z., Briggs, S., and Forbes, D.J. (2006). ELYS is a dual nucleoporin/kinetochore protein required for nuclear pore assembly and proper cell division. Proc Natl Acad Sci U S A *103*, 17801-17806.

Rasala, B.A., Ramos, C., Harel, A., and Forbes, D.F. Capture of AT-rich chromatin by ELYS recruits POM121 and NDC1 to initiate nuclear pore assembly. Mol Biol Cell, submitted.

Reeves, R., and Nissen, M.S. (1990). The A.T-DNA-binding domain of mammalian high mobility group I chromosomal proteins. A novel peptide motif for recognizing DNA structure. J Biol Chem *265*, 8573-8582.

Resendes, K.K., Rasala, B.A., and Forbes, D.J. (2008). Centrin 2 localizes to the vertebrate nuclear pore and plays a role in mRNA and protein export. Mol Cell Biol.

Ramos, C., Rasala, B.A., and Forbes, D.F. Structural intermediates in fusion mediated NPC assembly. In preparation.

Rout, M.P., Aitchison, J.D., Suprapto, A., Hjertaas, K., Zhao, Y., and Chait, B.T. (2000). The yeast nuclear pore complex: composition, architecture, and transport mechanism. J Cell Biol *148*, 635-651.

Ryan, K.J., and Wente, S.R. (2000). The nuclear pore complex: a protein machine bridging the nucleus and cytoplasm. Curr Opin Cell Biol *12*, 361-371.

Sheehan, M.A., Mills, A.D., Sleeman, A.M., Laskey, R.A., and Blow, J.J. (1988). Steps in the assembly of replication-competent nuclei in a cell-free system from Xenopus eggs. J Cell Biol *106*, 1-12.

Stavru, F., Hulsmann, B.B., Spang, A., Hartmann, E., Cordes, V.C., and Gorlich, D. (2006). NDC1: a crucial membrane-integral nucleoporin of metazoan nuclear pore complexes. J Cell Biol *173*, 509-519.

Suntharalingam, M., and Wente, S.R. (2003). Peering through the pore: nuclear pore complex structure, assembly, and function. Dev Cell *4*, 775-789.

Vasu, S., Shah, S., Orjalo, A., Park, M., Fischer, W.H., and Forbes, D.J. (2001). Novel vertebrate nucleoporins Nup133 and Nup160 play a role in mRNA export. J Cell Biol *155*, 339-354.

Vasu, S.K., and Forbes, D.J. (2001). Nuclear pores and nuclear assembly. Curr Opin Cell Biol *13*, 363-375.

Walther, T.C., Alves, A., Pickersgill, H., Loiodice, I., Hetzer, M., Galy, V., Hulsmann, B.B., Kocher, T., Wilm, M., Allen, T., Mattaj, I.W., and Doye, V. (2003a). The conserved Nup107-160 complex is critical for nuclear pore complex assembly. Cell *113*, 195-206.

Walther, T.C., Askjaer, P., Gentzel, M., Habermann, A., Griffiths, G., Wilm, M., Mattaj, I.W., and Hetzer, M. (2003b). RanGTP mediates nuclear pore complex assembly. Nature *424*, 689-694.

Wozniak, R., and Clarke, P.R. (2003). Nuclear pores: sowing the seeds of assembly on the chromatin landscape. Curr Biol *13*, R970-972.

Wozniak, R.W., Bartnik, E., and Blobel, G. (1989). Primary structure analysis of an integral membrane glycoprotein of the nuclear pore. J Cell Biol *108*, 2083-2092.

Yang, L., Guan, T., and Gerace, L. (1997). Integral membrane proteins of the nuclear envelope are dispersed throughout the endoplasmic reticulum during mitosis. J Cell Biol *137*, 1199-1210.

Yang, Q., Rout, M.P., and Akey, C.W. (1998). Three-dimensional architecture of the isolated yeast nuclear pore complex: functional and evolutionary implications. Mol Cell *1*, 223-234.

CHAPTER 1

ELYS is a dual nucleoporin/kinetochore protein required for nuclear pore assembly and proper cell division

Beth A. Rasala, Arturo V. Orjalo*, Zhouxin Shen, Steven Briggs†, and Douglass J. Forbes‡

Section of Cell and Developmental Biology, Division of Biological Sciences, University of California at San Diego, 9500 Gilman Drive, La Jolla, CA 92093-0347

Contributed by Steven Briggs, September 28, 2006 (sent for review July 26, 2006)

Nuclear pores span the nuclear envelope and act as gated aqueous channels to regulate the transport of macromolecules between the nucleus and cytoplasm, from individual proteins and RNAs to entire viral genomes. By far the largest subunit of the nuclear pore is the Nup107–160 complex, which consists of nine proteins and is critical for nuclear pore assembly. At mitosis, the Nup107–160 complex localizes to kinetochores, suggesting that it may also function in chromosome segregation. To investigate the dual roles of the Nup107–160 complex at the pore and during mitosis, we set out to identify binding partners by immunoprecipitation from both interphase and mitotic *Xenopus* egg extracts and mass spectrometry. ELYS, a putative transcription factor, was discovered to copurify with the Nup107–160 complex in *Xenopus* interphase extracts, *Xenopus* mitotic extracts, and human cell extracts. Indeed, a large fraction of ELYS localizes to the nuclear pore complexes of HeLa cells. Importantly, depletion of ELYS by RNAi leads to severe disruption of nuclear pores in the nuclear envelope, whereas lamin, Ran, and tubulin staining appear normal. At mitosis, ELYS targets to kinetochores, and RNAi depletion from HeLa cells leads to an increase in cytokinesis defects. Thus, we have identified an unexpected member of the nuclear pore and kinetochore that functions in both pore assembly at the nucleus and faithful cell division.

Nup107–160 complex | MEL-28 | Nup133 | mitosis

Essential for cell survival, nuclear pore complexes are large multiprotein assemblages, ≈30 times the size of the ribosome. Structurally, nuclear pores are comprised of three major domains inserted in the nuclear membranes. These domains include a massive central scaffold, cytoplasmic filaments, and a nuclear basket (1). Nuclear pores consist of multiple copies of ≈30 different proteins termed nucleoporins (Nups) (2). A third of these contain phenylalanine-glycine (FG) repeat domains, believed to be key sites for interaction with transport receptors (3).

During vertebrate mitosis, the nuclear pore disassembles into approximately a dozen subunits, concurrent with the breakdown of the nuclear envelope. Most diffuse throughout the mitotic cytoplasm, playing no role in mitotic progression identified to date. However, a small number of nuclear pore proteins, including the Nup107–160 complex, localize to regions of the mitotic kinetochore and/or spindle, pointing toward a function in mitotic chromosome segregation (4–15). We now know that, *in vitro*, the Nup107–160 complex is required for spindle assembly (15).

Nuclear reassembly, which begins in late anaphase and continues through telophase, occurs at the chromatin periphery. During this time, the nuclear pore subunits reassemble, stepwise, into pore complexes within the double nuclear membrane. The Nup107–160 complex, by far the largest of the pore subunits, has been shown to play a critical role in nuclear pore assembly. The Nup107–160 complex consists to date of nine proteins (Fig. 1*C*: Nup160, Nup133, Nup107, Nup96, Nup85, Nup43, Nup37, Sec13, and Seh1) and is part of the pore's central scaffold domain (5, 6, 8, 11). Immunodepletion of the Nup107–160 complex from *in vitro* nuclear reconstitution extracts, derived from *Xenopus* eggs, results in the assembly of nuclei completely devoid of nuclear pores (8, 9). Partial knockdown of members of the Nup107–160 complex in vertebrate tissue culture cells by RNAi also results in severe nuclear pore assembly defects in the nuclear envelope (4, 8, 9, 14). This complex is one of the first nuclear pore subunits recruited to the reforming nuclear envelope during pore assembly (5). Thus, the Nup107–160 complex is an essential and early determinant of nuclear pore assembly (5, 8, 9). However, its immediate binding partners within the vertebrate pore, as well as its kinetochore partners, remain speculative.

To begin to dissect the roles of the Nup107–160 complex in nuclear pore assembly and kinetochore function, a search for its protein-binding partners in both interphase and mitosis was initiated. We identified the protein ELYS, a putative transcription factor, to be a highly abundant binding partner of the Nup107–160 complex at both nuclear pores and kinetochores. We show that ELYS is essential not only for correct nuclear pore assembly but also for cell division.

Results

The Putative Transcription Factor ELYS Interacts with the Nup107–160 Complex. To identify binding partners of the Nup107–160 complex, extracts of *Xenopus laevis* eggs, prepared in either interphase or mitotic states, were used. Antibodies specific to Nup133 and Nup43, components of the Nup107–160 complex, were used separately to immunoprecipitate the complex from each type of cell cycle extract. The immunoprecipitates were proteolysed and subjected to liquid chromatography tandem MS (15). The MS spectra were searched against the National Center for Biotechnology Information (NCBI) *X. laevis* protein database. Because this database is incomplete, the NCBI human, fish, and reptile protein databases, plus the protein translations of our unpublished *Xenopus* Nup sequencing data, were included in the search. None of the Nup107–160 complex members were found in immunoprecipitations by control rabbit antisera. Seven of the nine Nup107–160 complex members were identified as highly abundant proteins in anti-Nup43 and anti-Nup133 immunoprecipitates from both interphase and mitotic extracts [Nup160, Nup107, Nup85, Nup43, Nup37, Sec13, and Seh1, denoted with dots (Table 1, which is published as supporting information on the PNAS web site)]. A search of the nearly complete NCBI *X.*

Author contributions: B.A.R. and D.J.F. designed research; B.A.R., A.V.O., and Z.S. performed research; Z.S. and S.B. contributed new reagents/analytic tools; B.A.R., A.V.O., Z.S., S.B., and D.J.F. analyzed data; and B.A.R. and D.J.F. wrote the paper.

The authors declare no conflict of interest.

Freely available online through the PNAS open access option.

Abbreviations: FG, phenylalanine-glycine; Nup, nucleoporin.

*Present address: The Buck Institute for Age Research, 8001 Redwood Boulevard, Novato, CA 94945.

†To whom correspondence may be addressed. E-mail: sbriggs@ucsd.edu.

‡To whom correspondence may be addressed at: Section of Cell and Developmental Biology, Division of Biological Sciences, University of California at San Diego, 9500 Gilman Drive, La Jolla, CA 92093-0347. E-mail: dforbes@ucsd.edu.

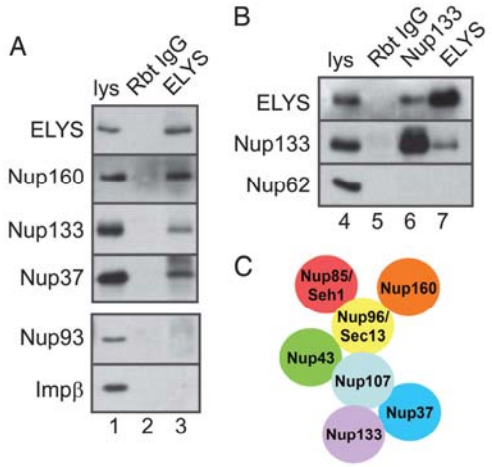

Fig. 1. ELYS coimmunoprecipitates with the Nup107–160 complex. (*A*) Immunoprecipitations from HeLa cell lysates. Anti-ELYS antibody immunoprecipitates ELYS, together with members of the Nup107–160 complex, such as Nup160, Nup133, and Nup37 (lane 3). Anti-ELYS antibodies do not immunoprecipitate the non-Nup107–160 complex Nup, Nup93, or the transport factor Importin β (lane 3). (*B*) Nup133 and ELYS are reciprocally coimmunoprecipitated with one another but not with the non-Nup107–160 complex Nup, Nup62 (lanes 6 and 7). (*A* and *B*) Immunoprecipitation with rabbit IgG serum (Rbt IgG) was used as a negative control (lanes 2 and 5). Lys, input HeLa cell lysate (lanes 1 and 4). (*C*) Cartoon representing the vertebrate Nup107–160 complex, including the nine constituents known before this study.

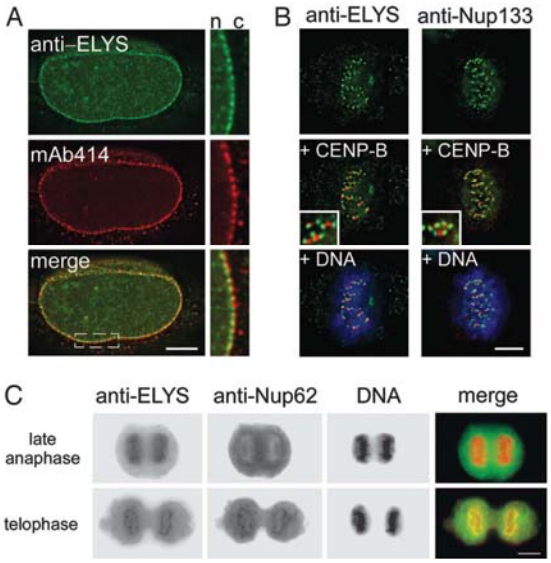

Fig. 2. ELYS localizes to the nuclear pore in interphase and to kinetochores during mitosis. (*A*) Double immunofluorescence on permeabilized, then fixed, HeLa cells with anti-ELYS antibody (*Top*, green) and the anti-FG Nup monoclonal antibody, mAb414 (*Middle*, red), revealing that both localize to the nuclear rim in a punctate pattern characteristic of nuclear pores. Superposition of the signals (*Bottom*) and a 250-fold magnification (see *Insets* to the right) show that ELYS colocalizes with the FG Nups. The nuclear (n) and cytoplasmic (c) sides of the nuclear envelope are indicated. (*B*) Immunofluorescence on mitotic HeLa cells extracted with PHEM buffer. Insets show a 250-fold magnification of kinetochore stains. ELYS (left column, green) and Nup133 (right column, green) show similar localization and bracket CENP-B (red) on the kinetochores. The DNA is stained with DAPI (blue). (*C*) During nuclear assembly in HeLa cells, ELYS (left column and red) associates with the chromatin periphery in late anaphase, whereas Nup62 (center column and green) associates in telophase. (Scale bars: *A* and *B*, 5 μm; *C*, 10 μm.)

laevis EST database confirmed these seven, as well as the two remaining Nup107–160 complex members, Nup133 and Nup96 whose sequences were not present in the *Xenopus* protein database (data not shown).

A limited set of proteins other than the Nup107–160 complex coimmunoprecipitated with antibodies to Nup43 and Nup133, but not with control antisera. A number were chaperone proteins, such as BiP, gp96, and FK506, likely reflecting a level of unfolding (Table 1). Interestingly, a major and unexpected constituent of the immunoprecipitates was the protein ELYS, which was found in both interphase and mitotic Nup107–160 complex immunoprecipitates and not in the controls.

ELYS (embryonic large molecule derived from yolk sac) is a large protein of ≈270 kDa with a predicted AT-hook DNA-binding motif (PRKRGRPRK). AT-hook motifs bind preferentially to the minor groove of DNA at stretches of AT-rich sequences (16). ELYS was originally identified in a mouse cDNA screen for potential regulatory genes involved in hematopoiesis but was simultaneously recognized to be expressed in a multitude of cell types (17). Because certain regions of ELYS, when fused to a yeast Gal4 DNA-binding domain, activated the transcription of a luciferase reporter gene in cultured cells, ELYS was designated as a putative transcription factor involved in hematopoiesis. In a subsequent mouse knockout study, however, it was found that ELYS-null mice die between embryonic days E3.5 and E5.5, well before the onset of hematopoiesis (day E9.5) (18). This finding suggests that ELYS functions in an unknown process that is essential to early mouse embryonic survival, either in addition to or instead of its function in hematopoeisis.

Using an anti-hELYS antibody, we found that Nup107–160 complex members consistently coimmunoprecipitated with ELYS in human cell lysates (Fig. 1*A*, lane 3). Nups not present in the Nup107–160 complex, such as Nup93 and Nup62, as well as the import receptor importin β, failed to immunoprecipitate with anti-ELYS antibody (Fig. 1 *A* and *B*), although a small amount of Nup358 and Nup153 were occasionally detected (data not shown). Importantly, anti-Nup133 antibody reciprocally immunoprecipitated ELYS (Fig. 1*B*, lane 6).

In summary, ELYS can be found in close association with the Nup107–160 complex throughout the cell cycle, and this interaction is evolutionarily conserved in vertebrates.

ELYS Localizes to both the Nuclear Pores and Nuclear Interior During Interphase. In the mouse study, ELYS was found to localize rather generally to the cytoplasm and nucleus with the authors' polyclonal antibody (17). When we performed immunofluorescence on HeLa cells using an affinity-purified commercially prepared anti-ELYS antibody, fixed either before or after Triton X-100 permeabilization, we did not see a significant cytoplasmic stain (Fig. 2*A*; and see Fig. 5, which is published as supporting information on the PNAS web site). Instead, ELYS was located at the nuclear rim in a punctate pattern typical of a nuclear pore stain as well as in the nuclear interior (Fig. 2*A*). Consistent with this finding, ELYS clearly colocalized with the FG Nups (mAb414) at the nuclear pore complexes (Fig. 2*A*).

ELYS Localizes to the Kinetochores in Mitosis. A fraction of the Nup107–160 complex is known to localize to the kinetochores from prophase to late anaphase (5, 8, 11). To determine whether ELYS is also present at kinetochores during mitosis, HeLa cells

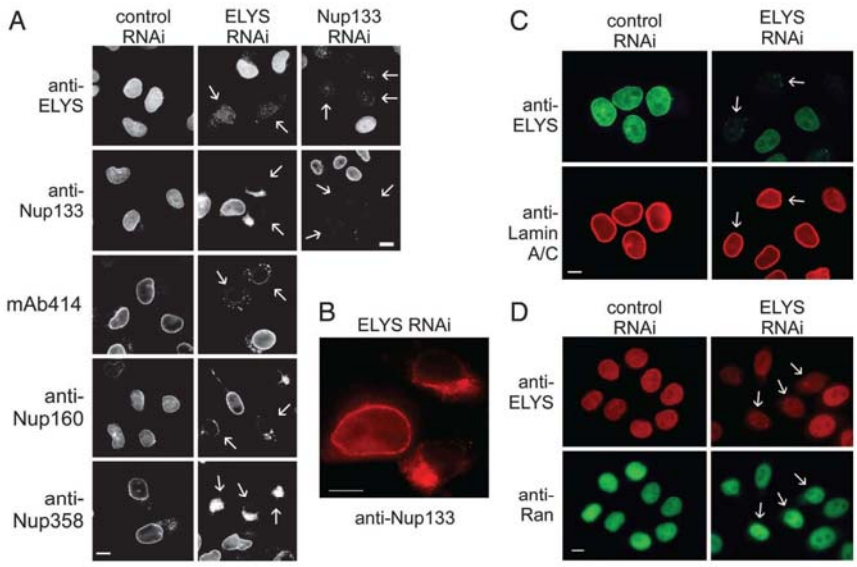

Fig. 3. ELYS is required for proper nuclear pore assembly. Immunofluorescence on HeLa cells transfected with control, ELYS, or Nup133 siRNA duplexes for 48–60 h. Cells were Triton X-100-extracted and then fixed and stained with the antibodies shown. Arrows indicate transfected cells. (*A*) ELYS RNAi results in a knockdown of ELYS and mislocalization of Nup133, whereas Nup133 RNAi similarly results in a knockdown of Nup133 and a reduction of ELYS in the nuclear envelope. ELYS RNAi leads to the mislocalization of the FG-Nups (mAb414), Nup160, and Nup358 from the nuclear rim to cytoplasmic aggregates (center column). (*B*) A magnification of ELYS-depleted cells clearly shows that Nup133 is greatly reduced in nuclear envelope pores and is mislocalized to cytoplasmic aggregates. (*C* and *D*) ELYS RNAi did not significantly affect lamin A/C localization to the nuclear lamina (*C*), or the nuclear accumulation of the transport factor Ran (fixed before permeabilization) (*D*). (Scale bars: 10 μm.)

were subjected to double immunofluorescence by using antibodies to ELYS and to the inner kinetochore protein, CENP-B. Strikingly, anti-ELYS antibodies stained mitotic cells in the paired dot-like pattern characteristic of kinetochore localization (Fig. 2*B* top left). Overlays of anti-ELYS and anti-CENP-B signals showed that ELYS brackets the CENP-B signal in a manner similar to an outer kinetochore protein (Fig. 2*B left*) and does so from prophase to late anaphase (Fig. 6, which is published as supporting information on the PNAS web site). A direct comparison of ELYS and Nup133 revealed that these proteins both localize to an identical region of the kinetochore in mitosis (Fig. 2*B*, compare left and right).

ELYS Is Recruited Early in the Nuclear Envelope Reassembly Process. To analyze the timing of ELYS recruitment during nuclear envelope reassembly, we compared its behavior to that of Nup62 and the Nup107–160 complex member, Nup133. Nup62, a component of the nuclear pore central channel domain, is recruited relatively late in the nuclear envelope reassembly process, i.e., during telophase (19, 20), whereas the Nup107–160 complex is recruited early (5). Immunofluorescence on HeLa cells revealed that ELYS begins to associate with the chromatin/nuclear periphery in late anaphase, well before Nup62 (Fig. 2*C*), in a manner similar to Nup133 (5) (see also Fig. 7, which is published as supporting information on the PNAS web site). Thus, ELYS is recruited early in the nuclear assembly process, with similar timing to that of the Nup107–160 complex.

ELYS Is Essential for Nuclear Pore Assembly. To investigate the role of ELYS at the nuclear pore, we depleted HeLa cells of ELYS by RNAi. HeLa cells transfected with ELYS siRNA oligonucleotides showed a drastic decrease in ELYS at both the nuclear rim and nuclear interior as compared with cells transfected with control oligonucleotides (Fig. 3*A Top*). Indeed, immunoblot analysis of lysates from cells transfected with ELYS siRNA oligonucleotides showed that the protein levels of ELYS were knocked down to very low levels (Fig. 8*A*, lane 2, which is published as supporting information on the PNAS web site).

Strikingly, in ELYS-depleted cells, Nup133 was mislocalized from the nuclear pores to cytoplasmic aggregates (Fig. 3 *A* and *B*). Moreover, RNAi depletion of Nup133 led to a much reduced level of ELYS at the nuclear envelope (Fig. 3*A*). Thus, ELYS and Nup133 are codependent for proper localization to the pore complexes of the nuclear envelope.

Further analysis revealed that RNAi depletion of ELYS affected the nuclear localization of all of the Nups we tested, including the FG Nups, the central scaffold proteins Nup93 and Nup53, the Nup107–160 complex members Nup85 and Nup160, and the cytoplasmic filament protein, Nup358 (Fig. 3*A* and data not shown). All exhibited reduced nuclear rim staining as well as increased cytoplasmic aggregate staining. Pom121, one of the few transmembrane pore proteins, and Tpr, a nuclear basket protein, also exhibited reduced nuclear rim staining upon ELYS depletion but showed few or smaller cytoplasmic aggregates (Fig. 8*B*). Clearly, with defects in all three domains of the nuclear pore complex (filaments, scaffold, and basket), ELYS is critical for the assembly and maintenance of nuclear pores.

Although the knockdown of ELYS by RNAi drastically affected nuclear pores, other cellular structures examined remained intact. ELYS RNAi did not substantially affect the nuclear lamina, (lamin A/C, Fig. 3*C*) or localization of the transport factor Ran to the nucleus, indicative of an intact nuclear envelope (Fig. 3*D*). Similarly, the microtubule cytoskeleton, as visualized by anti-tubulin staining, did not appear altered (Fig. 8*C*). Thus, our knockdown of ELYS does not have a global deleterious effect on cellular structure.

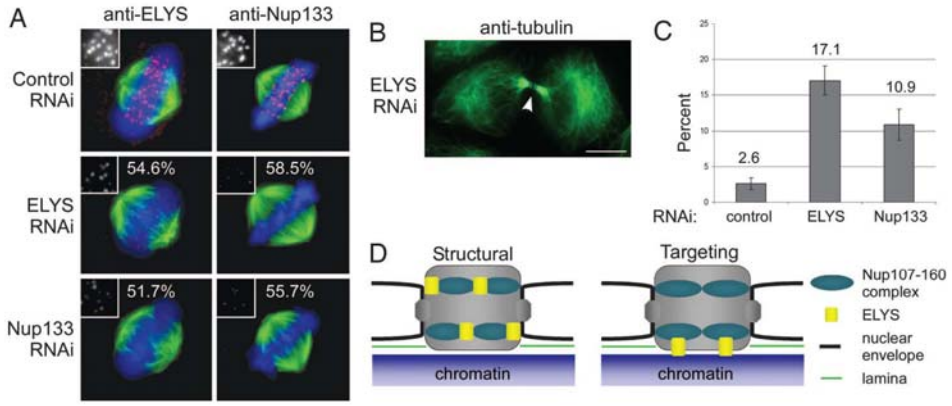

Fig. 4. Knockdown of ELYS leads to cell division defects. HeLa cells were transfected with control, ELYS or Nup133 siRNA duplexes for 48 h. (*A*) ELYS RNAi in HeLa cells leads to reduced levels of both ELYS and Nup133 (red, and *Insets*) at the kinetochores during mitosis, as compared with control-treated cells. Similarly, Nup133 RNAi leads to mitotic HeLa cells with reduced levels of both Nup133 and ELYS (red, and *Insets*) at the kinetochore. Numbers indicate the percentage of reduction of fluorescent intensities compared with those in the control RNAi transfections. (*B*) A large proportion of ELYS-depleted cells contain a midbody (arrowhead). (Scale bar: 10 μm.) (*C*) Percentage of cells with a midbody. Quantitation of the number of cells found in cytokinesis shows a significant increase in the occurrence of cells with midbody microtubules after ELYS and Nup133 RNAi, demonstrating a temporal block at this stage of the cell cycle, in comparison with transfections with the control siRNA duplex. (*D*) Two potential models for ELYS function. In the first model, ELYS serves as a core structural protein of the nuclear pore, one required for formation of the structure of nuclear pores. In the second model, ELYS is a nuclear pore-associated targeting protein that recruits Nups, such as the Nup107–160 complex, to assemble nuclear pores at the chromatin periphery. In its absence, pores would not be found at the nuclear rim.

Because ELYS has been hypothesized to be a transcription factor, we tested whether the nuclear pore defect might be due to decreased Nup protein levels, resulting from a failure in a possible ELYS-dependent Nup transcription. However, no difference in the protein levels of Nup160, Nup358, Nup214, Nup153, or Nup133 was seen after ELYS RNAi (Fig. 8*A*, lanes 1 and 2). These results indicate that ELYS plays an important and direct role in nuclear pore assembly and/or maintenance at the nuclear envelope.

Knockdown of ELYS Leads to Defects in Cytokinesis. To investigate the role of ELYS in targeting the Nup 107-160 complex to kinetochores, we depleted ELYS from HeLa cells by RNAi and quantitated the mitotic kinetochore signal intensities of ELYS or Nup133 for 46–200 kinetochores per condition. Notably, reducing the kinetochore signal of ELYS by RNAi resulted in a nearly identical reduction of Nup133 at the kinetochores (54.6% and 58.5%, Fig. 4*A*). Conversely, a reduction of the Nup133 kinetochore signal by Nup133 RNAi led to the same level of reduction of ELYS at the kinetochore (55.7% and 51.7%; Fig. 4*A*), indicating that ELYS and Nup133 are codependent for proper kinetochore targeting.

Although the partial loss of ELYS and Nup133 from the kinetochores after RNAi did not result in clear spindle assembly or mitotic chromosome alignment defects, it became quickly apparent that a significant number of the RNAi-depleted cells contained midbody microtubules, as visualized by β-tubulin immunofluorescence (Fig. 4*B*). Remarkably, ≈17% of ELYS-depleted cells and ≈11% of Nup133-depleted cells stained for midbody microtubules compared with only 2.6% of control RNAi-treated cells (Fig. 4*C*). These data indicate that depletion of either ELYS or Nup133 causes a delay in or failure to complete cytokinesis. Thus, ELYS and Nup133, a member of the Nup107–160 complex, are required for proper cell division.

Discussion

In this study, the major subunit of the nuclear pore, the Nup107–160 complex, was tested for molecular binding partners. The putative transcription factor ELYS was found to be such an interactor in both *Xenopus* and mammalian cells. Indeed, ELYS localizes to nuclear pores during interphase and to kinetochores throughout mitosis, in a manner virtually identical to that of the Nup107–160 complex. Both ELYS and the Nup107–160 complex are recruited early in the nuclear pore assembly process, i.e., in late anaphase. RNAi depletion of ELYS from HeLa cells resulted in severely reduced levels of Nups at the nuclear rim. Interestingly, ELYS RNAi often induced large cytoplasmic aggregates containing all of the Nups tested, with the exception of Tpr and, to a lesser extent, Pom121. We conclude that ELYS is an essential component for nuclear pore assembly and/or maintenance at the nuclear rim.

Mammalian ELYS is also a kinetochore-associated protein on mitotic chromosomes from prophase to late anaphase, akin to the Nup107–160 complex. Both bracket the inner kinetochore protein CENP-B and depend on one another for kinetochore localization. Although knockdown of ELYS from the kinetochores by ≈50% does not lead to significant chromosome segregation defects, we think it possible that the remaining protein is sufficient to carry out some ELYS function at the kinetochore. Strikingly, however, RNAi knockdown of ELYS does lead to a significant mitotic cell division defect, increasing the number of cells found detained in cytokinesis with midbody microtubules by ≈600%. A more detailed study of this defect will be needed to determine the precise role of ELYS in vertebrate cell division.

ELYS and the Nup107–160 complex plainly act in concert, both in nuclear pore assembly/maintenance and in proper cell division. However, they also differ: a substantial fraction of ELYS has a strong intranuclear presence. It has been shown that certain Nups, such as Nup98, Rae 1, and Nup50, shuttle into the nucleus and reside there part time (13, 20–24). ELYS may resemble these Nups. Alternatively, the intranuclear fraction of ELYS may have a function unrelated to nucleocytoplasmic trafficking. For example, Sec13, a member of the Nup107–160 complex, is both a Nup and a protein integral to the formation of the COPII-coated vesicles involved in cell secretion (2, 8, 11, 25–27). ELYS is referred to in gene databases as a transcription factor (ELYS or AT hook-containing transcription factor 1,

AHCTF1), based largely on the ability of certain regions to activate the transcription of a luciferase reporter (17). An important caveat, however, is that ELYS is a large, acidic protein; acidic domains often have the innate ability to activate transcription in reporter assays (28). A more in-depth analysis of its intranuclear pool is needed to determine whether ELYS is a bona fide transcription factor or has alternative functions inside the nucleus.

The demonstrated essential roles for ELYS in nuclear pore assembly and cytokinesis are consistent with the ELYS-null mouse data, which showed that ELYS is essential for very early embryonic survival. ELYS-null embryos die between days E3.5 and E5.5 (18). Mouse embryos null for Nup214, similarly, die between E4 and E4.5 (29), whereas embryos null for CENP-A, a protein critical for proper kinetochore function, die between E3.5 and E8.5 (30).

In this article, we show that ELYS is a previously uncharacterized resident of the nuclear pore. It is unusual to discover an unexpected member of the nuclear pore, because proteomics on the mammalian nuclear pore complex were completed in 2002 (2). In that study, mass spectrometry was performed on enriched Nup fractions from rat liver nuclei to determine the complete protein composition of the nuclear pore. A feasible explanation for why ELYS was not identified until now is that the human and mouse ELYS protein sequences (gi:17298096 and gi:17298098, respectively; 87% identity to rat ELYS, gi:34881056) were not placed in the NCBI database (September 2002) until after publication of the proteomics study (2). Another possibility is that ELYS was removed by the original rat pore purification protocol (2). We do find ELYS in purified HeLa nuclear pores, although the last purification step removes significant amounts (B.A.R., K. Gustin, and D.J.F., unpublished data).

BLAST searches reveal putative homologs of ELYS from species including *X. laevis* (gi:55250537), *Drosophila* (gi:24643345), and *Caenorhabditis elegans* (gi:42794020) but no obvious yeast homologs. The *C. elegans* gene, *C38D4.3*, which also contains an AT-hook motif, had been linked in a general genome-wide RNAi screen to the nuclear envelope in interphase and possibly to the kinetochore at metaphase (31, 32). Two studies published late after preparation of our report confirm this *C. elegans* link to nuclear pores and kinetochores (33, 34). However, gaps in the nuclear envelope induced by *C38D4.3/MEL-28* RNAi may have led to additional severe defects in the *C. elegans* embryos. Of note, the link to nuclear pores and kinetochores in worms is entirely consistent with our current findings in mammalian cells that ELYS RNAi disrupts the nuclear pore and cell division.

Considering the essential role of ELYS for nuclear pore assembly and maintenance, at least two basic models are possible (Fig. 4*D*). In the first, ELYS is an essential structural protein of the pore, associated with the Nup107–160 complex. The depletion of ELYS by RNAi in this model would result in no pores forming at any location within the cell. In the second model, ELYS is a nuclear pore-associated targeting protein that specifically recruits Nups, such as the Nup107–160 complex, to assemble into nuclear pores at the nuclear envelope rather than in membranes in cytoplasmic locations. Precedence for cytoplasmic pore complexes exists in annulate lamellae (AL), which are cytoplasmic structures that contain numerous nuclear pore-like complexes within stacks of double membranes. AL are present in cells but are not generally abundant (35). RNAi depletion of ELYS in this second model would also result in a clear loss of pores at the nuclear envelope. A potential secondary outcome, however, could be assembly into newly forming annulate lamellae pores. This possibility shows some support from the cytoplasmic aggregates of Nups that appear in ELYS RNAi-depleted cells (Figs. 3 *A* and *B* and 8*B*). Further work will be required to distinguish such models of ELYS function in nuclear pore assembly.

In summary, ELYS and the Nup107–160 complex biochemically interact and share strikingly similar localization and RNAi-depletion phenotypes. ELYS is a component of both the nuclear pore and the kinetochore as well as being intranuclear. RNAi confirms that ELYS is required for pore assembly at the nuclear envelope and for cell division. If it is a DNA-binding protein, as its AT-hook domain might suggest, ELYS could potentially use this domain to bind DNA and recruit pore subunits to the surface of the chromatin during mitosis. In interphase, ELYS could function similarly in new pore assembly or, alternatively, be involved in potential targeting of active vertebrate genes to the nuclear pore. As yet, gene targeting to the nuclear pore has been observed only in yeast (36–38), occurring through a set of specific yeast Nups.

Materials and Methods

Antibodies. The antibodies used included affinity-purified anti-hELYS (aa2220–2302; Bethyl Laboratories, Montgomery, TX), anti-hNup160, anti-hNup133 (6), anti-xNup43, anti-hNup37 (15), anti-Nup93 (39), anti-Nup358 (M. Dasso, National Institutes of Health, Bethesda, MD), anti-Tpr (40), anti-rat Pom121 (S. Tugendreich and D.J.F., unpublished data), anti-*Xenopus* importin β (R. Chan and D.J.F., unpublished data), anti-FG Nup antibody, mAb414 (Covance, Berkeley, CA), anti-CENP-B, [D. Cleveland, University of California at San Diego (UCSD)], anti-tubulin (A. Desai, UCSD), anti-hsp70, anti-Ran, and anti-Nup62 (BD Transduction Laboratories, Lexington, KY).

MS Analysis of Mitotic and Interphase Nup107–160 Complex Immunoprecipitations. Immunoprecipitation and MS analysis of the Nup107–160 complex from *Xenopus* egg extract were performed as recently published (15), except that the MS/MS spectra were searched against a combined forward–reverse database of NCBInr (National Center for Biotechnology Information nonredundant, version 1/10/2005) protein database limited to human, fish, and reptile taxonomies (345,250 sequences).

Immunoprecipitation from HeLa Cells. HeLa cells grown to 80% confluency in 10-cm dishes were washed twice with ice-cold PBS and 1 mM EDTA, lysed at 4°C in 1 ml of 50 mM Tris, pH 7.4, 150 mM NaCl, 1 mM EDTA, 1% Triton X-100, 0.25% sodium deoxycholate, and supplemented with 1 mM PMSF and a protease inhibitor mixture (P8340; Sigma, St. Louis, MO) for 30 min. Cell lysates were sonicated briefly and spun at 14,840 $\times$ *g* for 15 min. Immunoprecipitations were performed by adding 2–5 μg of anti-hNup133, anti-ELYS, or nonimmune rabbit IgG (Calbiochem/EMD Biosciences, San Diego, CA) coupled to protein A Sepharose beads (Amersham Biosciences, Piscataway, NJ).

Immunofluorescence and RNAi. For indirect immunofluorescence, HeLa cells were grown in DMEM/10% FCS on coverslips for 3 days. Cells were either 4% formaldehyde-fixed for 5 min or permeabilized with PHEM buffer (60 mM Pipes/20 mM Hepes, pH 6.9/10 mM EGTA/4 mM $MgSO_4$/0.2% Triton X-100) for 5 min, methanol-fixed for 10 min at −20°C or 4% formaldehyde-fixed for 10 min, and rehydrated with TBS-Tx (10 mM Tris, pH 7.4/150 mm NaCl/0.1% Triton X-100). The cells were processed for immunofluorescence as described (6). Images were acquired by using an optical sectioning deconvolution microscope (DeltaVision; Applied Precision, Issquah, WA; Figs. 2 *A* and B and 4*A*) or an Axioskop fluorescence microscope (Zeiss, Thornwood, NY) (Figs. 2*C*, 3, and 4*B*). Measurements of kinetochore intensity were conducted on nondeconvolved DeltaVision images. We believe that the $\approx$50% reduction in kinetochore staining (Fig. 4*A*), compared with the extensive reduction in total ELYS protein (Fig. 8A)

and ELYS at nuclear pores (Fig. 3 *A*, *C*, and *D*) after RNAi, derives from the finding that only a small percent of the Nup107–160 complex is found localized to the kinetochores at mitosis even in normal cells (5, 8, 11). Extensive cellular RNAi depletion would likely leave sufficient ELYS for the kinetochore stain observed here. All images used identical exposure settings, and scaling and intensities were determined by using Metamorph software (Universal Imaging, Downingtown, PA).

For the RNAi experiments, HeLa cells plated on coverslips were transfected for 48–60 h by using 0.84 μg of siRNA duplexes to ELYS (target: Exon 28 Silencer Pre-Designed siRNA #108720; Ambion, Austin, TX), Nup133 (target: AAGTCGATGACCAGCTGACCA) or Silencer Negative Control #1 siRNA (Ambion) in Oligofectamine (Invitrogen, Carlsbad, CA).

We thank Nick Herrera and Joe Pogliano for use of the deconvolution microscope. We especially thank Iain Cheeseman for experimental advice and aid and Arshad Desai, Don Cleveland, and members of the Forbes Laboratory for interesting discussion. This work was supported by National Institutes of Health Grant GM R01 GM33279 (to D.J.F.) and grants to S.B.

1. Suntharalingam M, Wente SR (2003) *Dev Cell* 4:775–789.
2. Cronshaw JM, Krutchinsky AN, Zhang W, Chait BT, Matunis MJ (2002) *J Cell Biol* 158:915–927.
3. Ryan KJ, Wente SR (2000) *Curr Opin Cell Biol* 12:361–371.
4. Boehmer T, Enninga J, Dales S, Blobel G, Zhong H (2003) *Proc Natl Acad Sci USA* 100:981–985.
5. Belgareh N, Rabut G, Bai SW, van Overbeek M, Beaudouin J, Daigle N, Zatsepina OV, Pasteau F, Labas V, Fromont-Racine M, Ellenberg J, Doye V (2001) *J Cell Biol* 154:1147–1160.
6. Vasu S, Shah S, Orjalo A, Park M, Fischer WH, Forbes DJ (2001) *J Cell Biol* 155:339–354.
7. Joseph J, Tan SH, Karpova TS, McNally JG, Dasso M (2002) *J Cell Biol* 156:595–602.
8. Harel A, Orjalo AV, Vincent T, Lachish-Zalait A, Vasu S, Shah S, Zimmerman E, Elbaum M, Forbes DJ (2003) *Mol Cell* 11:853–864.
9. Walther TC, Alves A, Pickersgill H, Loiodice I, Hetzer M, Galy V, Hulsmann BB, Kocher T, Wilm M, Allen T, *et al.* (2003) *Cell* 113:195–206.
10. Salina D, Enarson P, Rattner JB, Burke B (2003) *J Cell Biol* 162:991–1001.
11. Loiodice I, Alves A, Rabut G, Van Overbeek M, Ellenberg J, Sibarita JB, Doye V (2004) *Mol Biol Cell* 15:3333–3344.
12. Joseph J, Liu ST, Jablonski SA, Yen TJ, Dasso M (2004) *Curr Biol* 14:611–617.
13. Blower MD, Nachury M, Heald R, Weis K (2005) *Cell* 121:223–234.
14. Krull S, Thyberg J, Bjorkroth B, Rackwitz HR, Cordes VC (2004) *Mol Biol Cell* 15:4261–4277.
15. Orjalo AV, Arnaoutov A, Shen Z, Boyarchuk Y, Zeitlin SG, Fontoura B, Briggs S, Dasso M, Forbes DJ (2006) *Mol Biol Cell* 17:3806–3818.
16. Reeves R (2001) *Gene* 277:63–81.
17. Kimura N, Takizawa M, Okita K, Natori O, Igarashi K, Ueno M, Nakashima K, Nobuhisa I, Taga T (2002) *Genes Cells* 7:435–446.
18. Okita K, Kiyonari H, Nobuhisa I, Kimura N, Aizawa S, Taga T (2004) *Genes Cells* 9:1083–1091.
19. Bodoor K, Shaikh S, Salina D, Raharjo WH, Bastos R, Lohka M, Burke B (1999) *J Cell Sci* 112 (Pt 13):2253–2264.
20. Bodoor K, Shaikh S, Enarson P, Chowdhury S, Salina D, Raharjo WH, Burke B (1999) *Biochem Cell Biol* 77:321–329.
21. Harel A, Chan RC, Lachish-Zalait A, Zimmerman E, Elbaum M, Forbes DJ (2003) *Mol Biol Cell* 14:4387–4396.
22. Griffis ER, Altan N, Lippincott-Schwartz J, Powers MA (2002) *Mol Biol Cell* 13:1282–1297.
23. Guan T, Kehlenbach RH, Schirmer EC, Kehlenbach A, Fan F, Clurman BE, Arnheim N, Gerace L (2000) *Mol Cell Biol* 20:5619–5630.
24. Moore MS (2003) *Trends Cell Biol* 13:61–64.
25. Siniossoglou S, Wimmer C, Rieger M, Doye V, Tekotte H, Weise C, Emig S, Segref A, Hurt EC (1996) *Cell* 84:265–275.
26. Fontoura BM, Blobel G, Matunis MJ (1999) *J Cell Biol* 144:1097–1112.
27. Bickford LC, Mossessova E, Goldberg J (2004) *Curr Opin Struct Biol* 14:147–153.
28. Hope IA, Mahadevan S, Struhl K (1988) *Nature* 333:635–640.
29. van Deursen J, Boer J, Kasper L, Grosveld G (1996) *EMBO J* 15:5574–5583.
30. Howman EV, Fowler KJ, Newson AJ, Redward S, MacDonald AC, Kalitsis P, Choo KH (2000) *Proc Natl Acad Sci USA* 97:1148–1153.
31. Sonnichsen B, Koski LB, Walsh A, Marschall P, Neumann B, Brehm M, Alleaume AM, Artelt J, Bettencourt P, Cassin E, *et al.* (2005) *Nature* 434:462–469.
32. Gunsalus KC, Ge H, Schetter AJ, Goldberg DS, Han JD, Hao T, Berriz GF, Bertin N, Huang J, Chuang LS, *et al.* (2005) *Nature* 436:861–865.
33. Fernandez AG, Piano F (2006) *Curr Biol* 16:1757–1763.
34. Galy V, Askjaer P, Franz C, Lopez-Iglesias C, Mattaj IW (2006) *Curr Biol* 16:1748–1756.
35. Meier E, Miller BR, Forbes DJ (1995) *J Cell Biol* 129:1459–1472.
36. Galy V, Olivo-Marin JC, Scherthan H, Doye V, Rascalou N, Nehrbass U (2000) *Nature* 403:108–112.
37. Casolari JM, Brown CR, Komili S, West J, Hieronymus H, Silver PA (2004) *Cell* 117:427–439.
38. Dilworth DJ, Tackett AJ, Rogers RS, Yi EC, Christmas RH, Smith JJ, Siegel AF, Chait BT, Wozniak RW, Aitchison JD (2005) *J Cell Biol* 171:955–965.
39. Miller BR, Powers M, Park M, Fischer W, Forbes DJ (2000) *Mol Biol Cell* 11:3381–3396.
40. Shah S, Tugendreich S, Forbes D (1998) *J Cell Biol* 141:31–49.

Supplemental Data

Table 1.1. Summary of proteins identified in the Nup107-160 complex immunoprecipitation experiments by LC MS/MS. Numbers indicate the number of unique peptides identified in each immunoprecipitation reaction. The right-most column shows the total number of unique peptides identified. Dots denote known members of the Nup107-160 complex; the arrowhead highlights the novel Nup107-160 complex interactor, ELYS.

IP: / extract:	Nup133 Interphase	Nup133 Mitotic	Nup43 Interphase	Nup43 Mitotic	Rab IgG Interphase	Rab IgG Mitotic	**Total unique peptides**
Protein:							
• Nup160	7	9	11	14	0	0	13
➤ **ELYS**	**6**	**6**	**4**	**5**	**0**	**0**	**11**
• Nup85	2	6	4	8	0	0	8
P4hb	5	5	8	5	0	0	9
BiP	3	3	8	4	0	0	8
gp96	3	2	5	1	0	0	7
• Sec13	3	6	4	5	0	0	6
• Nup43	4	2	6	7	0	0	6
PPIB	6	4	6	4	0	0	5
• Nup37	2	3	3	4	0	0	6
• Seh1	2	1	2	4	0	0	4
• Nup107	0	1	3	3	0	0	3
FK506	3	2	2	2	0	0	3

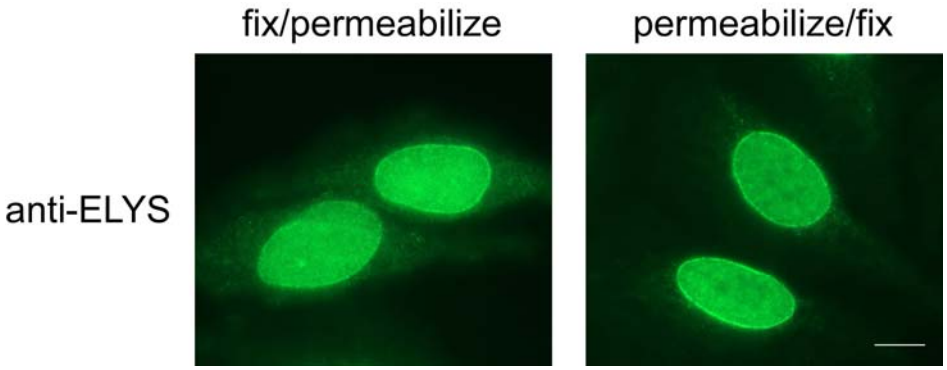

Figure 1.5. Immunofluorescence on HeLa cells with anti-ELYS antibody. Cells were either fixed prior to Triton X-100 permeabilization (left) or permeabilized and then fixed (right). Both methods show that anti-ELYS antibody primarily stains the nuclear rim and the nuclear interior.

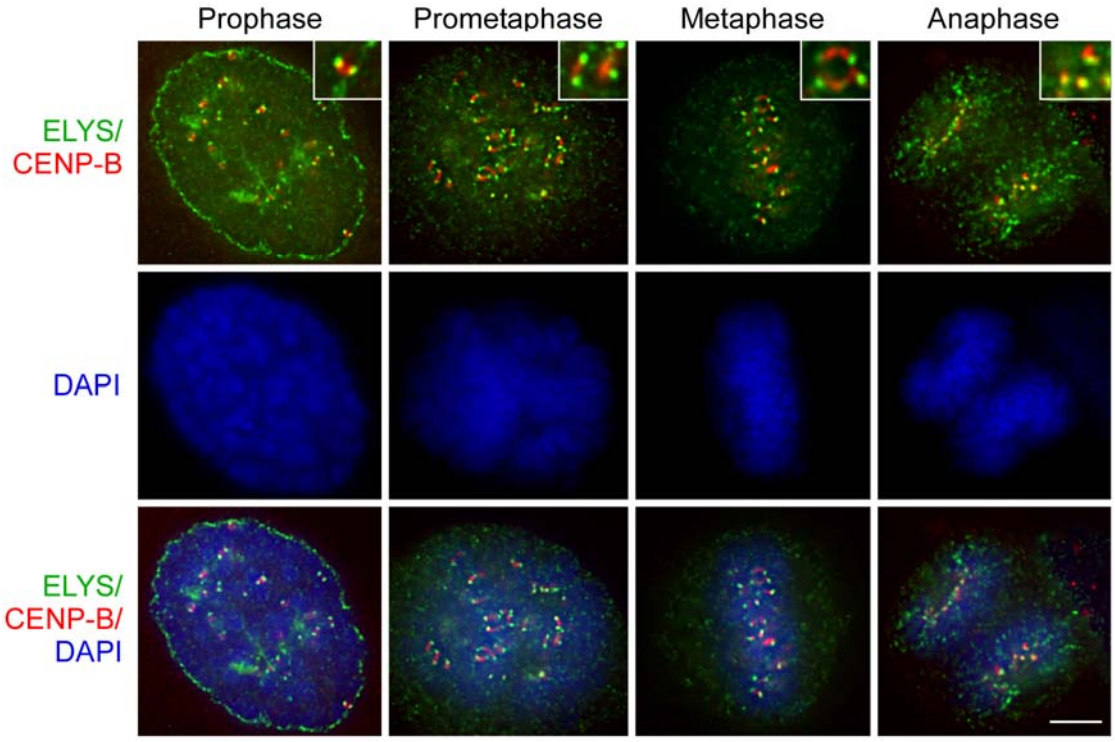

Figure 1.6. ELYS localizes to kinetochores throughout mitosis. Double immunofluorescence on mitotic HeLa cells show ELYS (green) is associated with the mitotic chromatin (i.e., kinetochore) bracketing CENP-B (red) from prophase to late anaphase. Bar, 5 μm.

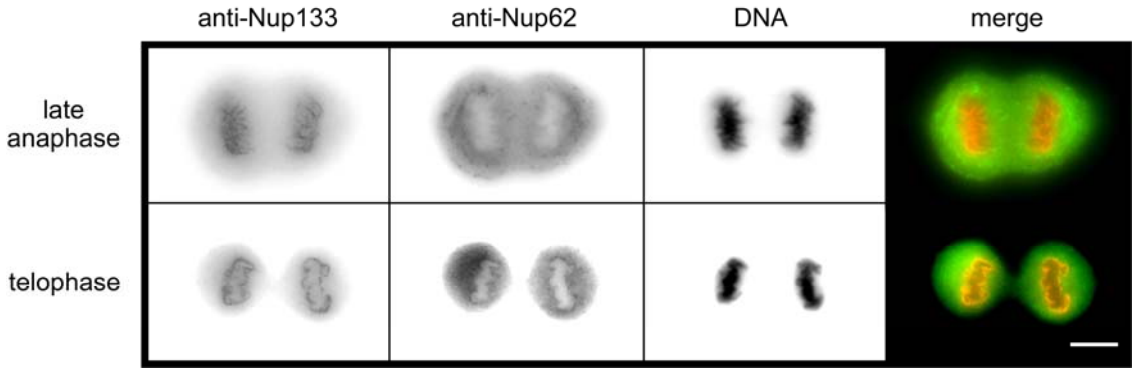

Figure 1.7. Nup133 associates with the reforming nuclear envelope in late anaphase with similar timing to ELYS. During nuclear assembly in HeLa cells, Nup133 (left column, red), a member of the Nup107-160 complex, associates with the reforming nuclear envelope in late anaphase while Nup62 (middle column, green) associates in telophase (as shown in (5)). Bar, 10 µm.

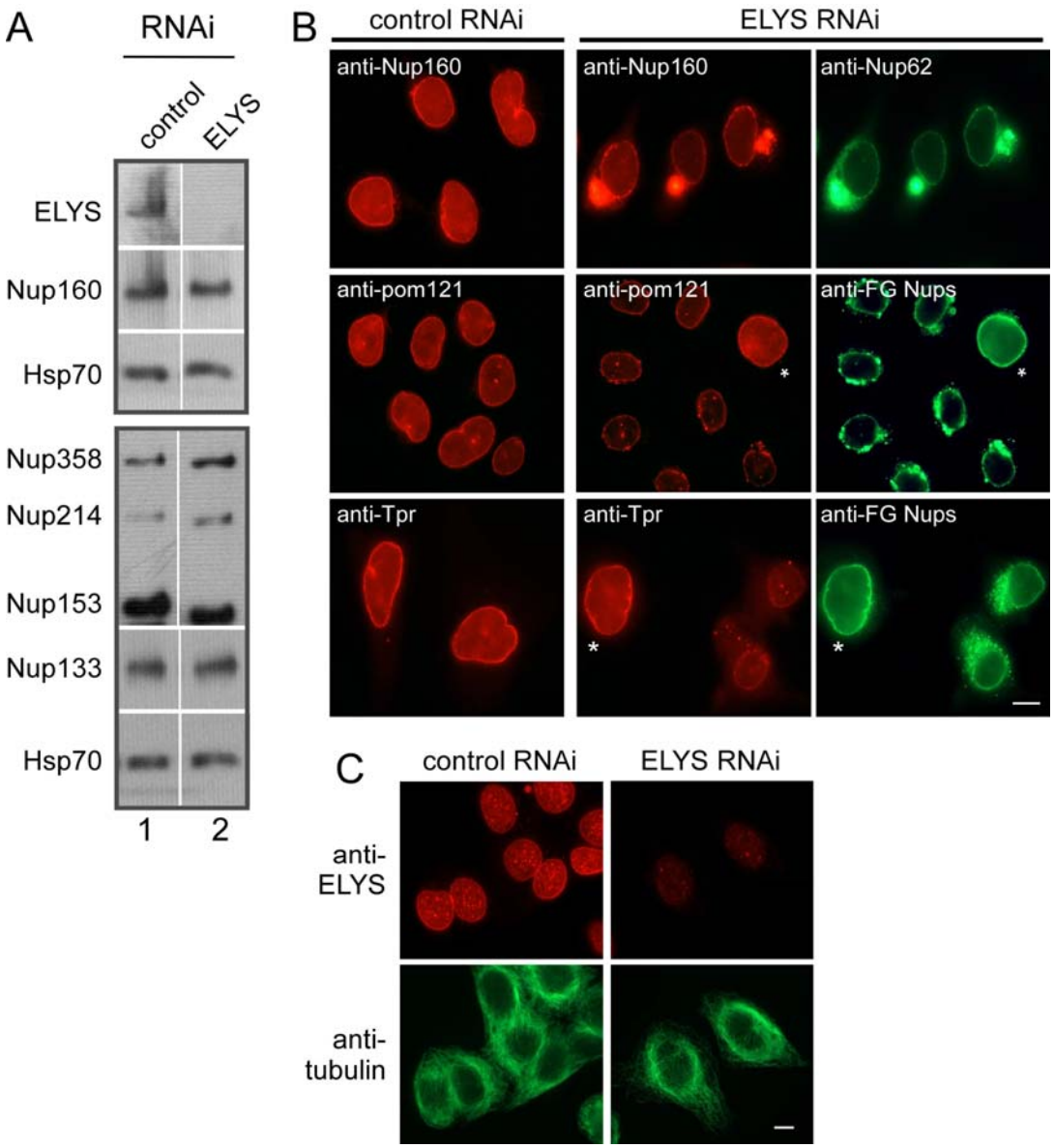

Figure 1.8. Analysis of ELYS RNAi on other nucleoporin proteins and tubulin.
(A) Immunoblots of HeLa cell lysates transfected for 60 hours with control siRNA (lane 1) or ELYS siRNA (lane 2) duplexes. The blots were cut horizontally into strips and probed with anti-ELYS, anti-Nup160, anti-Nup133, and mAb414 anti-FG Nup (Nup358, Nup214, Nup153) antibodies. An antibody to Hsp70 was used as a loading control. Note: in Nup133 RNAi experiments (not shown), ELYS protein remains present.
(B) HeLa cells were transfected with control or ELYS siRNA duplexes for 48 hours. ELYS depletion leads to mislocalization of Nup160 and Nup62 to the same cytoplasmic aggregates. Pom121 and Tpr show reduced staining at the nuclear rim following ELYS depletion, but only few, small cytoplasmic aggregates, in comparison to the anti-FG Nup staining.
(C) HeLa cells were transfected with control or ELYS siRNA duplexes. Depletion of ELYS did not alter the tubulin cytoskeleton, as visualized by anti-β-tubulin staining. Untransfected cells are denoted with asterisks (*). Bars, 10 μm.

Acknowledgements

Chapter 1, in full, is a reprint of the material as it appears in the **Proceedings of the National Academy of Sciences**: **Beth A. Rasala**, Art Orjalo, Zhouxin Shen, Steven Briggs, Douglass J Forbes. ELYS is a Dual Nucleoporin/Kinetochore Protein Required for Nuclear Pore Assembly and Proper Cell Division. PNAS, 2006 Nov 21; 103 (47): 17801-17806, by copyright permission from National Academy of Sciences, U.S.A. I was the primary investigator and author of this paper.

We thank Nick Herrera and Joe Pogliano for use of the deconvolution microscope. We especially thank Iain Cheeseman for experimental advice and aid, and Arshad Desai, Don Cleveland, and the Forbes lab, for interesting discussion.

CHAPTER 2

Capture of AT-rich chromatin by ELYS recruits POM121 and NDC1 to initiate nuclear pore assembly

Introduction

The nuclear envelope (NE), which encompasses the genome in eukaryotes, consists of double nuclear membranes, nuclear pore complexes (NPCs), and a nuclear lamina. Regulated, bidirectional nucleocytoplasmic transport of molecules is mediated by the nuclear pore complexes (Macara, 2001; Quimby and Corbett, 2001; Goldfarb *et al.*, 2004; Pemberton and Paschal, 2005; Patel *et al.*, 2007), massive protein structures ~125 MDa in size that span the nuclear envelope in vertebrates (Reichelt *et al.*, 1990). Although an intact and functioning NE is essential during interphase, in higher eukaryotes the nuclear envelope, including nuclear pore complexes, disassembles at the start of mitosis to allow for assembly of the mitotic spindle and division of the envelope and pore proteins into two daughter cells (reviewed in Burke and Ellenberg, 2002; Margalit *et al.*, 2005; Prunuske *et al.*, 2006). Following chromosome segregation, the nuclear envelope must reform around the daughter genomes, a process involving nuclear membrane recruitment and pore complex assembly.

Nuclear pore assembly is a complex process. Vertebrate NPCs are comprised of ~30 different proteins or nucleoporins (Nups), each in multiple copies (Cronshaw *et al.*, 2002). Nuclear pores disassemble at mitosis into ~14 soluble subunits and three integral membrane pore proteins, POM121, NDC1, and gp210, these latter being found in vesicles and ER sheets (Gerace *et al.*, 1982; Wozniak *et al.*, 1989; Greber *et al.*, 1990; Hallberg *et al.*, 1993; Ellenberg *et al.*, 1997; Yang *et al.*, 1997; Cotter *et al.*, 1998; Daigle *et al.*, 2001; Vasu and Forbes, 2001; Liu *et al.*, 2003; Suntharalingam and Wente, 2003; De Souza *et al.*, 2004; Hetzer *et al.*, 2005; Schwartz, 2005; Lau *et al.*, 2006; Madrid *et al.*, 2006; Mansfeld *et al.*, 2006; Stavru *et al.*, 2006).

Beginning late in anaphase, the soluble pore subunits and pore integral membrane proteins come together in multiple copies at the chromatin periphery to form nuclear pores within the newly formed nuclear membranes. Together the pore subunits build the asymmetric nuclear pore complex, containing a massive central scaffold, eight cytoplasmic filaments, and a nuclear basket. Post-mitotic NPC assembly is a stepwise process. Certain subunits have been classified by immunofluorescence *in vivo* into early, mid, or late-assembling proteins, but the order of assembly of most subunits remains unknown (Chaudhary and Courvalin, 1993; Bodoor *et al.*, 1999; Haraguchi *et al.*, 2000; Belgareh *et al.*, 2001; Daigle *et al.*, 2001; Rabut *et al.*, 2004; Rasala *et al.*, 2006; Franz *et al.*, 2007). An equally perplexing problem is the timing of membrane assembly. The two major mechanistic models that

have been proposed for the post-mitotic assembly of nuclear pores differ in regard to the role of the membrane component in this process. One model, and considerable data, indicates that NPCs assemble into regions of double nuclear membranes (Macaulay and Forbes, 1996; Goldberg *et al.*, 1997; Harel *et al.*, 2003a; Baur *et al.*, 2007). In this model, a distinct fusion event between the inner and outer nuclear membranes is then required for nuclear pore assembly. A competing model proposes that "pre-NPCs" form on chromatin, with the stepwise recruitment of all soluble subunits, and the nuclear membranes sealing around the structure only at the end of the process (Sheehan *et al.*, 1988; Burke and Ellenberg, 2002; Walther *et al.*, 2003a; Antonin *et al.*, 2005; Anderson and Hetzer, 2007). Clearly, many questions concerning how the process of nuclear pore assembly is initiated, ordered, and regulated thus remain unanswered.

The vertebrate protein ELYS, and presumably its homologue MEL-28 in *C. elegans*, have recently been shown to play the earliest essential role in nuclear pore assembly (Fernandez and Piano, 2006; Galy *et al.*, 2006; Rasala *et al.*, 2006; Franz *et al.*, 2007). Vertebrate ELYS/MEL-28 is a 270 kDa protein and contains putative NLSs, NESs, WD repeats and an AT-hook DNA-binding motif. ELYS was originally proposed to be a transcription factor involved in murine embryonic haematopoiesis (Kimura *et al.*, 2002). Full-length homologues of ELYS/MEL-28 can be found in most multicellular organisms from *C. elegans* to mammals. However, BLAST searches identify only a very

small ~300 aa protein in many fungi, including *S. pombe* (gi:4007794), although an *S. cerevisiae* homologue of this small protein has not been identified (D. Forbes, unpublished; Rasala *et al.*, 2006). The apparent lack of full-length homologues in fungi possibly suggests that the complete function of ELYS is conserved only in higher eukaryotes.

We first identified a link between ELYS and the vertebrate nuclear pore in a mass spectrometry search for proteins physically associated with the largest nuclear pore subunit, the nine member Nup107-160 subcomplex (Rasala *et al.*, 2006). In human tissue culture cells, RNAi-mediated knockdown of ELYS caused a greatly reduced pore number in the nuclear envelope, but a surprising increase in pores in the cytoplasm (Rasala *et al.*, 2006; Franz *et al.*, 2007). RNAi studies led to the important clue that ELYS is thus not an essential structural protein of the pore, but acts to target pore assembly specifically to the chromatin periphery. In the absence of ELYS, assembly occurs within the ER to give cytoplasmic pores, also known as annulate lamellae.

Both ELYS and the Nup107-160 complex were separately shown to bind to chromatin (Walther *et al.*, 2003a; Franz *et al.*, 2007; Gillespie *et al.*, 2007). It is now known that ELYS can bind to chromatin independently, while the Nup107-160 complex requires ELYS to achieve chromatin binding (Franz *et al.*, 2007). Immunodepletion of either ELYS or the Nup107-160 complex from *Xenopus* nuclear assembly extracts yields identical phenotypes, i.e.,

nuclei with intact nuclear membranes but devoid of nuclear pores (Harel *et al.*, 2003b; Walther *et al.*, 2003a; Franz *et al.*, 2007; Gillespie *et al.*, 2007). A recent study showed that a 208 aa C-terminal fragment of ELYS (rATH) that contains, among other sequences, NLSs and an AT-hook motif, outcompetes endogenous ELYS for chromatin binding (Gillespie *et al.*, 2007). This prevents the binding of the Nup107-160 complex and nuclear pore assembly, impacting DNA replication (Gillespie *et al.*, 2007). We and others have thus proposed a mechanism by which ELYS targets pore assembly to the nuclear periphery by first binding to chromatin, then recruiting its binding partner, the Nup107-160 complex to initiate pore assembly (Rasala *et al.*, 2006; Franz *et al.*, 2007; Gillespie *et al.*, 2007).

In this study we dissect the molecular role of ELYS in the early steps of NPC assembly. Using targeted deletion and point mutation analysis, sequence-specific DNA-binding antibiotics, and analysis of the recruitment of the soluble and pore integral membrane proteins to the forming nucleus, we address the steps in early pore assembly.

Material and Methods

Antibodies, constructs and protein expression. To generate the xELYS antiserum, *Xenopus ELYS* cDNA (LOC397707) was purchased from ATCC. The extreme C-terminus of this clone was PCR amplified using oligos 5'-CGGGATCCGAAATAAAGTTGATTTCTCCTC-3' and 5'-

ACGCGTCGACTCATCTCATCTTTCGCCGCGT-3' and sub-cloned into pET28a. Recombinant, his-tagged protein was expressed in *E. coli* BL21 expression cells, purified on Ni-NTA agarose (Qiagen, Valencia, CA), and used to immunize a rabbit. Other antibodies used in this study included anti-xNup160, anti-hNup133, anti-rat Nup98 GLFG (Harel *et al.*, 2003b); anti-hNup85, anti-*Xenopus* Pom121, anti-gp210 (Harel *et al.*, 2003b); anti-xNup43, anti-xNup37 (Orjalo *et al.*, 2006); anti-Nup93, anti-hNup205 (Miller and Forbes, 2000); anti-Tpr (Shah *et al.*, 1998); anti-*Xenopus* importin β (Rasala *et al.*, 2006); anti-xNup155 (S. Vasu and D.J.F, unpublished); anti-mNup53, anti--xNDC1 (V. Delmar and D.J.F, unpublished); anti-xNup50 (R. Sekhorn, unpublished); anti-Orc2, anti-RCC1, anti-Mcm3 (generous gifts from Z. You and J. Newport); anti-FG nucleoporin antibody mAb414 and anti-GST (Covance, Berkeley, CA); anti-human Importin α (BD Transduction Laboratories, Lexington, KY), anti-GAPDH (Calbiochem, San Diego, CA), and anti-ribophorin (Serotec, Ltd, Oxford, United Kingdom).

To generate recombinant GST-ΔAT-hook, the above oligos and cDNA clone were used and the PCR product was subcloned into pGEX-6P-3 (GE Healthcare, Uppsala, Sweden). To generate recombinant GST-AT-hook+, oligos 5'-CGGGATCCACCCAATATGTCTTCT-3' and 5'-ACGCGTCGACTCATCTCATCTTTCGCCGCGT-3' were used and the PCR product was subcloned into pGEX-6P-3. Stratagene's QuickChange Site-directed Mutagenesis Kit (Stratagene, La Jolla, CA) was utilized to generate

the GST-AT-hook 2R→A double point mutant using mutagenesis oligos 5'-GTTCCGGCCTCAAAACCGGCAGGCGCACCTCCAAAACACAAAGC-3' and 5'-GCTTTGTGTTTTGGAGGTGCGCCTGCCGGTTTTGAGGCCGGAAC-3' and following the manufacturer's protocol. All recombinant, GST tagged proteins were expressed in *E. coli* BL21 expression cells and purified on Glutathione Sepharose 4B beads (GE Healthcare).

RanQ69L was expressed, purified, and loaded with GTP as in (Orjalo, et al. 2006).

Nuclear and annulate lamellae reconstitution reactions. Cytosolic and membrane vesicle fractions of *Xenopus* egg extracts were prepared as in (Powers *et al.*, 1995). Nuclei were reconstituted at room temperature, by mixing *Xenopus* egg membrane vesicle and cytosolic fractions at a 1:20 ratio with an ATP-regeneration system and sperm chromatin (Macaulay *et al.*, 1995). Recombinant proteins (Figure 2.3) or buffer (0.35% ethanol), Distamycin A, or Chromomycin A_3 (Sigma, St. Louis, MO, Figure 2.4) were added to the cytosol and membranes on ice at the specified concentrations prior to chromatin addition. Note that Chromomycin A_3 is highly toxic and should be handled with care.

Annulate lamellae (AL) were assembled for two hours at room temperature, by mixing *Xenopus* egg membrane vesicle and cytosolic fractions at a ratio of 1:8, supplemented with glycogen as in (Meier *et al.*,

1995). Recombinant proteins, buffer (0.35% ethanol) or Distamycin A, or 2 mM GTPγS were added to the reactions, as indicated. AL were diluted in 1xELB (10 mM Hepes pH 7.6, 50 mM KCl, 25 mM Mg Cl_2), and pelleted through a 30% sucrose cushion. The membrane pellet was solubilized with SDS-containing sample buffer, and subjected to immunoblot analysis.

Immunofluorescence. For direct immunofluorescence, mAb414, affinity purified anti-POM121, or anti-xELYS were coupled to Alexa fluor dyes (Molecular Probes, Eugene, OR). To assay for the presence of nuclear pores or nucleoporins, nuclear reactions were stopped on ice one hour after the start of assembly. Directly labeled antibodies were added to the reactions for at least 10 min. The nuclei were mounted on mounting media containing 3,3-dihexyloxacarbocyanine (DHCC) membrane dye (green images) and Hoechst, or fixed with 3.2% formaldehyde, incubated with octadecyl rhodamine B chloride (R18, Molecular Probes) membrane dye (red images), and mounted on Vectashield with DAPI (Vector Laboratories, Burlingame, CA). Images were acquired using an Axiovert 200M (Carl Zeiss, Thornwood, NY) at a magnification of 63x using an oil objective (Carl Zeiss) with a 1.3 numerical aperture at 23ºC and with Immersol 518F (Carl Zeiss) as the imaging medium. Images were recorded using a Coolsnap HQ (Photometerics, Tucson, AZ) camera and Metavue software (Molecular Devices Corporation, Downingtown, PA).

POM121 pulldown. His-tagged *Xenopus* POM121 protein fragment aa 164-435 was expressed from a pET28a vector in *E. coli* BL21 expression cells and purified on Ni-NTA agarose (Qiagen). xPOM121 aa 164-435 was coupled to CnBr–Sepharose CL4B beads (GE Healthcare) prepared according to the manufacturer's instructions. Beads (5 mg) containing POM121 fragment or the control His-GFP (25 µg) were incubated with membrane-free *Xenopus* egg cytosol which had been diluted 1:20 in PBS with 1 mM PMSF and a protease inhibitor mixture (P8340; Sigma). This was incubated at room temperature with tumbling for one hour. The beads were washed three times with PBS. Proteins were eluted with 100 mM glycine, pH 2.5 and neutralized with 100 mM Tris-HCl, pH 7.9. SDS-PAGE and immunoblotting were performed as in Shah et al. (1998).

Anchored chromatin and anchored nuclei reactions. Protocols were adapted from (Macaulay and Forbes, 1996). Crude nucleoplasmin was prepared by heating egg cytosol to 100°C for 5 minutes. The denatured proteins were removed from nucleoplasmin by microcentrifugation at 14,840 x *g* for 20 minutes. Demembranated sperm chromatin was decondensed by addition of 2 volumes of crude nucleoplasmin for ~10 minutes at room temperature. Decondensation state was monitored by fluorescence microscopy. Decondensed chromatin was diluted to 2500 sperm/µl in 1xELB

(10 mM Hepes pH 7.6, 50 mM KCl, 25 mM Mg Cl_2). 50 μls of diluted sperm chromatin was used to coat each poly-L-lysine-treated 12 mm coverslip (Fisher Scientific, Pittsburg, PA). The swollen sperm chromatin was allowed to settle by gravity onto the coverslips for 2 hours in a humidified chamber. The chromatin-coated coverslips were then washed with 1xELB and blocked with 5% BSA/ELB for 20 minutes. For the anchored chromatin experiments, membrane-free *Xenopus* egg cytosol (which was subjected to an additional centrifugation at 14,840 x *g* for 20 minutes), an ATP-regenerating system, 25 μg/ml of nocodazole and recombinant proteins or antibiotics (where indicated) were combined on ice for a final volume of 30-40 μls, and then added to the chromatin-coated coverslips. Chromatin-binding reactions were allowed to continue for 20 minutes. Coverslips were washed 3 times with 1x ELB-K (10 mM Hepes pH 7.6, 125 mM KCl, 25 mM Mg Cl_2) to remove all unbound proteins. Chromatin-bound proteins were solubilized with SDS-containing sample buffer and subjected to immunoblotting analysis.

Anchored nuclei reactions were conducted as above, by mixing *Xenopus* egg membrane vesicle and cytosolic fractions at a ratio of 1:10, an ATP-regenerating system, 25 μg/ml of nocodazole, and recombinant proteins or antibiotics (where indicated) on ice for a final volume of 30-40 μls. Reactions were incubated with chromatin-coated coverslips for one hour at room temperature. 2 mM GTPγS was included in the reaction, where indicated, to prevent membrane vesicle fusion.

Results

Anti-ELYS antibody demonstrates that ELYS is abundant in nuclear pores, but not in annulate lamellae pores.

To investigate the molecular mechanism for ELYS function in nuclear pore assembly, we utilized a nuclear reconstitution system derived from *Xenopus* egg extract. The egg contains large stores of disassembled pore subunits and membrane vesicles; extracts of *Xenopus* eggs are well characterized for the study of nuclear and nuclear pore assembly (Forbes *et al.*, 1983; Lohka and Masui, 1983; Newport, 1987). To study the role of ELYS, we generated an antibody to aa 2358-2408 of the *Xenopus* ELYS protein (LOC397707). This antibody recognized a protein of the expected size of ~270 kDa in both *Xenopus* egg cytosol and XL177 cultured cell lysates (Figure 2.1A). Immunofluorescence revealed that the antibody stains *Xenopus* nuclei reconstituted in vitro in a punctate pattern that co-localizes, as expected, with nucleoporins containing phenylalanine-glycine repeat domains (FG-Nups) (Figure 2.1B).

The anti-xELYS antibody was next used to biochemically probe for the presence of ELYS in nuclear pores and annulate lamellae pores. Annulate lamellae (AL) are cytoplasmic stacks of membranes containing structures identical to pores, typically found in rapidly dividing cells such as gametes and tumor cells (Kessel, 1992; Meier *et al.*, 1995). AL can be readily assembled in vitro in *Xenopus* egg extracts in the absence of added chromatin (Dabauvalle

et al., 1991; Meier *et al.*, 1995; Miller and Forbes, 2000). Immunoblots using the anti-ELYS antibody showed that ELYS biochemically purifies with reconstituted nuclei, but not with annulate lamellae pore complexes assembled in vitro (Figure 2.1C, compare lanes 1 and 2). This data further supports the model that ELYS targets pore assembly to occur on the chromatin periphery (Rasala *et al.*, 2006; Franz *et al.*, 2007), rather than functioning as a structural component of the pore.

The ELYS C-terminus contains both AT-hook and non-AT-hook chromatin-binding domains.

ELYS has a putative AT-hook DNA-binding motif (Kimura *et al.*, 2002) and is a chromatin-associated protein (Galy *et al.*, 2006; Franz *et al.*, 2007; Gillespie *et al.*, 2007). To better understand the interaction between ELYS and chromatin, we set out to specifically mutate the AT-hook motif in order to test whether it actually plays a role in the chromatin binding of ELYS. This, though possibly assumed from recent work, has never been tested. We expressed a recombinant GST-tagged fragment corresponding to the C-terminal 128 aa of *Xenopus* ELYS that contained the 8 amino acid AT-hook motif, KPRGRPPK (AT-hook+, Figure 2.2A). We also expressed an identical fragment, but one into which we had introduced two arginine (R)→alanine (A) point mutations in the AT-hook motif (AT-hook-2R→A, Figure 2.2A) to give KP**A**G**A**PPK. These arginine residues have been shown to be crucial for the

interaction between AT-hook motifs and DNA in AT-hook chromatin-binding proteins such as HMGA1/HMG-I(Y) and Taf1 (Huth *et al.*, 1997; Metcalf and Wassarman, 2006). To test the ability of the ELYS GST-AT-hook+ and GST-AT-hook-2R→A fragments to bind to chromatin, we added decreasing concentrations of the fragments to egg cytosol and incubated this for 20 minutes with 'anchored chromatin' on coverslips (i.e., coverslips containing individual decondensed *Xenopus* sperm chromatin packets) (Macaulay and Forbes, 1996). The chromatin-containing coverslips were washed three times with buffer containing 125 mM KCl and any chromatin-bound proteins were solubilized with SDS-containing sample buffer. Immunoblot analysis revealed that the ELYS GST-AT-hook+ fragment bound to chromatin (Figure 2.2B). Surprisingly, ELYS GST-AT-hook-2R→A bound to chromatin with only a slightly reduced affinity (Figure 2.2B). The data suggest that, while the AT-hook motif contributes to the fragment's chromatin-binding ability, there might exist an additional chromatin-binding domain in the C-terminus of xELYS.

To test for this, we expressed a smaller fragment of the ELYS C-terminus that lacks the AT-hook motif, corresponding to the last 51 aa, and asked whether it also bound to anchored chromatin (ΔAT-hook, Figure 2.2A). Interestingly, ELYS GST-ΔAT-hook was able to bind to chromatin, although with a ~2-3 times lower affinity compared to ELYS GST-AT-hook+ (Figure 2.2C). GST was used as a control and did not bind to anchored chromatin

(Figure 2.2C). These data indicate that the C-terminus of *Xenopus* ELYS contains at least two chromatin-binding domains.

The AT-hook motif itself is required for the dominant negative effect of the ELYS C-terminus on nuclear pore assembly.

The ELYS GST-tagged recombinant protein fragments AT-hook+, AT-hook-2R→A, and ΔAT-hook are all capable of chromatin binding, albeit with slightly varying affinities (Figure 2.2). We next tested the effect these distinct ELYS fragments had on endogenous ELYS binding to chromatin. The addition of 5 or 10 μM ELYS AT-hook+ to egg cytosol readily blocked endogenous full-length ELYS from binding to anchored chromatin (Figure 2.3A, lane 3 and 6, top strip). Higher concentrations (10 μM) of ELYS AT-hook-2R→A also blocked endogenous ELYS chromatin binding; however, in the presence of 5 μM AT-hook-2R→A, we observed considerable ELYS chromatin binding (Figure 2.3A, lanes 4 and 7, top strip). The ELYS ΔAT-hook fragment had no effect on endogenous ELYS chromatin binding at either concentration (Figure 2.3A, lanes 5 and 8, top strip). Thus, the ELYS fragment containing a functional AT-hook, AT-hook+, most efficiently outcompeted endogenous ELYS for chromatin binding. Addition of the ELYS AT-hook+ fragment also efficiently blocked the chromatin binding of the Nup107-160 complex (Figure 2.3A, lanes 3 and 6, second strip). This

inhibition reinforced the conclusion that the binding of the Nup107-160 complex to chromatin is dependent on ELYS chromatin binding.

To compare the effects of ELYS AT-hook+, AT-hook-2R→A, and ΔAT-hook on nuclear pore assembly, we reconstituted nuclei in vitro in the presence of the recombinant fragments and probed for nuclear pores using a directly labeled antibody to FG-nucleoporins (Alexa-568-mAb414). The addition of high concentrations (15 μM) of exogenous GST, ELYS GST-ΔAT-hook, or ELYS GST-AT-hook-2R→A to nuclear assembly reactions had no detrimental effects on pore assembly (Figure 2.3B, FG-Nups). The rims of the nuclei stained brightly with directly-labeled anti-FG Nup antibody, mAb414. Additionally, nuclear membrane recruitment and fusion was normal in these nuclei, as determined by a continuous and smooth nuclear rim stain when the membrane dye, DHCC, was used; although nuclear shape and size was altered with GST-AT-hook-2R→A (Figure 2.3B, DHCC). In contrast, the addition of an equivalent concentration of ELYS GST-AT-hook+ to nuclear assembly reactions severely inhibited nuclear pore assembly and led to the assembly of very small nuclei (Figure 2.3B, FG-Nups, second column). (We note that the size difference is likely an effect on chromatin condensation induced by AT-hook+ and AT-hook-2R→A, as these also condense pre-swollen chromatin when that is used for nuclear assembly reactions; data not shown). Clearly, ELYS GST-AT-hook+ had no effect on nuclear membrane fusion (Figure 2.3B, DHCC). This phenotype of membrane-enclosed, but pore

assembly-inhibited nuclei mimics the ELYS immunodepletion phenotype (Franz *et al.*, 2007). Importantly, only ELYS GST-AT-hook+ inhibited nuclear pore assembly (Figure 2.3B), indicating that the pore assembly assay is exquisitely sensitive to a change in the 8-amino acid AT-hook of ELYS.

Near the completion of this work, a study was published that showed that a somewhat longer C-terminal recombinant fragment of *Xenopus* ELYS, which the authors termed rATH, bound to chromatin, inhibited endogenous ELYS and members of the Nup107-160 complex from binding to chromatin, and blocked NPC assembly (Gillespie *et al.*, 2007). rATH (208 aa; aa 2200-2408) contains our smaller GST-AT-hook+ fragment of ELYS (128 aa; aa 2281-2408) and their data is consistent with our own AT-hook+ data. However, that study did not in any way demonstrate that the AT-hook motif itself was the operationally important component of the 208 aa rATH fragment. With our results above, we now show that, while all three of our ELYS fragments bind to chromatin, only the fragment that contains a functional AT-hook motif efficiently blocks endogenous ELYS from binding to chromatin and inhibits the assembly of nuclear pores. These data demonstrate, for the first time, the importance of the specific amino acids of the AT-hook motif in nuclear pore assembly itself.

During this experiment, we also observed that the addition of the inhibitory AT-hook+ fragment to the anchored chromatin assay also reduced the amount of chromatin-bound RCC1 (Figure 2.3A, lane 3), of potential

interest to nuclear pore assembly. RCC1 is the chromatin-bound RanGEF that converts RanGDP to RanGTP (Bischoff and Ponstingl, 1991) and helps to establish a Ran gradient around the chromatin periphery that is important for nuclear pore assembly (Hetzer *et al.*, 2000; Zhang and Clarke, 2000; Harel *et al.*, 2003a; Walther *et al.*, 2003b; Wozniak and Clarke, 2003; Clarke and Zhang, 2004). One worry was that addition of ELYS AT-hook+ (Figure 2.3B), if it sufficiently inhibited RCC1 chromatin binding, could result in a defect in the generation of RanGTP which in turn could cause the failure in NPC assembly, both in our studies and those of (Gillespie *et al.*, 2007). To address this concern, we assembled nuclei in the presence of ELYS GST-AT-hook+, with and without added exogenous non-hydrolysable RanQ69L-GTP. We found that the nuclear pore assembly defect induced by AT-hook+ was not reversed by the addition of excess RanQ69L-GTP; no pores were seen on the surface of chromatin (Figure 2.3C, right panel) (also see below). These results indicate that the ELYS AT-hook+-induced pore assembly defect does not result from a defect in RanGTP generation. Taken together, we conclude that the presence of a wild type AT-hook is essential for the dominant negative effect of the ELYS AT-hook+ fragment on nuclear pore assembly.

The dominant negative fragment of ELYS does not block the assembly of annulate lamellae.

While our data seemed to suggest that the GST-AT-hook+ fragment inhibits nuclear pore assembly specifically by blocking the interaction between ELYS and chromatin, it is possible that the ELYS fragment could additionally or alternatively act as a dominant negative by sequestering away nucleoporins, such as the Nup107-160 complex, or other pore assembly factors. Interestingly, we noticed that in the nuclear reconstitution reactions assembled in the presence of both AT-hook+ and RanQ69L-GTP (Figure 2.3C, right panel), large aggregates of FG-Nup staining structures were observed in the cytoplasm, characteristic of the in vitro formation of annulate lamellae in the presence of excess RanQ69L-GTP (Harel *et al.*, 2003a; Walther *et al.*, 2003b). This observation seemed to directly rule out the sequestration possibility, as the ELYS AT-hook+ inhibits pore assembly only in the nuclear envelope, but does not block AL pore assembly in the cytoplasm.

To more definitively show this, we asked whether AT-hook+ had an effect on annulate lamellae pore assembly using an immunoblot analysis. As described previously, if interphase egg extract is incubated in the absence of any source of chromatin or DNA, annulate lamellae containing cytoplasmic pores readily form in vitro, presumably because the extract is so poised for pore assembly (Dabauvalle *et al.*, 1991; Meier *et al.*, 1995; Miller and Forbes, 2000). If the ELYS AT-hook+ fragment indeed blocks nuclear pore assembly solely by disrupting an interaction between ELYS and chromatin, then it should not affect AL pore assembly, which occurs in the absence of chromatin. An

AL pore assembly assay was carried out in vitro by incubating egg cytosol with membranes for 2 hours in the normal assay, except that equimolar amounts of GST or ELYS GST-AT-hook+ were added. Annulate lamellae containing pore complexes that formed during this incubation were isolated away from any soluble unincorporated pore proteins by high speed centrifugation and analyzed by gel electrophoresis and immunoblotting (Meier *et al.*, 1995). Immunoblot analysis revealed that there was no difference in the amounts of the FG-nucleoporins, Nup358, Nup214, Nup153 and Nup62, assembled into AL pore complexes in the presence of GST-AT-hook+ compared to that with GST alone (Figure 2.3D, lanes 1 and 2). An assembly reaction in the presence of 2 mM GTPγS, which inhibits annulate lamellae formation (Meier *et al.*, 1995), is shown for comparison (Figure 2.3D, lane 3). The AT-hook containing fragment of ELYS that blocks nuclear pore assembly clearly did not block AL pore assembly. We conclude that ELYS AT-hook+ does not act to block nuclear pore assembly through disruption of required Ran or through sequestration of necessary nucleoporins or factors, but through its action at the surface of the chromatin to deny endogenous ELYS access.

The antibiotic Distamycin A, which binds AT-rich DNA, blocks nuclear pore assembly.

AT-hook motifs are known to bind specifically to the minor groove of DNA at AT-rich sequences, and are found in a subset of DNA/chromatin-

binding proteins, such as the non-histone chromosomal high mobility group HMG protein family (Reeves and Nissen, 1990; Aravind and Landsman, 1998; Reeves, 2001). The importance of the ELYS AT-hook motif demonstrated above using the 2R→A point mutation implies that AT-rich DNA may play a role in NPC assembly. To test this, we set out to assemble reconstituted nuclei in vitro making use of two antibiotics: 1) Distamycin A which binds DNA in the minor groove of AT-rich regions, and 2) Chromomycin A_3 which binds DNA in the minor groove of GC-rich regions. These two antibiotics have been used previously to define the binding specificities for certain DNA/chromatin-binding proteins, such as histone H1 (Kas *et al.*, 1989), topoisomerase II (Bell *et al.*, 1997), and the nuclear envelope protein, Lamin B (Rzepecki *et al.*, 1998). Histone H1 and topoisomerase II are prevented from DNA binding by Distamycin A in vitro, while in vivo Lamin B is prevented from chromatin binding by Chromomycin A_3 and, to a lesser extent, Distamycin A.

Strikingly, we found that the AT-rich DNA binding antibiotic Distamycin A (10 μM) severely inhibited nuclear pore assembly (Figure 2.4A, Distamycin, top panel). An equimolar amount of the GC-rich DNA binding antibiotic, Chromomycin A_3, showed little effect on pore assembly, although the nuclei were somewhat altered in shape (Figure 2.4A). However, at high concentrations (>50 μM), Chromomycin A_3 did cause nuclear pore assembly defects, possibly by global alteration of chromatin structure or composition such that ELYS was lost through a more non-specific process (data not

shown; see Figure 2.4B for reduction at 10 μM Chromomycin A_3). Of note, at all concentrations tested, neither antibiotic affected nuclear membrane recruitment, or the fusion that is required to form the double nuclear membranes (Figure 2.4A, DHCC).

To determine whether the Distamycin A block to NPC assembly was dependent on the presence of DNA, we asked whether annulate lamellae pore complexes could assemble in the presence of Distamycin A. Indeed, we found that Distamycin A had no effect on AL pore assembly, confirming that the Distamycin inhibition of nuclear pore assembly is due to a specific interaction between the antibiotic and chromatin (Figure 2.5).

The data above implied that the AT-binding antibiotic Distamycin A inhibits NPC assembly by blocking endogenous ELYS from capturing its DNA binding sites, since both Distamycin A and AT-hook motif proteins are known to bind to the minor groove of DNA in AT-rich regions. To test this, we assayed the earliest step in nuclear pore assembly, by performing an anchored chromatin assay in the presence of either Distamycin A or Chromomycin A_3. Immunoblot analysis of the chromatin-bound proteins revealed that Distamycin A addition did indeed dramatically reduce the amount of ELYS and the Nup107-160 complex bound to chromatin (Figure 2.4B, lane 3). Chromomycin A_3 affected ELYS and the Nup107-160 proteins to a much lesser extent (Figure 2.4B, lane 4), while specifically reducing Mcm3 chromatin

binding. Thus, our data indicate that NPC assembly preferentially occurs on AT-rich sites in chromatin.

ELYS, the Nup107-160 complex, and Nup153 are the only soluble pore subunits to bind chromatin in the absence of membranes.

Overall, our data together with others suggest that NPC assembly begins with the binding of ELYS, followed by the recruitment of the Nup107-160 complex to chromatin (Figures 2.3 and 2.4; Franz *et al.*, 2007; Gillespie *et al.*, 2007). The next step in NPC assembly has remained unknown. Thus, we set out to investigate what occurs following the binding of ELYS and the Nup107-160 complex to AT-rich chromatin. Nuclear pore complexes are built, as far as is known, from 14 soluble subunits (Figure 2.6A) and three integral membrane proteins. The assembly order or addition of a few of the pore subunits has only been roughly estimated with respect to certain early or late assembling proteins and membrane fusion (Chaudhary and Courvalin, 1993; Macaulay and Forbes, 1996; Bodoor *et al.*, 1999; Haraguchi *et al.*, 2000; Belgareh *et al.*, 2001; Daigle *et al.*, 2001; Harel *et al.*, 2003a; Walther *et al.*, 2003a; Rabut *et al.*, 2004; Antonin *et al.*, 2005; Franz *et al.*, 2005; Rasala *et al.*, 2006; Baur *et al.*, 2007; Franz *et al.*, 2007). We hypothesize that the step in NPC assembly which immediately follows the chromatin-binding of ELYS and the Nup107-160 complex is either: (1) the recruitment of additional soluble pore subunits to the chromatin/ELYS/Nup107-160 precursor in a membrane-

independent manner, or (2) the recruitment of one or more integral membrane pore protein(s) with an associated membrane vesicle or sheet. To address the first possibility, we asked whether additional soluble pore subunits bind to chromatin in the complete absence of membranes. Because only a fraction of the nucleoporins have been tested for their ability to bind chromatin (Walther *et al.*, 2003a; Walther *et al.*, 2003b; Baur *et al.*, 2007; Franz *et al.*, 2007; Gillespie *et al.*, 2007), we set out to perform a near comprehensive analysis. Previous chromatin-binding experiments were done by incubating chromatin and cytosol together in vitro at room temperature, followed by a fixation step, and then a purification step to remove any unbound soluble proteins from the chromatin-bound proteins. The chromatin-bound Nups in those experiments were identified by immunofluorescence (Walther *et al.*, 2003a; Walther *et al.*, 2003b; Franz *et al.*, 2007). We thought this type of analysis had two flaws that could potentially result in an increase in false positives: (1) performing the fixation step before the separation of unbound soluble proteins from chromatin-bound proteins could increase the number of false-positives, and (2) any membrane contamination that occurred could induce pore assembly in the membrane-containing region and give the appearance of a false positive association of nucleoporins with the chromatin (Baur *et al.*, 2007). We used a biochemical assay which offered several advantages over the previous method and immunofluorescence in general. By immunoblotting, one could probe for a large number of nucleoporins in a single experiment and,

additionally, monitor for any membrane contamination by performing immunoblots for ER and integral membrane pore proteins. To avoid false positives and determine nucleoporin-chromatin binding accurately, sperm chromatin was decondensed with crude nucleoplasmin and allowed to settle onto poly-L-lysine treated coverslips for two hours. The coverslips were washed and non-specific sites blocked with BSA. Membrane-free cytosol, designated such by the absence of the membrane proteins ribophorin and gp210 (Figure 2.6C), was prepared and incubated with chromatin-coated coverslips for 60 minutes, before being washed three times with buffer containing 125 mM KCl. We asked which nucleoporin subcomplexes bound to chromatin by immunoblot analysis, using a battery of antibodies designed to probe for at least one member of each of the 14 soluble pore subunits (Figure 2.6A), with the exception of Aladin and Nup214. As negative controls, chromatin-coated coverslips were incubated with buffer alone (lane 6, Figure 2.6B and C), and coverslips lacking chromatin were incubated with cytosol (lane 5). Additionally, as a positive control membranes and cytosol were added to the anchored chromatin to assemble nuclei with nuclear pores (lane 3). Importantly, we found that when chromatin-coated coverslips were incubated with cytosol, the only pore subunits that bound to chromatin were ELYS and the Nup107-160 complex (Figure 2.6B, lane 7; ELYS, Nup160, Nup133). Likewise, when membranes and cytosol were added to anchored chromatin in the presence of GTPγS, which blocks vesicle fusion (Macaulay

and Forbes, 1996), only ELYS and the Nup107-160 complex bound (Figure 2.6B, lane 4).

RanGTP has been shown to promote nuclear pore assembly and furthermore to induce interaction between at least two soluble pore subunits, the Nup107-160 complex and Nup153, presumably by removing the negative regulator importin β (Hetzer *et al.*, 2000; Zhang and Clarke, 2000; Harel *et al.*, 2003a; Walther *et al.*, 2003b; Wozniak and Clarke, 2003; Clarke and Zhang, 2004; Quimby *et al.*, 2005). RanGTP has also been shown by immunofluorescence to increase the levels of ELYS and the Nup107-160 complex on chromatin (Franz *et al.*, 2007), and to induce the chromatin-binding of Nup153 and Nup358 (Walther *et al.*, 2003b). However, a different study showed that the chromatin binding of Nup153 and Nup358 was dependent not only on the presence of membranes, but also on vesicle fusion (Baur *et al.*, 2007). We wished to analyze whether RanGTP induced the binding of additional pore subunits, other than ELYS and the Nup107-160 complex, to chromatin in our more sensitive biochemical assay. For this, we incubated RanQ69L-GTP with cytosol and chromatin-coated coverslips. Immunoblot analysis of the bound proteins revealed that RanGTP did *not* increase the amount of ELYS or the Nup107-160 complex that bound to chromatin (Figure 2.6B, lane 8). Furthermore, RanQ69L-GTP induced only the binding of Nup153 to chromatin (Figure 2.6B and C, lane 8), indicating that the other soluble nuclear pore subunits (Figure 2.6A-C) do not bind to

chromatin in the absence of membranes, under these experimental conditions, even if excess RanGTP is present. Together, the data suggest that the assembly of these pore subunits not only requires the presence of membranes, but requires membrane fusion to form nuclear membranes.

POM121 interacts with the Nup107-160 and Nup93-205 pore subcomplexes.

We next set out to seek the link between the chromatin-bound Nups and the integral membrane pore proteins. Nuclei assembled in Nup107-160 complex-depleted egg extracts are encompassed by double nuclear membranes, but contain no nuclear pores (Vasu *et al.*, 2001; Harel *et al.*, 2003b; Walther *et al.*, 2003a). Previously, we showed that immunofluorescence on the pore integral membrane proteins POM121 and gp210 gave only a faint diffuse staining on nuclei depleted of the Nup107-160 complex (Harel *et al.*, 2003b). This suggested that either the Nup107-160 complex is required for normal recruitment of these pore membrane proteins or, alternatively, it is required for oligomerization of the pore membrane proteins (Harel *et al.*, 2003b).

While both POM121 and gp210 have been implicated in NPC assembly, POM121 appears early in nuclear assembly, making its binding partners in the nuclear pore of particular interest (Gerace *et al.*, 1982; Chaudhary and Courvalin, 1993; Hallberg *et al.*, 1993; Bodoor *et al.*, 1999;

Drummond and Wilson, 2002; Antonin *et al.*, 2005). In one study, in vitro immunodepletion of POM121 from membrane vesicles caused a defect in nuclear membrane formation that did not occur if the Nup107-160 complex was simultaneously depleted (Antonin *et al.*, 2005). Most relevant to the present study, RNAi knockdown of POM121 has, in many but not all cases, shown POM121 to be required for nuclear pore formation (Antonin *et al.*, 2005; Mansfeld *et al.*, 2006; Funakoshi *et al.*, 2007).

The ~120 kDa POM121 protein in *Xenopus* and mammals is a single transmembrane protein with the vast majority of the POM121 protein extending outside the ER lumen (Figure 2.7A) (Hallberg *et al.*, 1993; Soderqvist and Hallberg, 1994). The C-terminal third of POM121 contains FG repeat motifs (Figure 2.7A), which are present in a number of Nups and in general bind to transport receptors such as importin β (Hallberg *et al.*, 1993). No homologues of POM121 exist in yeast to provide genetic clues as to its near neighbor partners within the vertebrate nuclear pore.

To search for the soluble nucleoporins that link to POM121, pulldowns from *Xenopus* interphase extracts were performed using a POM121 fragment presumed to be available for potential interaction within the scaffold of the nuclear pore, one lacking FG repeats (aa144-435) (Figure 2.7A), in order to avoid transport receptor binding. Proteins that bound to this POM121 fragment in pulldowns were probed by immunoblotting with individual anti-nucleoporin and control antisera (Figure 2.7B). Notably, many nucleoporins,

such as Nup358, Nup214, Nup155, Nup62, and Nup53, showed no affinity for this POM121 fragment, demonstrating that the POM121 beads were not non-specifically sticky and, more importantly, that these Nups do not bind to this region of POM121 (aa144-435) under the experimental conditions used (Figure 2.7B, lanes 3 and 5). Importin α and β bound to the POM121 beads, but were largely removed by RanQ69L-GTP (Figure 2.7B, compare lanes 3 and 5). The FG nucleoporin Nup153 bound to the POM121 beads, but was also removed by RanQ69L-GTP, suggesting the interaction is indirect, perhaps through the known binding of Nup153 to importin β (Shah and Forbes, 1998; Shah *et al.*, 1998; Ben-Efraim and Gerace, 2001; Walther *et al.*, 2003b).

Strikingly, the Nup107-160 complex showed strong interaction with POM121 (Figure 2.7B, lane 3; Nup160, Nup133, Nup85, Nup43, Nup37). Its binding to the POM121 beads was unaffected by RanQ69L-GTP (Figure 2.7B, lane 5), indicating that the interaction is not non-specifically mediated through importin α and β. A lesser amount of ELYS was observed to bind the POM121 beads and may associate through its known interaction with the Nup107-160 complex (data not shown). Nup93 and to a smaller extent Nup205, members of the Nup93-188-205 subcomplex, were also seen to bind to the POM121 beads (Figure 2.7B, lane 3 and 5). None of the nucleoporins or importins bound to the negative control GFP (Figure 2.7B, lane 2 and 4). The Nup107-160 subcomplex and the Nup93-188-205 subcomplex are two

key subunits of the nuclear pore's central scaffold (Krull *et al.*, 2004). However, these two soluble pore subunits do not strongly interact with one another in immunoprecipitation experiments from *Xenopus* egg extract, even in the presence of RanGTP (data not shown). More importantly, we had shown above that the Nup93-188-205 subcomplex, as probed with anti-Nup93 antibody, does not bind to the Nup107-160 complex on anchored chromatin in the absence of membranes (Figure 2.6B). These data thus suggest that both the Nup107-160 and the Nup93 complexes bind to POM121 aa144-435 independently. The very strong and specific interaction of the Nup107-160 complex with POM121 implies that POM121 could be the next step in pore assembly after chromatin recruitment of ELYS and the Nup107-160 complex.

ELYS and the Nup107-160 complex recruit POM121- and NDC1-containing membrane vesicles.

We wished to determine whether the recruitment of POM121-containing membrane vesicles is dependent on chromatin-bound ELYS/Nup107-160 or is found in nuclear membranes independent of ELYS. To test this, we employed the tools we developed above to produce ELYS-minus nuclei. We assembled nuclei in the presence or absence of ELYS GST-AT-hook+ or in the presence or absence of Distamycin A and assayed for POM121. In nuclei assembled in the presence of 15 μM GST or ELYS GST-AT-hook 2R→A, immunofluorescence revealed that anti-POM121 antibodies stained the

nuclear rim in a normal punctate manner (Figure 2.8A). However, when nuclei were assembled in the presence of 15 μM GST-AT-hook+, no POM121 stain was observed (Figure 2.8A, middle panel). Thus, chromatin-bound ELYS/Nup107-160 complex is required either for the recruitment of POM121-containing membrane vesicles to the nucleus, or for the clustering of POM121 into early NPC structures within the fused nuclear membranes that can be visualized by immunofluorescence.

We next found that POM121 antibodies did not stain nuclei assembled in the presence of 10 μM Distamycin A. Thus, like the GST-AT-hook+, Distamycin A also prevents the recruitment of POM121-containing membrane vesicles, or the assembly of POM121 into visible protein oligomers.

A recent study showed that POM121 and NDC1 are co-enriched in the same membrane vesicles in *Xenopus* egg extracts, but are separate from the membrane vesicles containing gp210 (Antonin *et al.*, 2005; Mansfeld *et al.*, 2006). NDC1 in the only conserved integral membrane pore protein in both yeast and higher eukaryotes and has been shown to be essential for nuclear pore assembly (Chial *et al.*, 1998; West *et al.*, 1998; Lau *et al.*, 2004; Lau *et al.*, 2006; Madrid *et al.*, 2006; Mansfeld *et al.*, 2006; Stavru *et al.*, 2006). To determine whether the recruitment of NDC1 was dependent on chromatin-bound ELYS and the Nup107-160 complex, anchored nuclei were prepared, processed, and tested for protein content by immunoblotting (Macaulay and Forbes, 1996). This technique has the advantage of allowing one to

distinguish between the presence of a membrane protein in nuclei and the oligomerization of the protein. The anchored nuclei were assembled in the presence of GST, ELYS GST-AT-hook+ or GST-ΔAT-hook and assayed for the presence of NDC1 in the nuclei by immunoblot analysis (Figure 2.8C). We also probed the nuclei for the presence of the integral membrane pore protein, gp210 (Figure 2.8C).

We found that nuclei assembled in the presence of GST and ELYS ΔAT-hook contained all nucleoporins tested, including ELYS, Nup160, Nup133, Nup93, and the pore integral membrane proteins gp210 and NDC1 (Figure 2.8C, lanes 1 and 3). This normal phenotype agreed with that observed by immunofluorescence previously (Figure 2.3B). Anchored nuclei assembled in the presence of AT-hook+, however, lacked ELYS, Nup160, Nup133, and Nup93 (Figure 2.8C, lane 2). Interestingly, the anchored nuclei assembled in the presence of the ELYS AT-hook+ fragment contained gp210 in their nuclear membranes, but did not contain NDC1 (Figure 2.8C, lane 2). The integral membrane ER protein ribophorin, which is not associated with nuclear pore complexes, but is present in the nuclear membranes of *Xenopus* reconstituted nuclei (Drummond *et al.*, 1999), was also unaffected (Figure 2.8C, compare lanes 1-3). We thus conclude that the recruitment of POM121/NDC1-containing membrane vesicles to nuclei requires that ELYS and the Nup107-160 complex be present on the chromatin, but the recruitment of gp210-containing vesicles does not.

Discussion

The chromatin-binding protein ELYS targets nuclear pore assembly to the surface of chromosomes as nuclei form at the end of mitosis. In this study we have sought the molecular underpinnings of the action of ELYS in the early steps of nuclear pore assembly.

A model for the early steps in nuclear pore assembly.

The data support a model for the early steps in pore assembly where the binding of ELYS to AT-rich chromatin via the conserved AT-hook motif, together with a second non-AT-hook domain, marks the sites of nuclear pore assembly (Figure 2.9). ELYS binding to AT-rich DNA tracts "seeds" the chromatin with pore initiation sites. This achieves directionality for the membrane components that will come in next and also spatial localization to the correct area. This directionality fits the RanGTP gradient model for the regulation of nuclear envelope assembly (Hetzer *et al.*, 2002; Ryan *et al.*, 2003; Wozniak and Clarke, 2003; Clarke and Zhang, 2004; Harel and Forbes, 2004; Quimby *et al.*, 2005; Kalab *et al.*, 2006), but does not itself depend on Ran. None of this is needed for annulate lamellae formation.

Chromatin-bound ELYS targets the Nup107-160 complex to pore initiation sites (Franz *et al.*, 2007; Gillespie *et al.*, 2007). The recruitment of pore membrane components NDC1 and POM121 then occurs via an interaction between the Nup107-160 complex and the cytoplasmic domain of

POM121 (Figure 2.9). In the nuclear reconstitution system, this involves the recruitment of a specific pool of vesicles. In vivo, there would be extensive sheets or flattened cisternae of membranes present, with the inner nuclear membrane proteins associating with chromatin directly, or through lamins, lamin-binding proteins (Lopez-Soler *et al.*, 2001; Shumaker *et al.*, 2005; Ulbert *et al.*, 2006). The "bifunctional linker" Nup107-160 complex would attract POM121/NDC1 and place at least one copy of the pore-membrane proteins directly above the seeding point on chromatin. POM121 has previously been observed in vivo as an early assembling nucleoporin, appearing on chromosomes at the beginning of telophase; gp210 assembles late in telophase at the pore (Gerace *et al.*, 1982; Chaudhary and Courvalin, 1993; Bodoor *et al.*, 1999; Antonin *et al.*, 2005). Furthermore, POM121 and NDC1 are known to be co-enriched in the same membrane vesicles in *Xenopus* egg extracts, while gp210 is contained in separate vesicles (Antonin *et al.*, 2005; Mansfeld *et al.*, 2006).

Previous studies have identified a connection between the Nup107-160 complex, or its yeast homologue the Nup84 complex (Heath *et al.*, 1995; Li *et al.*, 1995), and membranes. Protein structure modeling revealed that the molecular architecture of the yeast Nup84 complex was similar to that of the vesicular-transport complexes COPI, COPII, and clathrin (Devos *et al.*, 2004). Sec13 is both a member of the Nup107-160 complex and of COPII vesicle-transport complexes (Siniossoglou *et al.*, 1996; Fontoura *et al.*, 1999; Harel *et*

al., 2003b; Bickford *et al.*, 2004; Loiodice *et al.*, 2004). Nup133 of the Nup107-160 complex was shown to contain a membrane-curvature-sensing ALPS-like motif with the ability to bind to small liposomes (Drin *et al.*, 2007). Finally, two recent models of the structure of the yeast NPC both place the Nup84 complex adjacent to the nuclear membranes (Alber *et al.*, 2007; Hsia *et al.*, 2007).

Data derived from our analysis of the chromatin-binding ability of the other soluble nucleoporins (Figure 2.6) argues that there would be no other obligatory components in the chromatin/ELYS/Nup107-160 complex/POM121 connection. The other soluble pore components therefore come in later in the assembly process. In vitro, their assembly is dependent on membrane vesicle fusion. Nup153 remains controversial in its potential role: it associates with chromatin in the presence of excess RanGTP (Walther *et al.*, 2003b), it has been seen early at the assembling pore (Bodoor *et al.*, 1999), however, depletion of Nup153 leads to the formation of functional pores lacking only the nuclear pore basket (Walther *et al.*, 2001; Hase and Cordes, 2003). Lastly, a recent study demonstrated that Nup153 and the other FG-nucleoporins Nup358, Nup214 and Nup62 do not associate with the nuclear periphery when nuclear membrane fusion is inhibited (Baur *et al.*, 2007). Thus, we believe that, under physiological conditions, large amounts of Nup153 would not be present early on. Together, the data imply that the assembly of the bulk of the

soluble pore subunits requires the presence of membranes and the fusion of the membrane vesicles (Figure 2.9).

Yeast lack a direct ELYS homologue.

The yeast *S. cerevisiae* and *S. pombe* lack a canonical ELYS homologue, although a small gene in *S. pombe* of 295 aa (gi:4007794) bears considerable homology to aa 694-972 in the central region of the 2266 amino acid human ELYS. No *S. cerevisiae* homologue to this small gene is readily apparent. Lacking the majority of ELYS structure, non-metazoans such as yeast may require a different initiation device for pore assembly in their intact nuclei. Considering that yeast do not undergo open mitosis and thus do not disassemble their NPCs, it is possible that a protein of ELYS' function is not required. However, a prediction from the metazoan precedent described here would be that any mechanism that acted to anchor the yeast Nup84 complex, which is the Nup107-160 complex homologue in yeast, to chromatin would be sufficient to initiate new pore assembly.

ELYS binds AT-rich chromatin through its AT-hook motif.

Interestingly, two *Xenopus* ELYS sequences have been published, one of 2201 amino acids (Galy *et al.*, 2006) and one of 2408 amino acids (Gillespie *et al.*, 2007). Ours is the longer one and identical to that used in the rATH study (Gillespie *et al.*, 2007). This sequence contains an extra 7 x ~31 aa

repeat upstream of the AT-hook which consists of both canonical AT-hook-like sequences and closely related sequences. *Xenopus* with its rapid cell division in early development, with cell division taking place every 30 minutes for the first 12 divisions (Newport and Kirschner, 1982), may potentially use these excess AT-hook-like sequences on ELYS to accomplish rapid nuclear pore assembly.

In our study, we demonstrate the importance of the primary ELYS AT-hook by showing that point mutations within the motif abolish the ability of the dominant negative to block NPC assembly (Figure 2.3). AT-hook motifs bind to the minor groove of DNA at AT-rich sequences (Reeves, 2001). Indeed, using the AT-binding antibiotic Distamycin A, we demonstrate that ELYS preferentially binds to AT-rich chromatin, and, likewise, NPC assembly is preferentially initiated from AT-rich chromatin (Figure 2.4).

The HMGA family of proteins is the best studied of the AT-hook-containing proteins. The HMGA family functions in a variety of nuclear processes, including gene transcription, DNA repair, and chromatin remodeling (Goodwin, 1998; Anand and Chada, 2000). While first described to bind DNA at any run of 5 to 6 AT base pairs, interestingly, more recent studies on the HMGA family of AT-hook proteins show that these proteins likely bind to DNA with sequence specificity. HMGA, which contains three AT-hook motifs, was shown to bind with higher affinity to two or three appropriately spaced AT tracts as opposed to a single AT tract (Maher and

Nathans, 1996). An NMR study of the HMGA1 AT-hook complexed to 5'-AAATT-3' reveled that the hook only bound in one orientation, with the N-terminal arginine of the RGR hook tripeptide located near the 5' end of the oligonucleotide (Huth *et al.*, 1997). Importantly, in a recent study using in vitro systematic evolution of ligands by exponential enrichment (SELEX) technology, the authors were able to identify a 15 bp consensus site for HMGA2 in which the first five base pairs are AT-rich, the middle four or five base pairs are GC-rich, and the last five or six base pairs are AT-rich (Cui and Leng, 2007). Together, these data suggest that the AT-hook containing HMGA proteins do not randomly bind to all AT-rich chromatin, but do so in a more sequence-specific manner. It would be intriguing to determine if ELYS, likewise, binds to chromatin in a restricted, sequence-specific manner.

AT-rich DNA is often found in gene-poor regions within the genome, while gene-rich regions generally have a high GC base composition (Bernardi *et al.*, 1985; Saccone *et al.*, 1993). There is also a large body of evidence which indicate that gene-poor/AT-rich regions of the genome are positioned at the nuclear periphery and gene-rich/GC-rich regions are positioned in the nuclear interior (Croft *et al.*, 1999; Saccone *et al.*, 2002; Zink *et al.*, 2004; Foster and Bridger, 2005). Thus, it is possible that the AT chromatin-binding of ELYS is at some level restricted to gene-poor regions and might aid in their localization to the nuclear periphery. Interestingly, a subset of genes act differently and instead move to the nuclear periphery upon transcriptional

activation in yeast, doing so through interaction with nuclear pore proteins (Casolari *et al.*, 2005; Cabal *et al.*, 2006). Recent work has now identified a subset of vertebrate genes that act similarly in that they move to the nuclear pore upon transcriptional activation (Brown *et al.*, in press). Moreover, certain nucleoporins change location upon transcription inhibition (Griffis *et al.*, 2002; Griffis *et al.*, 2004). In vertebrates, it would be intriguing to speculate whether ELYS might play a role at the pore in transcriptional activation of AT-rich promoters. Indeed, fragments of mammalian ELYS, when transfected, have been shown to activate the transcription of a luciferase reporter gene, leading to the initial proposal of ELYS as a transcription factor (Kimura *et al.*, 2002).

Nuclear pore assembly in S-phase.

Overall, the pore assembly mechanism proposed here would require only a small amount of alteration to function in the intact nucleus of an S phase cell, a time when pore number doubles. Import of ELYS and the Nup107-160 complex into the nucleus with sequential binding to chromatin would again be presumed to form a platform on AT-rich sites, where again POM121, moving laterally through the inner nuclear membrane, could anchor and initiate pore assembly. Indeed, both nuclear-cytoplasmic transport and a nuclear pool of the Nup107-160 complex have been shown to be required for pore insertion into intact nuclei (Walther *et al.*, 2003a; D'Angelo *et al.*, 2006).

One interpretation of our data is that there might be specific sites in the genome capable of initiating nuclear pore assembly. If true, this would have intriguing implications for the regulation of S-phase nuclear pore assembly. If NPC assembly were initiated from a limited number of chromatin sites, then the number and occupancy of these sites could control both the timing of NPC assembly and the number of pores assembled. For example, in S phase the pore initiation sites would double as the DNA is replicated, which would control the doubling in pore number previously described (Maul *et al.*, 1972). In order for this to occur, however, an intranuclear pool of soluble ELYS/MEL-28 must exist. Indeed, such a pool has already been described, both in HeLa cells (Rasala *et al.*, 2006) and in C elegans (Galy *et al.*, 2006). Intriguingly, Galy et al (2006) showed by FLIP that two pools of GFP-MEL-28 exist in C. elegans: one very stable pool associated with NPCs and a more mobile nucleoplasmic pool. This intriguing possibility awaits a more precise definition of what constitutes an ELYS-binding site on chromatin.

In a recent study of ELYS, chromatin immunoprecipitation data using an Mcm3 antibody led Gillespie et al (2007) to conclude that ELYS and the replication licensing complex, Mcm2-7, are in proximity on chromatin fragments, although the actual size of the average chromatin fragment in that study was not stated (Gillespie *et al.*, 2007). Using geminin, a protein which blocks Mcm2-7 loading onto chromatin, the authors saw delayed ELYS and nucleoporin incorporation into reconstituted nuclei. The authors proposed that

the presence of the Mcm2-7 complex promotes the affinity of ELYS for chromatin. In the present study, we found that the chromatin binding of Mcm3, as a representative member of the Mcm2-7 complex, was more sensitive to the GC-binding Chromomycin A_3, than the AT-binding Distamycin A (Figure 2.4B), and that this situation was the opposite to that seen for ELYS. We believe that further investigation is required to clearly define the potential relationship between replication licensing and nuclear pore assembly.

Taken together, our data indicate that the critical chromatin-membrane connection for pore assembly is the ELYS-Nup107-160-POM121 chain, which effectively marks the sites where pore assembly will initiate. The recruitment of the remaining soluble pore subunits follows and depends on membrane vesicle fusion.

Figures

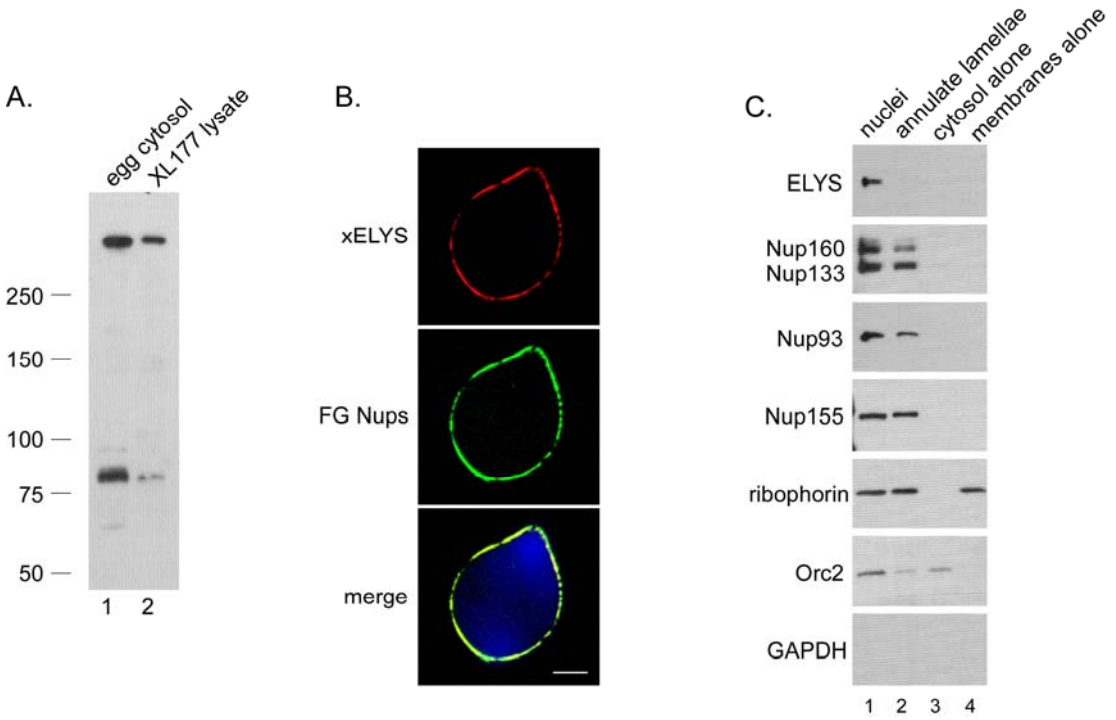

Figure 2.1. ELYS is abundant in nuclear pores, but not in annulate lamellae pores.
(A) Anti-*Xenopus* ELYS antibody recognizes two bands in *Xenopus* egg cytosol (lane 1) and XL177 *Xenopus* cell lysates (lane 2), one at the expected size of ~270 kDa, and one at ~80 kDa.
(B) *Xenopus* reconstituted nuclei were stained with directly-labeled anti-xELYS-AF568 (red), and mAb414-AF488 (FG-Nups, green). A merge shows the two stainings overlap at the nuclear rim. The DNA is stained with DAPI. Scale bar, 5 μm.
(C) Nuclear pores were assembled in the presence of *Xenopus* egg membranes, cytosol, and sperm chromatin (nuclei, lane 1). Annulate lamellae pores were assembled in the presence of only *Xenopus* egg membranes and cytosol (annulate lamellae, lane 2). Reactions assembled with cytosol only (lane 3) or membranes only (lane 4) were used as controls. All reactions were spun through a 30% sucrose cushion, with the heavy fractions, including the nuclei (lane 1), annulate lamellae (lane 2), membrane vesicles (lane 3) pelleting, while the soluble proteins (lane 4) remained in the supernatant. The pellets were solubilized with SDS-containing sample buffer and the presence of ELYS was determined by immunoblot. ELYS was enriched in the nuclear pore assembly reaction, while the rest of the soluble Nups (Nup160, Nup133, Nup93, and Nup155) purified with both nuclear and AL pores. Orc2, a nuclear protein not associated with pores, is enriched in the purified nuclei (lane 1). GAPDH, a cytosolic protein not associated with pores, is absent.

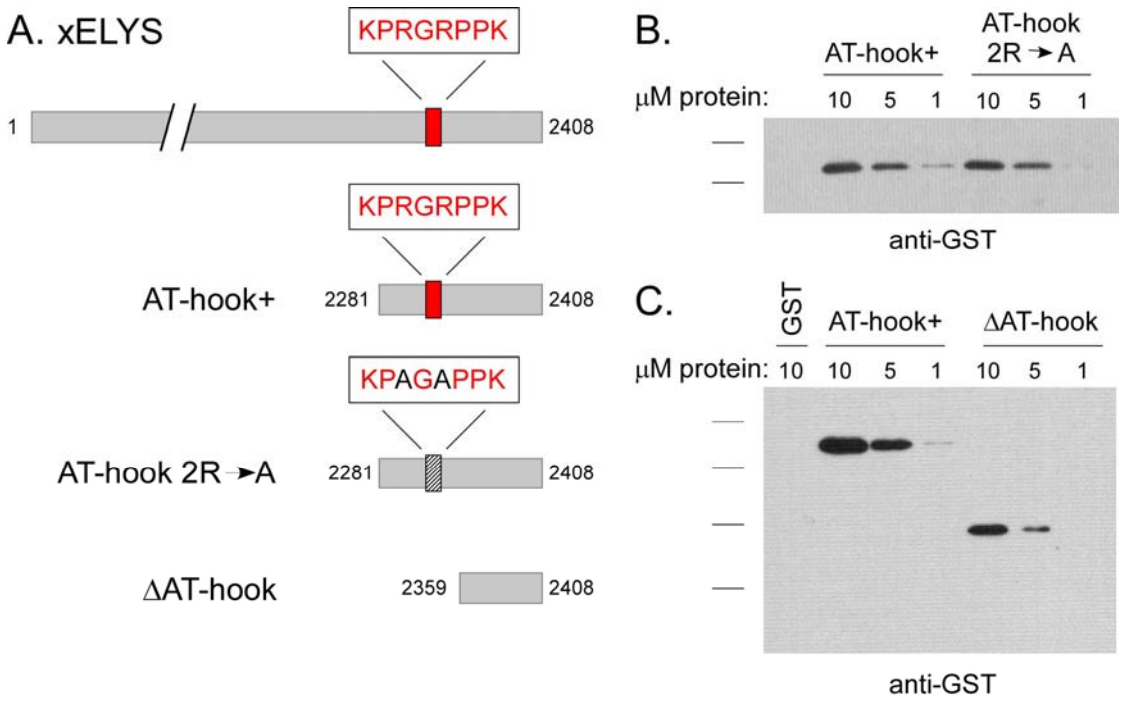

Figure 2.2. The ELYS C-terminus contains at least two chromatin-binding domains.
(A) Cartoons representing the xELYS C-terminal fragments used in this study. The red box represents the AT-hook motif; the black and white striped box represents the arginine (R) to alanine (A) AT-hook motif double point mutant.
(B) and (C) Anchored chromatin binding assays in which chromatin coated coverslips were incubated with *Xenopus* egg cytosol plus the indicated amounts of (B) GST-AT-hook+, GST-AT-hook 2R→A, or (C) GST, GST-AT-hook+, GST-ΔAT-hook. Immunoblots were probed with anti-GST antibody. GST-AT-hook+, GST-AT-hook 2R→A, and GST-ΔAT-hook all bound to the anchored chromatin with varying affinities, while GST did not. Dashes represent molecular weight markers (B) 55 and 40 kDa; and (C) 55, 40, 33 and 24 kDa.

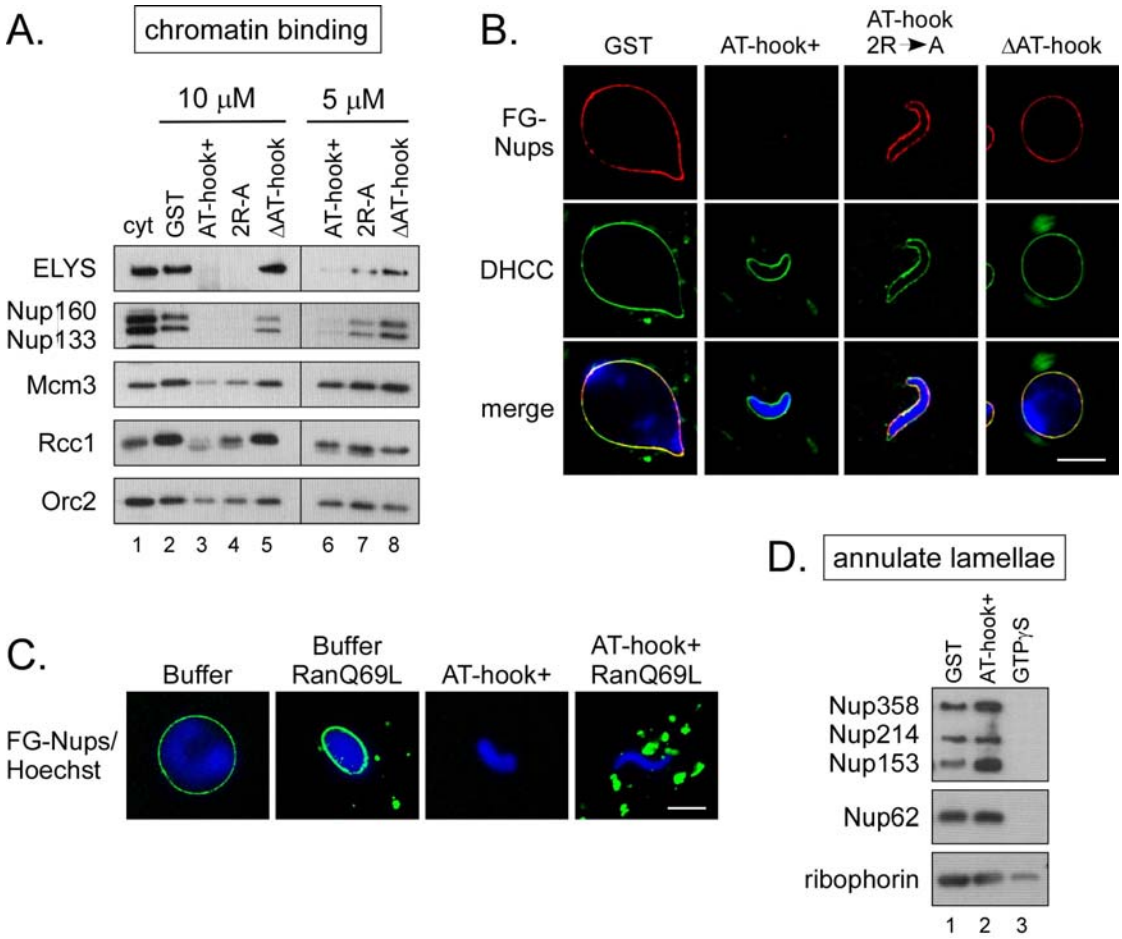

Figure 2.3. The AT-hook motif itself is required for the dominant negative effect of ELYS' C-terminus on nuclear pore assembly.

(A) Anchored chromatin binding assay in which chromatin coated coverslips were incubated with *Xenopus* egg cytosol plus 10 μM GST, or 5 or 10 μM GST-AT-hook+, GST-AT-hook 2R→A, or GST-ΔAT-hook. Immunoblot analysis revealed the relative amounts of chromatin binding for endogenous ELYS, Nup107-160 complex members Nup160 and Nup133, Mcm2-7 complex member Mcm3, and the RanGEF, RCC1. In this experiment, Orc2 served as a loading control. 'Cyt', *Xenopus* egg cytosol diluted 1:10, is shown for comparison (lane 1).

(B) Reconstituted nuclei were assembled in the presence of 15 μM GST, GST-AT-hook+, GST-AT-hook 2R→A, or GST-ΔAT-hook for 1 hour. The presence of mature nuclear pores was visualized by staining for the FG-Nups using directly labeled mAb414-AF568 (red). Membrane fusion was determined by continuous DHCC stain of the nuclear membranes (green). DNA was visualized with DAPI (blue, merge). Scale bar, 10 μm.

(C) Reconstituted nuclei were assembled in the presence of buffer or GST-AT-hook+; either in the presence or absence of 30 μM RanQ69L-GTP. The FG-Nups, representing mature nuclear pores, were stained with directly labeled mAb414-AF488 (green) and then fixed with 2% formaldehyde before being visualized by fluorescent microscopy. DNA was stained with Hoechst (blue). Scale bar, 10 μm.

(D) Annulate lamellae (AL) were assembled by combining purified *Xenopus* cytosol with membranes in the presence of either 20 μM GST (lane 1) or GST-AT-hook+ (lane 2) for 2 hours. The addition of 2 mM GTPγS to reactions containing membranes and cytosol inhibits AL assembly and is shown for comparison (lane 3). All membranes, including membrane-associated proteins, were purified by high-speed centrifugation through a 30% sucrose cushion and solubilized by SDS-containing sample buffer. Immunoblot analysis revealed that equal amounts of the soluble FG-nucleoporins, Nup358, Nup214, Nup153 and Nup62 assembled into AL supplemented with excess GST or GST-AT-hook+. Integral membrane protein ribophorin served as a loading control.

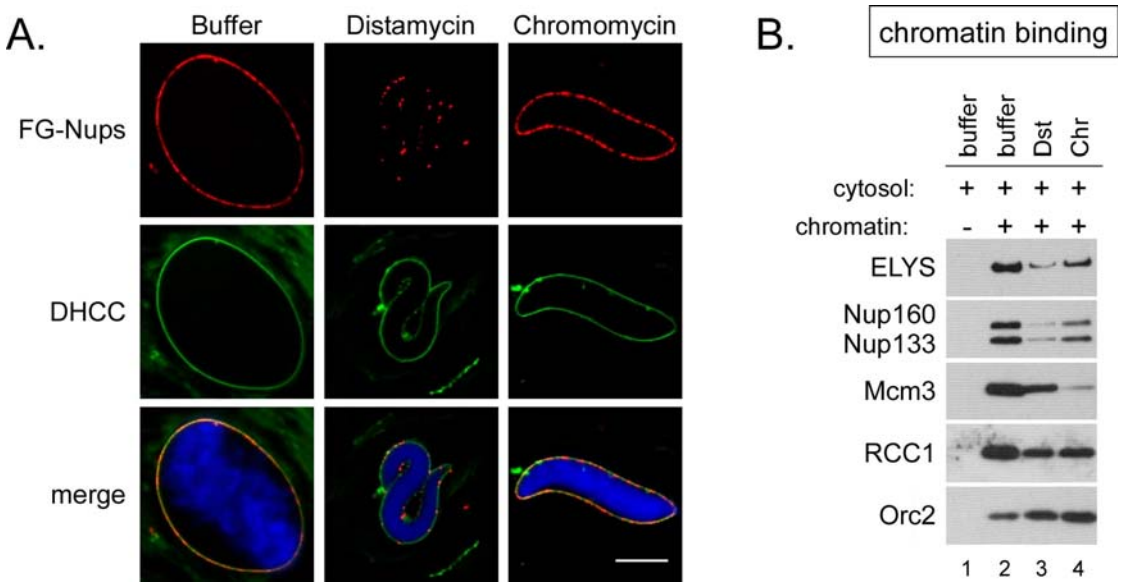

Figure 2.4. The antibiotic Distamycin A inhibits nuclear pore assembly.
(A) Reconstituted nuclei were assembled in the presence of buffer, 10 μM Distamycin A (AT-binder), or 10 μM Chromomycin A_3 (GC-binder). Nuclear pores were stained with directly labeled mAb414-AF568 (FG-Nups, red). Membrane fusion was determined by continuous DHCC stain of the nuclear membranes (green). DNA was stained with DAPI (blue, merge). Approximately 80% of the nuclei assembled in the presence of 10 μM Distamycin contained little to no visible nuclear pore staining, while the majority of the nuclei assembled in the presence of buffer or 10 μM Chromomycin displayed normal nuclear pore staining. Scale bar, 5 μm.
(B) Anchored chromatin binding assay in which chromatin coated coverslips were incubated with *Xenopus* egg cytosol plus buffer (lane 2), 10 μM Distamycin A (lane 3), or 10 μM Chromomycin A_3 (lane 4). Immunoblot analysis revealed the effect of each antibiotic on the relative amounts of chromatin binding for endogenous ELYS, Nup107-160 complex members Nup160 and Nup133, Mcm2-7 complex member Mcm3, and the RanGEF, RCC1. Chromatin was not added to the reaction in lane 1 to control for non-specific binding to the BSA-treated coverslips. In this experiment, Orc2 serves as a loading control.

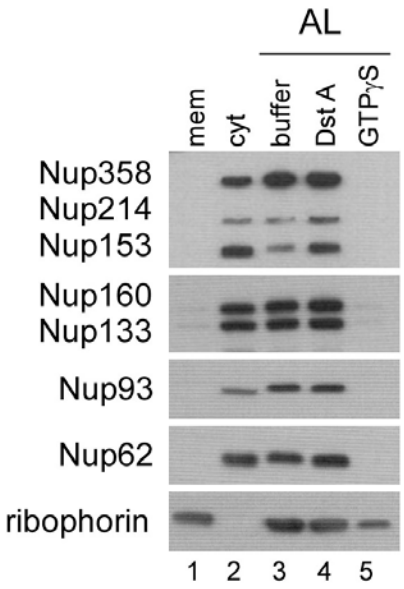

Figure 2.5. Distamycin A does not disrupt annulate lamellae pore assembly.
Annulate lamellae were assembled in vitro by incubating *Xenopus* egg membranes with cytosol, either in the presence of buffer or 10 μM Distamycin A (Dst A) (lanes 3 and 4). The purified membrane fractions were probed by immunoblotting. A reaction assembled in the presence of 2 mM GTPγS, which blocks membrane fusion and inhibits AL assembly (Meier *et al.*, 1995), was used as a negative control (lane 5). Distamycin A did not affect the assembly of soluble pore proteins Nup160, Nup133, Nup93 or Nup62 into AL. 'Mem', *Xenopus* egg membrane fraction diluted 1:20, and 'cyt', *Xenopus* egg cytosol diluted 1:10, are shown for comparison (lanes 1 and 2). Ribophorin was used as a loading control.

Figure 2.6. Only ELYS and the Nup107-160 pore subunits bind to chromatin in the absence of membranes and RanQ69L-GTP.
(A) A cartoon representing the known soluble nucleoporin subunits is shown (boxed), except for Aladin (for which we had no anti-*Xenopus* antisera). Nucleoporins highlighted in red were assayed for their ability to bind to anchored chromatin by immunoblotting.
(B-C) Anchored chromatin binding assay in which chromatin coated coverslips were incubated with *Xenopus* egg cytosol plus membranes to assemble nuclei (lane 3); egg cytosol plus membranes plus 2 mM GTPγS to block membrane vesicle fusion (lane 4); buffer alone (lane 6), membrane-free *Xenopus* egg cytosol (lane 7, arrowhead), or the identical cytosol plus 30 μM RanQ69L-GTP (lane 8). A coverslip not treated with chromatin and incubated with cytosol (lane 5) was used as a control for non-specific protein binding. In this experiment, Orc2 serves as a loading control. 'Mem,' *Xenopus* egg membrane fraction diluted 1:20, and 'cyt', *Xenopus* egg cytosol diluted 1:10, are shown for comparison (lanes 1 and 2). It should be noted that we did not detect chromatin-binding of Nup358 in the presence of excess RanGTP, as was previously published (Walther et al., 2003b).
(C) Immunoblots using antibodies to the integral membrane proteins gp210 and ribophorin show that membrane vesicles are not present in the *Xenopus* egg cytosol (lanes 2, 5-8).

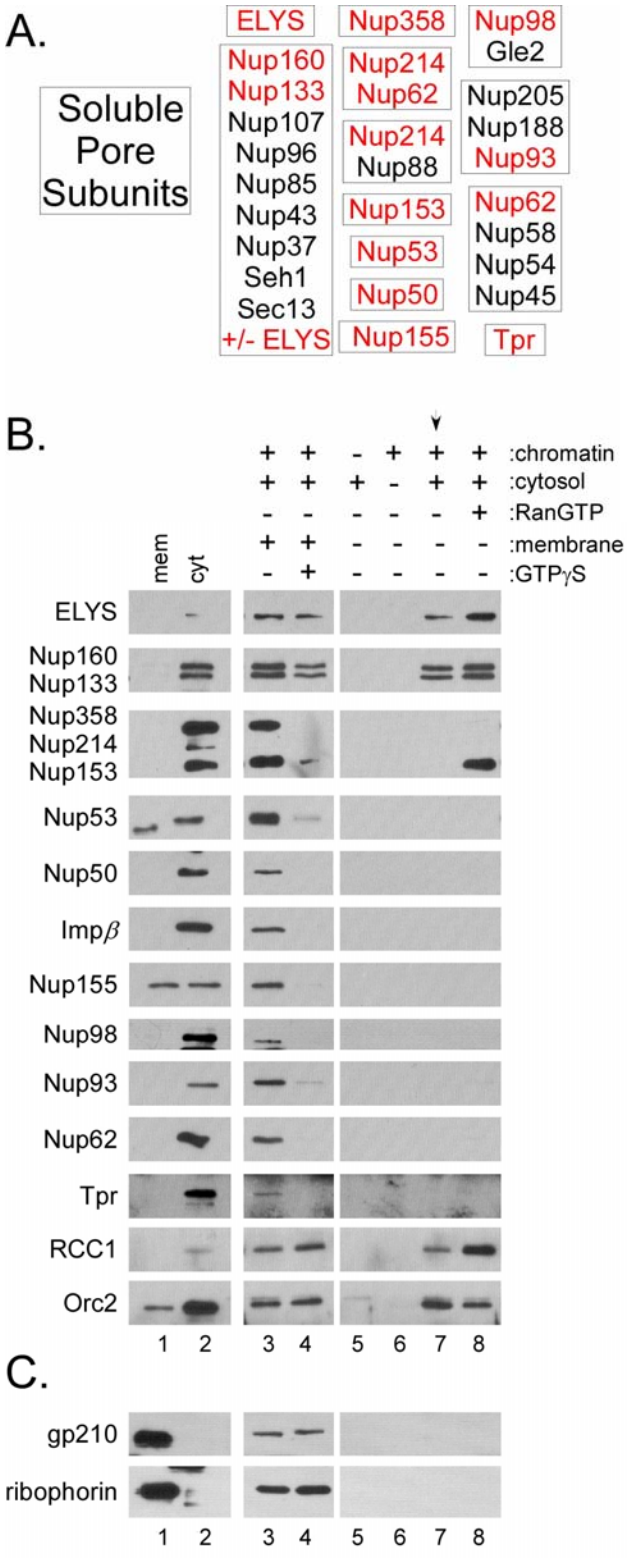
A.
Soluble Pore Subunits
ELYS
Nup160
Nup133
Nup107
Nup96
Nup85
Nup43
Nup37
Seh1
Sec13
+/- ELYS
Nup358
Nup214
Nup62
Nup214
Nup88
Nup153
Nup53
Nup50
Nup155
Nup98
Gle2
Nup205
Nup188
Nup93
Nup62
Nup58
Nup54
Nup45
Tpr
B.
:chromatin
:cytosol
:RanGTP
:membrane
:GTPγS
mem
cyt
ELYS
Nup160
Nup133
Nup358
Nup214
Nup153
Nup53
Nup50
Impβ
Nup155
Nup98
Nup93
Nup62
Tpr
RCC1
Orc2
1 2 3 4 5 6 7 8
C.
gp210
ribophorin
1 2 3 4 5 6 7 8

Figure 2.7. POM121 binds the Nup107-160 and the Nup93-205 complexes.
(A) A map of POM121 and the fragment used.
(B) The *Xenopus* POM121 fragment aa 144-435 (POM) was coupled to beads and mixed with *Xenopus* egg cytosol in pulldown reactions, in the presence or the absence of 10 μM RanQ69L-GTP. GFP-protein beads were used as a control. The bound proteins were probed by immunoblotting with different anti-nucleoporin and import factor antibodies, as shown in the figure. Nup160, Nup133, Nup85, Nup43, and Nup37 of the Nup107-160 complex, and Nup93 and Nup205 of the Nup93-205 complex specifically bound to the POM121 fragment. 'Cyt', *Xenopus* egg cytosol diluted 1:10, is shown for comparison (lane 1).

A. xenopus POM121

B.

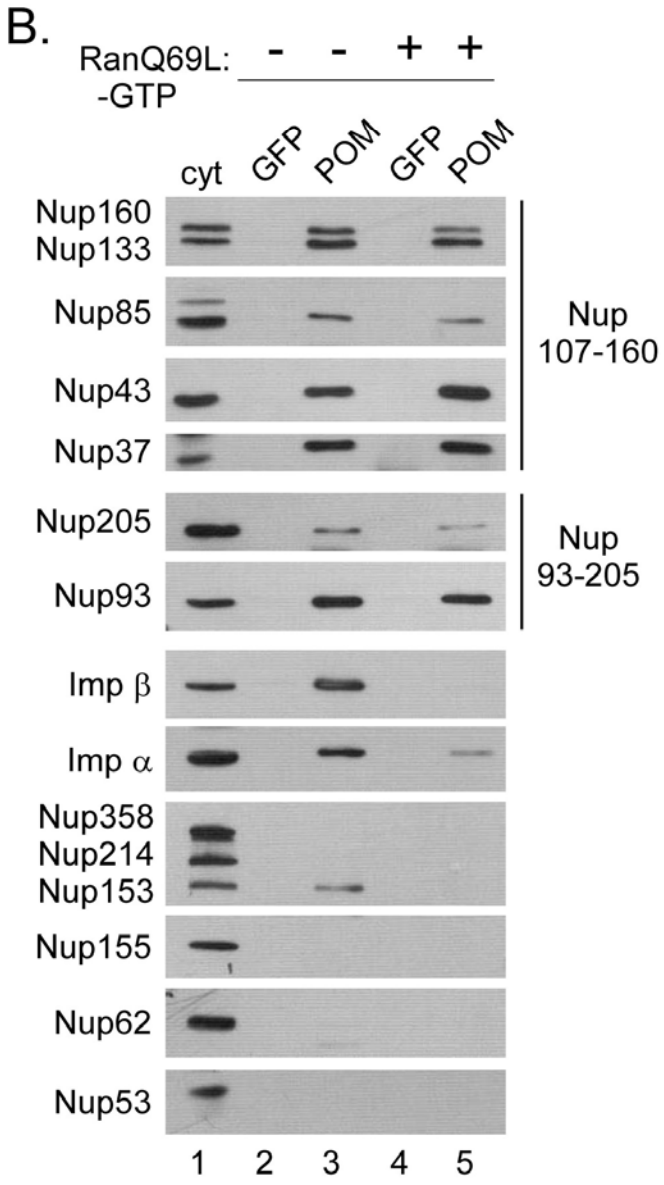

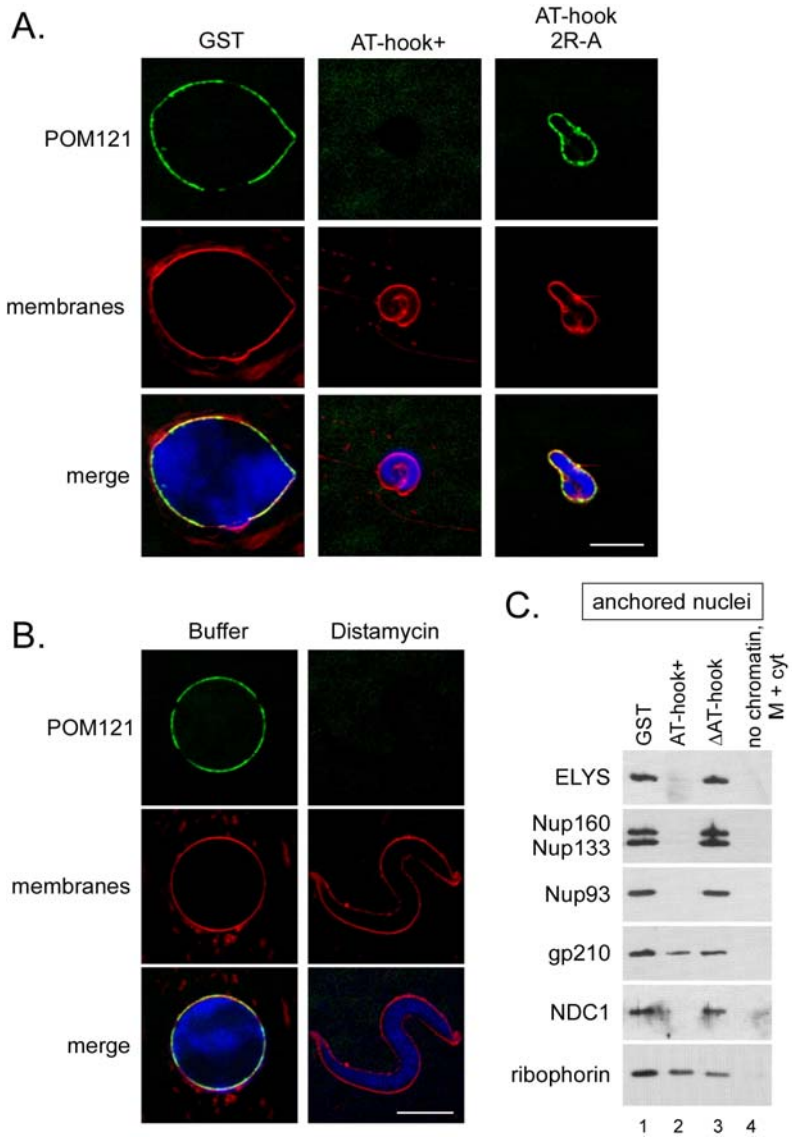

Figure 2.8. Chromatin-bound ELYS/Nup107-160 complex recruit POM121- and NDC1-containing membrane vesicles.

A) Reconstituted nuclei were assembled in the presence of 15 μM GST, GST-AT-hook+, or GST-AT-hook-2R→A. The presence of POM121 in the nuclear membranes was probed for with directly-labeled anti-POM121-AF488 (green). Membranes were stained with R18 membrane dye (red). DNA was stained with Hoechst (blue). Nuclei were fixed before mounting onto slides. Scale bar, 10 μm.

(B) Reconstituted nuclei were assembled in the presence of buffer or 10 μm Distamycin A and processed as in (A). Scale bar, 10 μm.

(C) Anchored nuclei were assembled by incubating chromatin-coated coverslips with membranes and cytosol for 1 hour; in the presence of either 15 μM GST, GST-AT-hook+, or GST-ΔAT-hook. A coverslip not treated with chromatin, but incubated with membranes 'M' and cytosol 'cyt', was used as a control for non-specific binding (lane 4). The recruitment of integral membrane pore proteins NDC1 and gp210, in the presence (GST and GST-ΔAT-hook, lane 1 and 3) or absence (GST-AT-hook+, lane 2) of chromatin-bound ELYS/Nup107-160 complex, was determined by immunoblot analysis.

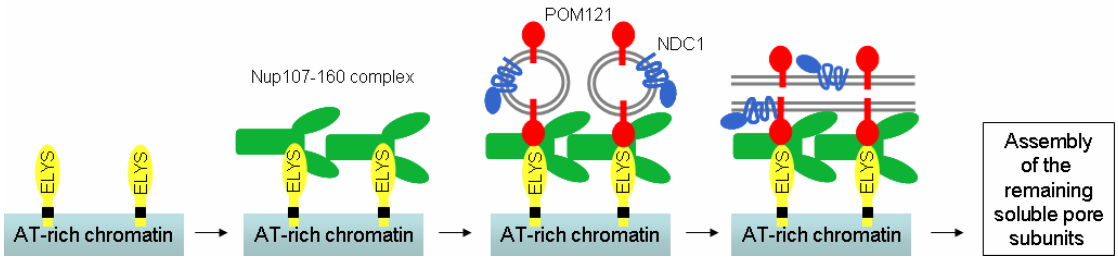

Figure 2.9. A model for the early steps in NPC assembly.
Based on our findings, we propose a model for the early steps in NPC assembly. The first step in pore assembly is the binding of ELYS (yellow) to AT-rich chromatin sites, selected via the high-affinity AT-hook motif (black box), and strengthened by its second chromatin binding domain. ELYS then acts as a bridge between the chromatin and the Nup107-160 complex (green) (Rasala *et al.*, 2006; Franz *et al.*, 2007; Gillespie *et al.*, 2007). Chromatin-bound ELYS/Nup107-160 complex actively recruits the integral membrane pore proteins POM121 (red) and NDC1 (blue), likely through interaction with the cytosolic domain of POM121. After membrane vesicle fusion, the rest of the soluble pore subunits assemble and a complete nuclear pore is formed. (Note, other vesicles/sheets bind to the chromatin via different linkages such as lamins to form the bulk of the nuclear membranes, but are not shown here.)

Acknowledgements

Chapter 2 is a modified version of a manuscript under submission for publication in **Molecular Biology of the Cell**: **Beth A. Rasala**, Corinne Ramos, Amnon Harel, and Douglass J. Forbes. Capture of AT-rich chromatin by ELYS recruits POM121 and NDC1 to initiate nuclear pore assembly. I was the primary investigator and author of this paper. We thank the members of the Forbes laboratory and Zhongsheng You for many helpful discussions regarding this work. We especially thank Valerie Delmar for critical reading of the manuscript and Corine Lau for reagents. We also thank Zhongsheng You for the kind gift of Orc2, RCC1, and Mcm3 antibodies.

References

Alber, F., Dokudovskaya, S., Veenhoff, L.M., Zhang, W., Kipper, J., Devos, D., Suprapto, A., Karni-Schmidt, O., Williams, R., Chait, B.T., Sali, A., and Rout, M.P. (2007). The molecular architecture of the nuclear pore complex. Nature *450*, 695-701.

Anand, A., and Chada, K. (2000). In vivo modulation of Hmgic reduces obesity. Nat Genet *24*, 377-380.

Anderson, D.J., and Hetzer, M.W. (2007). Nuclear envelope formation by chromatin-mediated reorganization of the endoplasmic reticulum. Nat Cell Biol *9*, 1160-1166.

Antonin, W., Franz, C., Haselmann, U., Antony, C., and Mattaj, I.W. (2005). The integral membrane nucleoporin pom121 functionally links nuclear pore complex assembly and nuclear envelope formation. Mol Cell *17*, 83-92.

Aravind, L., and Landsman, D. (1998). AT-hook motifs identified in a wide variety of DNA-binding proteins. Nucleic Acids Res *26*, 4413-4421.

Baur, T., Ramadan, K., Schlundt, A., Kartenbeck, J., and Meyer, H.H. (2007). NSF- and SNARE-mediated membrane fusion is required for nuclear envelope formation and completion of nuclear pore complex assembly in Xenopus laevis egg extracts. J Cell Sci *120*, 2895-2903.

Belgareh, N., Rabut, G., Bai, S.W., van Overbeek, M., Beaudouin, J., Daigle, N., Zatsepina, O.V., Pasteau, F., Labas, V., Fromont-Racine, M., Ellenberg, J., and Doye, V. (2001). An evolutionarily conserved NPC subcomplex, which redistributes in part to kinetochores in mammalian cells. J Cell Biol *154*, 1147-1160.

Bell, A., Kittler, L., Lober, G., and Zimmer, C. (1997). DNA binding properties of minor groove binders and their influence on the topoisomerase II cleavage reaction. J Mol Recognit *10*, 245-255.

Ben-Efraim, I., and Gerace, L. (2001). Gradient of increasing affinity of importin beta for nucleoporins along the pathway of nuclear import. J Cell Biol *152*, 411-417.

Bernardi, G., Olofsson, B., Filipski, J., Zerial, M., Salinas, J., Cuny, G., Meunier-Rotival, M., and Rodier, F. (1985). The mosaic genome of warm-blooded vertebrates. Science *228*, 953-958.

Bickford, L.C., Mossessova, E., and Goldberg, J. (2004). A structural view of the COPII vesicle coat. Curr Opin Struct Biol *14*, 147-153.

Bischoff, F.R., and Ponstingl, H. (1991). Catalysis of guanine nucleotide exchange on Ran by the mitotic regulator RCC1. Nature *354*, 80-82.

Bodoor, K., Shaikh, S., Salina, D., Raharjo, W.H., Bastos, R., Lohka, M., and Burke, B. (1999). Sequential recruitment of NPC proteins to the nuclear periphery at the end of mitosis. J Cell Sci *112 (Pt 13)*, 2253-2264.

Burke, B., and Ellenberg, J. (2002). Remodelling the walls of the nucleus. Nat Rev Mol Cell Biol *3*, 487-497.

Cabal, G.G., Genovesio, A., Rodriguez-Navarro, S., Zimmer, C., Gadal, O., Lesne, A., Buc, H., Feuerbach-Fournier, F., Olivo-Marin, J.C., Hurt, E.C., and Nehrbass, U. (2006). SAGA interacting factors confine sub-diffusion of transcribed genes to the nuclear envelope. Nature *441*, 770-773.

Casolari, J.M., Brown, C.R., Drubin, D.A., Rando, O.J., and Silver, P.A. (2005). Developmentally induced changes in transcriptional program alter spatial organization across chromosomes. Genes Dev *19*, 1188-1198.

Chaudhary, N., and Courvalin, J.C. (1993). Stepwise reassembly of the nuclear envelope at the end of mitosis. J Cell Biol *122*, 295-306.

Chial, H.J., Rout, M.P., Giddings, T.H., and Winey, M. (1998). Saccharomyces cerevisiae Ndc1p is a shared component of nuclear pore complexes and spindle pole bodies. J Cell Biol *143*, 1789-1800.

Clarke, P.R., and Zhang, C. (2004). Spatial and temporal control of nuclear envelope assembly by Ran GTPase. Symp Soc Exp Biol, 193-204.

Cotter, L.A., Goldberg, M.W., and Allen, T.D. (1998). Nuclear pore complex disassembly and nuclear envelope breakdown during mitosis may occur by both nuclear envelope vesicularisation and dispersion throughout the endoplasmic reticulum. Scanning *20*, 250-251.

Croft, J.A., Bridger, J.M., Boyle, S., Perry, P., Teague, P., and Bickmore, W.A. (1999). Differences in the localization and morphology of chromosomes in the human nucleus. J Cell Biol *145*, 1119-1131.

Cronshaw, J.M., Krutchinsky, A.N., Zhang, W., Chait, B.T., and Matunis, M.J. (2002). Proteomic analysis of the mammalian nuclear pore complex. J Cell Biol *158*, 915-927.

Cui, T., and Leng, F. (2007). Specific recognition of AT-rich DNA sequences by the mammalian high mobility group protein AT-hook 2: a SELEX study. Biochemistry *46*, 13059-13066.

Dabauvalle, M.C., Loos, K., Merkert, H., and Scheer, U. (1991). Spontaneous assembly of pore complex-containing membranes ("annulate lamellae") in Xenopus egg extract in the absence of chromatin. J Cell Biol *112*, 1073-1082.

Daigle, N., Beaudouin, J., Hartnell, L., Imreh, G., Hallberg, E., Lippincott-Schwartz, J., and Ellenberg, J. (2001). Nuclear pore complexes form immobile networks and have a very low turnover in live mammalian cells. J Cell Biol *154*, 71-84.

D'Angelo, M.A., Anderson, D.J., Richard, E., and Hetzer, M.W. (2006). Nuclear pores form de novo from both sides of the nuclear envelope. Science *312*, 440-443.

De Souza, C.P., Osmani, A.H., Hashmi, S.B., and Osmani, S.A. (2004). Partial nuclear pore complex disassembly during closed mitosis in Aspergillus nidulans. Curr Biol *14*, 1973-1984.

Devos, D., Dokudovskaya, S., Alber, F., Williams, R., Chait, B.T., Sali, A., and Rout, M.P. (2004). Components of coated vesicles and nuclear pore complexes share a common molecular architecture. PLoS Biol *2*, e380.

Drin, G., Casella, J.F., Gautier, R., Boehmer, T., Schwartz, T.U., and Antonny, B. (2007). A general amphipathic alpha-helical motif for sensing membrane curvature. Nat Struct Mol Biol *14*, 138-146.

Drummond, S., Ferrigno, P., Lyon, C., Murphy, J., Goldberg, M., Allen, T., Smythe, C., and Hutchison, C.J. (1999). Temporal differences in the appearance of NEP-B78 and an LBR-like protein during Xenopus nuclear envelope reassembly reflect the ordered recruitment of functionally discrete vesicle types. J Cell Biol *144*, 225-240.

Drummond, S.P., and Wilson, K.L. (2002). Interference with the cytoplasmic tail of gp210 disrupts "close apposition" of nuclear membranes and blocks nuclear pore dilation. J Cell Biol *158*, 53-62.

Ellenberg, J., Siggia, E.D., Moreira, J.E., Smith, C.L., Presley, J.F., Worman, H.J., and Lippincott-Schwartz, J. (1997). Nuclear membrane dynamics and reassembly in living cells: targeting of an inner nuclear membrane protein in interphase and mitosis. J Cell Biol *138*, 1193-1206.

Fernandez, A.G., and Piano, F. (2006). MEL-28 is downstream of the Ran cycle and is required for nuclear-envelope function and chromatin maintenance. Curr Biol *16*, 1757-1763.

Fontoura, B.M., Blobel, G., and Matunis, M.J. (1999). A conserved biogenesis pathway for nucleoporins: proteolytic processing of a 186-kilodalton precursor generates Nup98 and the novel nucleoporin, Nup96. J Cell Biol *144*, 1097-1112.

Forbes, D.J., Kirschner, M.W., and Newport, J.W. (1983). Spontaneous formation of nucleus-like structures around bacteriophage DNA microinjected into Xenopus eggs. Cell *34*, 13-23.

Foster, H.A., and Bridger, J.M. (2005). The genome and the nucleus: a marriage made by evolution. Genome organisation and nuclear architecture. Chromosoma *114*, 212-229.

Franz, C., Askjaer, P., Antonin, W., Iglesias, C.L., Haselmann, U., Schelder, M., de Marco, A., Wilm, M., Antony, C., and Mattaj, I.W. (2005). Nup155 regulates nuclear envelope and nuclear pore complex formation in nematodes and vertebrates. Embo J *24*, 3519-3531.

Franz, C., Walczak, R., Yavuz, S., Santarella, R., Gentzel, M., Askjaer, P., Galy, V., Hetzer, M., Mattaj, I.W., and Antonin, W. (2007). MEL-28/ELYS is required for the recruitment of nucleoporins to chromatin and postmitotic nuclear pore complex assembly. EMBO Rep *8*, 165-172.

Funakoshi, T., Maeshima, K., Yahata, K., Sugano, S., Imamoto, F., and Imamoto, N. (2007). Two distinct human POM121 genes: requirement for the formation of nuclear pore complexes. FEBS Lett *581*, 4910-4916.

Galy, V., Askjaer, P., Franz, C., Lopez-Iglesias, C., and Mattaj, I.W. (2006). MEL-28, a novel nuclear-envelope and kinetochore protein essential for zygotic nuclear-envelope assembly in C. elegans. Curr Biol *16*, 1748-1756.

Gerace, L., Ottaviano, Y., and Kondor-Koch, C. (1982). Identification of a major polypeptide of the nuclear pore complex. J Cell Biol *95*, 826-837.

Gillespie, P.J., Khoudoli, G.A., Stewart, G., Swedlow, J.R., and Blow, J.J. (2007). ELYS/MEL-28 chromatin association coordinates nuclear pore complex assembly and replication licensing. Curr Biol *17*, 1657-1662.

Goldberg, M.W., Wiese, C., Allen, T.D., and Wilson, K.L. (1997). Dimples, pores, star-rings, and thin rings on growing nuclear envelopes: evidence for structural intermediates in nuclear pore complex assembly. J Cell Sci *110 (Pt 4)*, 409-420.

Goldfarb, D.S., Corbett, A.H., Mason, D.A., Harreman, M.T., and Adam, S.A. (2004). Importin alpha: a multipurpose nuclear-transport receptor. Trends Cell Biol *14*, 505-514.

Goodwin, G. (1998). The high mobility group protein, HMGI-C. Int J Biochem Cell Biol *30*, 761-766.

Greber, U.F., Senior, A., and Gerace, L. (1990). A major glycoprotein of the nuclear pore complex is a membrane-spanning polypeptide with a large lumenal domain and a small cytoplasmic tail. Embo J *9*, 1495-1502.

Griffis, E.R., Altan, N., Lippincott-Schwartz, J., and Powers, M.A. (2002). Nup98 is a mobile nucleoporin with transcription-dependent dynamics. Mol Biol Cell *13*, 1282-1297.

Griffis, E.R., Craige, B., Dimaano, C., Ullman, K.S., and Powers, M.A. (2004). Distinct functional domains within nucleoporins Nup153 and Nup98 mediate transcription-dependent mobility. Mol Biol Cell *15*, 1991-2002.

Hallberg, E., Wozniak, R.W., and Blobel, G. (1993). An integral membrane protein of the pore membrane domain of the nuclear envelope contains a nucleoporin-like region. J Cell Biol *122*, 513-521.

Haraguchi, T., Koujin, T., Hayakawa, T., Kaneda, T., Tsutsumi, C., Imamoto, N., Akazawa, C., Sukegawa, J., Yoneda, Y., and Hiraoka, Y. (2000). Live fluorescence imaging reveals early recruitment of emerin, LBR, RanBP2, and Nup153 to reforming functional nuclear envelopes. J Cell Sci *113 (Pt 5)*, 779-794.

Harel, A., Chan, R.C., Lachish-Zalait, A., Zimmerman, E., Elbaum, M., and Forbes, D.J. (2003a). Importin beta negatively regulates nuclear membrane fusion and nuclear pore complex assembly. Mol Biol Cell *14*, 4387-4396.

Harel, A., and Forbes, D.J. (2004). Importin beta: conducting a much larger cellular symphony. Mol Cell *16*, 319-330.

Harel, A., Orjalo, A.V., Vincent, T., Lachish-Zalait, A., Vasu, S., Shah, S., Zimmerman, E., Elbaum, M., and Forbes, D.J. (2003b). Removal of a single pore subcomplex results in vertebrate nuclei devoid of nuclear pores. Mol Cell *11*, 853-864.

Hase, M.E., and Cordes, V.C. (2003). Direct interaction with nup153 mediates binding of Tpr to the periphery of the nuclear pore complex. Mol Biol Cell *14*, 1923-1940.

Heath, C.V., Copeland, C.S., Amberg, D.C., Del Priore, V., Snyder, M., and Cole, C.N. (1995). Nuclear pore complex clustering and nuclear accumulation of poly(A)+ RNA associated with mutation of the Saccharomyces cerevisiae RAT2/NUP120 gene. J Cell Biol *131*, 1677-1697.

Hetzer, M., Bilbao-Cortes, D., Walther, T.C., Gruss, O.J., and Mattaj, I.W. (2000). GTP hydrolysis by Ran is required for nuclear envelope assembly. Mol Cell *5*, 1013-1024.

Hetzer, M., Gruss, O.J., and Mattaj, I.W. (2002). The Ran GTPase as a marker of chromosome position in spindle formation and nuclear envelope assembly. Nat Cell Biol *4*, E177-184.

Hetzer, M., Walther, T.C., and Mattaj, I.W. (2005). Pushing the Envelope: Structure, Function, and Dynamics of the Nuclear Periphery. Annu Rev Cell Dev Biol.

Hsia, K.C., Stavropoulos, P., Blobel, G., and Hoelz, A. (2007). Architecture of a coat for the nuclear pore membrane. Cell *131*, 1313-1326.

Huth, J.R., Bewley, C.A., Nissen, M.S., Evans, J.N., Reeves, R., Gronenborn, A.M., and Clore, G.M. (1997). The solution structure of an HMG-I(Y)-DNA complex defines a new architectural minor groove binding motif. Nat Struct Biol *4*, 657-665.

Kalab, P., Pralle, A., Isacoff, E.Y., Heald, R., and Weis, K. (2006). Analysis of a RanGTP-regulated gradient in mitotic somatic cells. Nature *440*, 697-701.

Kas, E., Izaurralde, E., and Laemmli, U.K. (1989). Specific inhibition of DNA binding to nuclear scaffolds and histone H1 by distamycin. The role of oligo(dA).oligo(dT) tracts. J Mol Biol *210*, 587-599.

Kessel, R.G. (1992). Annulate lamellae: a last frontier in cellular organelles. Int Rev Cytol *133*, 43-120.

Kimura, N., Takizawa, M., Okita, K., Natori, O., Igarashi, K., Ueno, M., Nakashima, K., Nobuhisa, I., and Taga, T. (2002). Identification of a novel transcription factor, ELYS, expressed predominantly in mouse foetal haematopoietic tissues. Genes Cells *7*, 435-446.

Krull, S., Thyberg, J., Bjorkroth, B., Rackwitz, H.R., and Cordes, V.C. (2004). Nucleoporins as components of the nuclear pore complex core structure and Tpr as the architectural element of the nuclear basket. Mol Biol Cell *15*, 4261-4277.

Lau, C.K., Delmar, V.A., and Forbes, D.J. (2006). Topology of yeast Ndc1p: predictions for the human NDC1/NET3 homologue. Anat Rec A Discov Mol Cell Evol Biol *288*, 681-694.

Lau, C.K., Giddings, T.H., Jr., and Winey, M. (2004). A novel allele of Saccharomyces cerevisiae NDC1 reveals a potential role for the spindle pole body component Ndc1p in nuclear pore assembly. Eukaryot Cell *3*, 447-458.

Li, O., Heath, C.V., Amberg, D.C., Dockendorff, T.C., Copeland, C.S., Snyder, M., and Cole, C.N. (1995). Mutation or deletion of the Saccharomyces cerevisiae RAT3/NUP133 gene causes temperature-dependent nuclear accumulation of poly(A)+ RNA and constitutive clustering of nuclear pore complexes. Mol Biol Cell *6*, 401-417.

Liu, J., Prunuske, A.J., Fager, A.M., and Ullman, K.S. (2003). The COPI complex functions in nuclear envelope breakdown and is recruited by the nucleoporin Nup153. Dev Cell *5*, 487-498.

Lohka, M.J., and Masui, Y. (1983). Formation in vitro of sperm pronuclei and mitotic chromosomes induced by amphibian ooplasmic components. Science *220*, 719-721.

Loiodice, I., Alves, A., Rabut, G., Van Overbeek, M., Ellenberg, J., Sibarita, J.B., and Doye, V. (2004). The entire Nup107-160 complex, including three new members, is targeted as one entity to kinetochores in mitosis. Mol Biol Cell *15*, 3333-3344.

Lopez-Soler, R.I., Moir, R.D., Spann, T.P., Stick, R., and Goldman, R.D. (2001). A role for nuclear lamins in nuclear envelope assembly. J Cell Biol *154*, 61-70.

Macara, I.G. (2001). Transport into and out of the nucleus. Microbiol Mol Biol Rev *65*, 570-594, table of contents.

Macaulay, C., and Forbes, D.J. (1996). Assembly of the nuclear pore: biochemically distinct steps revealed with NEM, GTP gamma S, and BAPTA. J Cell Biol *132*, 5-20.

Macaulay, C., Meier, E., and Forbes, D.J. (1995). Differential mitotic phosphorylation of proteins of the nuclear pore complex. J Biol Chem *270*, 254-262.

Madrid, A.S., Mancuso, J., Cande, W.Z., and Weis, K. (2006). The role of the integral membrane nucleoporins Ndc1p and Pom152p in nuclear pore complex assembly and function. J Cell Biol *173*, 361-371.

Maher, J.F., and Nathans, D. (1996). Multivalent DNA-binding properties of the HMG-1 proteins. Proc Natl Acad Sci U S A *93*, 6716-6720.

Mansfeld, J., Guttinger, S., Hawryluk-Gara, L.A., Pante, N., Mall, M., Galy, V., Haselmann, U., Muhlhausser, P., Wozniak, R.W., Mattaj, I.W., Kutay, U., and Antonin, W. (2006). The conserved transmembrane nucleoporin NDC1 is required for nuclear pore complex assembly in vertebrate cells. Mol Cell *22*, 93-103.

Margalit, A., Vlcek, S., Gruenbaum, Y., and Foisner, R. (2005). Breaking and making of the nuclear envelope. J Cell Biochem *95*, 454-465.

Maul, G.G., Maul, H.M., Scogna, J.E., Lieberman, M.W., Stein, G.S., Hsu, B.Y., and Borun, T.W. (1972). Time sequence of nuclear pore formation in phytohemagglutinin-stimulated lymphocytes and in HeLa cells during the cell cycle. J Cell Biol *55*, 433-447.

Meier, E., Miller, B.R., and Forbes, D.J. (1995). Nuclear pore complex assembly studied with a biochemical assay for annulate lamellae formation. J Cell Biol *129*, 1459-1472.

Metcalf, C.E., and Wassarman, D.A. (2006). DNA binding properties of TAF1 isoforms with two AT-hooks. J Biol Chem *281*, 30015-30023.

Miller, B.R., and Forbes, D.J. (2000). Purification of the vertebrate nuclear pore complex by biochemical criteria. Traffic *1*, 941-951.

Newport, J. (1987). Nuclear reconstitution in vitro: stages of assembly around protein-free DNA. Cell *48*, 205-217.

Newport, J., and Kirschner, M. (1982). A major developmental transition in early Xenopus embryos: I. characterization and timing of cellular changes at the midblastula stage. Cell *30*, 675-686.

Orjalo, A.V., Arnaoutov, A., Shen, Z., Boyarchuk, Y., Zeitlin, S.G., Fontoura, B., Briggs, S., Dasso, M., and Forbes, D.J. (2006). The Nup107-160 nucleoporin complex is required for correct bipolar spindle assembly. Mol Biol Cell *17*, 3806-3818.

Patel, S.S., Belmont, B.J., Sante, J.M., and Rexach, M.F. (2007). Natively unfolded nucleoporins gate protein diffusion across the nuclear pore complex. Cell *129*, 83-96.

Pemberton, L.F., and Paschal, B.M. (2005). Mechanisms of receptor-mediated nuclear import and nuclear export. Traffic *6*, 187-198.

Powers, M.A., Macaulay, C., Masiarz, F.R., and Forbes, D.J. (1995). Reconstituted nuclei depleted of a vertebrate GLFG nuclear pore protein, p97, import but are defective in nuclear growth and replication. J Cell Biol *128*, 721-736.

Prunuske, A.J., Liu, J., Elgort, S., Joseph, J., Dasso, M., and Ullman, K.S. (2006). Nuclear envelope breakdown is coordinated by both Nup358/RanBP2 and Nup153, two nucleoporins with zinc finger modules. Mol Biol Cell *17*, 760-769.

Quimby, B.B., Arnaoutov, A., and Dasso, M. (2005). Ran GTPase regulates Mad2 localization to the nuclear pore complex. Eukaryot Cell *4*, 274-280.

Quimby, B.B., and Corbett, A.H. (2001). Nuclear transport mechanisms. Cell Mol Life Sci *58*, 1766-1773.

Rabut, G., Doye, V., and Ellenberg, J. (2004). Mapping the dynamic organization of the nuclear pore complex inside single living cells. Nat Cell Biol *6*, 1114-1121.

Rasala, B.A., Orjalo, A.V., Shen, Z., Briggs, S., and Forbes, D.J. (2006). ELYS is a dual nucleoporin/kinetochore protein required for nuclear pore

assembly and proper cell division. Proc Natl Acad Sci U S A *103*, 17801-17806.

Reeves, R. (2001). Molecular biology of HMGA proteins: hubs of nuclear function. Gene *277*, 63-81.

Reeves, R., and Nissen, M.S. (1990). The A.T-DNA-binding domain of mammalian high mobility group I chromosomal proteins. A novel peptide motif for recognizing DNA structure. J Biol Chem *265*, 8573-8582.

Reichelt, R., Holzenburg, A., Buhle, E.L., Jr., Jarnik, M., Engel, A., and Aebi, U. (1990). Correlation between structure and mass distribution of the nuclear pore complex and of distinct pore complex components. J Cell Biol *110*, 883-894.

Ryan, K.J., McCaffery, J.M., and Wente, S.R. (2003). The Ran GTPase cycle is required for yeast nuclear pore complex assembly. J Cell Biol *160*, 1041-1053.

Rzepecki, R., Bogachev, S.S., Kokoza, E., Stuurman, N., and Fisher, P.A. (1998). In vivo association of lamins with nucleic acids in Drosophila melanogaster. J Cell Sci *111 (Pt 1)*, 121-129.

Saccone, S., De Sario, A., Wiegant, J., Raap, A.K., Della Valle, G., and Bernardi, G. (1993). Correlations between isochores and chromosomal bands in the human genome. Proc Natl Acad Sci U S A *90*, 11929-11933.

Saccone, S., Federico, C., and Bernardi, G. (2002). Localization of the gene-richest and the gene-poorest isochores in the interphase nuclei of mammals and birds. Gene *300*, 169-178.

Schwartz, T.U. (2005). Modularity within the architecture of the nuclear pore complex. Curr Opin Struct Biol *15*, 221-226.

Shah, S., and Forbes, D.J. (1998). Separate nuclear import pathways converge on the nucleoporin Nup153 and can be dissected with dominant-negative inhibitors. Curr Biol *8*, 1376-1386.

Shah, S., Tugendreich, S., and Forbes, D. (1998). Major binding sites for the nuclear import receptor are the internal nucleoporin Nup153 and the adjacent nuclear filament protein Tpr. J Cell Biol *141*, 31-49.

Sheehan, M.A., Mills, A.D., Sleeman, A.M., Laskey, R.A., and Blow, J.J. (1988). Steps in the assembly of replication-competent nuclei in a cell-free system from Xenopus eggs. J Cell Biol *106*, 1-12.

Shumaker, D.K., Lopez-Soler, R.I., Adam, S.A., Herrmann, H., Moir, R.D., Spann, T.P., and Goldman, R.D. (2005). Functions and dysfunctions of the nuclear lamin Ig-fold domain in nuclear assembly, growth, and Emery-Dreifuss muscular dystrophy. Proc Natl Acad Sci U S A *102*, 15494-15499.

Siniossoglou, S., Wimmer, C., Rieger, M., Doye, V., Tekotte, H., Weise, C., Emig, S., Segref, A., and Hurt, E.C. (1996). A novel complex of nucleoporins, which includes Sec13p and a Sec13p homolog, is essential for normal nuclear pores. Cell *84*, 265-275.

Soderqvist, H., and Hallberg, E. (1994). The large C-terminal region of the integral pore membrane protein, POM121, is facing the nuclear pore complex. Eur J Cell Biol *64*, 186-191.

Stavru, F., Hulsmann, B.B., Spang, A., Hartmann, E., Cordes, V.C., and Gorlich, D. (2006). NDC1: a crucial membrane-integral nucleoporin of metazoan nuclear pore complexes. J Cell Biol *173*, 509-519.

Suntharalingam, M., and Wente, S.R. (2003). Peering through the pore: nuclear pore complex structure, assembly, and function. Dev Cell *4*, 775-789.

Ulbert, S., Platani, M., Boue, S., and Mattaj, I.W. (2006). Direct membrane protein-DNA interactions required early in nuclear envelope assembly. J Cell Biol *173*, 469-476.

Vasu, S., Shah, S., Orjalo, A., Park, M., Fischer, W.H., and Forbes, D.J. (2001). Novel vertebrate nucleoporins Nup133 and Nup160 play a role in mRNA export. J Cell Biol *155*, 339-354.

Vasu, S.K., and Forbes, D.J. (2001). Nuclear pores and nuclear assembly. Curr Opin Cell Biol *13*, 363-375.

Walther, T.C., Alves, A., Pickersgill, H., Loiodice, I., Hetzer, M., Galy, V., Hulsmann, B.B., Kocher, T., Wilm, M., Allen, T., Mattaj, I.W., and Doye, V. (2003a). The conserved Nup107-160 complex is critical for nuclear pore complex assembly. Cell *113*, 195-206.

Walther, T.C., Askjaer, P., Gentzel, M., Habermann, A., Griffiths, G., Wilm, M., Mattaj, I.W., and Hetzer, M. (2003b). RanGTP mediates nuclear pore complex assembly. Nature *424*, 689-694.

Walther, T.C., Fornerod, M., Pickersgill, H., Goldberg, M., Allen, T.D., and Mattaj, I.W. (2001). The nucleoporin Nup153 is required for nuclear pore basket formation, nuclear pore complex anchoring and import of a subset of nuclear proteins. Embo J *20*, 5703-5714.

West, R.R., Vaisberg, E.V., Ding, R., Nurse, P., and McIntosh, J.R. (1998). cut11(+): A gene required for cell cycle-dependent spindle pole body anchoring in the nuclear envelope and bipolar spindle formation in Schizosaccharomyces pombe. Mol Biol Cell *9*, 2839-2855.

Wozniak, R., and Clarke, P.R. (2003). Nuclear pores: sowing the seeds of assembly on the chromatin landscape. Curr Biol *13*, R970-972.

Wozniak, R.W., Bartnik, E., and Blobel, G. (1989). Primary structure analysis of an integral membrane glycoprotein of the nuclear pore. J Cell Biol *108*, 2083-2092.

Yang, L., Guan, T., and Gerace, L. (1997). Integral membrane proteins of the nuclear envelope are dispersed throughout the endoplasmic reticulum during mitosis. J Cell Biol *137*, 1199-1210.

Zhang, C., and Clarke, P.R. (2000). Chromatin-independent nuclear envelope assembly induced by Ran GTPase in Xenopus egg extracts. Science *288*, 1429-1432.

Zink, D., Fischer, A.H., and Nickerson, J.A. (2004). Nuclear structure in cancer cells. Nat Rev Cancer *4*, 677-687.

CHAPTER 3

Structural intermediates in fusion mediated NPC assembly

Introduction

Membrane fusion is one of the most fundamental, but tightly controlled, processes in life. Membranes merge during intracellular trafficking, fertilization, tissue formation, viral infection, and organelle biogenesis (Mohler *et al.*, 2002; Jahn *et al.*, 2003; Earp *et al.*, 2005). The formation of a nuclear envelope (NE) also requires membrane fusion events. The NE is composed of an outer nuclear membrane and an inner nuclear membrane, separated by a lumen and joined by nuclear pore complexes. Much of our knowledge of the mechanism of vertebrate NE assembly is derived from a cell-free system (Lohka and Masui, 1983; Newport, 1987; Newport and Dunphy, 1992). This has allowed the dissection of NE formation in vitro into distinct steps: recruitment of membrane vesicles to the chromatin surface, fusion of these vesicles, nuclear pore complex assembly, and expansion of the NE (Macaulay and Forbes, 1996; Hetzer *et al.*, 2001; Harel *et al.*, 2003a; D'Angelo *et al.*, 2006). The formation of the double nuclear membrane around chromatin requires extensive vesicle-vesicle fusion in vitro, promoted by the small GTPase Ran (Hetzer *et al.*, 2000; Zhang and Clarke, 2000) and regulated by importin β (Harel *et al.*, 2003a; Walther *et al.*, 2003). It is thought that nuclear

pores could form from a subsequent fusion event occurring between the two nuclear membranes. Indeed, cell-free experiments using the NPC assembly inhibitor BAPTA (Blobel *et al.*, 1992; Macaulay and Forbes, 1996; Schwander *et al.*, 2003) or an NPC insertion assay (D'Angelo *et al.*, 2006) show that NPCs can form into a completely closed NE in vitro, presumably through opposing bilayer fusion. This mimics the inner/outer nuclear membrane fusion process that must occur in S-phase vertebrate nuclei and yeast nuclei at all stages, where new nuclear pores form in the pre-existing nucleus.

Integral membrane proteins drive membrane fusion during enveloped virus entry into cells, SNARE-dependent intracellular fusion, and cell-cell fusion (Mohler *et al.*, 2002; Podbilewicz *et al.*, 2006). These fusion proteins are anchored in the membranes by one or more transmembrane domains. A recent study showed that the membrane vesicle-vesicle fusion event required for NE formation in vitro in *Xenopus* egg extracts is dependent on integral membrane SNARE proteins (Baur *et al.*, 2007). However, that study did not address inner/outer nuclear membrane fusion.

It is likely that one or more integral membrane proteins play a key role in the fusion event that must precede nuclear pore assembly in pre-existing enclosed nuclear membranes. To date, POM121, gp210, and NDC1 are the only known integral membrane proteins of the vertebrate nuclear pore (Gerace *et al.*, 1982; Hallberg *et al.*, 1993; Mansfeld *et al.*, 2006; Stavru *et al.*, 2006a). RNAi depletion of these transmembrane nucleoporins have shown that

POM121 and NDC1 are essential for nuclear pore formation (Antonin *et al.*, 2005; Mansfeld *et al.*, 2006; Stavru *et al.*, 2006a; Stavru *et al.*, 2006b; Funakoshi *et al.*, 2007), however their potential role in inner/outer nuclear membrane fusion has not been investigated. One possibility is that the proteins may work singularly or together to promote the fusion of the inner and outer nuclear membranes for nuclear pore assembly. Alternatively, an as yet unidentified transmembrane protein or soluble protein may be required for inner/outer nuclear membrane fusion in the process of nuclear pore assembly.

The most accepted molecular model for general membrane fusion is the "stalk-pore" mechanism for fusion events. This mechanism was first identified on artificial protein-free bilayers and then in viral fusion, intracellular fusion and, most recently, developmental cell fusion systems (Kozlov and Markin, 1983; Chernomordik *et al.*, 1987; Chernomordik *et al.*, 1993; Lu *et al.*, 2005; Reese *et al.*, 2005; Xu *et al.*, 2005; Podbilewicz *et al.*, 2006; Sapir *et al.*, 2007). In this mechanism, membrane fusion begins with the bending of the membranes and proceeds through a hemifusion intermediate (Figure 3.1), which consists of a stalk-like connection between the contacting membrane leaflets of two fusing bilayers. Hemifusion is followed by complete fusion, which involves the opening of a fusion pore connecting all four leaflets (Figure 3.1). Subsequent expansion of the fusion pore leads to a fully fused entity. Although fusion proteins are required to provide the driving force that induces hemifusion in biological membranes, the fusion reaction shows a striking

sensitivity to any alteration in membrane lipid composition (Chernomordik *et al.*, 1993). For biological membranes, hemifusion intermediates are strongly sensitive to the shapes of the lipid molecules in the proximal membrane leaflets. Cone-shaped lipids, if added, promote bending and therefore promote hemifusion. Inverted cone-shaped lipids inhibit bending and thus inhibit hemifusion. This is true for both viral and intracellular fusion events (Chernomordik and Kozlov, 2003; Melia *et al.*, 2006). The dependency on lipid shape is thought to be because of the bending specifically involved in forming the stalk-pore intermediate. In consequence, inverted cone-shaped lipids such as lysophosphatidylcholine (LPC) have been used to identify when a membrane fusion event occurs, since LPC acts as an inhibitor of that event. Post-hemifusion stages, which involve opening and expansion of a fusion pore, are found to be more protein dependent (Chernomordik and Kozlov, 2003; Lu *et al.*, 2005; Reese *et al.*, 2005; Xu *et al.*, 2005).

To form the nuclear pore, it is thought that sites of recruitment of soluble proteins on the chromatin surface act as nucleation points to delineate where the inner and outer nuclear membranes will be fused. The membrane fusion step has never been experimentally identified, nor has its temporal order with regard to nucleoporin recruitment and/or insertion been demonstrated. By using experimental approaches used previously to model membrane fusion reactions (Chernomordik *et al.*, 1998; Markosyan *et al.*, 2003; Henderson and Hope, 2006), we address questions with respect to the

fusion event between the inner and outer nuclear membranes in nuclear pore formation. Specifically, we describe a lipid-sensitive intermediate which occurs on a completely closed nuclear envelope downstream from the acquisition of early nuclear pore proteins, but prior to observation of NPC structures containing FG nucleoporins and channels functional for small molecule and dextran diffusion.

Material and Methods

Antibodies. The antibodies used in this study included affinity-purified anti-hNup133 (Vasu *et al.*, 2001), anti-*Xenopus* POM121 (Harel *et al.*, 2003b), which was raised to *Xenopus* POM121 aa144-435, anti-xELYS (Rasala, *et al.*, submitted), and anti-FG nucleoporin antibody, mAb414 (Covance, Berkeley, CA). Note that mAb414 recognizes most FG nucleoporins in *Xenopus*, but not *Xenopus* POM121, either on immunoblots or by immunofluorescence, presumably due to an inexact match of the FG epitopes in POM121.

Nuclear reconstitution and Immunofluorescence*. Xenopus* egg extracts, membrane vesicle and cytosolic fractions were prepared as in Harel *et al.* (2003). Nuclei were reconstituted at either room temperature or 15°C, by mixing *Xenopus* egg membrane vesicle and cytosolic fractions at a 1:20 ratio with an ATP-regeneration system and sperm chromatin (Macaulay and Forbes, 1996).

For direct immunofluorescence, mAb414, affinity purified anti-POM121, anti-xELYS or anti-Nup133 were coupled to Alexa fluor dyes (Molecular Probes, Eugene, OR). Nuclear reactions were stopped on ice at different times after the start of assembly. To assay for the presence of FG-Nups, POM121, or Nup133, the samples were mixed with 0.5 μg directly labeled antibodies for 10 min in 10 μl volume reaction before fixation with 3.2% paraformaldehyde and then monitored by confocal microscopy. To assay for the presence of nuclear ELYS, AF568-anti-xELYS was added at the start of the nuclear assembly reactions at a final concentration of 20 ng/μl. Nuclear assembly was then monitored as above.

Nuclear membrane formation was assayed by a continuous rim staining with the lipophilic dye 3,3-dihexyloxacarbocyanine iodide (DHCC) (Eastman Kodak, Rochester, NY) and the ability to exclude Alexa568-labeled anti-dsDNA antibody (Abcam, Cambridge, MA). For the latter, at the indicated time, nuclear assembly was stopped on ice and 0.2 μg Alexa568-anti-dsDNA was added for 10 min in 10 μl reaction sample. The samples were then fixed with 3.2% paraformaldehyde and monitored by microscopy.

Nuclei were visualized with an Axioskop 2 microscope (63x objective; Carl Zeiss, Thornwood, NY). Images were also acquired using an Axiovert 200M (Carl Zeiss, Thornwood, NY) at a magnification of 63x using an oil objective (Carl Zeiss) with a 1.3 numerical aperture at 23ºC and with Immersol 518F (Carl Zeiss) as the imaging medium. Images were recorded using a

Coolsnap HQ (Photometerics, Tucson, AZ) camera and Metavue software (Molecular Devices Corporation, Downingtown, PA). Trace images were produced using the trace contour function in Adobe Photoshop.

Application of exogenous lipids. Stock solutions of Lauroyl LysophosphatidylCholine (LPC; 12 carbon tail; Avanti Polar Lipids) and Oleic Acid (OA; Sigma Chemical Co.) were freshly prepared as 10 mM solutions in PBS and 25 mM ethanolic solution, respectively. At the indicated time, an assembly reaction was stopped on ice and LPC or LPC and OA were added directly to the samples at a final concentration of 600 μM by rapid injection of the stock solution into the tube under continuous flicking. The samples were returned to the working temperature (15°C or room temperature, as noted) and after further incubation, they were processed for direct immunofluorescence as previously described.

Diffusion assay. The presence of diffusion channels through the nuclear envelope was assayed by the ability of Alexa488-10kD or Alexa488-3kD dextrans to diffuse into the nucleus. Specifically, at the indicated time, a nuclear assembly reaction was stopped on ice and 1 μg Alexa488-10 kD or -3 kD dextrans (Molecular Probes, Eugene, OR) was added for 15 min to a 10 μl reaction sample. The samples were fixed with 3.2% paraformaldehyde for 20 min and then the fluorescence external to the nucleus was quenched by the

addition of 5 μg anti-Alexa Fluor 488 antibody for an additional 15 min. The samples were either directly monitored by microscopy, or were diluted to 200 μl in ELB buffer (10 mM HEPES-NaOH, pH 7.4, 3 mM $MgCl_2$, 50 mM KCl, 250 mM sucrose, 1 mM DTT, 100 μg/ml cycloheximide). These latter were subsequently centrifuged through a cushion of 30% (w/v) sucrose in ELB onto poly-L-Lysine-coated coverslips and then monitored by confocal microscopy. This assay was usually performed simultaneously with an Alexa568-anti-DNA antibody assay. Only nuclei that excluded the anti-DNA antibody (which marked them as intact) were assessed for their ability to exclude the labeled dextrans. Nuclear intermediates that excluded dextrans were designated as lacking diffusion channels. Under conditions where nuclei could proceed to a stage where they contained mature nuclear pores (for example, room temperature-30 minutes-no inhibitors, or 15°C-60 minutes), the Alexa 488-labeled 3 and 10 kD dextrans showed the expected diffusion into the nuclear interior. In these latter cases, intranuclear fluorescence would appear that was unquenchable by added150 kD anti-Alexa488 antibody.

Results

A temperature-sensitive intermediate in nuclear pore assembly.

Lowering the temperature is an approach long known to impair general membrane fusion. It has been used to stabilize and identify important steps in membrane fusion events, such as viral cell fusion, endocytosis, and cell-cell

fusion (Stegmann *et al.*, 1990; Schoch *et al.*, 1992; Melikyan *et al.*, 2000; Baur *et al.*, 2007; Gattegno *et al.*, 2007). Here, we combine lower temperature with a well-described nuclear assembly system derived from *Xenopus* egg extracts (Lohka and Masui, 1983; Newport, 1987) to ask whether one can isolate novel intermediates in nuclear pore assembly.

At room temperature, nuclear envelope formation and nuclear pore assembly are rather fast in the *Xenopus* system. Consistent with this, nuclear membranes visualized with the membrane dye DHCC formed by 15 min and grew and expanded over time (Figure 3.2A). Nuclear pore complexes (NPCs), as visualized by the anti-FG nucleoporin antibody mAb414, appeared at 15 min after initiation of the nuclear assembly reaction (Figure 3.2A). At room temperature, import-competent nuclei were readily apparent by 30 minutes (data not shown) and fully-grown by 60-120 minutes (Figure 3.2A). At 4ºC, we found that vesicle-vesicle fusion was arrested and no nuclear membranes were observed (data not shown).

We found, however, that at 15ºC over the long term was permissive for nuclear membrane assembly and NPC formation (Figure 3.2A). The lower temperature, however, affected the kinetics of nuclear formation (Figure 3.2A). Intact nuclei, complete with the FG nucleoporin rim staining characteristic of mature nuclear pores, were abundant only after 60 min at 15ºC. This indicates that nuclear assembly proceeds at 15ºC, but at a slower rate compared to room temperature. Strikingly, FG nucleoporin staining was not

detected at 30 min of assembly at 15ºC (asterisk, Figure 3.2A). Surface views and quantitation of NPCs/μm^2 confirmed the lack of FG-staining nuclear pores in this 30 min cold intermediate at 15°C (Figure 3.3).

Although nuclear assembly is slowed at 15°C, vesicle-vesicle fusion to form double nuclear membranes occurred. To show that the nuclear membranes indeed can completely enclose the chromatin at 15°C, we used an Alexa568-labeled anti-DNA antibody. Nuclear assembly reactions were initiated on chromatin templates with the addition of *Xenopus* egg membrane vesicles and cytosol. At the end of a reaction, Alexa568-labeled DNA antibody was added, with the presumption that it could only access the chromatin if the NE was not fully closed. Indeed, in nuclei incubated for 60 min at room temperature, the fluorescently labeled anti-DNA antibody did not access the chromatin in the great majority, as indicated by the absence of a red Alexa568 signal (Figure 3.4). In contrast, when GTPγS was added to prevent vesicle-vesicle fusion at the onset of the reaction (Boman *et al.*, 1992) or when Triton X100 was added to control nuclei at the end of the reaction, the chromatin substrates were uniformly stained with anti-DNA antibody (Figure 3.4). The calcium chelator BAPTA, however, known to cause formation of a nuclear membrane lacking nuclear pores (Macaulay and Forbes, 1996), gave closed nuclear structures that excluded entry of the anti-DNA antibody (Figure 3.4).

Having established that the anti-DNA antibody correctly monitors formation of completely fused nuclear membranes, we used this assay to

characterize nuclei assembled at 15°C for 30 min. Nearly half of the nuclei showed no labeling by the anti-DNA antibody *(*asterisks, Figure 3.2B), indicating that these were closed by 30 min. Most of the enclosed 15°C intermediates, when tested, did not contain FG nucleoporins (diamonds, Figure 3.2B and C). By 60 min, they had acquired FG Nups (Figure 3.2C; see also Figure 3.2A).

From these results, two possibilities exist in the 15°C 30 min intermediate. Either, (1) inner/outer nuclear membrane fusion takes place but a temperature-sensitive delay in FG recruitment is occurring, or (2) a temperature-sensitive impediment to inner/outer nuclear membrane fusion prevents the recruitment of FG nucleoporins.

Recruitment of POM121 and Nup133 into punctate structures characteristic of a partial pore intermediate in the membranes.

The 30min, 15°C cold intermediate lacks the FG Nups that are the hallmark of mature nuclear pores. We assessed, however, whether other nucleoporins were present in the intermediate. We found that POM121, an integral membrane pore protein, was indeed detectable by immunofluorescence and was observed in punctate structures in the membrane-enclosed intermediate (asterisk, 15°C, 30 min, Figure 3.5A). In these structures, no FG Nup staining was present. Nup133 was also observed to be present in this membrane intermediate (asterisk, Figure 3.5B). Nup133 is

a signature member of the Nup107-160 complex, indicating the presence of the entire complex at this time.

These entities were detected by directly labeled anti-Nup antibodies added to closed nuclear intermediates. Anti-DNA antibody identified completely enclosed intermediates. On enclosed nuclei, the anti-Nup antibodies can thus only access Nup-containing structures present on the outside of the nuclear membranes. This experimental design was planned so that it allowed us to detect membrane NPC intermediates, rather than earlier chromatin-bound Nups.

We previously identified a membrane-enclosed intermediate formed at room temperature by addition of the Ca++ chelator BAPTA. This BAPTA intermediate had no nuclear pores, as visualized by EM, and no FG Nups (Macaulay and Forbes, 1996). When we tested the BAPTA intermediate here for POM121 and Nup133, we found that neither was observable using the directly labeled antibodies (Figure 3.5C).

Thus, we conclude that both POM121 and Nup133 are present in the novel 30 min cold intermediate defined here. These nucleoporins are present in the nuclear membrane not as a diffuse stain, but as punctate entities and are already comparable in size to nuclear pores, indicating significant oligomerization of these nucleoporins might have occurred.

Oligomerization of ELYS is dependent on membranes and occurs

concurrently with the appearance of POM121 and Nup133 entities.

To determine what occurs on the nuclear face of the NE, we initiated nuclear assembly from chromatin templates at 15°C and stained for the chromatin-bound, pore targeting protein, ELYS (Rasala *et al.*, 2006; Franz *et al.*, 2007; Gillespie *et al.*, 2007). A timecourse at 15°C revealed that ELYS initially binds to chromatin in a diffuse pattern (Figure 3.6, 15 min). However, at 30 min 15°C, a punctate ELYS stain could be seen at the chromatin periphery (asterisk, Figure 3.6, 30 min; see also Figure 3.7, bottom row). As described above, these nuclei do not contain mature nuclear pores, as determined by the lack of FG-Nup staining. While punctate ELYS rim staining was observed in the 30 min 15°C intermediate, similar punctate staining was never seen when chromatin substrates were incubated with egg cytosol in the absence of membranes (Figure 3.7). Thus, these data suggest that the oligomerization of ELYS on the nuclear face of the NE occurs concurrently with the appearance of Nup133 and POM121 on the cytoplasmic face of the NE. Furthermore, the organization of ELYS into punctate entities is dependent on the presence of membranes.

A diffusion channel is lacking in the POM121^{+}/Nup133^{+} partial pore intermediate.

An important event in new pore assembly within an intact nucleus is the opening of a channel between the inner and outer nuclear membranes. This

channel presumably would begin in its simplest form as a fusion pore, grow to an expanded fusion pore, and eventually encompass the structure that includes the diffusion channel present in mature nuclear pores.

Nuclear pore complexes, while mediating active nucleocytoplasmic traffic of large proteins and RNAs, contain an effective aqueous channel which allows the non-specific passive diffusion of smaller macromolecules (Feldherr and Akin, 1997; Keminer and Peters, 1999; Peters, 2005; Naim *et al.*, 2007). Fluorescent molecules from dextrans to proteins have been used for decades to characterize the functional size for diffusion through mature vertebrate nuclear pores (Peters, 1984). Dextrans or proteins ≤20 kD (i.e., ≤10 nm in diameter) (Lenart *et al.*, 2003) can freely diffuse in and out of the nucleus through mature nuclear pores, using these aqueous channels.

To characterize whether the $POM121^{+}$/$Nup133^{+}$ partial pore cold nuclear intermediate described above contains open channels capable of diffusion, we developed a modified diffusion assay designed to detect small channels. This assay, first performed on control nuclei at room temperature, is as follows: Assembly reactions are initiated on chromatin templates at room temperature and incubated for 30 min (Figure 3.8A) or 60 min (data not shown). Completely enclosed nuclei are formed in both cases. At the end of the reaction, Alexa488-labeled 10 kD dextran is added. After 15 min on ice, anti-Alexa488 antibody is then added to quench all Alexa488-labeled dextran fluorescence that is *outside* the nucleus. After quenching of this external

fluorescence, the reactions are stopped by fixation and the nuclei are analyzed by fluorescence microscopy. In the room temperature control 30 min nuclei, channels clearly must be present, as Alexa488-10 kD dextran was visualized inside the nuclei (Figure 3.8A; RT, 30 min). In contrast, in BAPTA-treated pore-free nuclei, Alexa488-10kD dextran was absent (Figure 3.8A; BAPTA).

Using this novel quenching assay for channels, we assessed the 15°C, 30 min cold intermediate. We found that all cold intermediates that excluded Alexa568-labeled DNA antibody did not to allow the entry of Alexa488-10 kD dextran (asterisk, Figure 3.8B). These findings demonstrate that the $POM121^{+}/Nup133^{+}$ partial pore membrane intermediate lacks 10 kD-competent channels.

To determine whether a smaller channel might be present, we repeated the above using Alexa488-labled 3 kD dextran. This too was excluded from the cold intermediate (Figure 3.8C), indicating that the $POM121^{+}/Nup133^{+}$ cold intermediate lacks channels accessible to 3 kD dextran (Luby-Phelps, 1989).

As the reactions were allowed to proceed, 100% of the 15°C nuclei excluding anti-DNA antibody became permeable to Alexa488-3 kD or 10 kD dextran at 60 min (Figure 3.9 and data not shown). Thus, between 30 min and 60 min, diffusion channels formed in the double nuclear membrane. The development of channels coincides with the recruitment of FG Nups (Figure 3.2A). Stated differently, a $POM121^{+}/Nup133^{+}$ channel-negative intermediate is observed in the early stages of nuclear pore assembly. This then matures

into a channel-positive, FG Nup-containing nuclear pore complex.

The membrane fusion inhibitor LPC blocks channel formation and FG Nup recruitment.

If no channel exists in the 30 min cold intermediate, i.e., if the intermediate has not yet undergone fusion between the inner and outer nuclear membranes, this intermediate should be sensitive to membrane fusion inhibitors, such as lysophosphatidylcholine (LPC). LPC is an inverted cone-shaped lipid known to inhibit diverse biological fusion reactions by inhibiting the bending of the contacting leaflets of the fusing membranes; bending which is required to transition to the well-known hemifusion intermediate.

As a control for the efficacy of LPC in the in vitro reaction, nuclear membrane formation was tested in the presence of LPC. LPC was added to a nuclear assembly reaction at t=0 min and assembly was allowed to proceed at room temperature for 60 min. The addition of LPC did not prevent membrane vesicles from being recruited to the chromatin, but blocked their fusion into double nuclear membranes (Figure 3.10). The LPC block to nuclear membrane fusion was indistinguishable from that of the chemical fusion inhibitor GTPγS by confocal microscopy (Figure 3.10) (Boman *et al.*, 1992).

This LPC block to vesicle-vesicle fusion could be specifically counteracted: if the cone-shaped lipid oleic acid (OA) was added with LPC at t=0 min, formation of complete nuclear membranes was observed (LPC/OA,

Figure 3.10). We conclude that LPC and OA act in opposing ways on the vesicle-vesicle fusion required to form the two nuclear membranes, as expected from their effects on other known biological hemifusion reactions.

The critical question for the present study, however, was whether we could identify an LPC-sensitive fusion step in nuclear pore formation itself. To ask this, we started with the completely membrane-enclosed cold intermediate described above which contains ELYS, POM121 and Nup133, but lacks the FG nucleoporins and a dextran-accessible diffusion channel.

Buffer, LPC, or LPC+OA were added to reactions containing this 30 min cold intermediate. The reactions were allowed to proceed for an additional 90 min at 15°C, then assayed for the presence of 10 kD-competent channels, using Alexa488-10 kD dextran and Alexa568-anti DNA antibody. In the buffer control, the intermediate proceeded to a channel-positive state by 90 min (Figure 3.11, top panel). The addition of LPC, however, blocked the formation of 10 kD dextran-competent channels (asterisk, Figure 3.11). The presence of OA counteracted this block, i.e., 10 kD channels formed (Figure 3.11). These results indicate that LPC prevents channel formation. The specific counteraction of an LPC block to channel formation by OA addition further supports this conclusion.

Strikingly, no FG nucleoporin signal was observed on the LPC-treated nuclei, indicating that no accessible FG nucleoporins were present, even at 120 min of total incubation (asterisk, Figure 3.12A). A full block to FG Nup

staining was consistently seen with LPC, but the defect was prevented by inclusion of LPC+OA (Figure 3.12A and B). Thus, LPC causes a strong defect in mature NPC assembly.

In conclusion, a diffusion channel forms downstream from ELYS, POM121 and Nup133 recruitment and their organization into punctate entities, but upstream or coincident with FG nucleoporin recruitment.

Discussion

Here we arrest and isolate novel in vitro intermediates in nuclear pore assembly. We do so in two ways: (1) by slowing fusion progression through lowering the temperature of nuclear assembly, and (2) by blocking inner/outer membrane fusion by altering lipid composition with LPC. Sensitivity to LPC reveals that a hemifusion intermediate must occur in nuclear pore assembly and that lipid mixing between the inner and outer membranes is involved in the assembly of nuclear pore complexes. Our results show that inner/outer nuclear membrane fusion occurs following to the recruitment of ELYS, POM121, and Nup133 to the nuclear membrane, but precedes channel formation and recruitment of FG nucleoporins. These findings further argue that association of specific nucleoporins at the early stages of nuclear pore assembly sets the stage for fusion between the inner and outer nuclear membranes.

Low temperature has often been used as an inhibitor of biological

processes involving membrane fusion (Palade, 1975; Blumenthal *et al.*, 1987; Beckers and Rothman, 1992). Nuclear assembly in vitro with extracts of *Xenopus laevis* eggs is typically performed at room temperature, as the physiological temperature for *Xenopus laevis* is ~22-23ºC (Fort *et al.*, 2004). Nuclear assembly in vitro involves many steps including extensive vesicle-vesicle fusion, and, in intact nuclei, has been predicted to require a second fusion event between the nuclear membranes to form the multimeric pore complex (Macaulay and Forbes, 1996; Goldberg *et al.*, 1997; Harel *et al.*, 2003a; D'Angelo *et al.*, 2006). Each of these steps could theoretically be influenced by temperature, as lowered temperature has been shown to affect the lateral mobility of fusion proteins and to reduce the rate of fusion (Palade, 1975). In this study by lowering the temperature to 15ºC, we were able to slow down nuclear assembly. As a result, we observed a cold intermediate in nuclear pore assembly (Figure 3.2). Nuclear pore formation is thus temperature sensitive.

The formation of nuclear pores in existing nuclear membranes by definition must include an interaction between the lumenal domains of the inner and outer nuclear membranes. The fusogenic proteins in this event are unknown. The fusion machinery needs to bring the two membranes into sufficiently close proximity to allow membrane fusion to occur. For fusion to occur, the 20-25 nm distance between the inner and outer nuclear membranes needs to be bridged. One might predict that a transmembrane nucleoporin

with a large lumenal domain would be involved. To date, three integral membrane proteins are components of the vertebrate nuclear pore, POM121, gp210, and the recently discovered NDC1 (Gerace *et al.*, 1982; Wozniak *et al.*, 1989; Greber *et al.*, 1990; Hallberg *et al.*, 1993; Cotter *et al.*, 1998; Liu *et al.*, 2003; Lau *et al.*, 2006; Mansfeld *et al.*, 2006; Stavru *et al.*, 2006a). The majority of POM121 is not lumenal, nor is the majority of NDC1. Thus, both proteins lack significant lumenal parts to make direct contact between the opposing bilayers. In contrast, most of the mass of gp210 is lumenally located, which makes this protein a good candidate for playing a role in the inner/outer membrane fusion event (Wozniak *et al.*, 1989; Drummond and Wilson, 2002). However, during postmitotic nuclear envelope formation in mammalian cells, gp210 is recruited to the nuclear periphery at quite a late stage (Bodoor *et al.*, 1999). In addition, both biochemical depletion and RNAi depletion studies indicate that the nuclear pore can assemble in the absence of gp210 (Eriksson *et al.*, 2004; Olsson *et al.*, 2004; Antonin *et al.*, 2005; Stavru *et al.*, 2006b), and some mouse cell types have been shown to lack gp210 altogether (Olsson *et al.*, 2004).

Because of the large distance between the two membranes, the proteins involved in pore formation have to draw the membranes toward one another or bend them locally (Leikin *et al.*, 1987). It has been suggested that nuclear pore insertion could rely on ‘disposable‘ fusion proteins with the fusion factor being degraded and resynthesized during every cell cycle (Stavru *et al.*,

2006a). Alternatively, one could hypothesize that local oligomerization of the pore proteins could form a curved complex which would bend the membranes inward toward one another (Reynwar *et al.*, 2007). We were indeed able to detect an intermediate that contained oligomers of ELYS, POM121 and Nup133, but not FG nucleoporins (Figure 3.5 and 3.6).

We believe that the ELYS, POM121- and the Nup133-staining structures observed in the cold intermediate are much larger than single molecules. The punctate entities are indistinguishable in size from mature nuclear pores (Figure 3.5A and 3.5B). Interestingly, we show that the BAPTA pore-free intermediate that has been studied previously (Macaulay and Forbes, 1996; Harel *et al.*, 2003a) lacks accessible POM121 and Nup133 (Figure 3.5C) and thus is an earlier molecular intermediate to the intermediates described here.

When modeling a mechanism by which the pore can assemble in intact membranes, it would be logical to propose that a lateral association of individual membrane pore proteins within the bilayer would occur first. Our results suggest a specific homotypic/heterotypic lateral association of ELYS, POM121 and the Nup107-160 complex, represented by Nup133 staining, occurs at early stages of nuclear pore formation in the nuclear membranes. Indeed, the Nup107-160 complex binds to POM121 in biochemical assays (Rasala, *et al*., submitted). These proteins could: (1) initiate this lateral aggregation, or (2) could be aggregated by an unknown lumenal protein.

Even though it is thought that nuclear pores develop through membrane fusion between the outer and inner membranes in intact nuclei (Macaulay and Forbes, 1996; Goldberg *et al.*, 1997; D'Angelo *et al.*, 2006), this membrane fusion step has never been biochemically identified nor mapped in its temporal order with respect to specific nucleoporin recruitment. We demonstrate here that the addition of LPC to the $POM121^{+}$/$Nup133^{+}$ cold intermediate prevents the recruitment of FG nucleoporins and, strikingly, the formation of a 3 kD dextran-competent channel (Figure 3.11 and 3.12). Thus, LPC inhibits nuclear pore formation and is concluded to do so through its block of hemifusion between the inner and outer nuclear membrane lipid bilayers. We believe that normally fusion to form a membrane channel must precede or be concomitant with recruitment of the soluble FG proteins of the pore, forming a complete nuclear pore complex. A model incorporating these findings is shown in Figure 3.13.

Figures

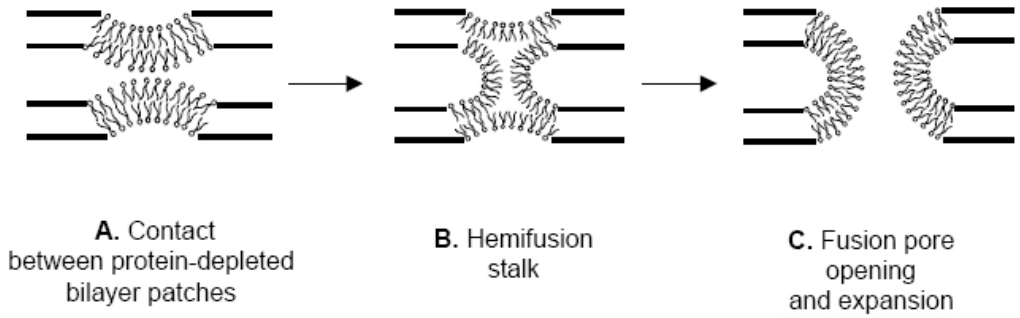

Adapted from Chernomordik et al., 2006

Figure 3.1. The "stalk-pore" pathway of membrane fusion. After establishing contact, membrane-associated proteins (not shown) move apart to allow local close physical contact (A) between the contacting leaflets of two membrane bilayers. This is followed by a merger of the contacting leaflets into a stalk-like hemifusion complex (B). The hemifusion complex then progresses and a lipidic fusion pore opens and expands, which completes the fusion reaction (C).

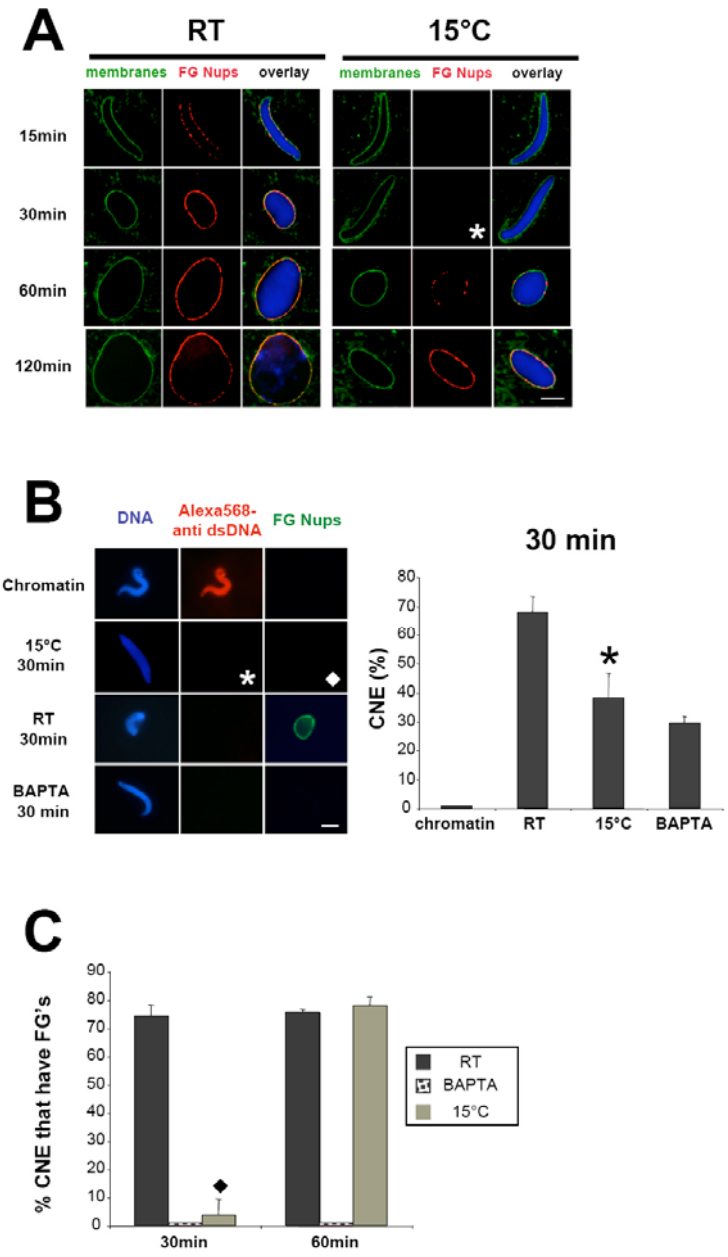

Figure 3.2. Cold temperature produces a novel intermediate in NPC assembly.
(A) The progression of nuclear envelope assembly is slowed down at 15ºC. Nuclear assembly reactions containing chromatin, cytosol and membranes were set up at different temperatures. Reactions were stopped at the indicated time points and analyzed by confocal microscopy after direct immunofluorescence with mAb414 (red). Nuclear membranes were visualized with the fluorescent membrane dye DHCC (green) and chromatin was stained with DAPI (blue). Scale bars, 10 μm. (B) A DNA antibody exclusion assay was used to determine the formation of closed nuclear envelope (CNE) at indicated times at room temperature (RT) and 15ºC on regular and BAPTA-treated nuclei. The formation of CNE was quantified for at least 100 randomly chosen chromatin substrates in three independent experiments (histogram). Scale bars, 10 μm. (C) The percentage of CNE containing FG Nups was plotted using three different experiments. Errors bars indicate the standard deviation SD.

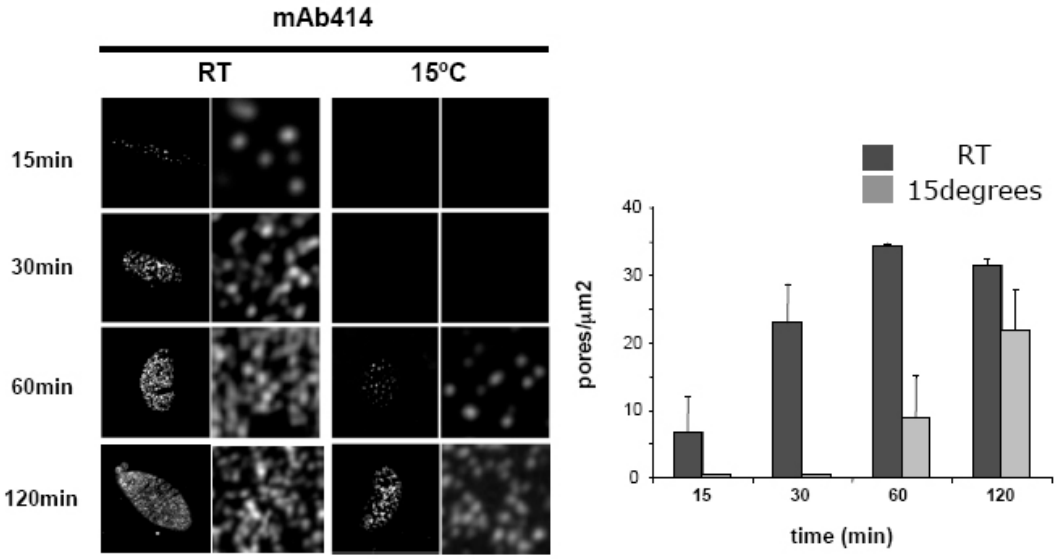

Figure 3.3. NPC density increases over time at 15°C. Individual NPCs were visualized by immunofluorescence with Alexa568-mAb414 on the surface at low magnification and with 8x zoom. Pore density for each condition was calculated using three independent experiments as described in the Methods and plotted. Error bars indicate SD.

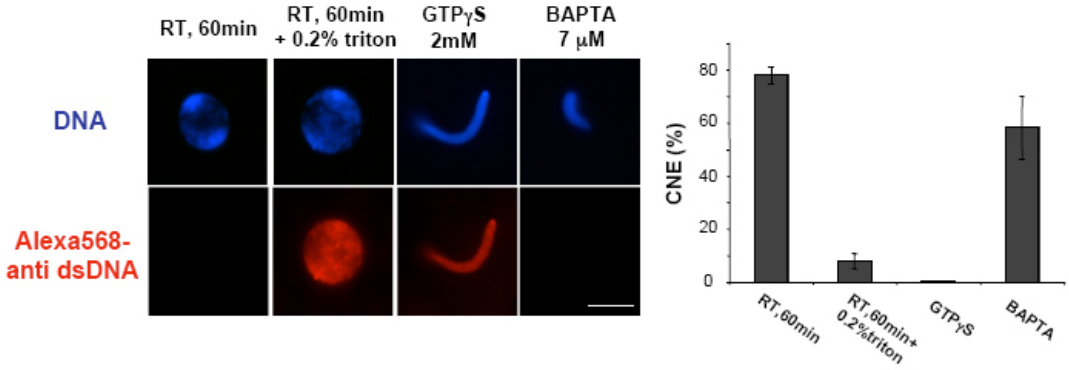

Figure 3.4. Closed nuclear envelope (CNE) analysis with an Alexa568-α-DNA antibody. An exclusion assay to determine the formation of a completely enclosed nuclear envelope was carried out on chromatin incubated with GTPγS-treated, BAPTA-treated or regular extract. Nuclei were also permeabilized with TritonX-100, as control. Labeling of chromatin with the Alexa568-α-dsDNA indicates that a fully closed NE has not formed; absence of antibody indicates that it has formed. Scale bars, 10 µm. Error bars indicate SD.

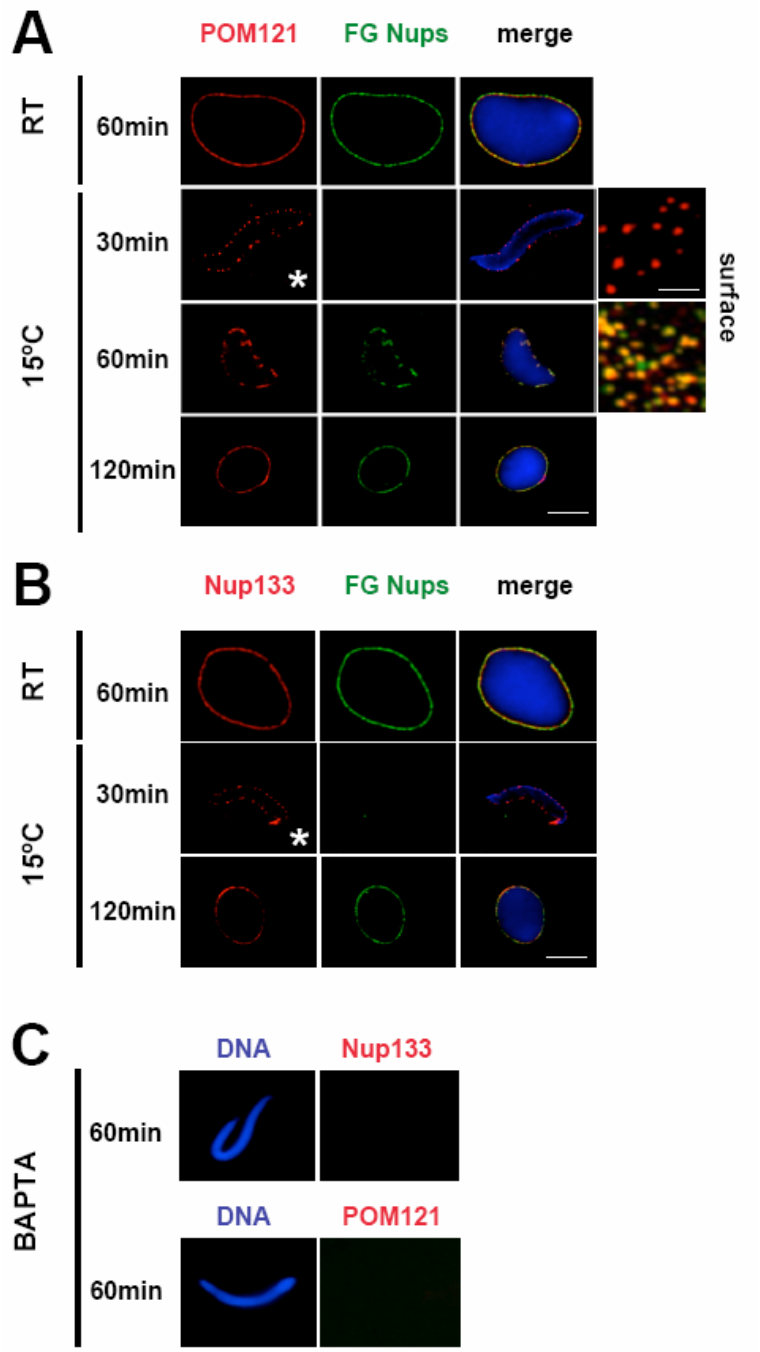

Figure 3.5. The cold intermediate contains punctate POM121 and Nup133.
(A) Nuclear assembly reactions were stopped at the indicated times at 15ºC and analyzed by confocal microscopy after direct immunofluorescence with Alexa568-α-POM121 and Alexa488-mAb414. The merged images (yellow) are at the right. Chromatin was stained with DAPI (blue). Scale bars, 10 μm. Individual NPCs were visualized on the surface of the intermediates at high magnification for the 30 min and 60 min nuclei assembled at 15°C. (B) The assembly reaction at 15° was also analyzed with Alexa568-α-Nup133 and Alexa488-mAb414. Scale bars, 10 μm. (C) Nuclei assembled in the presence of the pore-inhibitor BAPTA do not contain POM121 and Nup133 in their nuclear membranes.

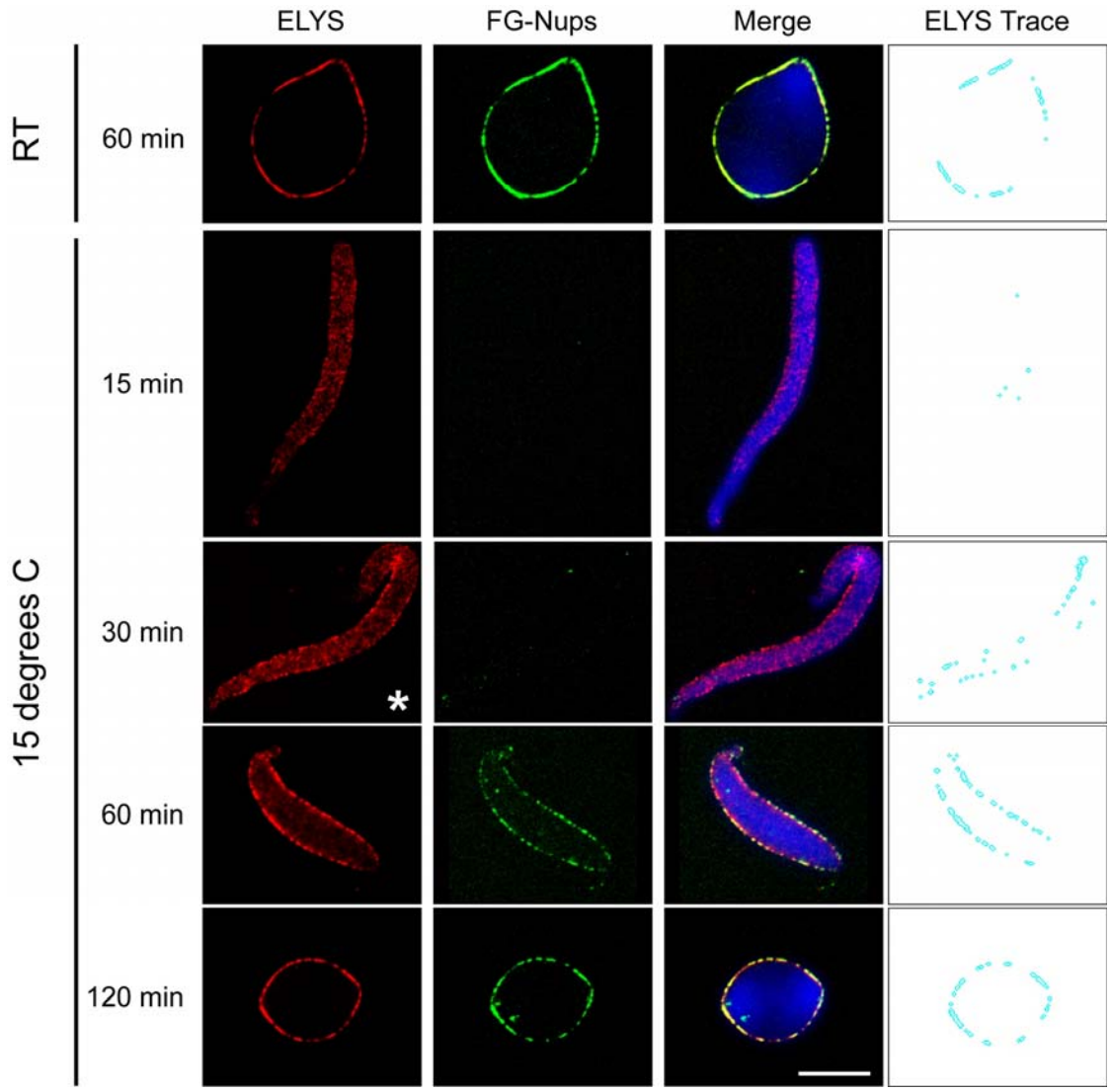

Figure 3.6. A timecourse of ELYS at 15°C. Nuclear assembly reactions were stopped at the indicated times at 15ºC and analyzed by confocal microscopy after direct immunofluorescence with Alexa568-α-xELYS (red) and Alexa488-mAb414 (green). DNA was stained with DAPI (blue). The images on the right show the contour traces of the Alexa568-α-xELYS antibody signals. Scale bars, 10 μm.

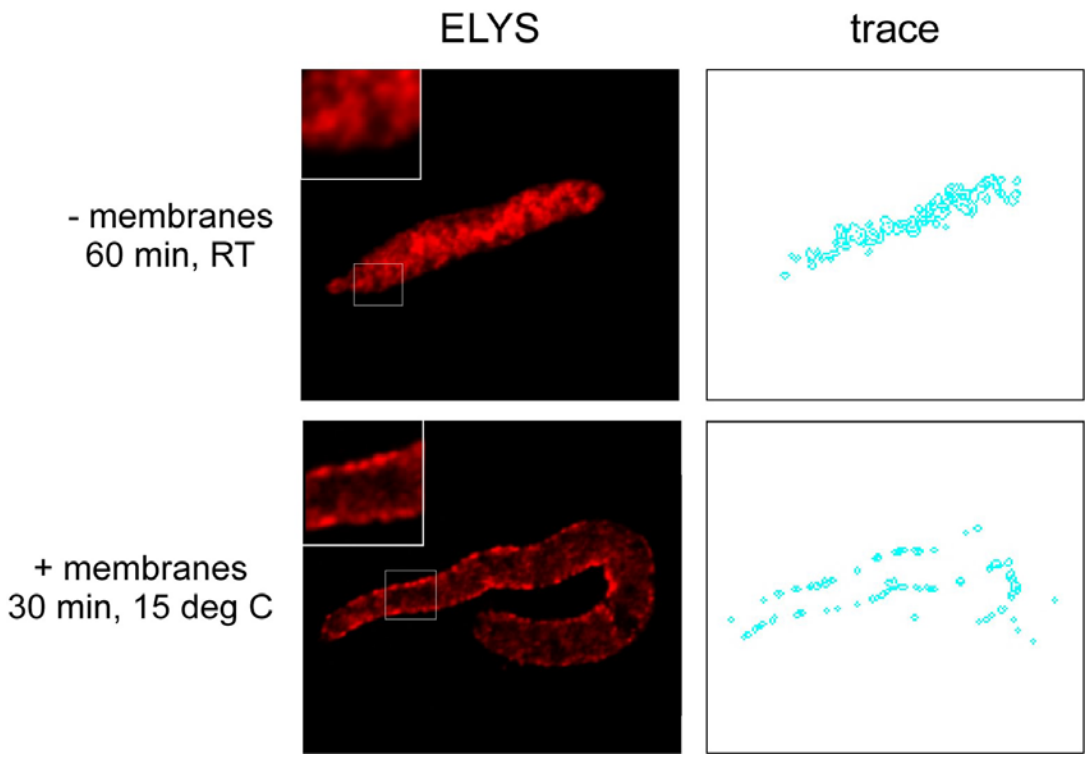

Figure 3.7. The oligomerization of ELYS at the nuclear periphery is dependent on membranes. In the absence of membranes, Alexa568-α-xELYS stains chromatin in a diffuse pattern, even when reactions are allowed to proceed for 60 minutes at room temperature (RT, top). In the presence of membranes, the majority of the Alexa568-α-xELYS fluorescent signal is localized to the nuclear periphery in punctate dots after only 30 minutes at 15°C. The insets are 200% magnifications of the indicated areas. The images on the right show the contour traces of the Alexa568-α-xELYS antibody signals.

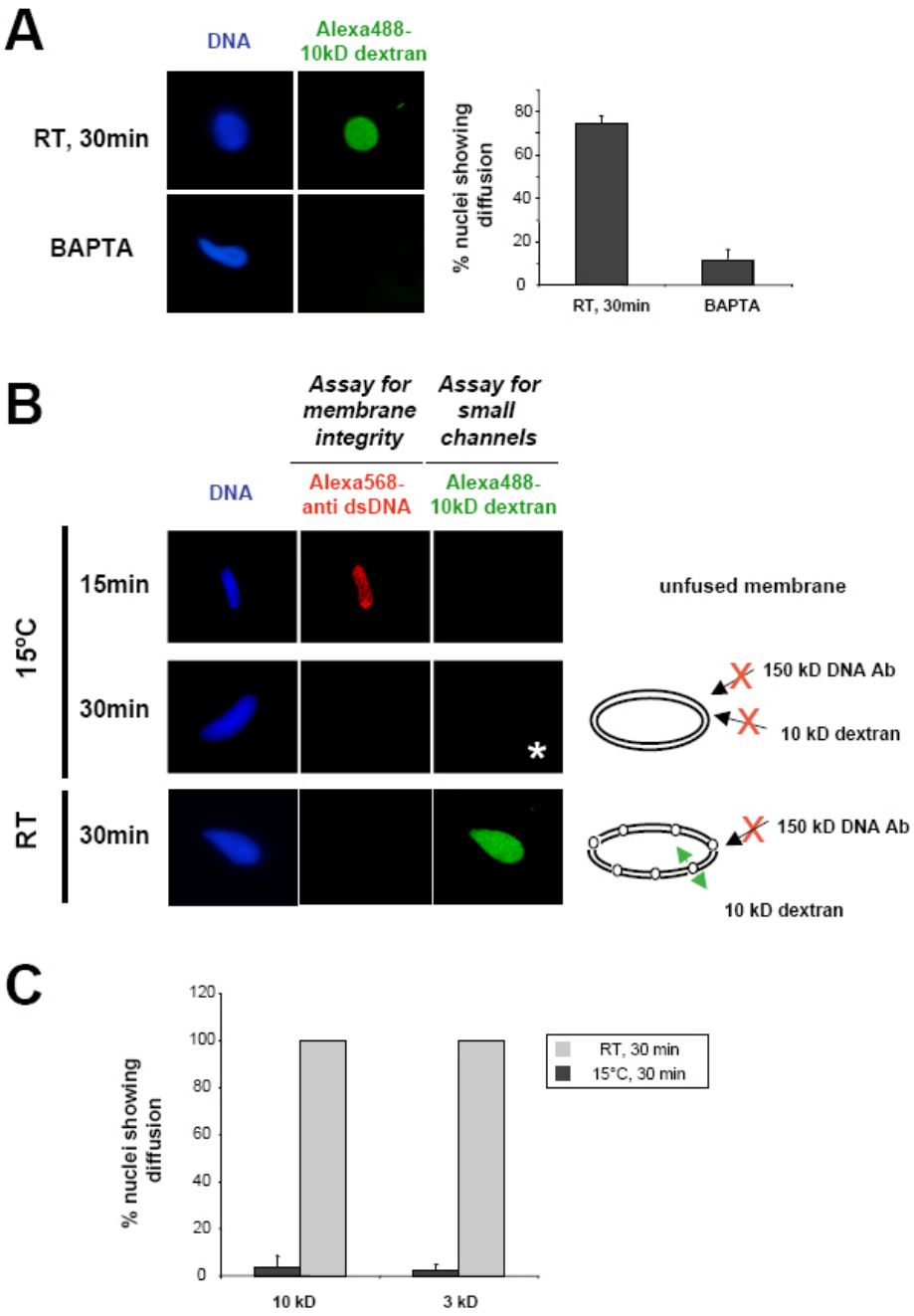

Figure 3.8. The cold intermediate lacks a diffusion channel. (A) In order to check for the presence of diffusion channels through the nuclear envelope, we used a dextran-diffusion assay on control nuclei and BAPTA-treated nuclei. The percentage of nuclei showing diffusion of Alexa488 10kD dextran was quantified for at least 100 randomly chosen nuclear intermediates in three independent experiments (histogram). Errors bars indicate SD. (B) The same assay was used to determine the presence of 10kD competent-diffusion channels on a closed nuclear envelope at 15 and 30 min at 15°C. (C) The percentage of enclosed nuclei showing diffusion of Alexa488-10kD or Alexa488-3kD dextrans was plotted using three different experiments. Errors bars indicate the standard deviation SD.

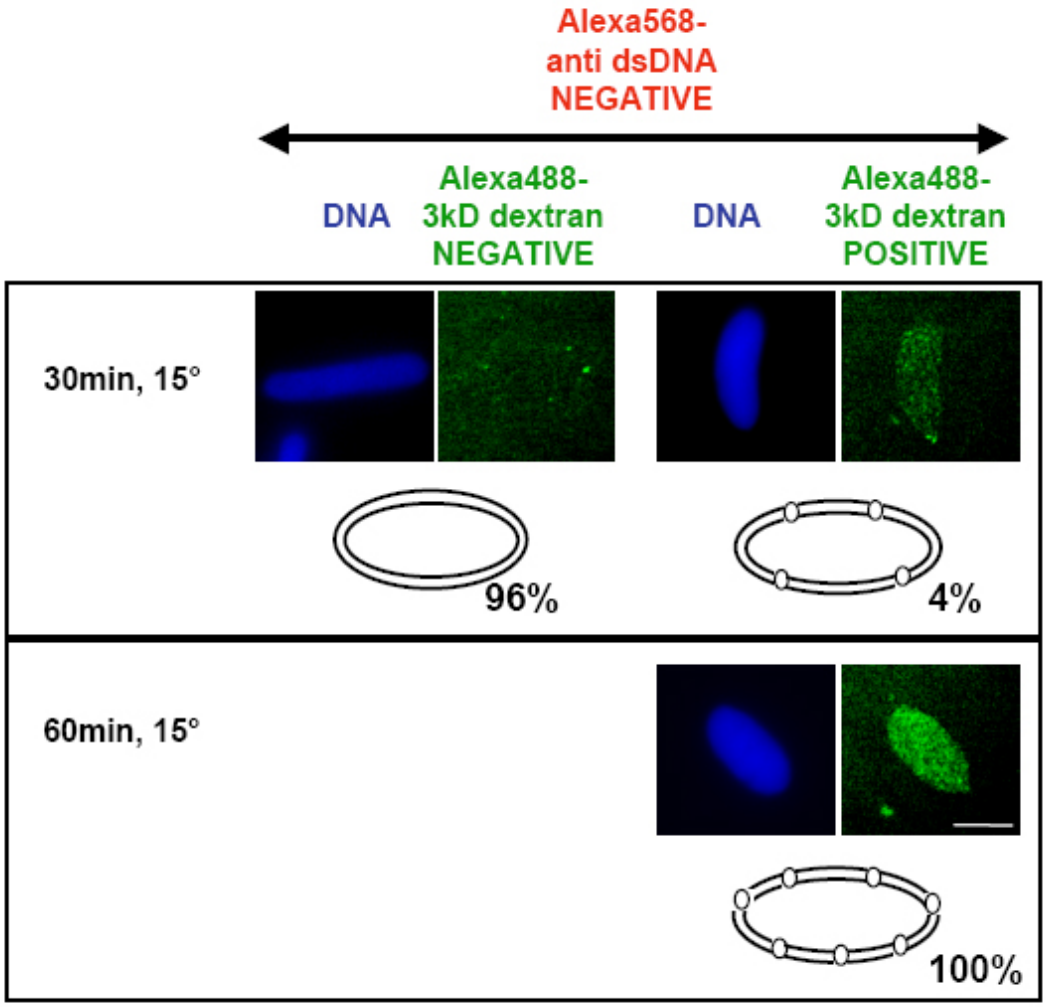

Figure 3.9. A timecourse indicates that the diffusion channel develops late at 15°C, coinciding with FG Nup assembly. The diffusion assay was performed at different times on nuclei formed at 15°C. Only the nuclei showing closed nuclear envelopes (CNE) according to our DNA antibody exclusion assay were analyzed for 3kD-dextran uptake. Scale bars, 10 μm.

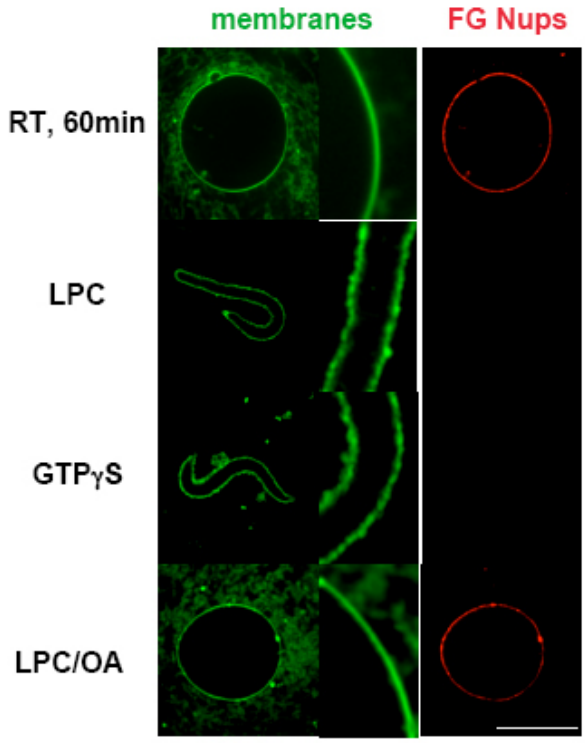

Figure 3.10. LPC inhibits vesicle-vesicle fusion and nuclear pore assembly at room temperature. Nuclear reconstitution reactions were set up at room temperature and supplemented at t=0 with buffer (RT, 60min), LPC, or LPC and OA. The formation of nuclear membranes was assayed at 1h with DHCC (green). The enlargements are magnified 3x. FG nucleoporins were detected with Alexa568-mAb414 antibody. LPC blocks vesicle-vesicle fusion in a manner similar to GTPγS. LPC and OA added together compensate the effects of each other on lipid mixing. Fusion was restored and FG nucleoporins incorporated, as shown by the nuclear rim staining with Alexa568-mAb414 (LPC/OA). Scale bars, 10 μm.

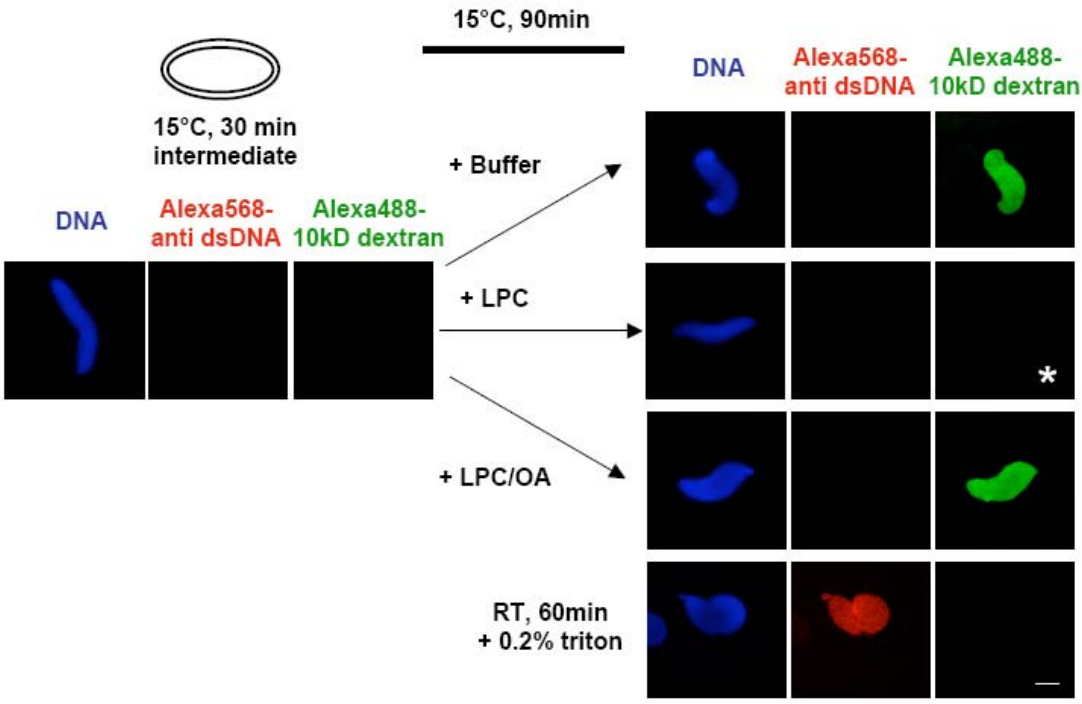

Figure 3.11. The fusion inhibitor LPC blocks diffusion channel formation. Nuclei were formed for 30 min at 15°C and the preparation was verified for the absence of diffusion channels with Alexa488-10 kD dextran. LPC was added to these nuclei, followed by incubation for 90 min, in order to assess the affect of LPC on channel formation. A block was observed. To confirm that LPC blocks at the lipid-mixing stage in NPC formation, LPC and OA were added together to the cold-arrested, followed by incubation for 90 min. The nuclei were then assayed for channel formation with Alexa488-10 kD dextran. Diffusion of Alexa488-10 kD dextran into the nuclei was now observed. Scale bars, 10 μm.

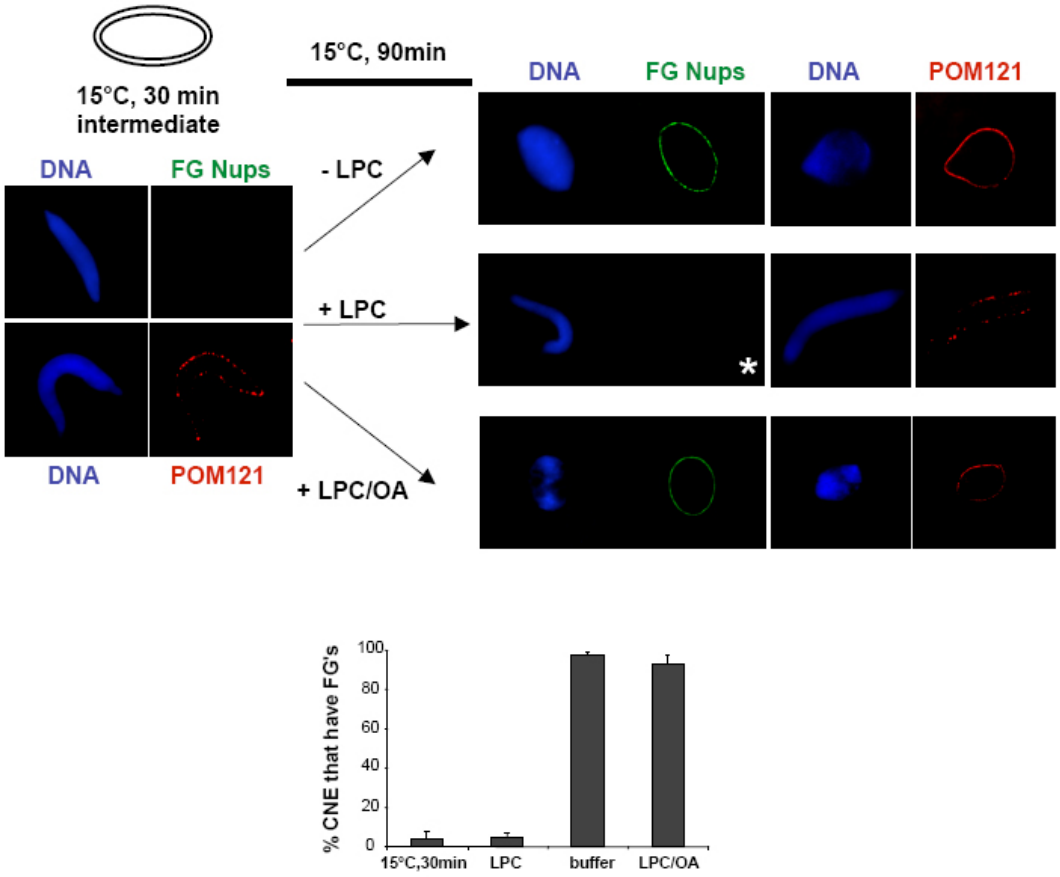

Figure 3.12. The fusion inhibitor LPC prevents FG Nups assembly into the cold intermediate. (A) Nuclei were formed for 30 min at 15°C and the preparation was verified for the presence for POM121 with Alexa568-α-POM121 and the absence of FG Nups with Alexa488-mAb414. Buffer (-LPC), LPC, or LPC/OA were added to these nuclei, followed by incubation for 90 min. **(B)** The percentage of closed nuclei containing FG Nups, was plotted using three different experiments. Errors bars indicate SD.

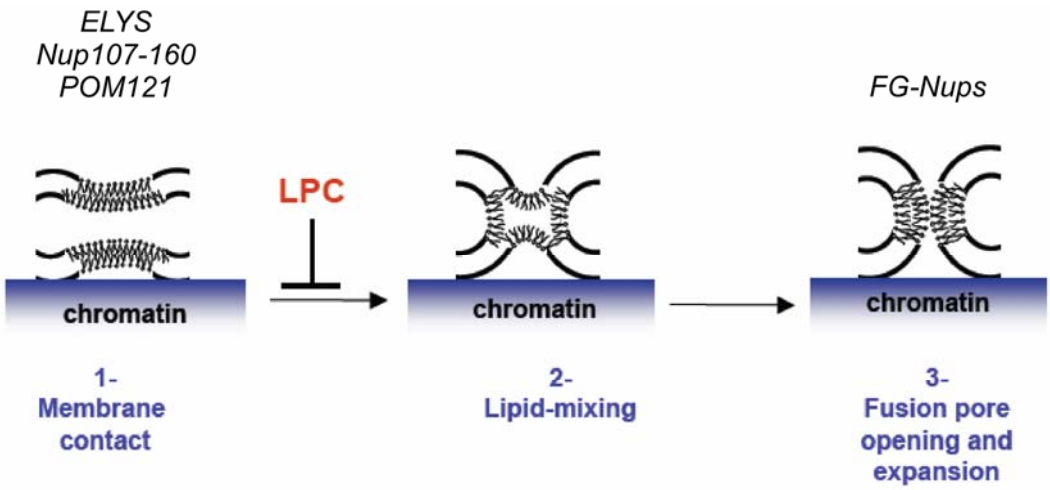

Figure 3.13. A model for fusion-dependent nuclear pore assembly. Our data demonstrate that nuclear pore assembly is dependent on inner/outer nuclear membrane fusion. Furthermore, we show that the opening of a diffusion channel and FG Nup recruitment are late events in NPC assembly.

Acknowledgements

The text in Chapter 3 is a modified version of a manuscript in preparation for publication: Corinne Ramos, **Beth A. Rasala**, and Douglass J. Forbes, Structural intermediates in fusion mediated NPC assembly. I was the secondary researcher listed in this publication which forms the basis for this chapter.

References

Antonin, W., Franz, C., Haselmann, U., Antony, C., and Mattaj, I.W. (2005). The integral membrane nucleoporin pom121 functionally links nuclear pore complex assembly and nuclear envelope formation. Mol Cell *17*, 83-92.

Baur, T., Ramadan, K., Schlundt, A., Kartenbeck, J., and Meyer, H.H. (2007). NSF- and SNARE-mediated membrane fusion is required for nuclear envelope formation and completion of nuclear pore complex assembly in Xenopus laevis egg extracts. J Cell Sci *120*, 2895-2903.

Beckers, J.M., and Rothman, J.E. (1992). Transport between Golgi cisternae. Methods Enzymol *219*, 5-12.

Blobel, C.P., Wolfsberg, T.G., Turck, C.W., Myles, D.G., Primakoff, P., and White, J.M. (1992). A potential fusion peptide and an integrin ligand domain in a protein active in sperm-egg fusion. Nature *356*, 248-252.

Blumenthal, R., Bali-Puri, A., Walter, A., Covell, D., and Eidelman, O. (1987). pH-dependent fusion of vesicular stomatitis virus with Vero cells. Measurement by dequenching of octadecyl rhodamine fluorescence. J Biol Chem *262*, 13614-13619.

Bodoor, K., Shaikh, S., Salina, D., Raharjo, W.H., Bastos, R., Lohka, M., and Burke, B. (1999). Sequential recruitment of NPC proteins to the nuclear periphery at the end of mitosis. J Cell Sci *112 (Pt 13)*, 2253-2264.

Boman, A.L., Delannoy, M.R., and Wilson, K.L. (1992). GTP hydrolysis is required for vesicle fusion during nuclear envelope assembly in vitro. J Cell Biol *116*, 281-294.

Chernomordik, L.V., Frolov, V.A., Leikina, E., Bronk, P., and Zimmerberg, J. (1998). The pathway of membrane fusion catalyzed by influenza hemagglutinin: restriction of lipids, hemifusion, and lipidic fusion pore formation. J Cell Biol *140*, 1369-1382.

Chernomordik, L.V., and Kozlov, M.M. (2003). Protein-lipid interplay in fusion and fission of biological membranes. Annu Rev Biochem *72*, 175-207.

Chernomordik, L.V., Melikyan, G.B., and Chizmadzhev, Y.A. (1987). Biomembrane fusion: a new concept derived from model studies using two interacting planar lipid bilayers. Biochim Biophys Acta *906*, 309-352.

Chernomordik, L.V., Vogel, S.S., Sokoloff, A., Onaran, H.O., Leikina, E.A., and Zimmerberg, J. (1993). Lysolipids reversibly inhibit Ca(2+)-, GTP- and pH-

dependent fusion of biological membranes. FEBS Lett *318*, 71-76.

Cotter, L.A., Goldberg, M.W., and Allen, T.D. (1998). Nuclear pore complex disassembly and nuclear envelope breakdown during mitosis may occur by both nuclear envelope vesicularisation and dispersion throughout the endoplasmic reticulum. Scanning *20*, 250-251.

D'Angelo, M.A., Anderson, D.J., Richard, E., and Hetzer, M.W. (2006). Nuclear pores form de novo from both sides of the nuclear envelope. Science *312*, 440-443.

Drummond, S.P., and Wilson, K.L. (2002). Interference with the cytoplasmic tail of gp210 disrupts "close apposition" of nuclear membranes and blocks nuclear pore dilation. J Cell Biol *158*, 53-62.

Earp, L.J., Delos, S.E., Park, H.E., and White, J.M. (2005). The many mechanisms of viral membrane fusion proteins. Curr Top Microbiol Immunol *285*, 25-66.

Eriksson, C., Rustum, C., and Hallberg, E. (2004). Dynamic properties of nuclear pore complex proteins in gp210 deficient cells. FEBS Lett *572*, 261-265.

Feldherr, C.M., and Akin, D. (1997). The location of the transport gate in the nuclear pore complex. J Cell Sci *110 (Pt 24)*, 3065-3070.

Fort, D.J., Rogers, R.L., Thomas, J.H., Buzzard, B.O., Noll, A.M., and Spaulding, C.D. (2004). Comparative sensitivity of Xenopus tropicalis and Xenopus laevis as test species for the FETAX model. J Appl Toxicol *24*, 443-457.

Franz, C., Walczak, R., Yavuz, S., Santarella, R., Gentzel, M., Askjaer, P., Galy, V., Hetzer, M., Mattaj, I.W., and Antonin, W. (2007). MEL-28/ELYS is required for the recruitment of nucleoporins to chromatin and postmitotic nuclear pore complex assembly. EMBO Rep *8*, 165-172.

Funakoshi, T., Maeshima, K., Yahata, K., Sugano, S., Imamoto, F., and Imamoto, N. (2007). Two distinct human POM121 genes: requirement for the formation of nuclear pore complexes. FEBS Lett *581*, 4910-4916.

Gattegno, T., Mittal, A., Valansi, C., Nguyen, K.C., Hall, D.H., Chernomordik, L.V., and Podbilewicz, B. (2007). Genetic control of fusion pore expansion in the epidermis of Caenorhabditis elegans. Mol Biol Cell *18*, 1153-1166.

Gerace, L., Ottaviano, Y., and Kondor-Koch, C. (1982). Identification of a major polypeptide of the nuclear pore complex. J Cell Biol *95*, 826-837.

Gillespie, P.J., Khoudoli, G.A., Stewart, G., Swedlow, J.R., and Blow, J.J. (2007). ELYS/MEL-28 chromatin association coordinates nuclear pore complex assembly and replication licensing. Curr Biol *17*, 1657-1662.

Goldberg, M.W., Wiese, C., Allen, T.D., and Wilson, K.L. (1997). Dimples, pores, star-rings, and thin rings on growing nuclear envelopes: evidence for structural intermediates in nuclear pore complex assembly. J Cell Sci *110 (Pt 4)*, 409-420.

Greber, U.F., Senior, A., and Gerace, L. (1990). A major glycoprotein of the nuclear pore complex is a membrane-spanning polypeptide with a large lumenal domain and a small cytoplasmic tail. Embo J *9*, 1495-1502.

Hallberg, E., Wozniak, R.W., and Blobel, G. (1993). An integral membrane protein of the pore membrane domain of the nuclear envelope contains a nucleoporin-like region. J Cell Biol *122*, 513-521.

Harel, A., Chan, R.C., Lachish-Zalait, A., Zimmerman, E., Elbaum, M., and Forbes, D.J. (2003a). Importin beta negatively regulates nuclear membrane fusion and nuclear pore complex assembly. Mol Biol Cell *14*, 4387-4396.

Harel, A., Orjalo, A.V., Vincent, T., Lachish-Zalait, A., Vasu, S., Shah, S., Zimmerman, E., Elbaum, M., and Forbes, D.J. (2003b). Removal of a single pore subcomplex results in vertebrate nuclei devoid of nuclear pores. Mol Cell *11*, 853-864.

Henderson, H.I., and Hope, T.J. (2006). The temperature arrested intermediate of virus-cell fusion is a functional step in HIV infection. Virol J *3*, 36.

Hetzer, M., Bilbao-Cortes, D., Walther, T.C., Gruss, O.J., and Mattaj, I.W. (2000). GTP hydrolysis by Ran is required for nuclear envelope assembly. Mol Cell *5*, 1013-1024.

Hetzer, M., Meyer, H.H., Walther, T.C., Bilbao-Cortes, D., Warren, G., and Mattaj, I.W. (2001). Distinct AAA-ATPase p97 complexes function in discrete steps of nuclear assembly. Nat Cell Biol *3*, 1086-1091.

Jahn, R., Lang, T., and Sudhof, T.C. (2003). Membrane fusion. Cell *112*, 519-533.

Keminer, O., and Peters, R. (1999). Permeability of single nuclear pores. Biophys J *77*, 217-228.

Kozlov, M.M., and Markin, V.S. (1983). [Possible mechanism of membrane fusion]. Biofizika *28*, 242-247.

Lau, C.K., Delmar, V.A., and Forbes, D.J. (2006). Topology of yeast Ndc1p: predictions for the human NDC1/NET3 homologue. Anat Rec A Discov Mol Cell Evol Biol *288*, 681-694.

Leikin, S.L., Kozlov, M.M., Chernomordik, L.V., Markin, V.S., and Chizmadzhev, Y.A. (1987). Membrane fusion: overcoming of the hydration barrier and local restructuring. J Theor Biol *129*, 411-425.

Lenart, P., Rabut, G., Daigle, N., Hand, A.R., Terasaki, M., and Ellenberg, J. (2003). Nuclear envelope breakdown in starfish oocytes proceeds by partial NPC disassembly followed by a rapidly spreading fenestration of nuclear membranes. J Cell Biol *160*, 1055-1068.

Liu, J., Prunuske, A.J., Fager, A.M., and Ullman, K.S. (2003). The COPI complex functions in nuclear envelope breakdown and is recruited by the nucleoporin Nup153. Dev Cell *5*, 487-498.

Lohka, M.J., and Masui, Y. (1983). Formation in vitro of sperm pronuclei and mitotic chromosomes induced by amphibian ooplasmic components. Science *220*, 719-721.

Lu, X., Zhang, F., McNew, J.A., and Shin, Y.K. (2005). Membrane fusion induced by neuronal SNAREs transits through hemifusion. J Biol Chem *280*, 30538-30541.

Luby-Phelps, K. (1989). Preparation of fluorescently labeled dextrans and ficolls. Methods Cell Biol *29*, 59-73.

Macaulay, C., and Forbes, D.J. (1996). Assembly of the nuclear pore: biochemically distinct steps revealed with NEM, GTP gamma S, and BAPTA. J Cell Biol *132*, 5-20.

Mansfeld, J., Guttinger, S., Hawryluk-Gara, L.A., Pante, N., Mall, M., Galy, V., Haselmann, U., Muhlhausser, P., Wozniak, R.W., Mattaj, I.W., Kutay, U., and Antonin, W. (2006). The conserved transmembrane nucleoporin NDC1 is required for nuclear pore complex assembly in vertebrate cells. Mol Cell *22*, 93-103.

Markosyan, R.M., Cohen, F.S., and Melikyan, G.B. (2003). HIV-1 envelope proteins complete their folding into six-helix bundles immediately after fusion pore formation. Mol Biol Cell *14*, 926-938.

Melia, T.J., You, D., Tareste, D.C., and Rothman, J.E. (2006). Lipidic antagonists to SNARE-mediated fusion. J Biol Chem *281*, 29597-29605.

Melikyan, G.B., Markosyan, R.M., Hemmati, H., Delmedico, M.K., Lambert, D.M., and Cohen, F.S. (2000). Evidence that the transition of HIV-1 gp41 into a six-helix bundle, not the bundle configuration, induces membrane fusion. J Cell Biol *151*, 413-423.

Mohler, W.A., Shemer, G., del Campo, J.J., Valansi, C., Opoku-Serebuoh, E., Scranton, V., Assaf, N., White, J.G., and Podbilewicz, B. (2002). The type I membrane protein EFF-1 is essential for developmental cell fusion. Dev Cell *2*, 355-362.

Naim, B., Brumfeld, V., Kapon, R., Kiss, V., Nevo, R., and Reich, Z. (2007). Passive and facilitated transport in nuclear pore complexes is largely uncoupled. J Biol Chem *282*, 3881-3888.

Newport, J. (1987). Nuclear reconstitution in vitro: stages of assembly around protein-free DNA. Cell *48*, 205-217.

Newport, J., and Dunphy, W. (1992). Characterization of the membrane binding and fusion events during nuclear envelope assembly using purified components. J Cell Biol *116*, 295-306.

Olsson, M., Scheele, S., and Ekblom, P. (2004). Limited expression of nuclear pore membrane glycoprotein 210 in cell lines and tissues suggests cell-type specific nuclear pores in metazoans. Exp Cell Res *292*, 359-370.

Palade, G. (1975). Intracellular Aspects of the Process of Protein Synthesis. Science *189*, 867.

Peters, R. (1984). Nucleo-cytoplasmic flux and intracellular mobility in single hepatocytes measured by fluorescence microphotolysis. Embo J *3*, 1831-1836.

Peters, R. (2005). The nanopore connection to cell membrane unitary permeability. Traffic *6*, 199-204.

Podbilewicz, B., Leikina, E., Sapir, A., Valansi, C., Suissa, M., Shemer, G.,

and Chernomordik, L.V. (2006). The C. elegans developmental fusogen EFF-1 mediates homotypic fusion in heterologous cells and in vivo. Dev Cell *11*, 471-481.

Rasala, B.A., Orjalo, A.V., Shen, Z., Briggs, S., and Forbes, D.J. (2006). ELYS is a dual nucleoporin/kinetochore protein required for nuclear pore assembly and proper cell division. Proc Natl Acad Sci U S A *103*, 17801-17806.

Rasala, B.A., Ramos, C., Harel, A., and Forbes, D.F. Capture of AT-rich chromatin by ELYS recruits POM121 and NDC1 to initiate nuclear pore assembly. Mol Biol Cell, submitted.

Reese, C., Heise, F., and Mayer, A. (2005). Trans-SNARE pairing can precede a hemifusion intermediate in intracellular membrane fusion. Nature *436*, 410-414.

Reynwar, B.J., Illya, G., Harmandaris, V.A., Muller, M.M., Kremer, K., and Deserno, M. (2007). Aggregation and vesiculation of membrane proteins by curvature-mediated interactions. Nature *447*, 461-464.

Sapir, A., Choi, J., Leikina, E., Avinoam, O., Valansi, C., Chernomordik, L.V., Newman, A.P., and Podbilewicz, B. (2007). AFF-1, a FOS-1-regulated fusogen, mediates fusion of the anchor cell in C. elegans. Dev Cell *12*, 683-698.

Schoch, C., Blumenthal, R., and Clague, M.J. (1992). A long-lived state for influenza virus-erythrocyte complexes committed to fusion at neutral pH. FEBS Lett *311*, 221-225.

Schwander, M., Leu, M., Stumm, M., Dorchies, O.M., Ruegg, U.T., Schittny, J., and Muller, U. (2003). Beta1 integrins regulate myoblast fusion and sarcomere assembly. Dev Cell *4*, 673-685.

Stavru, F., Hulsmann, B.B., Spang, A., Hartmann, E., Cordes, V.C., and Gorlich, D. (2006a). NDC1: a crucial membrane-integral nucleoporin of metazoan nuclear pore complexes. J Cell Biol *173*, 509-519.

Stavru, F., Nautrup-Pedersen, G., Cordes, V.C., and Gorlich, D. (2006b). Nuclear pore complex assembly and maintenance in POM121- and gp210-deficient cells. J Cell Biol *173*, 477-483.

Stegmann, T., White, J.M., and Helenius, A. (1990). Intermediates in influenza induced membrane fusion. Embo J *9*, 4231-4241.

Vasu, S., Shah, S., Orjalo, A., Park, M., Fischer, W.H., and Forbes, D.J. (2001). Novel vertebrate nucleoporins Nup133 and Nup160 play a role in mRNA export. J Cell Biol *155*, 339-354.

Walther, T.C., Askjaer, P., Gentzel, M., Habermann, A., Griffiths, G., Wilm, M., Mattaj, I.W., and Hetzer, M. (2003). RanGTP mediates nuclear pore complex assembly. Nature *424*, 689-694.

Wozniak, R.W., Bartnik, E., and Blobel, G. (1989). Primary structure analysis of an integral membrane glycoprotein of the nuclear pore. J Cell Biol *108*, 2083-2092.

Xu, Y., Zhang, F., Su, Z., McNew, J.A., and Shin, Y.K. (2005). Hemifusion in SNARE-mediated membrane fusion. Nat Struct Mol Biol *12*, 417-422.

Zhang, C., and Clarke, P.R. (2000). Chromatin-independent nuclear envelope assembly induced by Ran GTPase in Xenopus egg extracts. Science *288*, 1429-1432.

CHAPTER 4

Centrin 2 localizes to the vertebrate nuclear pore and plays a role in mRNA and protein export

Introduction

The nuclear pore complex (NPC) is the sole mediator of traffic between the nucleus and cytoplasm (3, 15, 16, 27, 39, 66, 134). The vertebrate NPC is a massive 125 MDa complex, comprised of ~30 different proteins in multiple copies per pore (18, 102). Together these proteins, or nucleoporins, create a structure composed of three distinct domains: cytoplasmic filaments, a central scaffold with 8 large spokes, and a nuclear basket (120). The overall structure of the vertebrate NPC exhibits striking similarity to the smaller yeast NPC (129, 140). The yeast and vertebrate nucleoporins, despite the fact that their protein components have extensive sequence divergence, show much structural and functional similarity with few exceptions (18, 84, 103). One major exception was thought to be the integral membrane proteins that anchor the NPC to the nuclear envelope. These were thought to differ completely from yeast to humans (14, 24, 45, 85). The recent discovery of a vertebrate Ndc1, a homologue for yeast Ndc1, now provides a common integral membrane pore protein between the species (63, 81, 114). The second exception was the yeast centrin protein, Cdc31, which was designated a nucleoporin based on its presence in highly purified yeast nuclear pores (31, 103). Despite extensive purification of rat nuclear pores (18,

84) and the existence of multiple human centrin genes, there has been no experimental evidence to date linking centrin to the vertebrate nuclear pore. Here we have addressed the unusual finding of centrin in the yeast nuclear pore and its absence in the vertebrate pore.

As a group, centrins are small calcium-binding proteins traditionally associated with essential cellular structures responsible for nucleating microtubules (105, 136). This nucleation function for centrin is evolutionarily conserved from the flagella of algae to the spindle pole body of yeast to their vertebrate equivalent, the centrosome (10, 29, 65, 105, 107, 113). For this reason, it was unexpected to find centrin in the yeast nuclear pore (103).

In humans, three different centrin genes have been identified: human centrin 1 (HsCen1), centrin 2 (HsCen2) and centrin 3 (HsCen3) (29, 65, 87). HsCen1 and HsCen2 show substantial identity with one another (84%), but only 54% identity with HsCen3 (87). HsCen1 is distinct in that it exhibits tissue-specific expression, being expressed primarily in the testes and retina which have flagella and cilia, respectively (48, 137, 138). In contrast, HsCen2 and HsCen3 are ubiquitously expressed throughout the body where they have been demonstrated to play critical roles in centriole/centrosome duplication and cell division (86, 108, 138).

Despite known localization to the centrosome, however, most human centrin 2 is in fact not centrosome-associated, but is present in both the cytosol and nucleus, as shown by cell fractionation and immunofluorescence (94). Thus, it is highly possible that centrin 2 has further functions, ones outside

microtubule nucleation. At least one other role for centrin 2 has indeed been found in higher eukaryotes. In both humans and Arabidopsis, centrin 2 has been shown to be a functional part of the Xeroderma Pigmentosum Group C (XPC) complex which initiates nucleotide excision repair as a part of a global DNA repair pathway (4, 72, 90, 92). In addition, as stated above, the single yeast centrin homologue Cdc31 has been identified to be a component of the yeast nuclear pore (103). Indeed, Cdc31 has a role in yeast mRNA export, interacting with the Sac3-Thp1-Sus1 mRNA export complex. Most strikingly, Cdc31 mutants are severely defective in mRNA export (31).

Within the vertebrate nuclear pore, a number of nucleoporins have been found to be essential for mRNA export. These include multiple FG (phenylalanine-glycine)-containing nucleoporins (Nup358, Nup214, Nup153 and Nup98), which interact with the mRNA export cargo as it transits the pore (8, 13, 34, 43, 52, 98, 112, 127, 133). In addition, a critical subcomplex of the scaffold of the nuclear pore, the Nup107-160 complex, has been implicated in mRNA export. Overexpression of a specific fragment of either Nup133 or Nup160, two components of the Nup107-160 complex, causes strong defects in mRNA export (128). Similarly, mutations of the yeast homologues of these proteins (S.c. Nup133 and S.c. Nup120) were among the first of the yeast nucleoporins to show defects in mRNA export (2, 7, 22, 23, 38, 50, 70).

Globally, a subset of nucleoporins, including the vital Nup107-160 complex, has also been shown to have mitotic functions. These nucleoporins move to the kinetochore and/or spindle poles during mitosis (5, 11, 12, 25, 56,

74, 79, 93, 104, 119, 142). Focusing specifically on the Nup107-160 complex, this large 9-10 member complex, essential for mRNA export, pore assembly, and structure, is also absolutely required for correct spindle assembly (93), likely due to its mitotic location at the kinetochores and spindle poles (11, 47, 93, 96, 100, 111, 128, 131).

In the present study, we observed an interaction of centrin 2 with the vertebrate Nup107-160 complex in both *Xenopus* and human cells. Strikingly, we found centrin 2 to be strongly enriched at the vertebrate nuclear pore. Moreover, misexpression of centrin 2 led to defects in nuclear export. Our results demonstrate that vertebrate centrin 2 not only interacts with the nuclear pore, but that this interaction has a role in vertebrate mRNA and protein export.

Materials and Methods

Antibodies. Two commercial antibodies were used to detect human and *Xenopus* centrin 2. Centrin Ab A, raised to an undisclosed sequence located within aa 50-100 of human centrin 2, crossreacts with human centrin 1 and 2, but not centrin 3 (Santa Cruz Biotechnology, Santa Cruz, CA). Centrin Ab B, raised to the C-terminus of human centrin 1 (aa 152-172), similarly crossreacts with human centrin 1 and 2, but not centrin 3 (Sigma, St. Louis, MO). Other antibodies used include anti-hNup160, anti-xNup160, anti-hNup133 (128), anti-hNup93, anti-hNup205 (89), anti-mNup85 (46), anti-hNup43, anti-xNup43, anti-hNup37, anti-xNup37 (Orjalo, 2006), mAb414 anti-FG Nups; (Covance, Berkeley, CA),

anti-xNup155 (47), anti-mNup53, anti-xNup50 (gift from V. Delmar), and anti-myc (Calbiochem/EMD Biosciences, San Diego, CA).

GST Pulldowns. 50 μg of GST or GST-xNup160 C-terminus was crosslinked to CNBr beads in PBS (8 g/L NaCl, 0.2 g/L KCl, 0.14 g/L Na_2HPO_4, 0.24 g/L KH_2PO_4). The beads were then incubated with 50 μls of *Xenopus* cytosol plus or minus 10 μM RanQ69L-GTP in a final volume of 500 μls of PBS, 50 mM NaF, 50 mM β-glycerophosphate, 1 mM $NaVO_4$, plus protease inhibitors (P3840 Sigma Aldrich, St. Louis, MO) for one hour at room temperature. The reactions were washed three times with PBS, eluted with 0.1 M glycine, pH 2.5, and neutralized with 100 mM Tris, pH 7.9. The eluate was then subjected to LC-tandem mass spectrometry (Rasala *et al*, 2006).

Immunoprecipitation. HeLa cells grown to 80% confluency in 10 cm dishes were washed with 1X PBS and lysed at 4°C in 1ml of 50 mM Tris, pH 7.4, 150 mM NaCl, 1mM EDTA, 1% Triton X-100, 0.25% sodium deoxycholate, supplemented with aprotinin and leupeptin (final concentration 10μg/mL) for 30 min. Cells lysates were vortexed briefly and spun at 14,840 x *g* for 10 min. Immunoprecipitations were performed by adding 2-5 μg of anti-centrin (Ab A or Ab B, where indicated), anti-hNup160, or non-immune rabbit or goat IgG, followed by the addition of Protein A (for rabbit IgG) or Protein G (for goat IgG) Sepharose beads (Amersham Biosciences, Piscataway, NJ). Centrin antibody

co-immunoprecipitation of myc-tagged proteins was performed as above except HeLa cells were transfected 24 hrs prior to lysis with the indicated constructs using Lipofectamine (Invitrogen, Carlsbad, CA).

Immunofluorescence. For indirect immunofluorescence, HeLa cells were grown at 37°C in DMEM (Mediatech, Herndon, VA)/10% FCS (Invitrogen, Carlsbad, CA). XL177 *Xenopus* cells were grown in L-15 media (Mediatech, Herndon, VA)/15% FCS at room temperature on coverslips for 1-2 days. Cells were washed with 1X PBS and fixed with 2% formaldehyde for 10 min. Cells were then permeabilized with 0.005% digitonin in transport buffer (TB: 20 mM HEPES, 110 mM potassium acetate, 2 mM magnesium acetate, 1 mM EGTA, pH 7.4) for 5 min at 4°C followed by a 20 min wash in TB, or permeabilized in 0.5% Triton X-100 in 1X PBS for 10 min at room temperature. Cells were blocked 2 hrs to overnight in PBS containing 2% FCS, 2% BSA, and 0.02% NaN_3. Where indicated, the fixation step was carried out after permeabilization (Supplemental Figure S4.3). Cells were stained with anti-centrin (Sigma, 1:750, or Santa Cruz Biotechnology, 1:100) or anti-lamin B (Santa Cruz Biotechnology) antibodies together with mAb414 (Covance) for 1h. Staining was detected with Alexa Fluor 568-labeled goat anti-rabbit IgG (for the centrin antibody) or Alexa Fluor 568-labeled donkey anti-goat IgG (for the lamin B antibody), each with Alexa Fluor 488-labeled donkey anti-mouse IgG (for mAb414) (Molecular Probes/Invitrogen, Carlsbad, CA). Coverslips were mounted on Vectashield (Vector Laboratories, Burlingame, CA) and visualized with an Axiovert 200M microscope (Carl Zeiss,

Thornwood, NY) at a magnification of 63X using an oil objective with a 1.3 numerical aperture at 23°C, with Immersol 518F (Carl Zeiss) as the imaging medium. Images were recorded using a Coolsnap HQ camera (Photometrics, Tucson, AZ) and Metavue software (Molecular Devices Corporation, Downingtown, PA). Trace images were produced using the trace contour function in Adobe Photoshop.

Nuclear Reconstitution. Cytosolic and membrane vesicle fractions of *Xenopus* egg extracts were prepared as in (99). The membranes were stored in 10 μl aliquots at -80°C, and used as a 20X stock. Nuclei were reconstituted by mixing *Xenopus* egg membrane and cytosolic fractions at a 1:20 ratio with an ATP-regeneration system and sperm chromatin (80). For indirect immunofluorescence, reconstituted nuclei were formaldehyde fixed, pelleted onto poly-L-lysine-coated coverslips (15 min at 750 rpm) and probed with mAb414 and either of the anti-centrin antibodies described above. Where indicated, pelleted nuclei were permeabilized with Triton X-100 (Supplemental Figure S4.3). Both centrin antibodies A and B exhibited NPC staining of reconstituted nuclei in the absence or presence of Triton X-100 treatment; however, NPC staining was more pronounced if Triton X-100 was not used.

Constructs. The C-terminus of *Xenopus* Nup160 was obtained by PCR from a non-full length xNup160 cDNA clone (Primer 1: CCCGAATTCCAGCCGGTATCAGGAGCTGTG, Primer 2:

TTTCTCGAGTTACGCCCGTAGAGGCTTC) (128). This fragment, containing the last ~297 aa of the *Xenopus* Nup160 C-terminus, was subcloned into a pGEX-4T-1 GST tag vector (GE Healthcare, Piscataway, NJ). The xNup160 sequence is homologous to amino acids 1144-1429 of human Nup160. A full-length cDNA clone of HsCen2 (Accession No NM_004344.1) was obtained from Origene (Rockville, MD). Oligonucleotides were used to amplify either the HsCen2 N-terminus (aa 1-98) or the HsCen2 C-terminus (aa 94-172), which were subcloned as EcoRI-Kpn1 fragments into a pCDNA3.1 myc-tagging transfection vector (Invitrogen, Carlsbad, CA). For the myc-tag transfection experiments, a cDNA of human Nup160 aa 912-1436 was reverse transcribed from HeLa total RNA, amplified by PCR, and cloned into the pBluescript vector (Stratagene, La Jolla, CA). Nup160 amino acids 1146–1436 from this cDNA clone were then subcloned as an XhoI-BamHI fragment into pcDNA 3.1.

RNAi and Transfection. For the RNAi experiments, HeLa cells plated on coverslips were transfected for 48–60 h by using 0.84 μg of siRNA duplexes to ELYS (target: Exon 28 Silencer Pre-Designed siRNA #108720; Ambion, Austin, TX) (60hrs) or Centrin 2 (target: 5′-AAGAGCAAAAGCAGGAGATCC-3) Ambion, Austin TX) (48 hrs) (108) and Silencer Negative Control #1 siRNA (Ambion) in Oligofectamine (Invitrogen, Carlsbad, CA) as in (101).

HeLa cells were transfected 24 hrs prior to immunoprecipitation or poly [A+] RNA assays with the indicated constructs using Lipofectamine 2000 (Invitrogen, Carlsbad, CA) (2.5:1, Lipofectamine to DNA). Where

immunofluorescence was performed, successfully transfected cells were identified by positive staining for the myc epitope using FITC-labeled anti-myc antibody (Santa Cruz Biotechnology, Santa Cruz, CA). *Xenopus* XL177 cells were transfected 48 hrs prior to poly [A+] RNA assays using Lipofectamine at an increased ratio (5:1, Lipofectamine to DNA) at room temperature. XL177 cells were changed to fresh L-15 medium four hours following transfection.

Poly [A+] RNA Nuclear Accumulation Assay. Cells were grown on coverslips for 1 day, then transfected for ~24 hrs with control plasmids, or plasmids encoding Nup160 fragments or HsCen2 fragments in pCDNA3.1 using Lipofectamine 2000 (Invitrogen, Carlsbad, CA) (128). For siRNA experiments, cells were transfected with the indicated siRNA 48 hrs before performing the poly [A+] RNA accumulation assay. Cells were fixed (3% formaldehyde in PBS, 20 min on ice), permeabilized (0.5% Triton X-100 in PBS), incubated 5 min with PBS +1 mM vanadyl ribonucleoside complexes (VRC) and 5 min with 2X SSC+VRC (0.3M NaCl, 0.03M sodium citrate, pH 7), then prehybridized with 50% formamide, 2X SSC, 1 mg/ml BSA, 1 mM VRC, and 10% dextran sulfate (1hr, 37°C). The cells were hybridized with Cy3-oligo$[dT]_{50}$ (GeneLink, Hawthorne, NY) at 100 pg/μl in the same buffer (overnight, 37°), washed three times in 2X SSC (37°C, 5 min each), then refixed with 3% formaldehyde in PBS, 20 min on ice. Expression of transfected proteins was detected with FITC-labeled anti-myc antibody (1:100, Santa Cruz Biotechnology, Santa Cruz, CA).

Nuclear Protein Import and Export. Cells were grown on coverslips for 1 day, then cotransfected for ~16 hrs with the pXRGG (Rev-Glucocorticoid-GFP) plasmid (44, 75, 128) and either: (1) control plasmid encoding malate dehydrogenase, (2) plasmids encoding Nup160 fragments, or (3) HsCen2 fragments in pCDNA3.1, using Lipofectamine 2000 (Invitrogen, Carlsbad, CA). All of the latter plasmids were myc-tagged. For siRNA experiments, cells were transfected with RGG and the indicated siRNA 48 hrs before performing the import/export assay. After transfection, the cells were treated with dexamethasone (final concentration 1μM) (Sigma Aldrich, St. Louis, MO) for 60 min to induce RGG import. In parallel, an identical set of transfected cells were treated with dexamethasone for 60 min to induce RGG import, washed, then incubated with media lacking dexamethasone (2 hr, 37°C) to promote RGG export. Cells were fixed (3% formaldehyde in PBS, 15 min on ice), permeabilized (0.5% Triton X-100 in PBS, 10 min), and blocked (5% FBS in PBS, 10 min). The transfected expressed proteins were detected with TRITC-labeled anti-myc antibody (1:100, Santa Cruz Biotechnology, Santa Cruz, CA) or in the case of RGG, by its GFP moiety.

Results

Centrin 2 interacts with the Nup107-160 complex.

Many of the vertebrate nucleoporins exhibit low homology to their yeast counterparts (≤25%). Despite this, the vertebrate Nups are found in subcomplexes akin to the subcomplexes derived from the yeast nuclear pore.

The yeast homologue of the Nup107-160 complex, the Nup84 complex, exhibits a Y-shaped structure as determined by electron microscopy and in vivo reconstitution (77, 78, 110). Fluorescence resonance energy transfer or FRET experiments between Nup120 (the yeast homologue of Nup160) and an adjacent central component of the Nup84 complex suggest that the C-terminus of Nup120 faces away from the center of the Y and is thus free to interact with other proteins outside of the Y-shaped complex (21). In vertebrates, its homologue Nup160 is ~300 amino acids longer than yeast Nup120, thus increasing the extension of this protein away from the core of the Nup107-160 complex (128).

Higher metazoan nuclear pores experience unique situations that yeast nuclear pores do not, such as mitotic nuclear pore disassembly and subsequent reassembly. Thus, for multiple reasons, we sought to identify novel protein binding partners for the C-terminus of vertebrate Nup160. We used *Xenopus* egg extracts as a source for cellular proteins (46, 88). *Xenopus* Nup160 C-terminal fragment pulldowns were performed in the presence or absence of 10 μM RanQ69L-GTP. Pulldowns with GST alone served as negative controls. The proteins bound were identified by mass spectrometry.

One intriguing candidate found to bind to the GST-xNup160 C-terminus was *Xenopus laevis* centrin. Six full-length *Xenopus* centrin protein sequence isolates are present in the Entrez protein database at this time. Four contain the three peptides identified by our mass spectrometry screen and are either identical to one another or contain three amino acid differences. These four sequences are designated in the database as *Xenopus* centrin 2 or, more

generically, centrin. The fifth and sixth sequences are clear *Xenopus* homologues of centrin 3, as they share only 58% identity to the sequences above, but 88% identity with human centrin 3. No *Xenopus* centrin 1 has yet been identified.

We thus believe that the interacting protein that we have found is *Xenopus* centrin 2. It has 85% identity to human centrin 2, an ubiquitously expressed centrin, versus 81% identity to human centrin 1, the testes/retina-specific centrin. While human centrin 1 and 2 are similar, in the sequence locations where they differ *Xenopus* centrin more closely resembles human centrin 2 than centrin 1 (14 vs. 6 identities, Supplemental Figure S4.1). In consequence, we conclude that this interacting protein is *Xenopus* centrin 2.

To analyze the *Xenopus* centrin 2 interaction with Nup160 further, two commercially prepared antibodies to human centrin proved to be of value (Figure 4.1A). Centrin antibody A, raised to an internal region of human centrin 2, is known to recognize human centrin 1 and 2, but not centrin 3 (Figure 4.1A, Santa Cruz Biotechnology). Similarly, centrin antibody B, raised to the C-terminus of human centrin 1, recognizes both human centrin 1 and 2, but not centrin 3 (Figure 4.1A, Sigma Aldrich). In HeLa cells, centrin 2 is the only protein that should be recognized by each of these antibodies, as the testis/retinal-specific centrin 1 protein should not be present (138). Both antibodies detected a protein of the appropriate size in human HeLa cell lysates (Figure 4.1B, lanes 6 and 7). These anti-centrin antibodies also recognized an identically sized protein of 20

kDa on immunoblots of *Xenopus* egg cytosol and lysates of *Xenopus* XL177 cultured cells (Figure 4.1B, lanes 1-4).

To confirm the mass spectrometry interaction between the C-terminus of xNup160 and centrin 2, we again performed a GST-xNup160 C-terminal pulldown from *Xenopus* egg cytosol and probed with centrin antibody B (Figure 4.1C). A centrin band was indeed observed in the Nup160 C-terminal pulldown (white arrow, lanes 3 and 5, Figure 4.1C), but not in control GST pulldowns (lanes 2 and 4, Figure 4.1C).

We next looked for evidence that centrin 2 interacts with the full Nup107-160 complex. Centrin antibody B was used to immunoprecipitate *Xenopus* centrin 2 from interphase egg cytosol (white arrow, Figure 4.2A, lane 2). Importantly, this centrin antibody B also co-immunoprecipitated all tested members of the Nup107-160 complex, including Nup160, Nup133, Nup85, and Nup43 (black arrows, Figure 4.2A, lane 2). Similar results were observed with centrin antibody A (data not shown). However, Nup93, which is not a member of the Nup107-160 complex (40), did not co-immunoprecipitate significantly with either centrin antibody (Figure 4.2A, lane 2, and data not shown)

A Nup107-160 complex interaction with centrin 2 was also observed in human cells. Of the anti-centrin antibodies, centrin antibody A proved the most efficient at immunoprecipitation of centrin 2 from HeLa cell lysates prepared by Triton X-100/deoxycholate lysis (white arrow, Figure 4.2B, lane 2). When analyzed, this antibody consistently co-immunoprecipitated all tested members of the human Nup107-160 complex (black arrows, Figure 4.2B, lane 2).

Importantly, antibody to Nup160 reciprocally co-immunoprecipitated centrin 2 from HeLa cells (white arrow, Figure 4.2C, lane 2). Nup93 and several other nucleoporins not in the Nup107-160 subcomplex, such as Nup205, Nup155, Nup53, and Nup50, were not co-immunoprecipitated by the centrin antibody (Figure 4.2B and Supplemental Figure S4.2), although the FG proteins Nup358, Nup214, and Nup62 were sometimes observed in small amounts (data not shown). Thus, centrin 2 and the Nup107-160 complex show a specific interaction.

Testing other nucleoporins involved in mRNA export.

Mass spectrometry of the *Xenopus* proteins pulled down by the GST-xNup160 C-terminus also revealed Nup153 (data not shown), a known Nup107-160 complex interacting partner that plays an important role in mRNA export (8, 91, 112, 127, 128). We therefore asked whether centrin 2 interacts with Nup153 or other nucleoporins involved in mRNA export. Centrin antibody A did indeed co-immunoprecipitate Nup153 from HeLa cell and *Xenopus* egg extracts (black arrow, Figure 4.2D, lane 2, and data not shown). However, Nup98, also involved in mRNA export, did not co-immunoprecipitate with the centrin antibody (Figure 4.2D, lane 2). In summary, we have identified interactions between centrin 2 and specific nucleoporins involved in mRNA export, i.e., the Nup107-160 complex and Nup153.

Centrin 2 is found at the nuclear pores of *Xenopus* reconstituted nuclei and cultured cells.

The interaction between *Xenopus* centrin 2 and specific nucleoporins suggested that centrin 2 could be located at the nuclear pore as previously seen in yeast (103). However, our previous finding of the Nup107-160 complex at the spindle poles (93) made it equally possible that the centrin-Nup107-160 interaction could in fact be occuring at the spindle pole, and not at the nuclear pore. To address this, immunofluorescence was performed on nuclei assembled in vitro in *Xenopus* interphase egg extracts (30, 46, 73, 109, 126, 141). This system provides a powerful tool by which robust assembly of functional nuclei occurs around chromatin templates in vitro. Using immunofluorescence with both centrin antibody A and B, we found that *Xenopus* centrin 2 was indeed localized at the nuclear rim, as well as to a lesser extent the nuclear interior (Figure 4.3A). Moreover, the centrin 2 at the nuclear rim was observed in a punctate pattern that closely co-localized with that of FG nucleoporins (Figure 4.3A, 5X magnification).

When immunofluorescence was performed on XL177 *Xenopus* cultured cells, centrin antibody A and B again consistently gave a nuclear pore stain (Figure 4.3B and data not shown). Centrin 2 was also observed in the cytoplasm of XL177 cells, consistent with the previous finding (94) that the majority of centrin 2 in animal cells is not associated with the centrosome, but is cytoplasmic and nuclear. A specific centrosomal stain was not seen, likely because the

cytoplasmic stain obscures it. Taken together, the above results demonstrate that *Xenopus* centrin 2 is clearly present at the nuclear pore.

Centrin 2 is at the nuclear pores of human cells.

In human and mouse cells, vertebrate centrin has long been observed at the centrosome, when either immunofluorescence or GFP-tagging was used (19, 29, 49, 51, 65, 76, 86, 87, 105, 108, 135). In prior studies where centrin 2 was identified visually as being primarily at the centrosome with no NPC localization, the human cells were either methanol fixed or formaldehyde fixed and then Triton X-100 permeabilized (29, 62, 94, 108). When we fixed human HeLa cells with formaldehyde, followed by permeabilization with Triton X-100 and performed immunofluorescence with centrin antibody A in the traditional manner, we saw no centrin staining of any sort (data not shown). Notably, even yeast cdc31 could not be visualized at the NPC by immunofluorescence (31). When we performed formaldehyde fixation and permeabilization with Triton X-100 and used centrin antibody B on HeLa cells, we saw distinct centrosomal staining and little other stain (white arrow, Figure 4.4A), as previously observed by others.

However, if HeLa cells were permeabilized with the more mild detergent digitonin and immunofluorescence was performed with anti-centrin antibody A or B, we observed centrin 2 in a punctate stain at the nuclear rim (Figure 4.4B and Supplemental Figure S4.3B). This stain was seen to co-localize with that of the FG nucleoporins. Nuclear pore staining was observed whether formaldehyde fixation preceded (Figure 4.4B) or followed (Supplemental Figure 4.3B) digitonin

permeabilization of the HeLa cells. Some nuclear and cytoplasmic centrin 2 was additionally observed, but the nuclear pore stain was prominent.

In summary, we find that centrin 2 is observed primarily at the centrosome in Triton-X100-permeabilized human cells, in accordance with previous immunofluorescence studies. However, milder digitonin treatment conditions after fixation reveals that centrin 2 is clearly located in a punctate pattern at the nuclear rim in human cells, co-localizing with FG nucleoporins.

Centrin 2 staining is disrupted by the loss of nuclear pores.

To further test the nuclear pore localization of centrin 2, we disrupted nuclear pores in HeLa cells using RNAi. It has been shown by us and others that RNAi of the critical nuclear pore assembly protein, ELYS/MEL-28, leads to a dramatic loss of nuclear pores at the nuclear envelope in human cells and, instead, promotes the formation of annulate lamellae, cytoplasmic stacks of membranes with pore complexes that contain virtually all nucleoporins tested (17, 20, 36, 101). Furthermore, ELYS RNAi in HeLa cells was previously shown by us to leave the nuclear membranes and Ran gradient unaltered (101).

We examined the effect of ELYS/MEL-28 RNAi on human centrin 2. ELYS/MEL-28 RNAi of HeLa cells led to a dramatic loss of FG nucleoporins at the nuclear rim and a concomitant increase in large cytoplasmic aggregates containing FG nucleoporins, near but not part of the nuclear rim (ELYS RNAi, green panel, Figure 4.5A). Neither of these changes was observed with a control RNAi oligo (Figure 4.5A, compare green panels). Strikingly, RNAi depletion of

ELYS/MEL-28 led to a decrease in the centrin 2 punctate nuclear rim stain, as compared to that of the control cells (Figure 4.5A, compare red panels). Disruption of the nuclear pores caused centrin 2 protein to aggregate in the cytoplasm in locations often coincident with FG nucleoporins (Merge, Figure 4.5A; see also 5X Trace). As these FG nucleoporin-containing aggregates have previously been characterized by electron microscopy to be annulate lamellae, i.e., stacks of cytoplasmic pores (36), our data support the finding that centrin 2 is associated with the pore both in nuclear pores and in cytoplasmic annulate lamellae pores.

It should be noted that in some ELYS/MEL-28 RNAi depleted cells, a population of centrin 2 also accumulated in the nucleus (Figure 4.5A); these nuclear aggregates did not overlap with FG nucleoporins. As expected, ELYS/MEL-28 RNAi did not disrupt the nuclear envelope overall (101), as lamin B staining remained unchanged (Figure 4.5B, red panels).

We conclude that disruption of the nuclear pores reduces centrin 2 nuclear pore staining and causes localization of a population of centrin 2 to the FG nucleoporin-containing cytoplasmic aggregates presumed to be annulate lamellae. Thus, the RNAi result is entirely consistent with the localization of centrin 2 at nuclear pores.

Centrin 2 is involved in vertebrate mRNA export.

The localization of centrin 2 at the vertebrate nuclear pore suggested that it might have a functional role at the pore. Vertebrate Nup160 has previously

been shown to play a role in mRNA export: transfection of a fragment of Nup160, specifically aa 317-697, into HeLa cells had a dominant negative effect on mRNA export, resulting in nuclear poly [A]+ RNA accumulation (128). One possibility is that this fragment of Nup160 might, when overexpressed, sequester centrin away. Thus, we pursued a two-fold strategy to determine whether centrin 2 plays a role in mRNA export.

We first asked which domains of human Nup160 are involved in the interaction with centrin 2. HeLa cells were transfected either with specific myc-tagged fragments of the Nup160 gene or with a full-length malate dehydrogenase gene as a control. After transfection, the cells were lysed and subjected to immunoprecipitation with centrin antibody A. Both the myc-tagged C-terminus of Nup160 (aa 912-1436) and the internal fragment of Nup160 (aa 317-697) co-immunoprecipitated with centrin 2 (black arrows, Figure 4.6A, lane 2). The Nup160 fragments may bind directly to centrin 2 or indirectly via a secondary protein. The negative control protein malate dehydrogenase did not immunoprecipitate with centrin 2 (white arrow, Figure 4.6A, lane 2). We conclude that centrin 2 biochemically interacts with at least two regions of human Nup160, and that the C-terminal region of Nup160 appears to be involved in the stronger interaction of the two, as shown by its distinct enrichment (Figure 4.6A).

We asked whether overexpression of the strong centrin-interacting Nup160 C-terminus (aa 912-1436) had an effect on mRNA export. Plasmids containing the two different myc-tagged Nup160 fragments or malate dehydrogenase were transfected into HeLa cells for 24 hours and poly [A]+ RNA

localization monitored by hybridization with Cy3-oligo-$[dT]_{50}$. Successfully transfected cells were identified with FITC-labeled anti-myc antibody. The location of poly [A]+ RNA in the cells was determined in 500 transfected myc+ cells per experiment and the experiment was done in triplicate. Quantitation of the results indicated that transfection of human cells with the negative control malate dehydrogenase gene inhibited mRNA export in only 2% of the myc+ transfected cells (Figure 4.6B). Expression of Nup160 aa 317-697, previously shown to inhibit mRNA export, led to nuclear accumulation of poly [A]+ RNA, as expected, in 30% of the myc-positive transfected cells (Figure 4.6B). Expression of the strong centrin-binding C-terminus of Nup160 (aa 912-1436) had an even greater effect, inhibiting mRNA export in nearly 50% of the transfected cells (Figure 4.6B). Sample images of transfected human cells inhibited for mRNA export by the Nup160 fragments are shown in Figure 4.6C (red: poly [A]+ RNA; green: myc transfection).

Transfection of *Xenopus* cultured cells, as opposed to human cell transfection, has historically proven difficult. Conditions that allowed transfection of our myc-tagged constructs into XL177 cells were worked out (see Materials and Methods). Transfection of each of the human Nup160 fragments into *Xenopus* XL177 cells led to nuclear accumulation of poly [A]+ RNA (Figure 4.6D). However, due to the low overall transfection efficiency of the XL177 cells, we were unable to precisely quantify and graph this effect. We conclude, however, from the human and *Xenopus* transfection results that domains of Nup160 that interact with centrin 2 elicit a dominant negative effect on mRNA export.

Approaching the role of centrin 2 in mRNA export more directly, we asked whether transfection of fragments of the human centrin 2 gene would have an effect on poly [A]+ RNA export. Centrin 2 protein has been shown by X-ray crystallography to have a dumbbell-shaped structure consisting of two domains, an N-terminal half containing two Ca2+ binding EF-hand motifs and a C-terminal half also containing two Ca2+ binding EF-hand motifs, with the individual halves separated by a helical linker (124). We created separate myc-tagged constructs, an HsCen2 N-terminal half (aa 1-98) and an HsCen2 C-terminal half (aa 94-172), based on the published structures of these domains (83, 139). We found that expression of either half of human centrin 2 led to nuclear poly [A]+ RNA accumulation in ~20-25% of the transfected cells (Figure 4.7A). In contrast, transfection of either of two myc-tagged negative control genes, malate dehydrogenase (data not shown) or pyruvate kinase (PK-Myc, Figure 4.7A), inhibited export in only 5% of transfected cells. The majority of cells transfected with the control constructs showed a largely cytoplasmic stain, indicating that mRNA had been exported. Sample images of centrin 2-transfected cells with inhibition of mRNA export are shown in Figure 4.7B (red: poly [A]+ RNA; green: myc transfected). We conclude that the overexpression of either the N- or C-terminal half of human centrin 2 inhibits vertebrate mRNA export in a dominant negative manner.

We also determined the effect of centrin 2 depletion on mRNA export by using a specific siRNA oligo known to knock down centrin 2 (108) (Supplemental Figure S4.4A-C). Because centrin 2 RNAi is known to disrupt centriole

duplication and lead to mitotic defects, we were only able to look for potential effects of centrin 2 knockdown on mRNA export in those cells which were not arrested in mitosis (without nuclei) or were multinucleate (as a result of inaccurate exit from mitosis). This made approximately half the transfected cells available for poly [A]+ RNA assessment. Centrin 2 RNAi depletion led to poly [A]+ RNA accumulation in ~20% of this group of cells. We thus conclude that overexpression of either the N- or C-terminal half of human centrin 2, as well as depletion of the centrin 2 protein via RNAi, inhibits vertebrate mRNA export.

Dominant negative fragments of centrin 2 block protein export, but not import.

Nuclear protein import and export can be measured with an NES/NLS-bearing protein construct, RGG, which contains the HIV protein REV with its NES, the ligand binding domain of the glucocorticoid receptor which contains a hormone-dependent NLS, and GFP (44, 75). When transfected alone, the RGG protein is cytoplasmic until the introduction of dexamethasone, which induces its import into the nucleus (Figure 4.8A). Upon removal of dexamethasone the RGG construct protein is exported, which is presumed to occur through the Crm1 export receptor. Co-transfection of the RGG construct with a control malate dehydrogenase gene had no effect on either RGG protein import or export (Figure 4.8B-E). Co-transfection of RGG with either Nup160 aa 317-697 or the Nup160 C-terminus (aa 912-1436) also had no effect on nuclear RGG protein import or export induced by dexamethasone (Figure 4.8B-E). Interestlingly,

siRNA depletion of centrin 2 had no effect on RGG protein import, but led to a block in RGG export, disrupting RGG protein export in 23-32% of depleted cells without mitotic defects (Supplemental Figure S4.4D-F). Similarly, each half of centrin 2 showed no effect on RGG protein import (Figure 4.8B and D). However, both centrin fragments exhibited a dominant negative effect on RGG protein export (Figure 4.8C and E). Specifically, expression of either the N or C-terminus of human centrin 2 led a block in RGG protein export in ~20-30% of the transfected cells (Figure 4.8E). Strikingly, this effect on RGG protein export appears to mirror exactly the effect of the centrin halves on mRNA export (Figure 4.7A). In this context, it is significant to the consideration of mechanism of action to note that Rev NES protein export uses the receptor Crm-1, while mRNA export employs a different set of transport factors which include Tap1/Mex67 and associated proteins (6, 28, 33, 35, 54, 57, 68, 69, 117, 118). Thus, while overexpression of fragments of Nup160 only affect mRNA export (Figures 4.6 and 4.8) (128), our results support that centrin 2 acts on both protein and mRNA export pathways.

Discussion

A new role for vertebrate centrin at the nuclear pore has been identified in this study. Despite being observed to be a structural component of the yeast nuclear pore in 2000 (103) with a functional role later revealed (31), the intervening years have never shown a hint that centrin has any connection to the vertebrate nuclear pore, either structurally or functionally. We have now

observed interaction between vertebrate centrin 2 and the critical Nup107-160 complex of the nuclear pore from *Xenopus* to human cells (Figures 4.1 and 4.2). Indeed, although previously visualized to be a centrosomal protein by immunofluorescence, we have found that centrin 2 co-localizes extensively with nuclear pores in human and *Xenopus* cultured cells, as well as with the pores of nuclei reconstituted in vitro in *Xenopus* egg extracts (Figures 4.3 and 4.4). Although readily apparent at the NPCs of *Xenopus* cells and in vitro reconstituted nuclei, substitution of digitonin for Triton X-100 is required to observe NPC association in HeLa cells. Disruption of the nuclear pore targeting/assembly protein ELYS/MEL-28 by RNAi, known to lead to a loss of nuclear pores, causes a dramatic decrease in centrin 2 at the nuclear pore under conditions where the nuclear lamina remains unaltered (Figure 4.5). Instead, in ELYS RNAi-treated cells centrin 2 relocates to FG nucleoporin-containing cytoplasmic aggregates (annulate lamellae), demonstrating that centrin 2 interacts with both nuclear and cytoplasmic pore complexes (Figure 4.5). We additionally identify a functional role for centrin 2 at the nuclear pore. Overexpression of either the N-terminal or C-terminal Ca^{2+} binding EF hand domains of human centrin 2 leads to the nuclear accumulation of poly [A]+ RNA, consistent with a disruption of mRNA export (Figure 4.7). This mRNA export defect mirrors the nuclear poly [A]+ RNA accumulation caused by overexpression of Nup160 fragments, which are either direct or indirect binding sites for centrin 2 (Figure 4.6), and also mirrors the Cdc31 defect observed in yeast (31). In addition, overexpression of either half of human centrin 2 has a dominant negative effect on RGG protein export, but not

its import (Figure 4.8). Depletion of centrin 2 by RNAi causes similar disruptions of both mRNA and protein export (Supplemental Figure S4.4). We conclude that centrin 2 interacts with a major subunit of the nuclear pore, exhibits a nuclear pore localization, and has a functional role in mRNA and protein export.

Centrins have long been associated structurally with the centrosome (105). Traditional immunofluorescence on human cells using methanol or formaldehyde/Triton X-100 has previously revealed centrin 2 to be localized at the centrosome (29, 94, 108). RNAi experiments demonstrated that centrin 2 is required for centriole duplication (108). Moreover, a physical interaction between centrin 2 and the centrosomal protein Sfi-1, observed both in yeast and humans, plays a key role in the regulation of centrosome structure and centriole duplication (59, 71, 82, 106). It is thus clear that centrins are an essential component of the vertebrate centrosome and yeast spindle pole body. A single higher eukaryotic, non-centrosomal nuclear function for centrin 2 was previously observed in the XPC nucleotide excision repair complex, as described in the Introduction (4, 72, 90, 92).

Our identification of vertebrate centrin 2 as a novel binding partner for the Nup107-160 complex in immunoprecipitations originally suggested a possible mitotic, centrosome-related role for the interaction. Indeed, the Nup107-160 complex moves to the kinetochores and spindle poles at mitosis (11, 25, 74, 93, 142) and we previously demonstrated that it is required for correct bipolar spindle assembly: immunodepletion of the Nup107-160 complex from *Xenopus* mitotic extracts results in severely defective spindle assembly in vitro (93).

Our finding, however, that centrin 2, is present at the nuclear pore in interphase and is involved in mRNA and protein export now shows that centrin 2 has another important novel interphase function in vertebrates. This conclusion brings an unexpected, but remarkable symmetry to the studies of yeast and vertebrate centrin. The single centrin of *S. cerevisiae,* Cdc31, is an essential component of the yeast centrosome equivalent, the spindle pole body, and an established member of the yeast nuclear pore complex (31, 53, 103, 113). Indeed, a functional role for yeast Cdc31 in mRNA export was identified; expression of a mutant Cdc31 allele (Cdc31-151) or absence of Cdc31 expression leads to nuclear accumulation of poly [A]+ RNA (31). Here, we find that overexpression of either half of human centrin 2 has a dominant negative effect on mRNA export, both in human and *Xenopus* cultured cells (Figure 4.7). Moreover, centrin 2 affects Crm-1 mediated protein export, but not at least one major type of protein import (Figure 4.8). Thus, our data indicates for the first time that vertebrate centrin 2 is at the nuclear pore and plays a role in mRNA and nuclear protein export during interphase. The recent discovery of dynein at the yeast nuclear pore now presents a new and interesting difference between the yeast and vertebrate nuclear pore (115).

In yeast, the function of Cdc31 in mRNA export appears to be mediated through interaction with an mRNA export complex, the yeast Sac3-Thp1-Sus1 complex (31, 130). Specifically, Cdc31 interacts with yeast Sac3p, a 150 kDa protein (9, 31). Vertebrate centrin 2 might also possibly bind and/or function through an as yet undiscovered vertebrate Sac3-Thp1-Sus1 complex.

Three vertebrate homologues of Sac3 have been identified, GANP, MCM3AP and Shd1 (1, 58). GANP (B-cell germinal center-associated protein) and MCM3AP (MCM3 associated protein) are derived from the same gene by alternative splicing (1). GANP is 210 kDa; 60 kDa of which has 23% homology with a region of yeast Sac3 (aa 129-803). This region of yeast Sac3 contains its centrin-interaction domain (1, 60, 61). GANP also has several N-terminal degenerate FG motifs (32), a motif found almost exclusively in nucleoporins. However, the large GANP protein and its smaller alternatively spliced C-terminal isoform, MCM3AP, contain other non-Sac3 domains, including a GCN5-related N-acetyltransferase domain and a DNA primase activity, both required for their function in DNA replication (60, 61, 121-123).

The third vertebrate relative of Sac3p, SHD1 (Sac3 homology domain protein 1), is a third the size of yeast Sac3p and lacks the yeast centrin-interaction domain (58). However, SHD1 localizes to centrosomes and RNAi of SHD1 causes abnormalities in centrosome duplication and spindle formation (58). Thus, while both Shd1 and GANP/MCM3AP contain similarities to yeast Sac3, they contain unrelated additional domains. We cannot rule in or out a role for these proteins at the nuclear pore in mRNA export. As yet, however, they have no direct connection to vertebrate centrins.

Our work identifies interactions between centrin 2 and several major nucleoporins involved in mRNA export. In addition to the Nup107-160 complex, we observed centrin 2 interacting with the FG nucleoporin Nup153 (Figure 4.2). Interestingly, yeast Sac3 is known to bind to the yeast FG nucleoporin Nup1, a

distant homologue of Nup153 (31, 32, 55, 67). Our observed interaction of vertebrate centrin 2 with Nup153 may be direct or indirect and involve a vertebrate Sac3 equivalent, such as Shd1. Alternatively, the interaction between vertebrate centrin 2 and Nup153 may use the Nup107-Nup160 complex as an intermediary, since we have shown this complex binds both centrin 2 and Nup153 (Figure 4.2) (128, 132).

Structurally, the major domains of centrins are comprised of Ca^{2+}-binding EF hand motifs. It has been observed that mutations that specifically affect the calcium-binding of yeast Cdc31 cause nuclear accumulation of poly (A)+ RNA (31). Other actions of centrins are also altered by calcium. The affinity of Cdc31 for its spindle pole body partner Kar1 increases 10-fold with calcium, which affects its role in spindle pole body duplication (37). The affinity of human centrin 2 for XPC similarly increases 28-fold in the presence of calcium, although, how this affects XPC activity has not yet been determined (92, 97).

Calcium has been separately implicated as a possible regulator of the nuclear pore in a handful of studies [see (26, 125) and references therein]. For example, atomic force microscopy observes structural changes in the pore with calcium addition, described as a calcium-induced, iris-like opening of the nuclear basket ring, the first pore structure encountered by proteins and mRNAs before export (116). Specific changes in nucleoporin localization include the FG domain of Nup153, which changes its position within the pore with the addition of 2 mM Ca^{2+} (95), a Ca^{2+} change comparable to typical calcium flux from the ER.

Calcium changes have been observed to influence not only pore structure, but pore function. Thapsigargin, which depletes the ER calcium stores, is seen to disrupt passive diffusion and nuclear transport through the vertebrate NPC in living cells (41, 64). Because the integral membrane pore protein, gp210, contains lumenal calcium-binding motifs, and expression of an antibody to this portion of gp210 within the ER lumen inhibits both passive diffusion and signal-mediated transport, one hypothesis has been that gp210 could be a calcium sensor that triggers such conformational NPC changes (26, 42). However, our identification of centrin 2 at the vertebrate nuclear pore introduces a potential more centrally located calcium sensor for the NPC, one that is not lumenal.

In summary, we conclude that a population of vertebrate centrin 2 interacts with nuclear pore subcomplexes, localizes to the nuclear pore, and plays a role in mRNA and protein export. Thus, we have identified a new and distinct interphase function for vertebrate centrin 2. Possible interaction of centrin 2 in an mRNA export complex, such as the yeast Sac3-Thp1-Sus1-Cdc31 complex, which is as yet undiscovered in vertebrates, may be of future interest. In addition, the ability of centrin 2 to bind calcium provides interesting potential roles for this protein as a regulatory or structural component of the nuclear pore.

Figures

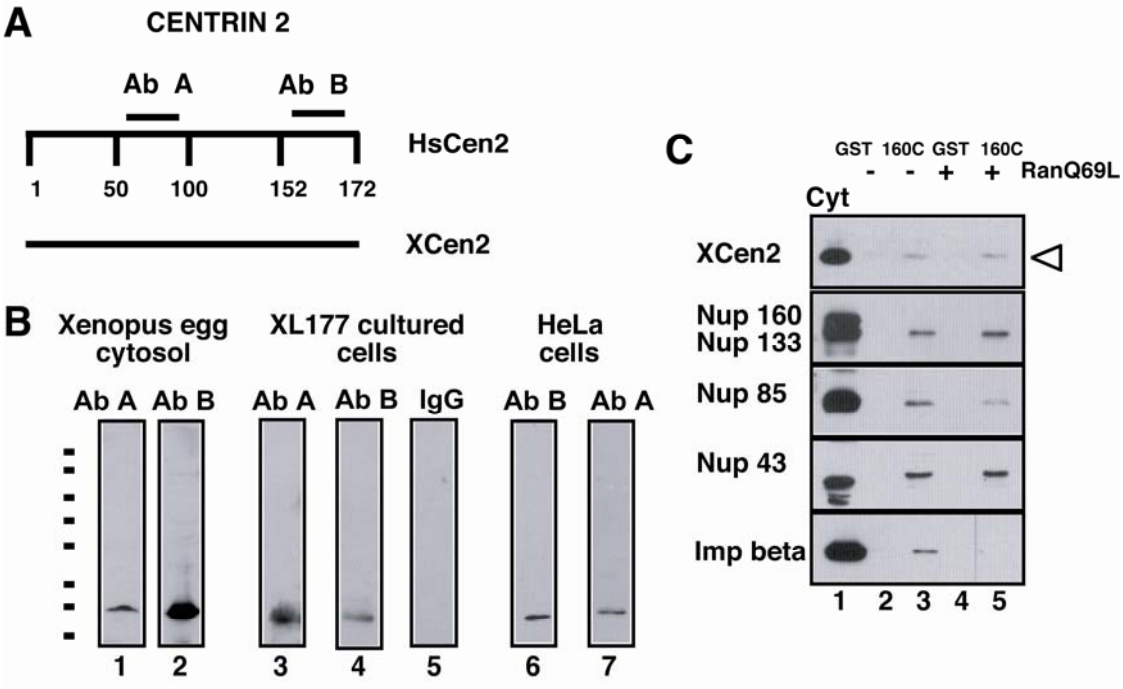

Figure 4.1. Scheme of proteins and antibodies used.
(A) *Xenopus* centrin 2 and human centrin 2 both consist of 172 amino acids and share 85% identity. Two antibodies were used to recognize both human and *Xenopus* centrin 2 in this study. Centrin antibody A (Ab A) recognizes a region between residues 50-100 of human centrin 2; *Xenopus* centrin 2 shares 80% identity with human centrin 2 in this domain. Centrin antibody B (Ab B) was raised to C-terminal residues 152-172 of human centrin 1, which because of high homology also recognizes human centrin 2. *Xenopus* centrin 2 differs from human centrin 1 at only one position from aa 152-172. (B) Both anti-centrin antibodies recognize an apparent single band in *Xenopus* egg extract (lanes 1 and 2), *Xenopus* XL177 cell lysate (lanes 3 and 4), and HeLa cells (lanes 6 and 7). Control IgG did not recognize this band (lane 5). Hatch marks on the left indicate the molecular weight markers (From top: 150, 100, 75, 50, 37, 25, 20, 15 kDa). (C) The GST-tagged C-terminus of xNup160 interacts with *Xenopus* centrin 2, as well as members of the Nup107-160 complex in the presence or absence of RanQ69L-GTP (black arrow, lanes 3 and 5). Certain nucleoporins interact only when excess RanGTP is added, presumably due to removal of endogenous importin β, a negative inhibitor of interaction. We observed no effect of RanQ69L-GTP addition here, other than removal of peripheral importin β. GST alone was used as a negative control (lanes 2 and 4). 'Cyt' indicates a fraction of input *Xenopus* egg cytosolic extract (lane 1).

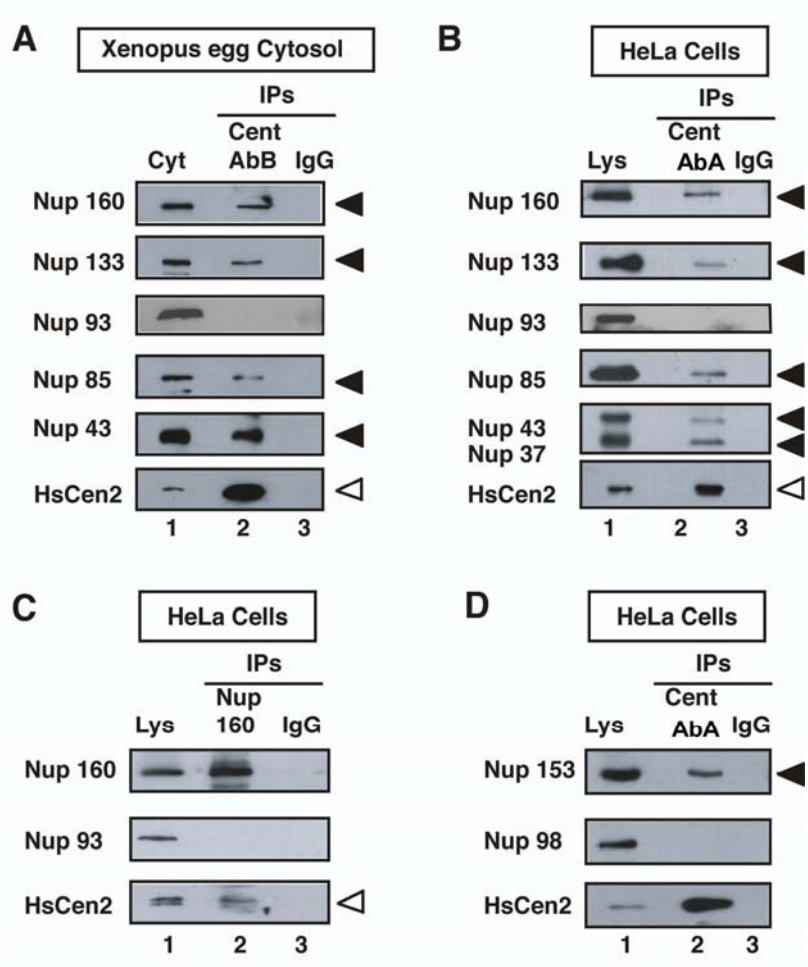

Figure 4.2. Centrin 2 antibody co-immunoprecipitates nucleoporins involved in mRNA export from human cells and *Xenopus* egg extracts.
(A) Anti-centrin antibody B (Ab B) immunoprecipitates *Xenopus* centrin 2 (white arrow), along with members of the Nup107-160 complex, such as Nup160, Nup133, Nup85 and Nup43 (black arrows; lane 2) from *Xenopus* egg extract. Nup37 was also occasionally immunoprecipitated by centrin 2 antibody B (data not shown). Centrin antibody B did not immunoprecipitate the non-Nup107-160 complex member, Nup93 (lane 2). Immunoprecipitation with rabbit IgG was used as a negative control (lane 3). 'Cyt' indicates a fraction of input *Xenopus* egg cytosolic extract. Centrin antibody A also co-immunoprecipitated both centrin 2 and Nup160 (data not shown). Because of its superior efficiency, centrin antibody B was used for the majority of subsequent *Xenopus* centrin 2 immunoprecipitation experiments. (B) Anti-centrin antibody A (Ab A) immunoprecipitates human centrin 2 (white arrow), and all tested members of the Nup107-160 complex (Nup160, Nup133, Nup85, Nup43 and Nup37; black arrows) from HeLa cells, but does not immunoprecipitate the non-complex member Nup93 (lane 2). Immunoprecipitation with goat IgG (lane 3) was used as a negative control. 'Lys' indicates a fraction of the input HeLa cell lysate (B-D). Centrin antibody B also co-immunoprecipitated both centrin 2 and Nup160 (data not shown); however, because of the superior levels of human centrin 2 immunoprecipitated by centrin antibody A, we used this antibody for the majority of HeLa immunoprecipitation experiments. (C) Nup160 antibody reciprocally co-immunoprecipitated human centrin 2 (lane 2). Immunoprecipitation with rabbit IgG (lane 3) was used as a negative control (C and D). (D) Anti-centrin antibody A (Ab A) immunoprecipitates Nup153 (black arrow), but not Nup98 from HeLa cell lysate.

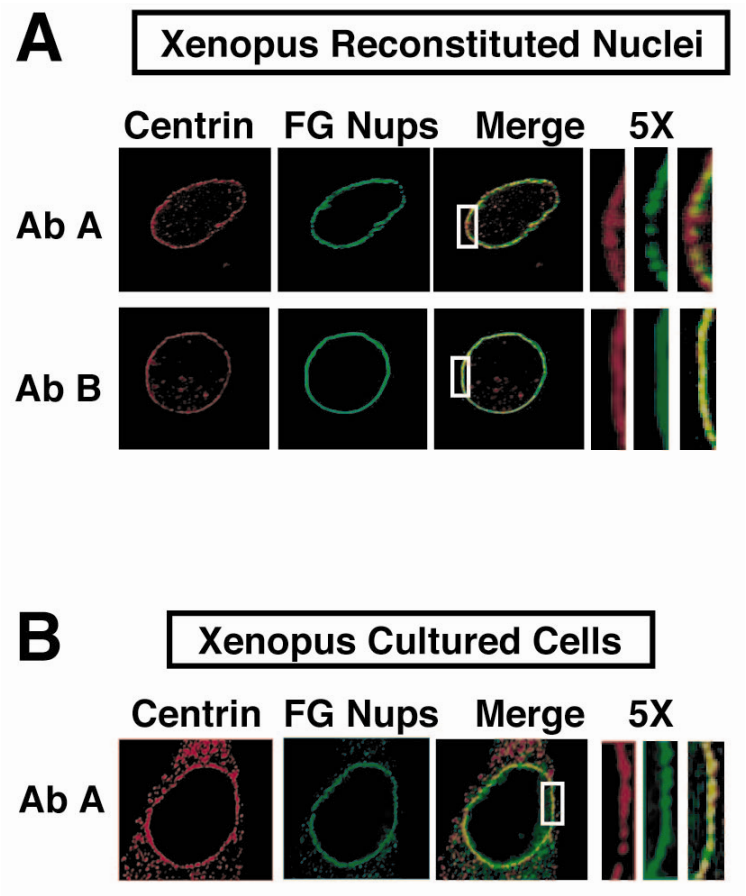

Figure 4.3. Centrin 2 is located at the nuclear pore in *Xenopus* nuclei assembled in vitro and in cultured cells.
(A) *Xenopus* centrin 2 localizes to the rim of in vitro reconstituted nuclei. Double immunofluorescence of spun down reconstituted nuclei, stained with anti-centrin 2 antibody (Ab A or B; left panels) and anti-FG Nup antibody mAb414 (middle panels) with merged images (right panels). Insets (far right) are a 5X magnification. See also Supplemental Figure S4.3A for parallel images from this experiment performed under different conditions. (B) Anti-centrin antibody A shows localization of centrin 2 at the nuclear rim of *Xenopus* XL177 cells fixed with formaldehyde and permeabilized with Triton X-100. Double immunofluorescence with anti-FG Nup antibody mAb414 is shown with the merged image at the right. Insets (far right) are a 5X magnification.

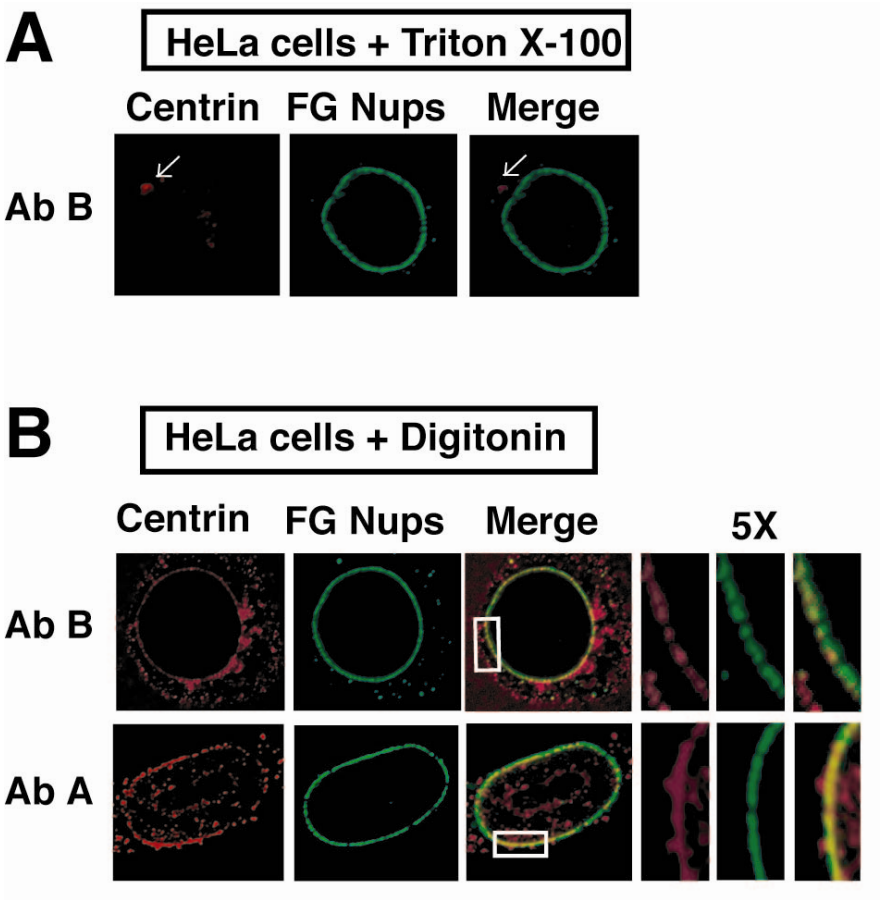

Figure 4.4. Centrin 2 is located at the centrosome and the nuclear pore in human cells. (A) Human centrin 2 localizes to the centrosome in HeLa cells fixed with formaldehyde and permeabilized with Triton X-100. Double immunofluorescence of HeLa cells with anti-centrin antibody B (left) and the FG Nup antibody mAb414 (middle) is shown with the merged image at the right. (B) Immunofluorescence with Centrin Ab B or A performed on HeLa cells fixed with formaldehyde and treated with digitonin. Centrin antibody B reveals more extensive centrin 2 staining with clear human centrin 2 staining present at the nuclear rim in a punctate pattern. Double immunofluorescence of HeLa cells with either anti-centrin antibody A or B and anti-FG Nup monoclonal antibody mAb414 is shown with the merged image at the right. Insets (far right) are a 5X magnification.

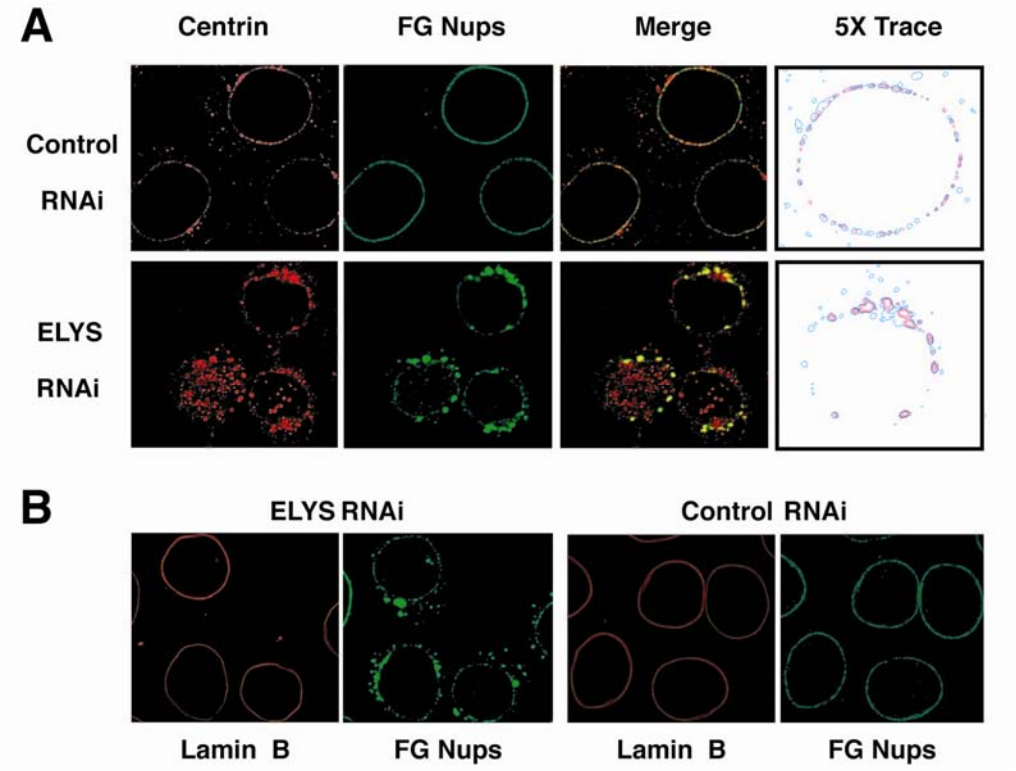

Figure 4.5. ELYS/MEL-28 RNAi disrupts centrin 2 at the nuclear pore.
Immunofluorescence on HeLa cells transfected with ELYS siRNA duplexes, known to disrupt nuclear pore structure, for 48 h. After ELYS or control RNAi, the cells were digitonin permeabilized and fixed with formaldehyde. (A) Double immunofluorescence, performed with anti-centrin antibody A and anti-FG Nup monoclonal antibody mAb414, is shown with the merged image at the right. The far right image is a contour trace of the individual antibody signals as a representative of a transfected cell. (B) Double immunofluorescence performed with anti-lamin B and anti-FG Nup monoclonal antibody mAb414 is shown. ELYS RNAi disrupts centrin 2 at the nuclear rim, while leaving the nuclear lamina unaltered.

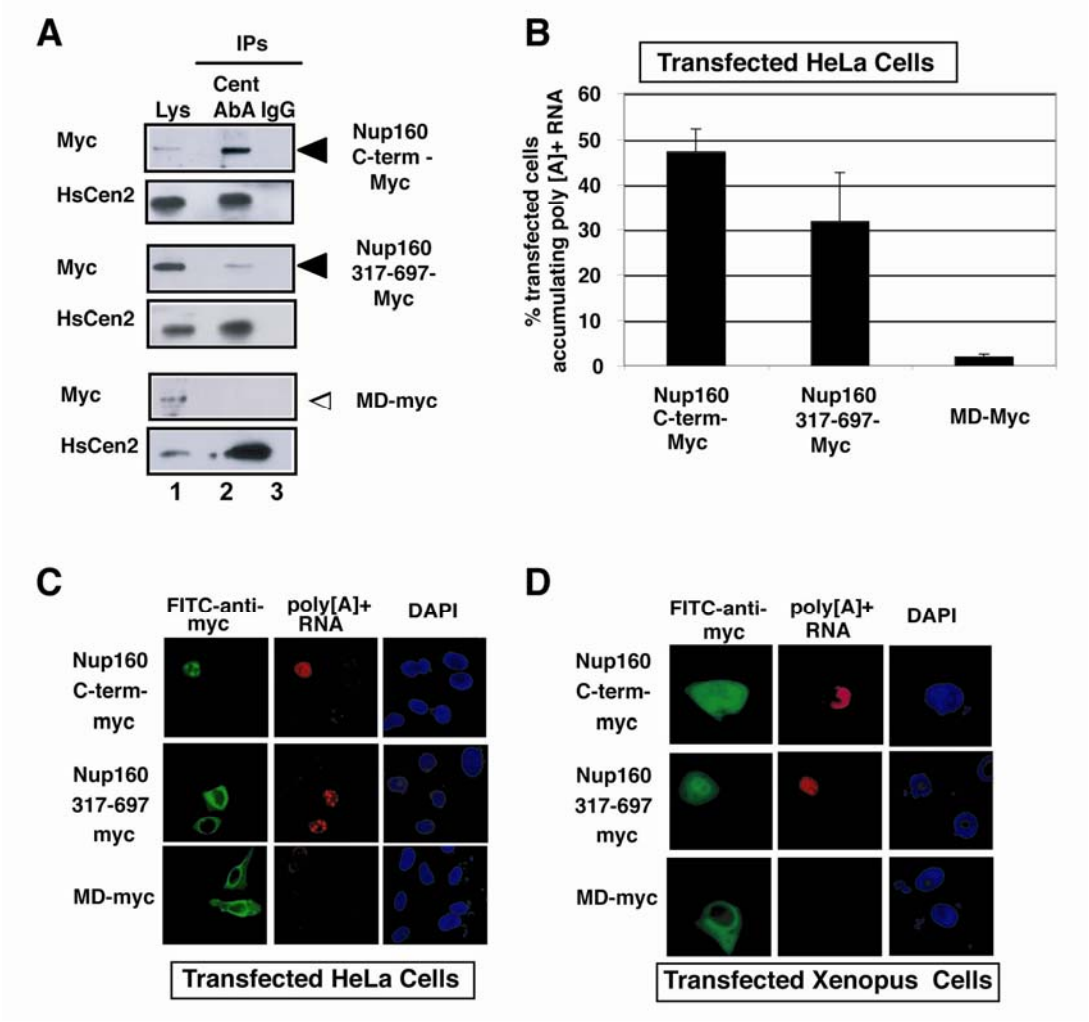

Figure 4.6. Fragments of Nup160 that interact with centrin 2 cause nuclear accumulation of poly [A]+ RNA. (A) Anti-centrin antibody A co-immunoprecipitates Myc-tagged Nup160 C-terminus (aa 912-1436) and Myc-tagged Nup160 aa 317-697 (lane 2), but not malate dehydrogenase (MD, lane 2) from transfected HeLa cells. Lane 1 indicates the amount of transfected protein produced. Lane 2 measures whether and how much of the protein is immunoprecipitated by the anti-centrin antibody, as revealed by probing with an anti-Myc antibody. Differences in transfection efficiency or the level of construct protein expression between the constructs were present (see Lane 1); however, in this experiment at least as much Myc-malate dehydrogenase was expressed as was Myc-Nup160 C-terminus (lane 1, compare Myc-MD to Myc-Nup160 C-term). Immunoprecipitation with goat IgG serum (IgG) was used as a negative control (lane 3). 'Lys' indicates a lane with 10% of the input transfected HeLa cell lysate shown (lane 1); the remaining 90% was used for the anti-centrin 2 immunoprecipitation (lane 2). (B) Overexpression of Nup160 aa 317-697 or Nup160 C-terminus (aa 912-1436), but not malate dehydrogenase, causes nuclear accumulation of poly [A]+ RNA. HeLa cells were transfected with the myc-tagged Nup160 fragments or malate dehydrogenase 24 hours before the poly [A]+ RNA accumulation assay was performed. Quantitation of nuclear poly [A]+ RNA accumulation was done on 500 cells per experiment. The percentage of transfected HeLa cells with nuclear poly [A]+ RNA accumulation was calculated in three independent experiments and averaged. (C) Typical views of HeLa cells successfully transfected with the myc-tagged Nup160 fragments or malate dehydrogenase are shown. Left panels show expression of the myc tagged constructs using FITC-labeled myc antibody (green). The center panels are the same cells hybridized with Cy3-oligo[dT]$_{50}$ to show nuclear poly [A]+ RNA accumulation (red). Right panels show the complete field of cells by DAPI DNA staining. (D) Typical views of *Xenopus* XL177 cells successfully transfected, as described in Materials and Methods, with the myc-tagged Nup160 fragments or malate dehydrogenase are shown. The cells were visualized as in (C).

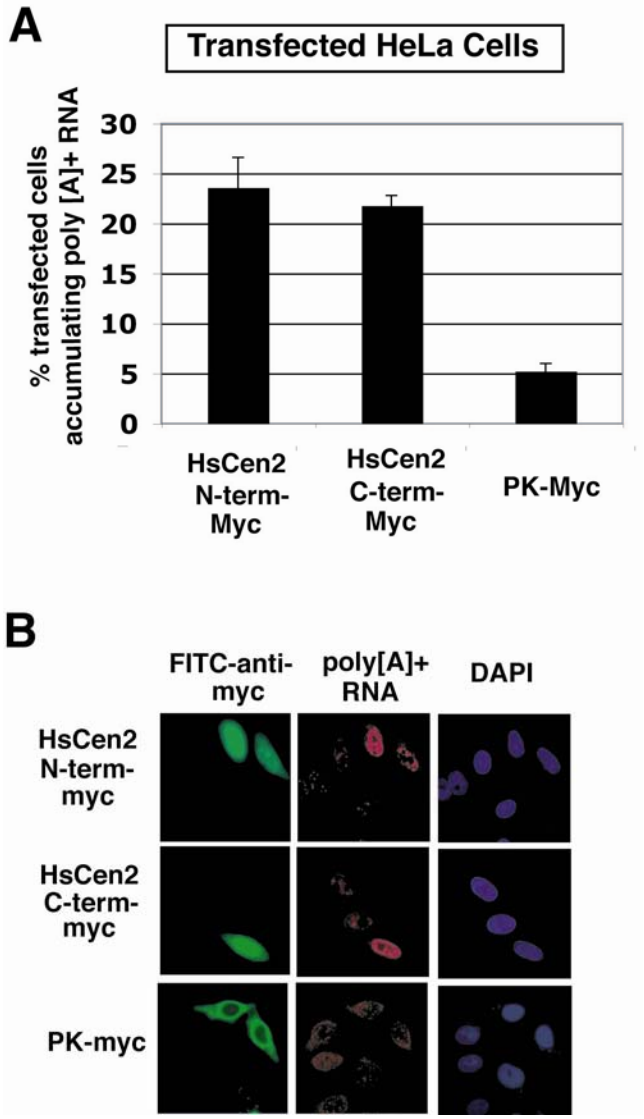

Figure 4.7. Overexpression of the N- or C-terminal half of centrin 2 causes nuclear accumulation of poly [A]+ RNA in human cells.

(A) Overexpression of the human centrin 2 N-terminus or C-terminus, but not pyruvate kinase, causes nuclear accumulation of poly [A]+ RNA. HeLa cells were transfected with the indicated construct 24 hours before the poly [A]+ RNA accumulation assay was performed. Quantitation of nuclear poly [A]+ RNA accumulation in cells transfected with either of the two human centrin 2 fragments or the control pyruvate kinase gene was done on 500 cells per experiment. The percentage of transfected HeLa cells with nuclear poly [A]+ RNA accumulation was calculated in three independent experiments and averaged. (B) Typical views of HeLa cells successfully transfected with the myc-tagged centrin fragments or pyruvate kinase control gene are shown. The cells were transfected as in (A). Left panels show expression of the myc tagged constructs using FITC-labeled myc antibody (green). The center panels are the same cells hybridized with Cy3-oligo $[dT]_{50}$ to show nuclear poly [A]+ RNA accumulation (red). Right panels show the complete field of cells by DAPI DNA staining.

Figure 4.8. Overexpression of the N- or C-terminal half of centrin 2 blocks protein export, but not import.
(A) HeLa cells were transfected with the Rev-Glucocorticoid ligand binding domain-GFP (RGG) plasmid for 16 hours before the addition of dexamethasone to induce RGG import which occurred exactly as in (44, 75, 128). (B) Overexpression of the human centrin 2 N-terminus or C-terminus, Nup160 aa 317-697 or Nup160 C-terminus (aa 912-1436) or malate dehydrogenase, have no effect on RGG protein import. HeLa cells were co-transfected with the indicated constructs plus the RGG construct 16 hours before the addition of dexamethasone to induce RGG protein import. Typical views of HeLa cells successfully transfected with the myc-tagged constructs and the RGG construct following induced protein import are shown. Top panels show expression of the myc-tagged constructs using TRITC-labeled myc antibody (red). The bottom panels are the same cells showing the location of the RGG protein via its GFP tag (green). Typically, the RGG protein targets to the nucleoli within the nucleus (44, 75, 128) as observed here. (C) Overexpression of the human centrin 2 N-terminus or C-terminus, but not Nup160 aa 317-697 or C-terminus (aa 912-1436) and malate dehydrogenase, blocks RGG protein export. Cells were transfected and treated with dexamethasone as in (B). Following RGG protein import, the cells were switched to fresh media lacking dexamethasone for two hours to induce RGG protein export. Typical views of HeLa cells successfully transfected with the myc-tagged proteins and RGG construct following induced protein export are shown and were visualized as in (B). Of the transfected cells 24% were inhibited for RGG export by the N-terminal half of centrin 2 and 22% by the C-terminal half of centrin 2 while only 5% of control malate dehydrogenase transfected cells showed inhibition of export. (D) Quantitation of RGG protein import in cells co-transfected with the human centrin 2 N-terminus or C-terminus, Nup160 aa 317-697 or C-terminus (aa 912-1436) or malate dehydrogenase. The cells were transfected as in (B). The percentage of transfected HeLa cells with blocked RGG protein import was calculated in three independent experiments and averaged. 500 transfected cells were counted per experiment. (E) Quantitation of RGG protein export in cells co-transfected with the myc-tagged constructs as in (B) was performed as in (D).

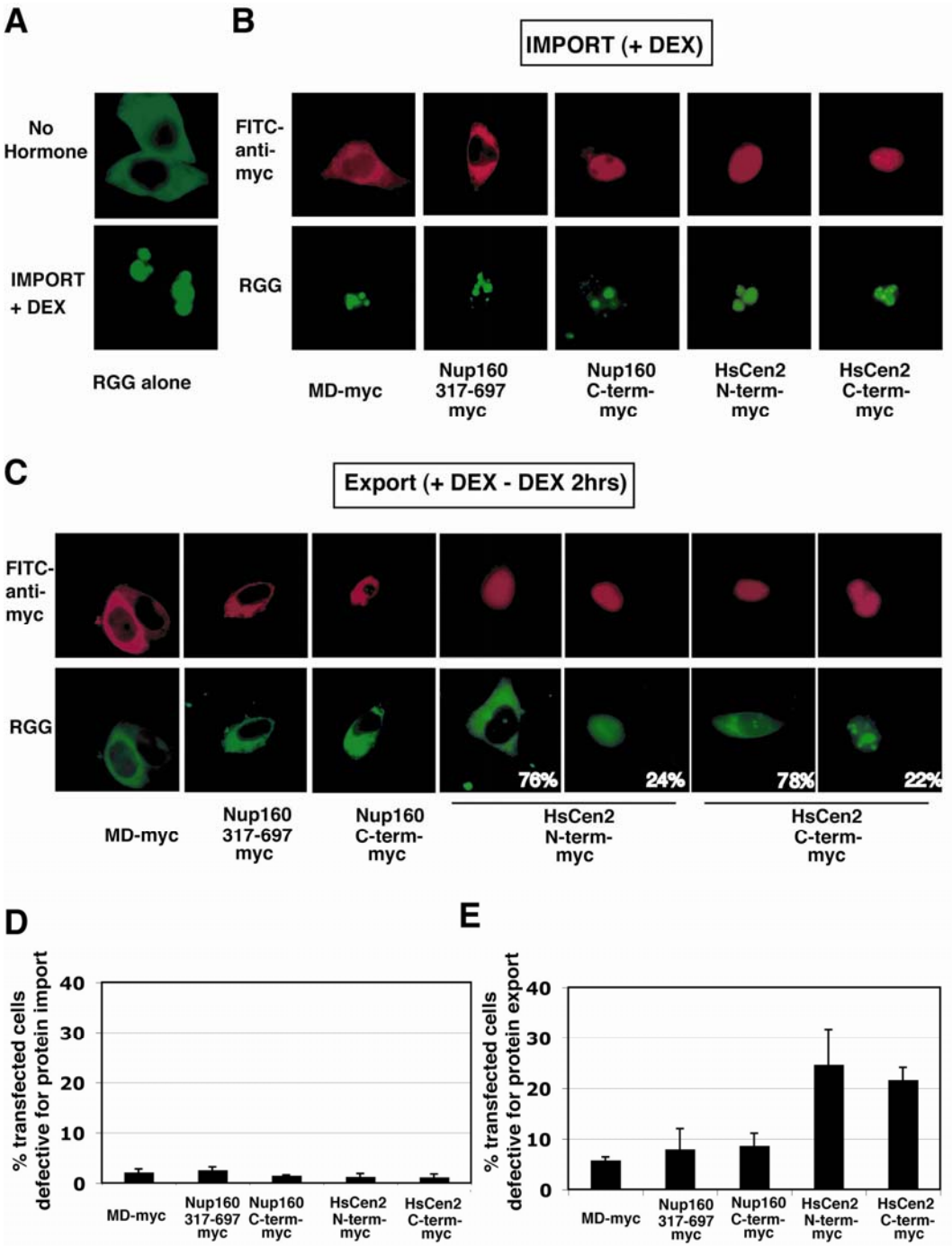
A
B
IMPORT (+ DEX)
No Hormone
IMPORT + DEX
FITC-anti-myc
RGG
RGG alone
MD-myc
Nup160 317-697 myc
Nup160 C-term-myc
HsCen2 N-term-myc
HsCen2 C-term-myc
C
Export (+ DEX - DEX 2hrs)
FITC-anti-myc
RGG
76%
24%
78%
22%
MD-myc
Nup160 317-697 myc
Nup160 C-term-myc
HsCen2 N-term-myc
HsCen2 C-term-myc
D
% transfected cells defective for protein import
0
10
20
30
40
MD-myc
Nup160 317-697 myc
Nup160 C-term-myc
HsCen2 N-term-myc
HsCen2 C-term-myc
E
% transfected cells defective for protein export
0
10
20
30
40
MD-myc
Nup160 317-697 myc
Nup160 C-term-myc
HsCen2 N-term-myc
HsCen2 C-term-myc

Supplemental Data

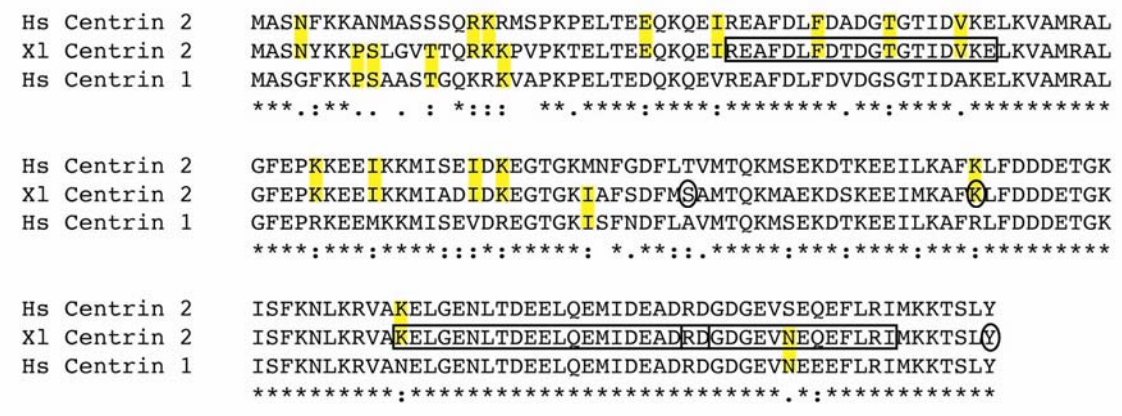

Supplemental Figure S4.1. *Xenopus* Centrin 2/Centrin shares 85% identity with human centrin 2. A mass spectrometry screen identified three protein fragments that corresponded to amino acids 34-52, 131-152, and 151-165 of *Xenopus* centrin 2 (NP_001080127) and Cetn2-prov protein (AAH54948). The sequence of *Xenopus* centrin 2 is shown with the boxes indicating the peptide fragments. A Blast search of the Entrez protein database identified 2 additional homologous *Xenopus* protein isolates (AAA79194 and AAH84063) that displayed only a three amino acid difference (circled amino acids 91, 111, and 172) from the *Xenopus* centrin 2 protein shown. These were referred to in the Entrez database generically as centrin. Alignment of these sequences with the human centrin 1 (NP_004057) and 2 (NP_004335) sequence (shown) reveals that these *Xenopus* sequences display 85% identity to human centrin 2 and only 80% identity to human centrin 1. Human centrin 1 and centrin 2 differ at 28 residues. Of these residues that distinguish human centrin 1 and 2, *Xenopus* centrin 2 matches human centrin 2 at 14 sites, but only matches human centrin 1 at 6 of these sites (highlighted residues). (Note that in a number of places, *Xenopus* centrin 2 differs from both human centrin 1 and 2, unmarked).

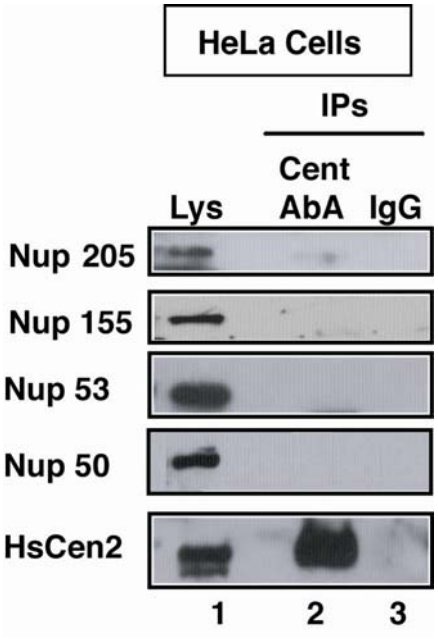

Supplemental Figure S4.2. Lack of centrin interaction with multiple non-Nup107-160 complex nucleoporins. Additional immunoblots were done in parallel to Figure 4.2B-D. These confirm that anti-centrin antibody A (Ab A) immunoprecipitates human centrin 2, and reveal that it does not immunoprecipitate the non-Nup107-160 complex nucleoporins Nup205, Nup155, Nup53, or Nup 50 (lane 2). Immunoprecipitation with goat IgG (lane 3) was used as a negative control. 'Lys' indicates a fraction of input HeLa cell lysate.

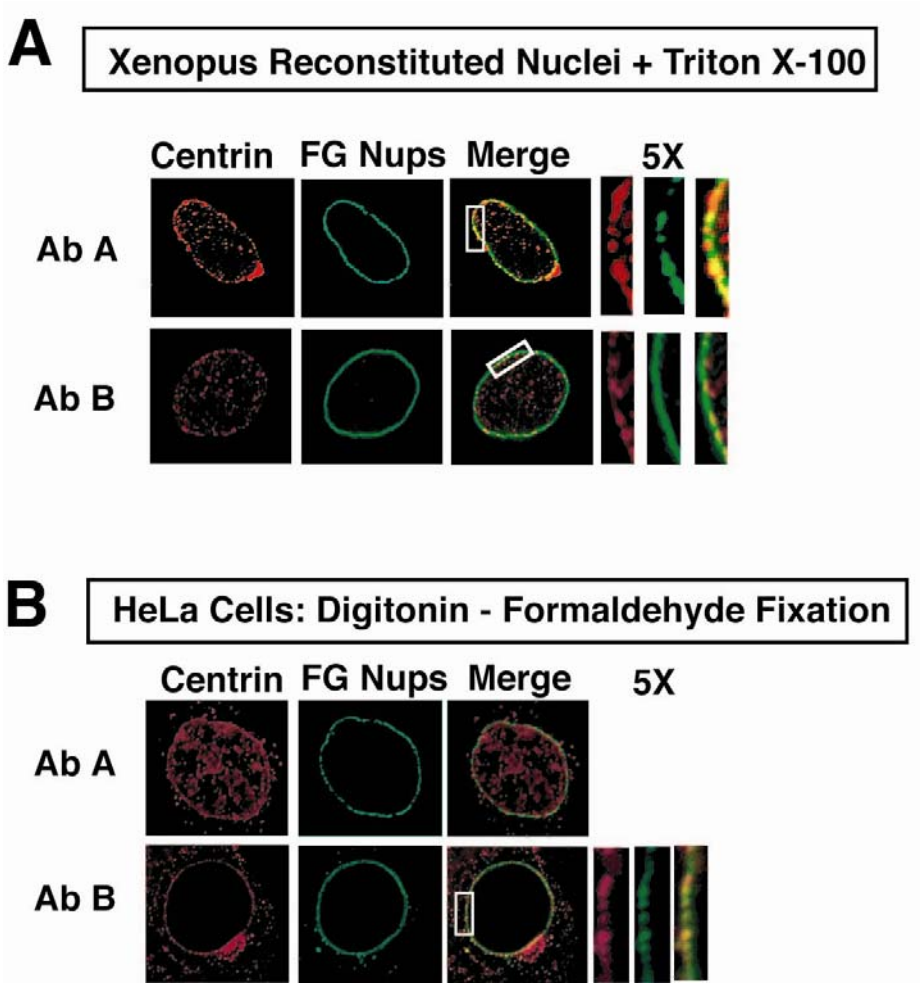

Supplemental Figure S4.3. Additional conditions demonstrating localization of centrin 2 at the nuclear rim.
(A) *Xenopus* centrin 2 localizes to the rim of in vitro reconstituted nuclei. Double immunofluorescence of reconstituted nuclei, spun down, and Triton X-100 permeabilized were stained with anti-centrin 2 antibodies (Ab A or B) (left panels) and mAb414 (middle panels) with merged images (right panels). Insets (far right) are a 5X magnification. A punctate rim is observed, but is not as distinct as in Figure 4.3A, where Triton X-100 was not used. This experiment was performed on the same day as those in Figure 4.3A. (B) Immunofluorescence performed with either centrin antibody A or B demonstrates that human centrin 2 is present at nuclear rim in a punctate pattern in HeLa cells treated with digitonin before formaldehyde fixation. Double immunofluorescence of HeLa cells with anti-centrin Ab A or B and anti-FG Nup monoclonal antibody mAb414 is shown with the merged image at the right. The inset (far right) is a 5X magnification, with the nuclear (N) and cytoplasmic (C) sides of the nuclear envelope indicated. A punctate rim is observed, but is not as distinct as in Figure 4.4B where digitonin treatment was performed after formaldehyde fixation. This experiment was performed on the same day as those in Figure 4.4B.

Supplemental Figure S4.4. Centrin 2 siRNA disrupts mRNA and protein export, but not protein import.

(A) Depletion of centrin 2 protein by siRNA. Immunoblotting for centrin 2 (Ab B), Nup160, and γ-tubulin was performed on HeLa cells transfected with control (lane 1) or centrin 2 (lane 2) siRNA for 48 hours. (B) Depletion of centrin 2 by siRNA causes nuclear accumulation of poly [A]+ RNA. HeLa cells were transfected with control or centrin 2 siRNA duplexes 48 hours before the poly [A]+ RNA accumulation assay was performed. Only cells which had a single nucleus were quantitated (~half the total cells on the coverslip). The figure indicates the % of single nucleate cells accumulating poly [A]+ RNA. Multinucleate cells and cells arrested in mitosis were not assessed. Quantitation of nuclear poly [A]+ RNA accumulation was performed on 500 single nucleate cells per experiment. The percentage of these transfected HeLa cells with nuclear poly [A]+ RNA accumulation was calculated form three independent experiments and averaged. (C) Typical views of HeLa cells transfected with control or centrin 2 siRNA are shown. The cells were transfected as in (B). The red panels show cells hybridized with Cy3-oligo $[dT]_{50}$ to assess nuclear poly [A]+ RNA accumulation. The blue panels show the complete field of cells stained with DAPI DNA dye. (D) HeLa cells were transfected with the RGG protein import/export plasmid together with control or centrin 2 siRNA oligonucleotides for 48 hours, followed by the addition of dexamethasone to induce RGG import. In parallel, a second set of similarly transfected cells where RGG protein import had been induced were switched to fresh media lacking dexamethasone and incubated for two additional hours, in order to induce RGG protein export. Typical views are shown of siRNA transfected HeLa cells (control or centrin 2) expressing the RGG construct visualized via its GFP tag following the induction or either protein import or export. (E) Quantitation of RGG protein import in single nucleate interphase cells is shown after transfection with control or centrin 2 siRNA. The cells were transfected as in (D). The percentage of transfected single nucleate HeLa cells which contained blocked RGG protein import was calculated in three independent experiments and averaged. 500 transfected cells were counted per experiment. (F) Quantitation of RGG protein *export* in cells co-transfected as in (E). The experiments presented in panels D-F were performed at the same time.

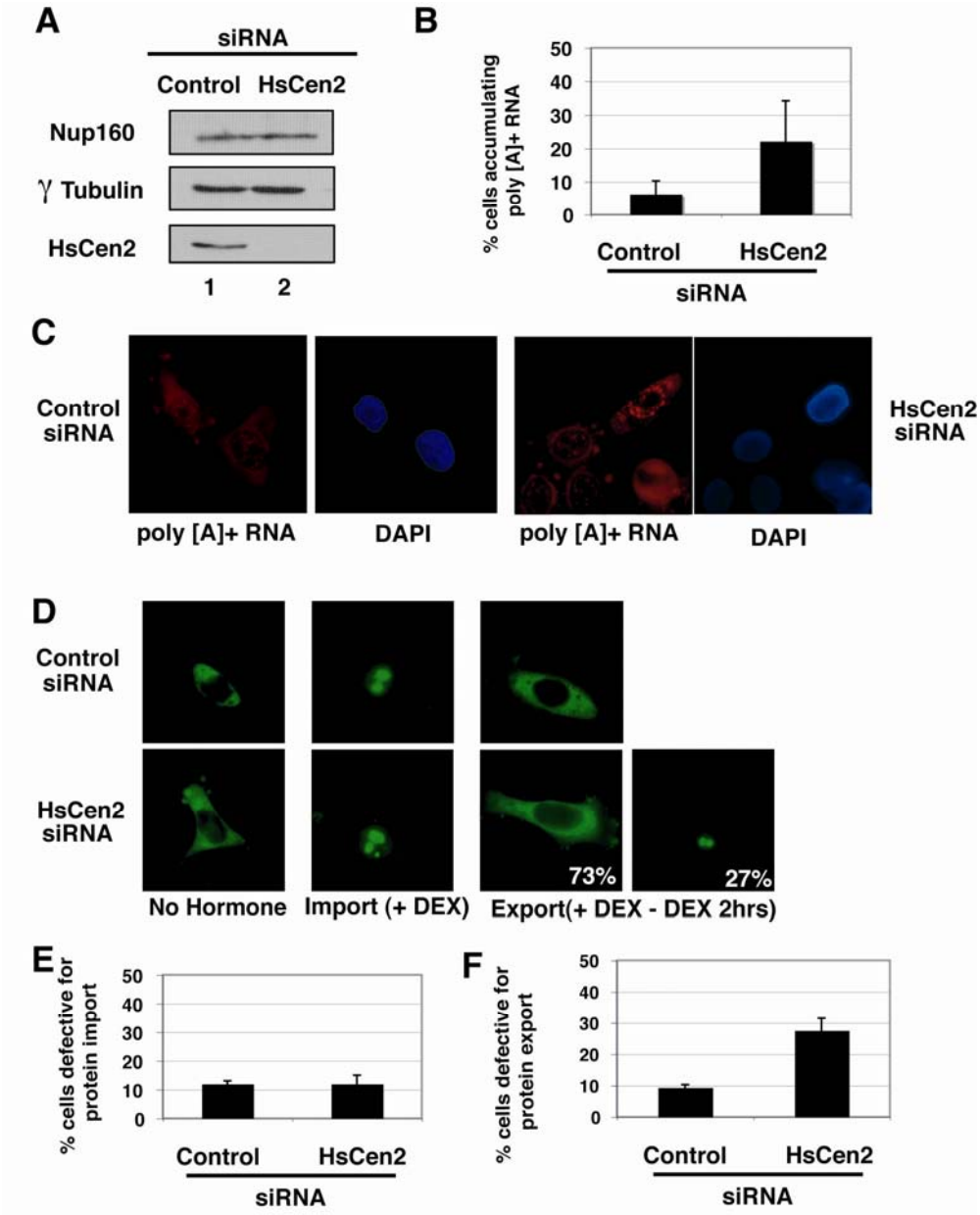
A
siRNA
Control
HsCen2
Nup160
γ Tubulin
HsCen2
1
2
B
% cells accumulating poly [A]+ RNA
50
40
30
20
10
0
Control
HsCen2
siRNA
C
Control siRNA
HsCen2 siRNA
poly [A]+ RNA
DAPI
poly [A]+ RNA
DAPI
D
Control siRNA
HsCen2 siRNA
73%
27%
No Hormone
Import (+ DEX)
Export(+ DEX - DEX 2hrs)
E
% cells defective for protein import
50
40
30
20
10
0
Control
HsCen2
siRNA
F
% cells defective for protein export
50
40
30
20
10
0
Control
HsCen2
siRNA

Acknowledgements

The text in Chapter 4 is a modified version of a manuscript in press in **Molecular and Cellular Biology:** Resendes K, **Rasala BA,** and Forbes DF, Centrin 2 localizes to the vertebrate nuclear pore and is involved in mRNA and protein export. Mol Cell Biol. In press. I was the second author listed in this publication which forms that basis of Chapter 4. We thank Leonie Heyworth and Art Orjalo for help in the initial cloning of the Nup160 C-terminal fragments, Zhouxin Shen and Steven Briggs for performing the mass spectrometry, and members of the Forbes lab for helpful discussions.

References

1. Abe, E., K. Kuwahara, M. Yoshida, M. Suzuki, H. Terasaki, Y. Matsuo, E. I. Takahashi, and N. Sakaguchi. 2000. Structure, expression, and chromosomal localization of the human gene encoding a germinal center-associated nuclear protein (GANP) that associates with MCM3 involved in the initiation of DNA replication. Gene 255:219-27.

2. Aitchison, J. D., G. Blobel, and M. P. Rout. 1995. Nup120p: a yeast nucleoporin required for NPC distribution and mRNA transport. J Cell Biol 131:1659-75.

3. Allen, T. D., J. M. Cronshaw, S. Bagley, E. Kiseleva, and M. W. Goldberg. 2000. The nuclear pore complex: mediator of translocation between nucleus and cytoplasm. J Cell Sci 113 (Pt 10):1651-9.

4. Araki, M., C. Masutani, M. Takemura, A. Uchida, K. Sugasawa, J. Kondoh, Y. Ohkuma, and F. Hanaoka. 2001. Centrosome protein centrin 2/caltractin 1 is part of the xeroderma pigmentosum group C complex that initiates global genome nucleotide excision repair. J Biol Chem 276:18665-72.

5. Arnaoutov, A., Y. Azuma, K. Ribbeck, J. Joseph, Y. Boyarchuk, T. Karpova, J. McNally, and M. Dasso. 2005. Crm1 is a mitotic effector of Ran-GTP in somatic cells. Nat Cell Biol 7:626-32.

6. Bachi, A., I. C. Braun, J. P. Rodrigues, N. Pante, K. Ribbeck, C. von Kobbe, U. Kutay, M. Wilm, D. Gorlich, M. Carmo-Fonseca, and E. Izaurralde. 2000. The C-terminal domain of TAP interacts with the nuclear pore complex and promotes export of specific CTE-bearing RNA substrates. Rna 6:136-58.

7. Bai, S. W., J. Rouquette, M. Umeda, W. Faigle, D. Loew, S. Sazer, and V. Doye. 2004. The fission yeast Nup107-120 complex functionally interacts with the small GTPase Ran/Spi1 and is required for mRNA export, nuclear pore distribution, and proper cell division. Mol Cell Biol 24:6379-92.

8. Bastos, R., A. Lin, M. Enarson, and B. Burke. 1996. Targeting and function in mRNA export of nuclear pore complex protein Nup153. J Cell Biol 134:1141-56.

9. Bauer, A., and R. Kolling. 1996. The SAC3 gene encodes a nuclear protein required for normal progression of mitosis. J Cell Sci 109 (Pt 6):1575-83.

10. Baum, P., C. Furlong, and B. Byers. 1986. Yeast gene required for spindle pole body duplication: homology of its product with Ca2+-binding proteins. Proc Natl Acad Sci U S A 83:5512-6.

11. Belgareh, N., G. Rabut, S. W. Bai, M. van Overbeek, J. Beaudouin, N. Daigle, O. V. Zatsepina, F. Pasteau, V. Labas, M. Fromont-Racine, J. Ellenberg, and V. Doye. 2001. An evolutionarily conserved NPC subcomplex, which redistributes in part to kinetochores in mammalian cells. J Cell Biol 154:1147-60.

12. Blower, M. D., M. Nachury, R. Heald, and K. Weis. 2005. A Rae1-containing ribonucleoprotein complex is required for mitotic spindle assembly. Cell 121:223-34.

13. Boer, J., J. Bonten-Surtel, and G. Grosveld. 1998. Overexpression of the nucleoporin CAN/NUP214 induces growth arrest, nucleocytoplasmic transport defects, and apoptosis. Mol Cell Biol 18:1236-47.

14. Cohen, M., N. Feinstein, K. L. Wilson, and Y. Gruenbaum. 2003. Nuclear pore protein gp210 is essential for viability in HeLa cells and Caenorhabditis elegans. Mol Biol Cell 14:4230-7.

15. Cole, C. N., and J. J. Scarcelli. 2006. Transport of messenger RNA from the nucleus to the cytoplasm. Curr Opin Cell Biol 18:299-306.

16. Conti, E., and E. Izaurralde. 2001. Nucleocytoplasmic transport enters the atomic age. Curr Opin Cell Biol 13:310-9.

17. Cordes, V. C., S. Reidenbach, and W. W. Franke. 1995. High content of a nuclear pore complex protein in cytoplasmic annulate lamellae of Xenopus oocytes. Eur J Cell Biol 68:240-55.

18. Cronshaw, J. M., A. N. Krutchinsky, W. Zhang, B. T. Chait, and M. J. Matunis. 2002. Proteomic analysis of the mammalian nuclear pore complex. J Cell Biol 158:915-27.

19. D'Assoro, A. B., F. Stivala, S. Barrett, G. Ferrigno, and J. L. Salisbury. 2001. GFP-centrin as a marker for centriole dynamics in the human breast cancer cell line MCF-7. Ital J Anat Embryol 106:103-10.

20. Dabauvalle, M. C., K. Loos, H. Merkert, and U. Scheer. 1991. Spontaneous assembly of pore complex-containing membranes ("annulate lamellae") in Xenopus egg extract in the absence of chromatin. J Cell Biol 112:1073-82.

21. Damelin, M., and P. A. Silver. 2002. In situ analysis of spatial relationships between proteins of the nuclear pore complex. Biophys J 83:3626-36.

22. Dockendorff, T. C., C. V. Heath, A. L. Goldstein, C. A. Snay, and C. N. Cole. 1997. C-terminal truncations of the yeast nucleoporin Nup145p produce a rapid temperature-conditional mRNA export defect and alterations to nuclear structure. Mol Cell Biol 17:906-20.

23. Doye, V., R. Wepf, and E. C. Hurt. 1994. A novel nuclear pore protein Nup133p with distinct roles in poly(A)+ RNA transport and nuclear pore distribution. Embo J 13:6062-75.

24. Drummond, S. P., and K. L. Wilson. 2002. Interference with the cytoplasmic tail of gp210 disrupts "close apposition" of nuclear membranes and blocks nuclear pore dilation. J Cell Biol 158:53-62.

25. Enninga, J., A. Levay, and B. M. Fontoura. 2003. Sec13 shuttles between the nucleus and the cytoplasm and stably interacts with Nup96 at the nuclear pore complex. Mol Cell Biol 23:7271-84.

26. Erickson, E. S., O. L. Mooren, D. Moore, J. R. Krogmeier, and R. C. Dunn. 2006. The role of nuclear envelope calcium in modifying nuclear pore complex structure. Can J Physiol Pharmacol 84:309-18.

27. Erkmann, J. A., and U. Kutay. 2004. Nuclear export of mRNA: from the site of transcription to the cytoplasm. Exp Cell Res 296:12-20.

28. Erkmann, J. A., R. Sanchez, N. Treichel, W. F. Marzluff, and U. Kutay. 2005. Nuclear export of metazoan replication-dependent histone mRNAs is dependent on RNA length and is mediated by TAP. Rna 11:45-58.

29. Errabolu, R., M. A. Sanders, and J. L. Salisbury. 1994. Cloning of a cDNA encoding human centrin, an EF-hand protein of centrosomes and mitotic spindle poles. J Cell Sci 107 (Pt 1):9-16.

30. Finlay, D. R., and D. J. Forbes. 1990. Reconstitution of biochemically altered nuclear pores: transport can be eliminated and restored. Cell 60:17-29.

31. Fischer, T., S. Rodriguez-Navarro, G. Pereira, A. Racz, E. Schiebel, and E. Hurt. 2004. Yeast centrin Cdc31 is linked to the nuclear mRNA export machinery. Nat Cell Biol 6:840-8.

32. Fischer, T., K. Strasser, A. Racz, S. Rodriguez-Navarro, M. Oppizzi, P. Ihrig, J. Lechner, and E. Hurt. 2002. The mRNA export machinery requires

the novel Sac3p-Thp1p complex to dock at the nucleoplasmic entrance of the nuclear pores. Embo J 21:5843-52.

33. Fischer, U., J. Huber, W. C. Boelens, I. W. Mattaj, and R. Luhrmann. 1995. The HIV-1 Rev activation domain is a nuclear export signal that accesses an export pathway used by specific cellular RNAs. Cell 82:475-83.

34. Forler, D., G. Rabut, F. D. Ciccarelli, A. Herold, T. Kocher, R. Niggeweg, P. Bork, J. Ellenberg, and E. Izaurralde. 2004. RanBP2/Nup358 provides a major binding site for NXF1-p15 dimers at the nuclear pore complex and functions in nuclear mRNA export. Mol Cell Biol 24:1155-67.

35. Fornerod, M., M. Ohno, M. Yoshida, and I. W. Mattaj. 1997. CRM1 is an export receptor for leucine-rich nuclear export signals. Cell 90:1051-60.

36. Franz, C., R. Walczak, S. Yavuz, R. Santarella, M. Gentzel, P. Askjaer, V. Galy, M. Hetzer, I. W. Mattaj, and W. Antonin. 2007. MEL-28/ELYS is required for the recruitment of nucleoporins to chromatin and postmitotic nuclear pore complex assembly. EMBO Rep 8:165-72.

37. Geier, B. M., H. Wiech, and E. Schiebel. 1996. Binding of centrins and yeast calmodulin to synthetic peptides corresponding to binding sites in the spindle pole body components Kar1p and Spc110p. J Biol Chem 271:28366-74.

38. Goldstein, A. L., C. A. Snay, C. V. Heath, and C. N. Cole. 1996. Pleiotropic nuclear defects associated with a conditional allele of the novel nucleoporin Rat9p/Nup85p. Mol Biol Cell 7:917-34.

39. Gorlich, D., and U. Kutay. 1999. Transport between the cell nucleus and the cytoplasm. Annu Rev Cell Dev Biol 15:607-60.

40. Grandi, P., T. Dang, N. Pane, A. Shevchenko, M. Mann, D. Forbes, and E. Hurt. 1997. Nup93, a vertebrate homologue of yeast Nic96p, forms a complex with a novel 205-kDa protein and is required for correct nuclear pore assembly. Mol Biol Cell 8:2017-38.

41. Greber, U. F., and L. Gerace. 1995. Depletion of calcium from the lumen of endoplasmic reticulum reversibly inhibits passive diffusion and signal-mediated transport into the nucleus. J Cell Biol 128:5-14.

42. Greber, U. F., and L. Gerace. 1992. Nuclear protein import is inhibited by an antibody to a lumenal epitope of a nuclear pore complex glycoprotein. J Cell Biol 116:15-30.

43. Griffis, E. R., N. Altan, J. Lippincott-Schwartz, and M. A. Powers. 2002. Nup98 is a mobile nucleoporin with transcription-dependent dynamics. Mol Biol Cell 13:1282-97.

44. Gustin, K. E., and P. Sarnow. 2001. Effects of poliovirus infection on nucleo-cytoplasmic trafficking and nuclear pore complex composition. Embo J 20:240-9.

45. Hallberg, E., R. W. Wozniak, and G. Blobel. 1993. An integral membrane protein of the pore membrane domain of the nuclear envelope contains a nucleoporin-like region. J Cell Biol 122:513-21.

46. Harel, A., R. C. Chan, A. Lachish-Zalait, E. Zimmerman, M. Elbaum, and D. J. Forbes. 2003. Importin beta negatively regulates nuclear membrane fusion and nuclear pore complex assembly. Mol Biol Cell 14:4387-96.

47. Harel, A., and D. J. Forbes. 2004. Importin beta: conducting a much larger cellular symphony. Mol Cell 16:319-30.

48. Hart, P. E., J. N. Glantz, J. D. Orth, G. M. Poynter, and J. L. Salisbury. 1999. Testis-specific murine centrin, Cetn1: genomic characterization and evidence for retroposition of a gene encoding a centrosome protein. Genomics 60:111-20.

49. Hart, P. E., G. M. Poynter, C. M. Whitehead, J. D. Orth, J. N. Glantz, R. C. Busby, S. L. Barrett, and J. L. Salisbury. 2001. Characterization of the X-linked murine centrin Cetn2 gene. Gene 264:205-13.

50. Heath, C. V., C. S. Copeland, D. C. Amberg, V. Del Priore, M. Snyder, and C. N. Cole. 1995. Nuclear pore complex clustering and nuclear accumulation of poly(A)+ RNA associated with mutation of the Saccharomyces cerevisiae RAT2/NUP120 gene. J Cell Biol 131:1677-97.

51. Higginbotham, H., S. Bielas, T. Tanaka, and J. G. Gleeson. 2004. Transgenic mouse line with green-fluorescent protein-labeled Centrin 2 allows visualization of the centrosome in living cells. Transgenic Res 13:155-64.

52. Hutten, S., and R. H. Kehlenbach. 2006. Nup214 is required for CRM1-dependent nuclear protein export in vivo. Mol Cell Biol 26:6772-85.

53. Ivanovska, I., and M. D. Rose. 2001. Fine structure analysis of the yeast centrin, Cdc31p, identifies residues specific for cell morphology and spindle pole body duplication. Genetics 157:503-18.

54. Izaurralde, E. 2002. A novel family of nuclear transport receptors mediates the export of messenger RNA to the cytoplasm. Eur J Cell Biol 81:577-84.

55. Jones, A. L., B. B. Quimby, J. K. Hood, P. Ferrigno, P. H. Keshava, P. A. Silver, and A. H. Corbett. 2000. SAC3 may link nuclear protein export to cell cycle progression. Proc Natl Acad Sci U S A 97:3224-9.

56. Joseph, J., S. T. Liu, S. A. Jablonski, T. J. Yen, and M. Dasso. 2004. The RanGAP1-RanBP2 complex is essential for microtubule-kinetochore interactions in vivo. Curr Biol 14:611-7.

57. Katahira, J., K. Strasser, A. Podtelejnikov, M. Mann, J. U. Jung, and E. Hurt. 1999. The Mex67p-mediated nuclear mRNA export pathway is conserved from yeast to human. Embo J 18:2593-609.

58. Khuda, S. E., M. Yoshida, Y. Xing, T. Shimasaki, M. Takeya, K. Kuwahara, and N. Sakaguchi. 2004. The Sac3 homologue shd1 is involved in mitotic progression in mammalian cells. J Biol Chem 279:46182-90.

59. Kilmartin, J. V. 2003. Sfi1p has conserved centrin-binding sites and an essential function in budding yeast spindle pole body duplication. J Cell Biol 162:1211-21.

60. Kuwahara, K., S. Tomiyasu, S. Fujimura, K. Nomura, Y. Xing, N. Nishiyama, M. Ogawa, S. Imajoh-Ohmi, S. Izuta, and N. Sakaguchi. 2001. Germinal center-associated nuclear protein (GANP) has a phosphorylation-dependent DNA-primase activity that is up-regulated in germinal center regions. Proc Natl Acad Sci U S A 98:10279-83.

61. Kuwahara, K., M. Yoshida, E. Kondo, A. Sakata, Y. Watanabe, E. Abe, Y. Kouno, S. Tomiyasu, S. Fujimura, T. Tokuhisa, H. Kimura, T. Ezaki, and N. Sakaguchi. 2000. A novel nuclear phosphoprotein, GANP, is up-regulated in centrocytes of the germinal center and associated with MCM3, a protein essential for DNA replication. Blood 95:2321-8.

62. Laoukili, J., E. Perret, S. Middendorp, O. Houcine, C. Guennou, F. Marano, M. Bornens, and F. Tournier. 2000. Differential expression and cellular distribution of centrin isoforms during human ciliated cell differentiation in vitro. J Cell Sci 113 (Pt 8):1355-64.

63. Lau, C. K., V. A. Delmar, and D. J. Forbes. 2006. Topology of yeast Ndc1p: predictions for the human NDC1/NET3 homologue. Anat Rec A Discov Mol Cell Evol Biol 288:681-94.

64. Lee, M. A., R. C. Dunn, D. E. Clapham, and L. Stehno-Bittel. 1998. Calcium regulation of nuclear pore permeability. Cell Calcium 23:91-101.

65. Lee, V. D., and B. Huang. 1993. Molecular cloning and centrosomal localization of human caltractin. Proc Natl Acad Sci U S A 90:11039-43.

66. Lei, E. P., and P. A. Silver. 2002. Protein and RNA export from the nucleus. Dev Cell 2:261-72.

67. Lei, E. P., C. A. Stern, B. Fahrenkrog, H. Krebber, T. I. Moy, U. Aebi, and P. A. Silver. 2003. Sac3 is an mRNA export factor that localizes to cytoplasmic fibrils of nuclear pore complex. Mol Biol Cell 14:836-47.

68. Levesque, L., Y. C. Bor, L. H. Matzat, L. Jin, S. Berberoglu, D. Rekosh, M. L. Hammarskjold, and B. M. Paschal. 2006. Mutations in tap uncouple RNA export activity from translocation through the nuclear pore complex. Mol Biol Cell 17:931-43.

69. Levesque, L., B. Guzik, T. Guan, J. Coyle, B. E. Black, D. Rekosh, M. L. Hammarskjold, and B. M. Paschal. 2001. RNA export mediated by tap involves NXT1-dependent interactions with the nuclear pore complex. J Biol Chem 276:44953-62.

70. Li, O., C. V. Heath, D. C. Amberg, T. C. Dockendorff, C. S. Copeland, M. Snyder, and C. N. Cole. 1995. Mutation or deletion of the Saccharomyces cerevisiae RAT3/NUP133 gene causes temperature-dependent nuclear accumulation of poly(A)+ RNA and constitutive clustering of nuclear pore complexes. Mol Biol Cell 6:401-417.

71. Li, S., A. M. Sandercock, P. Conduit, C. V. Robinson, R. L. Williams, and J. V. Kilmartin. 2006. Structural role of Sfi1p-centrin filaments in budding yeast spindle pole body duplication. J Cell Biol 173:867-77.

72. Liang, L., S. Flury, V. Kalck, B. Hohn, and J. Molinier. 2006. CENTRIN2 interacts with the Arabidopsis homolog of the human XPC protein (AtRAD4) and contributes to efficient synthesis-dependent repair of bulky DNA lesions. Plant Mol Biol 61:345-56.

73. Lohka, M. J., and Y. Masui. 1983. Formation in vitro of sperm pronuclei and mitotic chromosomes induced by amphibian ooplasmic components. Science 220:719-21.

74. Loiodice, I., A. Alves, G. Rabut, M. Van Overbeek, J. Ellenberg, J. B. Sibarita, and V. Doye. 2004. The entire Nup107-160 complex, including

three new members, is targeted as one entity to kinetochores in mitosis. Mol Biol Cell 15:3333-44.

75. Love, D. C., T. D. Sweitzer, and J. A. Hanover. 1998. Reconstitution of HIV-1 rev nuclear export: independent requirements for nuclear import and export. Proc Natl Acad Sci U S A 95:10608-13.

76. Lutz, W., W. L. Lingle, D. McCormick, T. M. Greenwood, and J. L. Salisbury. 2001. Phosphorylation of centrin during the cell cycle and its role in centriole separation preceding centrosome duplication. J Biol Chem 276:20774-80.

77. Lutzmann, M., R. Kunze, A. Buerer, U. Aebi, and E. Hurt. 2002. Modular self-assembly of a Y-shaped multiprotein complex from seven nucleoporins. Embo J 21:387-97.

78. Lutzmann, M., R. Kunze, K. Stangl, P. Stelter, K. F. Toth, B. Bottcher, and E. Hurt. 2005. Reconstitution of Nup157 and Nup145N into the Nup84 complex. J Biol Chem 280:18442-51.

79. Lyman, S. K., and L. Gerace. 2001. Nuclear pore complexes: dynamics in unexpected places. J Cell Biol 154:17-20.

80. Macaulay, C., and D. J. Forbes. 1996. Assembly of the nuclear pore: biochemically distinct steps revealed with NEM, GTP gamma S, and BAPTA. J Cell Biol 132:5-20.

81. Mansfeld, J., S. Guttinger, L. A. Hawryluk-Gara, N. Pante, M. Mall, V. Galy, U. Haselmann, P. Muhlhausser, R. W. Wozniak, I. W. Mattaj, U. Kutay, and W. Antonin. 2006. The conserved transmembrane nucleoporin NDC1 is required for nuclear pore complex assembly in vertebrate cells. Mol Cell 22:93-103.

82. Martinez-Sanz, J., A. Yang, Y. Blouquit, P. Duchambon, L. Assairi, and C. T. Craescu. 2006. Binding of human centrin 2 to the centrosomal protein hSfi1. Febs J 273:4504-15.

83. Matei, E., S. Miron, Y. Blouquit, P. Duchambon, I. Durussel, J. A. Cox, and C. T. Craescu. 2003. C-terminal half of human centrin 2 behaves like a regulatory EF-hand domain. Biochemistry 42:1439-50.

84. Matunis, M. J. 2006. Isolation and fractionation of rat liver nuclear envelopes and nuclear pore complexes. Methods 39:277-83.

85. Miao, M., K. J. Ryan, and S. R. Wente. 2006. The integral membrane protein Pom34p functionally links nucleoporin subcomplexes. Genetics 172:1441-57.

86. Middendorp, S., T. Kuntziger, Y. Abraham, S. Holmes, N. Bordes, M. Paintrand, A. Paoletti, and M. Bornens. 2000. A role for centrin 3 in centrosome reproduction. J Cell Biol 148:405-16.

87. Middendorp, S., A. Paoletti, E. Schiebel, and M. Bornens. 1997. Identification of a new mammalian centrin gene, more closely related to Saccharomyces cerevisiae CDC31 gene. Proc Natl Acad Sci U S A 94:9141-6.

88. Miller, B. R., and D. J. Forbes. 2000. Purification of the vertebrate nuclear pore complex by biochemical criteria. Traffic 1:941-51.

89. Miller, B. R., M. Powers, M. Park, W. Fischer, and D. J. Forbes. 2000. Identification of a new vertebrate nucleoporin, Nup188, with the use of a novel organelle trap assay. Mol Biol Cell 11:3381-96.

90. Molinier, J., C. Ramos, O. Fritsch, and B. Hohn. 2004. CENTRIN2 modulates homologous recombination and nucleotide excision repair in Arabidopsis. Plant Cell 16:1633-43.

91. Nakielny, S., S. Shaikh, B. Burke, and G. Dreyfuss. 1999. Nup153 is an M9-containing mobile nucleoporin with a novel Ran-binding domain. Embo J 18:1982-95.

92. Nishi, R., Y. Okuda, E. Watanabe, T. Mori, S. Iwai, C. Masutani, K. Sugasawa, and F. Hanaoka. 2005. Centrin 2 stimulates nucleotide excision repair by interacting with xeroderma pigmentosum group C protein. Mol Cell Biol 25:5664-74.

93. Orjalo, A. V., A. Arnaoutov, Z. Shen, Y. Boyarchuk, S. G. Zeitlin, B. Fontoura, S. Briggs, M. Dasso, and D. J. Forbes. 2006. The Nup107-160 nucleoporin complex is required for correct bipolar spindle assembly. Mol Biol Cell 17:3806-18.

94. Paoletti, A., M. Moudjou, M. Paintrand, J. L. Salisbury, and M. Bornens. 1996. Most of centrin in animal cells is not centrosome-associated and centrosomal centrin is confined to the distal lumen of centrioles. J Cell Sci 109 (Pt 13):3089-102.

95. Paulillo, S. M., M. A. Powers, K. S. Ullman, and B. Fahrenkrog. 2006. Changes in nucleoporin domain topology in response to chemical effectors. J Mol Biol 363:39-50.

96. Pemberton, L. F., M. P. Rout, and G. Blobel. 1995. Disruption of the nucleoporin gene NUP133 results in clustering of nuclear pore complexes. Proc Natl Acad Sci U S A 92:1187-91.

97. Popescu, A., S. Miron, Y. Blouquit, P. Duchambon, P. Christova, and C. T. Craescu. 2003. Xeroderma pigmentosum group C protein possesses a high affinity binding site to human centrin 2 and calmodulin. J Biol Chem 278:40252-61.

98. Powers, M. A., D. J. Forbes, J. E. Dahlberg, and E. Lund. 1997. The vertebrate GLFG nucleoporin, Nup98, is an essential component of multiple RNA export pathways. J Cell Biol 136:241-50.

99. Powers, M. A., C. Macaulay, F. R. Masiarz, and D. J. Forbes. 1995. Reconstituted nuclei depleted of a vertebrate GLFG nuclear pore protein, p97, import but are defective in nuclear growth and replication. J Cell Biol 128:721-36.

100. Radu, A., G. Blobel, and R. W. Wozniak. 1994. Nup107 is a novel nuclear pore complex protein that contains a leucine zipper. J Biol Chem 269:17600-5.

101. Rasala, B. A., A. V. Orjalo, Z. Shen, S. Briggs, and D. J. Forbes. 2006. ELYS is a dual nucleoporin/kinetochore protein required for nuclear pore assembly and proper cell division. Proc Natl Acad Sci U S A 103:17801-6.

102. Reichelt, R., A. Holzenburg, E. L. Buhle, Jr., M. Jarnik, A. Engel, and U. Aebi. 1990. Correlation between structure and mass distribution of the nuclear pore complex and of distinct pore complex components. J Cell Biol 110:883-94.

103. Rout, M. P., J. D. Aitchison, A. Suprapto, K. Hjertaas, Y. Zhao, and B. T. Chait. 2000. The yeast nuclear pore complex: composition, architecture, and transport mechanism. J Cell Biol 148:635-51.

104. Salina, D., P. Enarson, J. B. Rattner, and B. Burke. 2003. Nup358 integrates nuclear envelope breakdown with kinetochore assembly. J Cell Biol 162:991-1001.

105. Salisbury, J. L. 1995. Centrin, centrosomes, and mitotic spindle poles. Curr Opin Cell Biol 7:39-45.

106. Salisbury, J. L. 2004. Centrosomes: Sfi1p and centrin unravel a structural riddle. Curr Biol 14:R27-9.

107. Salisbury, J. L., A. Baron, B. Surek, and M. Melkonian. 1984. Striated flagellar roots: isolation and partial characterization of a calcium-modulated contractile organelle. J Cell Biol 99:962-70.

108. Salisbury, J. L., K. M. Suino, R. Busby, and M. Springett. 2002. Centrin-2 is required for centriole duplication in mammalian cells. Curr Biol 12:1287-92.

109. Segura-Totten, M., A. K. Kowalski, R. Craigie, and K. L. Wilson. 2002. Barrier-to-autointegration factor: major roles in chromatin decondensation and nuclear assembly. J Cell Biol 158:475-85.

110. Siniossoglou, S., M. Lutzmann, H. Santos-Rosa, K. Leonard, S. Mueller, U. Aebi, and E. Hurt. 2000. Structure and assembly of the Nup84p complex. J Cell Biol 149:41-54.

111. Siniossoglou, S., C. Wimmer, M. Rieger, V. Doye, H. Tekotte, C. Weise, S. Emig, A. Segref, and E. C. Hurt. 1996. A novel complex of nucleoporins, which includes Sec13p and a Sec13p homolog, is essential for normal nuclear pores. Cell 84:265-75.

112. Soop, T., B. Ivarsson, B. Bjorkroth, N. Fomproix, S. Masich, V. C. Cordes, and B. Daneholt. 2005. Nup153 affects entry of messenger and ribosomal ribonucleoproteins into the nuclear basket during export. Mol Biol Cell 16:5610-20.

113. Spang, A., I. Courtney, U. Fackler, M. Matzner, and E. Schiebel. 1993. The calcium-binding protein cell division cycle 31 of Saccharomyces cerevisiae is a component of the half bridge of the spindle pole body. J Cell Biol 123:405-16.

114. Stavru, F., B. B. Hulsmann, A. Spang, E. Hartmann, V. C. Cordes, and D. Gorlich. 2006. NDC1: a crucial membrane-integral nucleoporin of metazoan nuclear pore complexes. J Cell Biol 173:509-19.

115. Stelter, P., R. Kunze, D. Flemming, D. Hopfner, M. Diepholz, P. Philippsen, B. Bottcher, and E. Hurt. 2007. Molecular basis for the functional interaction of dynein light chain with the nuclear-pore complex. Nat Cell Biol 9:788-96.

116. Stoffler, D., K. N. Goldie, B. Feja, and U. Aebi. 1999. Calcium-mediated structural changes of native nuclear pore complexes monitored by time-lapse atomic force microscopy. J Mol Biol 287:741-52.

117. Strasser, K., J. Bassler, and E. Hurt. 2000. Binding of the Mex67p/Mtr2p heterodimer to FXFG, GLFG, and FG repeat nucleoporins is essential for nuclear mRNA export. J Cell Biol 150:695-706.

118. Strawn, L. A., T. Shen, and S. R. Wente. 2001. The GLFG regions of Nup116p and Nup100p serve as binding sites for both Kap95p and Mex67p at the nuclear pore complex. J Biol Chem 276:6445-52.

119. Stukenberg, P. T., and I. G. Macara. 2003. The kinetochore NUPtials. Nat Cell Biol 5:945-7.

120. Suntharalingam, M., and S. R. Wente. 2003. Peering through the pore: nuclear pore complex structure, assembly, and function. Dev Cell 4:775-89.

121. Takei, Y., M. Assenberg, G. Tsujimoto, and R. Laskey. 2002. The MCM3 acetylase MCM3AP inhibits initiation, but not elongation, of DNA replication via interaction with MCM3. J Biol Chem 277:43121-5.

122. Takei, Y., M. Swietlik, A. Tanoue, G. Tsujimoto, T. Kouzarides, and R. Laskey. 2001. MCM3AP, a novel acetyltransferase that acetylates replication protein MCM3. EMBO Rep 2:119-23.

123. Takei, Y., and G. Tsujimoto. 1998. Identification of a novel MCM3-associated protein that facilitates MCM3 nuclear localization. J Biol Chem 273:22177-80.

124. Thompson, J. R., Z. C. Ryan, J. L. Salisbury, and R. Kumar. 2006. The structure of the human centrin 2-xeroderma pigmentosum group C protein complex. J Biol Chem 281:18746-52.

125. Thorogate, R., and K. Torok. 2007. Role of Ca2+ activation and bilobal structure of calmodulin in nuclear and nucleolar localization. Biochem J 402:71-80.

126. Tsai, M. Y., S. Wang, J. M. Heidinger, D. K. Shumaker, S. A. Adam, R. D. Goldman, and Y. Zheng. 2006. A mitotic lamin B matrix induced by RanGTP required for spindle assembly. Science 311:1887-93.

127. Ullman, K. S., S. Shah, M. A. Powers, and D. J. Forbes. 1999. The nucleoporin nup153 plays a critical role in multiple types of nuclear export. Mol Biol Cell 10:649-64.

128. Vasu, S., S. Shah, A. Orjalo, M. Park, W. H. Fischer, and D. J. Forbes. 2001. Novel vertebrate nucleoporins Nup133 and Nup160 play a role in mRNA export. J Cell Biol 155:339-54.

129. Vasu, S. K., and D. J. Forbes. 2001. Nuclear pores and nuclear assembly. Curr Opin Cell Biol 13:363-75.

130. Vinciguerra, P., and F. Stutz. 2004. mRNA export: an assembly line from genes to nuclear pores. Curr Opin Cell Biol 16:285-92.

131. Walther, T. C., A. Alves, H. Pickersgill, I. Loiodice, M. Hetzer, V. Galy, B. B. Hulsmann, T. Kocher, M. Wilm, T. Allen, I. W. Mattaj, and V. Doye. 2003. The conserved Nup107-160 complex is critical for nuclear pore complex assembly. Cell 113:195-206.

132. Walther, T. C., P. Askjaer, M. Gentzel, A. Habermann, G. Griffiths, M. Wilm, I. W. Mattaj, and M. Hetzer. 2003. RanGTP mediates nuclear pore complex assembly. Nature 424:689-94.

133. Walther, T. C., M. Fornerod, H. Pickersgill, M. Goldberg, T. D. Allen, and I. W. Mattaj. 2001. The nucleoporin Nup153 is required for nuclear pore basket formation, nuclear pore complex anchoring and import of a subset of nuclear proteins. Embo J 20:5703-14.

134. Weis, K. 2002. Nucleocytoplasmic transport: cargo trafficking across the border. Curr Opin Cell Biol 14:328-35.

135. White, R. A., Z. Pan, and J. L. Salisbury. 2000. GFP-centrin as a marker for centriole dynamics in living cells. Microsc Res Tech 49:451-7.

136. Wiese, C., and Y. Zheng. 2006. Microtubule nucleation: gamma-tubulin and beyond. J Cell Sci 119:4143-53.

137. Wolfrum, U., A. Giessl, and A. Pulvermuller. 2002. Centrins, a novel group of Ca2+-binding proteins in vertebrate photoreceptor cells. Adv Exp Med Biol 514:155-78.

138. Wolfrum, U., and J. L. Salisbury. 1998. Expression of centrin isoforms in the mammalian retina. Exp Cell Res 242:10-7.

139. Yang, A., S. Miron, P. Duchambon, L. Assairi, Y. Blouquit, and C. T. Craescu. 2006. The N-terminal domain of human centrin 2 has a closed structure, binds calcium with a very low affinity, and plays a role in the protein self-assembly. Biochemistry 45:880-9.

140. Yang, Q., M. P. Rout, and C. W. Akey. 1998. Three-dimensional architecture of the isolated yeast nuclear pore complex: functional and evolutionary implications. Mol Cell 1:223-34.

141. Zhang, C., M. W. Goldberg, W. J. Moore, T. D. Allen, and P. R. Clarke. 2002. Concentration of Ran on chromatin induces decondensation, nuclear envelope formation and nuclear pore complex assembly. Eur J Cell Biol 81:623-33.

142. Zuccolo, M., A. Alves, V. Galy, S. Bolhy, E. Formstecher, V. Racine, J. B. Sibarita, T. Fukagawa, R. Shiekhattar, T. Yen, and V. Doye. 2007. The human Nup107-160 nuclear pore subcomplex contributes to proper kinetochore functions. Embo J 26:1853-64.

FUTURE DIRECTIONS

Defining the steps required to initiate nuclear pore assembly.

In Chapter 1-3, I described the progress I made toward understanding how nuclear pore assembly is initiated, as well as toward defining the early steps in this process. Based on my results and others, I propose a highly detailed model for nuclear pore assembly (Figure F.1). In this model, the binding of ELYS to AT-rich chromatin sites is the first step in nuclear pore assembly. Chromatin-bound ELYS then recruits the Nup107-160 complex, the major structural subunit of the pore (Rasala *et al.*, 2006; Franz *et al.*, 2007; Gillespie *et al.*, 2007). The ELYS/Nup107-160 pore platform then actively recruits membranes containing POM121 and NDC1, the two early assembling and essential integral membrane pore proteins (Bodoor *et al.*, 1999; Antonin *et al.*, 2005; Mansfeld *et al.*, 2006; Stavru *et al.*, 2006a; Funakoshi *et al.*, 2007). Nuclear recruitment of gp210, the third integral membrane pore protein which is thought to be dispensable for pore assembly (Gerace *et al.*, 1982; Chaudhary and Courvalin, 1993; Bodoor *et al.*, 1999; Eriksson *et al.*, 2004; Antonin *et al.*, 2005; Stavru *et al.*, 2006b), does not depend on chromatin-bound ELYS/Nup107-160 complex. In vitro, vesicle-vesicle fusion then occurs. In vivo, the membranes would likely be recruited in sheets from the ER or in tubules at the end of mitosis (Ellenberg *et al.*, 1997; Yang *et al.*, 1997; Daigle *et al.*, 2001; Anderson and Hetzer, 2007), thus vesicle fusion would not

be required. At this point, the Nup107-160 complex would be located on both sides of the nuclear membrane. Oligomerization of ELYS/Nup107-160/POM121 on the surface of the chromatin and an equivalent oligomerization of Nup107-160 and POM121 on the opposing outer nuclear membrane then precedes and possibly induces the fusion between the inner and outer nuclear membranes. This involves an LPC-sensitive hemifusion intermediate. The assembly of the remaining soluble pore subunits is likely a stepwise process and their order still remains to be defined in regard to one another and to the inner/outer nuclear membrane fusion step, except the FG-Nups, whose assembly is concurrent with or follows the fusion event. Taken together, this data strongly supports the fusion-mediated model for nuclear pore assembly which describes pore insertion within a continuous double membrane that is dependent on inner/outer membrane fusion, and convincingly refutes the alternative, pre-pore model, where membrane sheets engulf a preformed pore 'plug' or complex (see Introduction, Figure I.3). Importantly, because my model describes pore insertion into a double nuclear membrane, it is valid during both post-mitotic and S-phase nuclear pore assembly.

While molecular details of nuclear pore assembly are becoming clearer with the studies described here, many questions still remain to be answered. In the remainder of this section, I will summarize these questions as I see them.

Further characterization of ELYS' AT-rich chromatin binding

My data suggest that ELYS is restricted, at some level, to bind certain AT-rich regions or sites on the genome. Indeed, preliminary data I have obtained suggests that ELYS cannot bind a chromatinized pBluescript plasmid, but can bind the pEGPF plasmid which contains a eukaryotic promoter insert, even though the plasmids have comparable amounts of A-T DNA (49.6% verses 46.6%, respectively; data not shown). It would be extremely interesting to identify the chromatin binding sites for ELYS that my data suggests exist. Is there a specific AT-rich DNA sequence that ELYS recognizes? If so, where on the chromatin is that sequence found? ELYS chromatin immunoprecipitation and then chip hybridization (ChIP-chip) would be one way to identify specific DNA sequences associated with ELYS. Alternatively, high throughput technology such as in vitro systematic evolution of ligands by exponential enrichment (SELEX) could also be used to characterize high affinity DNA sequences for ELYS binding.

Another question concerning ELYS chromatin binding is: Does the population of ELYS that is associated with nuclear pores remain chromatin-bound throughout the cell cycle? Or does it release the chromatin after pore assembly is complete? If ELYS doesn't remain bound to chromatin, what is the signal to release it? In contrast, if ELYS does remain bound to chromatin throughout interphase, does it play a role in chromatin biology, such as

chromatin organization or gene expression? Indeed, ELYS was originally proposed to be a transcription factor involved in embryonic haematopoiesis (Kimura *et al.*, 2002). That study demonstrated that certain fragments of ELYS, when fused to a GAL4 DNA binding domain, could activate transcription of a luciferase reporter gene upon transfection, while other fragments acted to suppress transcription.

Finally, are other chromatin proteins involved in ELYS binding? Interestingly, in Chapter 2 I demonstrated that two overlapping fragments of xELYS, one that contains the AT-hook and one that does not, could bind to chromatin. Mass spectrometry analysis of GST pulldown reactions using these fragments revealed a variety of chromatin-associated proteins to be potential binding partners for both the AT-hook+ and ΔAT-hook fragments (data not shown). Further analysis of these potential binding partners should yield insight into how ELYS is targeted to chromatin.

Oligomerization of the early assembling nucleoporins and membrane fusion

In Chapter 3, we demonstrate that ELYS, the Nup107-160 complex, and POM121 are found in punctate entities before the fusion of the inner and outer nuclear membranes. What about NDC1? Is it also located in these structures (see below)? Interestingly, we show that the presence of membranes is required to induce the organization of ELYS into these punctate

entities. The nuclear pore has an eight-fold rotational symmetry, so each pore subunit is found in copies of eight or multiples of eight. Indeed, the yeast homologue of the Nup107-160 complex, the Nup84 complex, is found in 16-32 copies per pore and recent modeling analyses suggest that it makes up the primary pore scaffold (Rout *et al.*, 2000; Cronshaw *et al.*, 2002; Krull *et al.*, 2004; Alber *et al.*, 2007; Hsia *et al.*, 2007). We believe the punctate structures visualized by immunofluorescence at 15°C 30 min (Chapter 3, Figures 3.5 and 3.6) represent early intermediates of this 8-fold symmetrical pore scaffold and contain multiple copies of ELYS, POM121, and the Nup107-160 complex. However further characterization of these early pore entities would be required to verify this hypothesis. Co-localization of these proteins by immunofluorescence or immunoelectron microscopy could be used to show whether they are found in the same punctate entities. Preliminary data using directly-labeled antibodies to POM121 and Nup133 suggest that they do indeed co-localize at 15°C 30 min (data not shown). A biochemical analysis could be employed to determine the copy number for ELYS, the Nup107-160 complex, and POM121 per punctate early pore intermediates. Specifically, the early pore intermediate could be isolated by lightly crosslinking the 15°C 30 min nuclei. The subsequent solublization of the reaction followed by immunoprecipitation with, for example, anti-Nup133 antibodies, should result in the purification of Nup107-160 complex-containing intermediate. The molecular mass of this structure could be determined by analytical

ultracentrifugation. Immunoblots on the purified pore intermediate would allow us to verify that ELYS, POM121, and the Nup107-160 complex are indeed organized within the same punctate entity. Of course, we could also test for the presence of all the other pore subunits. Once the mass of the early pore intermediate is determined and the components have been identified, an estimate of the copy number for each protein could be made.

We also show in Chapter 3 that the early, punctate pore entities are present before the inner/outer membrane fusion event. What remains to be answered is: what are the minimal requirements to induce membrane fusion? Is ELYS/Nup107-160/POM121 sufficient? Is an as yet unidentified protein required? What is the mechanism of fusion? Is protein oligomerization sufficient to bend the membranes and induce fusion as we have proposed? Or is a 'hit-and-run' fusogen required, as others have proposed (Stavru *et al.*, 2006a)? The early pore intermediate could be isolated as above from LPC-treated 15°C 30 min nuclei, which are arrested just prior to inner/outer nuclear membrane fusion. Immunoblot and/or mass spectrometry analysis on isolated the LPC-arrested pore intermediate would allow one to determine which known nucleoporins and potential fusogens are present on the membranes and associated with the pore intermediate at this time.

Finally, in Chapter 3 we demonstrated that early, punctate pore intermediates appear on the chromatin side of the nuclear envelope (as visualized by ELYS) and on the cytoplasmic side of the nuclear envelope (as

visualized by externally added anti-POM121 and anti-Nup133 antibodies) at the same time in nuclear assembly. Can we show a biochemical connection between the nuclear Nups with those on the cytoplasmic face? If so, how does the interaction span the two lipid bilayers and the lumen which lies between them? Neither POM121 nor NDC1 have large luminal domains.

I believe finding the answers to these important questions will greatly improve our understanding of the mechanism of nuclear pore insertion.

What role does NDC1 play in nuclear pore initiation?

In Chapter 2, I show that chromatin-bound ELYS and the Nup107-160 complex are required for the recruitment of POM121- and NDC1-containing membrane vesicles to the nucleus. POM121 and NDC1 are co-enriched on the same membrane vesicle population in vitro (Mansfeld *et al.*, 2006), so NDC1 should presumably be recruited to the nuclear membranes early in nuclear pore assembly, i.e. with the same timing as POM121. What role, then, does NDC1 play in nuclear pore assembly? Both yeast and vertebrate nuclear pore complexes contain three known integral membrane pore proteins; however NDC1 is the only protein that is conserved over this evolutionary distance. Ndc1 is essential in yeast (Chial *et al.*, 1998; West *et al.*, 1998; Lau *et al.*, 2004). In vertebrates, RNAi knockdown of NDC1 disrupts proper pore assembly and/or structure (Mansfeld *et al.*, 2006; Stavru *et al.*, 2006a). Together, these data suggest that NDC1 plays an essential role in nuclear

pore assembly. Thus, it would be of interest to determine whether NDC1 localizes with ELYS/Nup107-160/POM121 in the punctate early pore intermediate, which could be done by performing indirect immunofluorescence on 15°C 30 min nuclei (unfortunately, our lab does not have the tools to do this as of yet). Based on my data and others, I would predict that NDC1 does assemble into the early pore intermediate.

Determining the order of the remaining pore subunits in nuclear pore assembly

In Chapter 2, I show that the assembly of most of the soluble pore subunits (with the exception of ELYS and the Nup107-160 complex) occurs following membrane recruitment and formation of the double nuclear membranes (Chapter 2, Figure 2.6). In Chapter 3, we demonstrate that the FG-Nups recognized by mAb414 (Nup358, Nup214, Nup153, and Nup62), either assemble concurrently with or following the second fusion event, inner/outer nuclear membrane fusion (Chapter 3, Figure 3.12). However, the assembly order of the remaining soluble pore subunits with respect to one another and to the second fusion event remains to be determined. In Chapter 2, I show that a POM121 fragment interacts not only with the Nup107-160 complex, but with the Nup93-205 complex (Chapter 2, Figure 2.7). Like the Nup107-160 complex, the Nup93-205 complex, and its yeast counterpart the Nic96 complex, is believed to be part of the pore scaffold. It is located on both

the nuclear and cytoplasmic face of the pore, and has been predicted to be close in proximity to the membranes (Rout *et al.*, 2000; Krull *et al.*, 2004; Hawryluk-Gara *et al.*, 2005; Alber *et al.*, 2007). In support of our POM121 pulldown data, a cytoplasmic fragment of POM121, when expressed in the membranes of mitochondria, was able to recruit Nup205 to the mitochondria (Stavru *et al.*, 2006b). Furthermore, NDC1 has been linked to the Nup93-205 complex and was shown to interact with Nup53 (which itself binds to Nup93-205) (Hawryluk-Gara *et al.*, 2005; Mansfeld *et al.*, 2006). Thus, it is likely that the Nup93-205 complex assembles soon after membrane vesicle recruitment and fusion, possibly between the first and second fusion events. Indeed, our preliminary data suggest that Nup93 is located in punctate entities in the cold intermediate, suggesting that the Nup93-205 complex assembles before fusion between the inner and outer nuclear membranes (data not shown). Immunoblot analysis on a 15°C anchored nuclear assembly timecourse, in combination with addition of pore assembly inhibitors such as LPC, GTPγS, and excess importin β (see below), could be used to determine the order of assembly of the remaining soluble pore subunits with respect to one another and to membrane fusion.

The role of Ran and Importin β regulation in the early steps in nuclear pore assembly

Nuclear membrane formation and nuclear pore assembly are controlled by the GTPase Ran and its antagonist, importin β. Importin β negatively regulates nuclear membrane fusion and nucleoporin assembly (Harel *et al.*, 2003; Walther *et al.*, 2003), while RanGTP promotes these processes (Wozniak and Clarke, 2003; Clarke and Zhang, 2004; Harel and Forbes, 2004). It is believed that importin β acts by binding to its targets such as individual nucleoporins, thereby preventing key interactions. RanGTP positively regulates nuclear membrane formation and pore assembly by binding to importin β, which results in the release of β's targets. This release occurs only near the chromatin, due to the chromatin localization of RCC1, the RanGEF that exchanges GDP for GTP (Bischoff and Ponstingl, 1991). What remains unknown is how Ran/importin β mediate the pore assembly steps that I have defined above. Importin β binds to the Nup107-160 complex (Walther *et al.*, 2003) and to ELYS (Appendix B, Figure A.4). Is the chromatin binding of ELYS and/or the Nup107-160 complex regulated by Ran/importin β? Several studies have shown that the addition of Ran69L-GTP induces excess chromatin binding of ELYS and the Nup107-160 complex (Walther *et al.*, 2003; Franz *et al.*, 2007), however my own data do not support this, although the experiments were not performed in the same manner (Chapter 2, Figure 2.6). To answer whether RanGTP/importin β regulate the chromatin binding of ELYS and the Nup107-160 complex more conclusively, one could immunodeplete Ran and ask whether ELYS and/or the Nup107-160 complex

can still bind to chromatin. Alternatively, one could add excess importin β to chromatin binding assays to determine whether excess β blocks the ability of ELYS/Nup107-160 to bind to chromatin. Indeed, our lab has performed these experiments and our results indicate that the chromatin binding of ELYS is negatively regulated by importin β (data not shown). Similar experiments could be done to determine whether the recruitment of POM121- and NDC1-containing membrane vesicles is also regulated by Ran/importin β.

While we have come a long way in our understanding of nuclear pore assembly and function, many questions remain unanswered. I believe that future studies that strive to answer the questions above will greatly enhance not only our knowledge of nuclear pore complexes, but our understanding of many cellular functions involving nuclear-cytoplasmic communication, including the regulation of gene expression, DNA damage responses, cell-cycle control, extra-cellular signaling, and apoptosis.

Figures

Figure F.1. A combined model for the early steps in fusion-dependent nuclear pore assembly. Nuclear pore assembly is initiated from AT-rich chromatin through the binding of ELYS (yellow) via its AT-hook motif and a second chromatin binding domain. ELYS recruits its binding partner, the Nup107-160 complex (green). The chromatin-bound ELYS/ Nup107-160 pore platform then actively recruits the integral membrane pore proteins, POM121 (red) and NDC1 (not shown) and their associated membrane vesicles (black lines) in vitro, or associated membrane tubules or sheets in vivo. In vitro, membrane vesicle fusion occurs. ELYS, POM121 and the Nup107-160 complex organize into punctate early pore intermediates. This protein clustering or oligo-merization leads to the bending of the nuclear membranes and results in the fusion of the inner and outer nuclear membranes and the formation of a diffusion channel. Maturation to a functional pore, which involves the recruitment of the remaining soluble pore subunits, occurs concurrently or following the inner/outer nuclear membrane fusion event. Of note, the nuclear basket and cytoplasmic filaments of the NPC, as well as the integral membrane pore proteins gp210 and NDC1, were excluded from the model for simplicity.

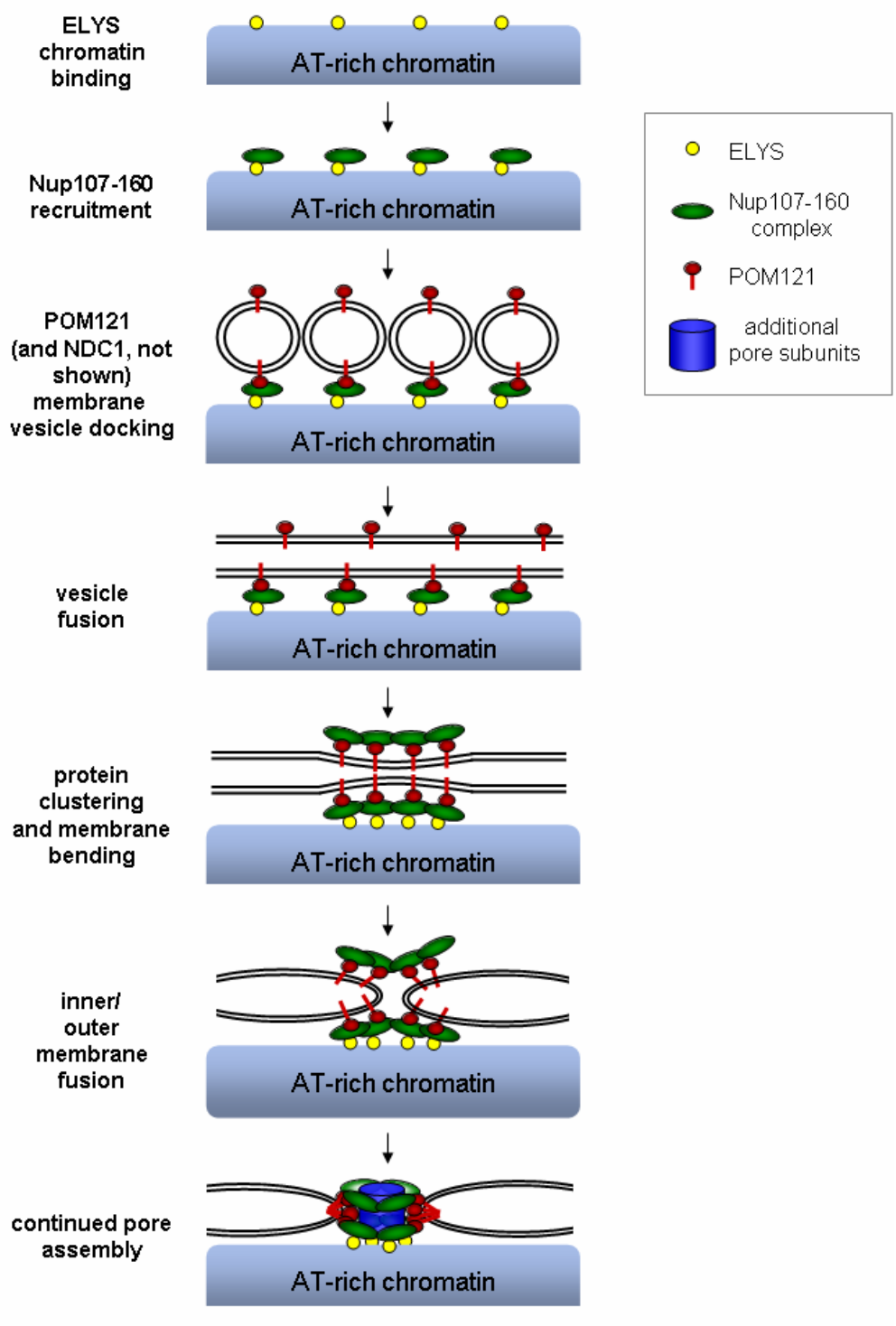
ELYS chromatin binding
AT-rich chromatin
Nup107-160 recruitment
AT-rich chromatin
POM121 (and NDC1, not shown) membrane vesicle docking
AT-rich chromatin
vesicle fusion
AT-rich chromatin
protein clustering and membrane bending
AT-rich chromatin
inner/ outer membrane fusion
AT-rich chromatin
continued pore assembly
AT-rich chromatin
ELYS
Nup107-160 complex
POM121
additional pore subunits

References

Alber, F., Dokudovskaya, S., Veenhoff, L.M., Zhang, W., Kipper, J., Devos, D., Suprapto, A., Karni-Schmidt, O., Williams, R., Chait, B.T., Sali, A., and Rout, M.P. (2007). The molecular architecture of the nuclear pore complex. Nature *450*, 695-701.

Anderson, D.J., and Hetzer, M.W. (2007). Nuclear envelope formation by chromatin-mediated reorganization of the endoplasmic reticulum. Nat Cell Biol *9*, 1160-1166.

Antonin, W., Franz, C., Haselmann, U., Antony, C., and Mattaj, I.W. (2005). The integral membrane nucleoporin pom121 functionally links nuclear pore complex assembly and nuclear envelope formation. Mol Cell *17*, 83-92.

Bischoff, F.R., and Ponstingl, H. (1991). Catalysis of guanine nucleotide exchange on Ran by the mitotic regulator RCC1. Nature *354*, 80-82.

Bodoor, K., Shaikh, S., Salina, D., Raharjo, W.H., Bastos, R., Lohka, M., and Burke, B. (1999). Sequential recruitment of NPC proteins to the nuclear periphery at the end of mitosis. J Cell Sci *112 (Pt 13)*, 2253-2264.

Chaudhary, N., and Courvalin, J.C. (1993). Stepwise reassembly of the nuclear envelope at the end of mitosis. J Cell Biol *122*, 295-306.

Chial, H.J., Rout, M.P., Giddings, T.H., and Winey, M. (1998). Saccharomyces cerevisiae Ndc1p is a shared component of nuclear pore complexes and spindle pole bodies. J Cell Biol *143*, 1789-1800.

Clarke, P.R., and Zhang, C. (2004). Spatial and temporal control of nuclear envelope assembly by Ran GTPase. Symp Soc Exp Biol, 193-204.

Cronshaw, J.M., Krutchinsky, A.N., Zhang, W., Chait, B.T., and Matunis, M.J. (2002). Proteomic analysis of the mammalian nuclear pore complex. J Cell Biol *158*, 915-927.

Daigle, N., Beaudouin, J., Hartnell, L., Imreh, G., Hallberg, E., Lippincott-Schwartz, J., and Ellenberg, J. (2001). Nuclear pore complexes form immobile networks and have a very low turnover in live mammalian cells. J Cell Biol *154*, 71-84.

Ellenberg, J., Siggia, E.D., Moreira, J.E., Smith, C.L., Presley, J.F., Worman, H.J., and Lippincott-Schwartz, J. (1997). Nuclear membrane dynamics and

reassembly in living cells: targeting of an inner nuclear membrane protein in interphase and mitosis. J Cell Biol *138*, 1193-1206.

Eriksson, C., Rustum, C., and Hallberg, E. (2004). Dynamic properties of nuclear pore complex proteins in gp210 deficient cells. FEBS Lett *572*, 261-265.

Franz, C., Walczak, R., Yavuz, S., Santarella, R., Gentzel, M., Askjaer, P., Galy, V., Hetzer, M., Mattaj, I.W., and Antonin, W. (2007). MEL-28/ELYS is required for the recruitment of nucleoporins to chromatin and postmitotic nuclear pore complex assembly. EMBO Rep *8*, 165-172.

Funakoshi, T., Maeshima, K., Yahata, K., Sugano, S., Imamoto, F., and Imamoto, N. (2007). Two distinct human POM121 genes: requirement for the formation of nuclear pore complexes. FEBS Lett *581*, 4910-4916.

Gerace, L., Ottaviano, Y., and Kondor-Koch, C. (1982). Identification of a major polypeptide of the nuclear pore complex. J Cell Biol *95*, 826-837.

Gillespie, P.J., Khoudoli, G.A., Stewart, G., Swedlow, J.R., and Blow, J.J. (2007). ELYS/MEL-28 chromatin association coordinates nuclear pore complex assembly and replication licensing. Curr Biol *17*, 1657-1662.

Harel, A., Chan, R.C., Lachish-Zalait, A., Zimmerman, E., Elbaum, M., and Forbes, D.J. (2003). Importin beta negatively regulates nuclear membrane fusion and nuclear pore complex assembly. Mol Biol Cell *14*, 4387-4396.

Harel, A., and Forbes, D.J. (2004). Importin beta: conducting a much larger cellular symphony. Mol Cell *16*, 319-330.

Hawryluk-Gara, L.A., Shibuya, E.K., and Wozniak, R.W. (2005). Vertebrate Nup53 interacts with the nuclear lamina and is required for the assembly of a Nup93-containing complex. Mol Biol Cell *16*, 2382-2394.

Hsia, K.C., Stavropoulos, P., Blobel, G., and Hoelz, A. (2007). Architecture of a coat for the nuclear pore membrane. Cell *131*, 1313-1326.

Kimura, N., Takizawa, M., Okita, K., Natori, O., Igarashi, K., Ueno, M., Nakashima, K., Nobuhisa, I., and Taga, T. (2002). Identification of a novel transcription factor, ELYS, expressed predominantly in mouse foetal haematopoietic tissues. Genes Cells *7*, 435-446.

Krull, S., Thyberg, J., Bjorkroth, B., Rackwitz, H.R., and Cordes, V.C. (2004). Nucleoporins as components of the nuclear pore complex core structure

and Tpr as the architectural element of the nuclear basket. Mol Biol Cell *15*, 4261-4277.

Lau, C.K., Giddings, T.H., Jr., and Winey, M. (2004). A novel allele of Saccharomyces cerevisiae NDC1 reveals a potential role for the spindle pole body component Ndc1p in nuclear pore assembly. Eukaryot Cell *3*, 447-458.

Mansfeld, J., Guttinger, S., Hawryluk-Gara, L.A., Pante, N., Mall, M., Galy, V., Haselmann, U., Muhlhausser, P., Wozniak, R.W., Mattaj, I.W., Kutay, U., and Antonin, W. (2006). The conserved transmembrane nucleoporin NDC1 is required for nuclear pore complex assembly in vertebrate cells. Mol Cell *22*, 93-103.

Rasala, B.A., Orjalo, A.V., Shen, Z., Briggs, S., and Forbes, D.J. (2006). ELYS is a dual nucleoporin/kinetochore protein required for nuclear pore assembly and proper cell division. Proc Natl Acad Sci U S A *103*, 17801-17806.

Rout, M.P., Aitchison, J.D., Suprapto, A., Hjertaas, K., Zhao, Y., and Chait, B.T. (2000). The yeast nuclear pore complex: composition, architecture, and transport mechanism. J Cell Biol *148*, 635-651.

Stavru, F., Hulsmann, B.B., Spang, A., Hartmann, E., Cordes, V.C., and Gorlich, D. (2006a). NDC1: a crucial membrane-integral nucleoporin of metazoan nuclear pore complexes. J Cell Biol *173*, 509-519.

Stavru, F., Nautrup-Pedersen, G., Cordes, V.C., and Gorlich, D. (2006b). Nuclear pore complex assembly and maintenance in POM121- and gp210-deficient cells. J Cell Biol *173*, 477-483.

Walther, T.C., Askjaer, P., Gentzel, M., Habermann, A., Griffiths, G., Wilm, M., Mattaj, I.W., and Hetzer, M. (2003). RanGTP mediates nuclear pore complex assembly. Nature *424*, 689-694.

West, R.R., Vaisberg, E.V., Ding, R., Nurse, P., and McIntosh, J.R. (1998). cut11(+): A gene required for cell cycle-dependent spindle pole body anchoring in the nuclear envelope and bipolar spindle formation in Schizosaccharomyces pombe. Mol Biol Cell *9*, 2839-2855.

Wozniak, R., and Clarke, P.R. (2003). Nuclear pores: sowing the seeds of assembly on the chromatin landscape. Curr Biol *13*, R970-972.

Yang, L., Guan, T., and Gerace, L. (1997). Integral membrane proteins of the nuclear envelope are dispersed throughout the endoplasmic reticulum during mitosis. J Cell Biol *137*, 1199-1210.

APPENDIX A

ELYS localization with respect to the nuclear envelope

ELYS resides on the nuclear face of the nuclear pore.

Using RNAi in HeLa cells, we were able to show that ELYS is essential for nuclear pore assembly (Rasala *et al.*, 2006). We proposed two potential models for ELYS' role in NPC assembly (see Chapter 1, Figure 1.4D). The first was that ELYS was a key structural component of the nuclear pore, similar to its binding partner, the Nup107-160 complex. The second model, which we favored, was that ELYS functions to target pore assembly to the nuclear envelope through an interaction with the chromatin. To distinguish between these two models, we began by investigating the localization of ELYS in regards to the nuclear envelope. The nuclear pore is composed of three asymmetrical domains: the central scaffold which spans the nuclear membranes, the cytoplasmic filaments, and the nuclear basket. The key *structural* components of the pore, like the Nup107-160 complex and the Nup93-205 complex, reside in the central scaffold domain and can therefore be accessed by antibodies from both sides of the nuclear envelope (Belgareh *et al.*, 2001; Krull *et al.*, 2004). To determine whether ELYS localizes to the cytoplasmic face to the nuclear pore, I performed indirect immunofluorescence on HeLa cells using the commercially available anti-human ELYS antibody. I

treated cells with either digitonin to selectively permeabilize the plasma membrane, or TritonX-100 to permeabilize both the plasma and nuclear membranes. Indeed, the anti-human ELYS antibody only stained the nuclear rim in the presence of TritonX-100, while the antibody to Nup133, a member of the Nup107-160 complex that has been shown to localize to both sides on the NE (Belgareh *et al.*, 2001), stained in both digitonin- and TritonX-100-treated cells (Figure A.1A). These data suggest that either: (1) ELYS resides solely on the nuclear side of the NE or (2) ELYS, once assembled into pore complexes, is masked and immunofluorescence detection requires TritonX-100 extraction/permeabilization.

To distinguish between these possibilities, I co-stained TritonX-100 treated HeLa cells with ELYS and either the nuclear pore cytoplasmic filament protein, Nup88, or the nuclear lamina protein, Lamin A/C. Deconvolution microscopy allowed for visualization of the location of ELYS with respect to nuclear envelope. Nup88 resides on the cytoplasmic side of the NE while Lamin A/C resides on the nuclear side (Figure A.1B). As a control, we also co-stained cells with Nup133. As expected, Nup133 co-localized with both cytoplasmic Nup88 and nuclear Lamin A/C (Figure A.1B, left column). The anti-ELYS signal, however, was slightly more interior to the Lamin A/C signal and significantly more nuclear than the Nup88 signal (Figure A.2B, right column). Taken together, these data indicate that ELYS is located on the nuclear side of the nuclear envelope, and suggest that ELYS is not part of the

nuclear pore central scaffold. Furthermore, the data argue against ELYS as a structural protein of the nuclear pore.

To determine more conclusively whether ELYS is a structural component of the pore, I asked if ELYS assembles into annulate lamellae (AL). AL are cytoplasmic stacks of ER membranes embedded with structurally correct pore complexes (Dabauvalle *et al.*, 1991; Kessel, 1992). If ELYS is an essential structural component of the nuclear pore, then it must also be present in the structurally correct AL-pore complexes. HeLa cells were co-stained with mAb414 to visual the FG-Nups in the cytoplasm at AL-pore complexes, and either ELYS or Nup133. Immunofluorescence revealed that ELYS does not co-localize with the FG-Nups in the cytoplasm at AL-pore complexes, while Nup133, a key structural pore protein does (Figure A.2). In a separate experiment, I quantitated the percent co-localization of ELYS with the cytoplasmic AL-pores in HeLa cells (Figure A.3). Z-projections through HeLa cells were used to determine the frequency in which ELYS co-localized to AL-pores, as visualized with the anti-FG-Nup antibody, mAb414. Cells were co-stained with ELYS, Nup133, and Tpr. Nup133 is known to assemble into AL-pores, while Tpr is the only identified soluble nucleoporin that does not assemble into AL, to date (Cordes *et al.*, 1997). Quantitation revealed that anti-Nup133 antibodies co-stained with cytoplasmic FG-nups at a high frequency, while anti-Tpr antibodies do so at a low frequency (Figure A.3). Anti-ELYS antibodies also only stained AL-pores at a low frequency (Figure

A.3). Similar results were seen by immunofluorescence using U2OS cells (data not shown), and biochemically for *Xenopus* AL assembled in vitro (see Chapter 2, Figure A.1). These data suggest that ELYS is not necessary for the assembly of AL-pore complexes and thus implies that ELYS is not an essential factor for pore structure.

In conclusion, ELYS is resides solely on the nuclear face of the nuclear pore, and does not significantly associate with cytoplasmic AL-pore complexes. Thus, my data indicate that the essential pore assembly protein, ELYS, does not function as a keystone structural component of the nuclear pore, but rather as a spatial regulator required to target pore assembly to the nuclear envelope.

Figures

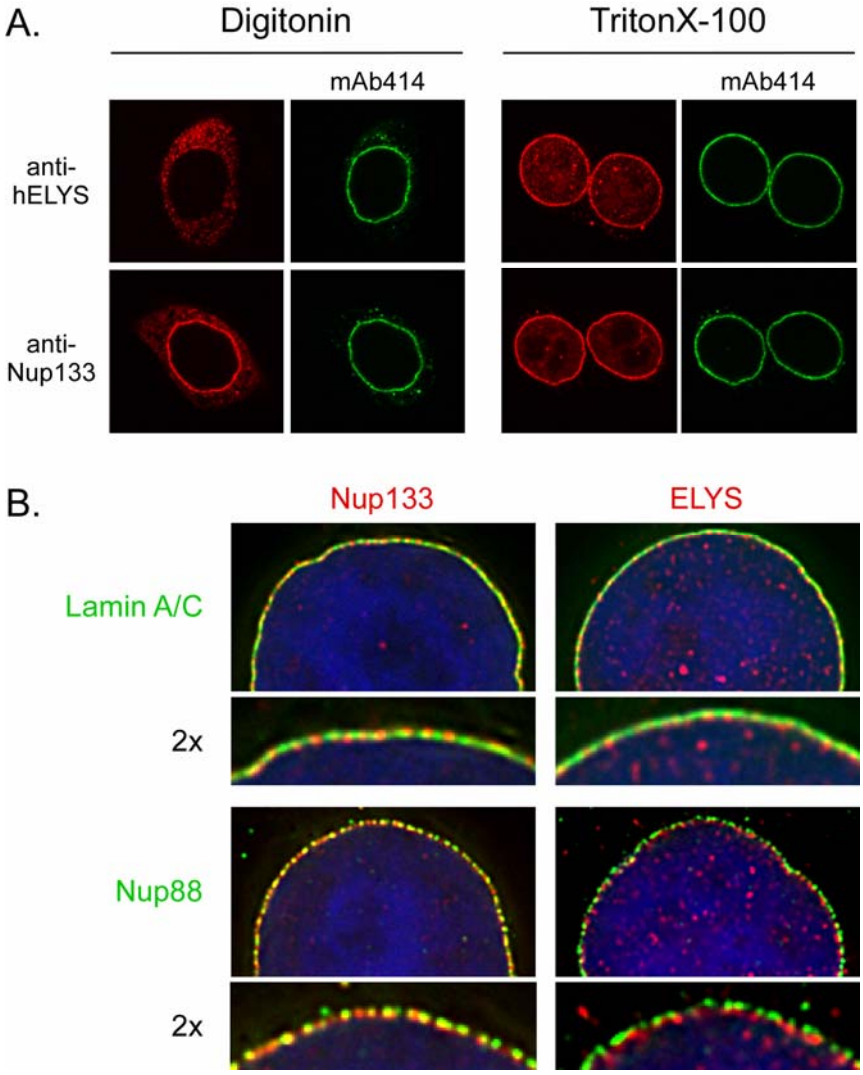

Figure A.1. ELYS is located on the nuclear face of the nuclear envelope.
A. HeLa cells were treated with either Digitonin to permeabilize only the plasma membrane or TritonX-100 to permeabilize both the plasma and nuclear membranes. Antibodies to human ELYS (red, top row) only detect ELYS at the pore when the nuclear membrane is permeabilized with TritonX-100, while antibodies to Nup133, which localizes to both sides on the nuclear pore, are able to detect Nup133 under both treatments (red, bottom row).

B. Indirect immunofluorescence on HeLa cells permeabilized with TritonX-100. At the nuclear rim, ELYS (red) co-localizes with the nuclear protein Lamin A/C (green) and is interior to Nup88 (green), a cytoplasmic filament protein. Nup133 (red), which localizes to both sides on the nuclear pore, co-localizes with both Lamin A/C and Nup88.

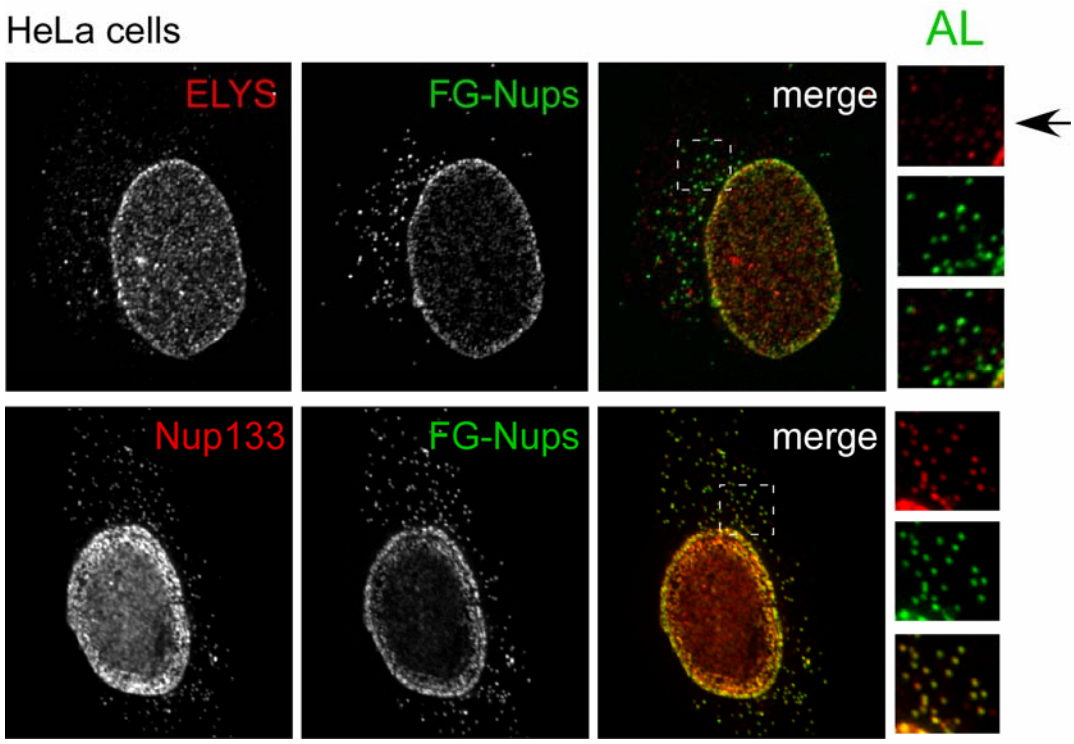

Figure A.2. ELYS does not localize to annulate lamellae in HeLa cells. Z-stack projections acquired by confocal microscopy on HeLa cells indicate that human ELYS (red, top row) does not co-localize with the FG-Nups (green) at cytoplasmic pores, called annulate lamellae (see insets, 2x). Arrow points to anti-ELYS staining in the insets. Nup133 (red, bottom row), however, does assemble into annulate lamellae, as expected.

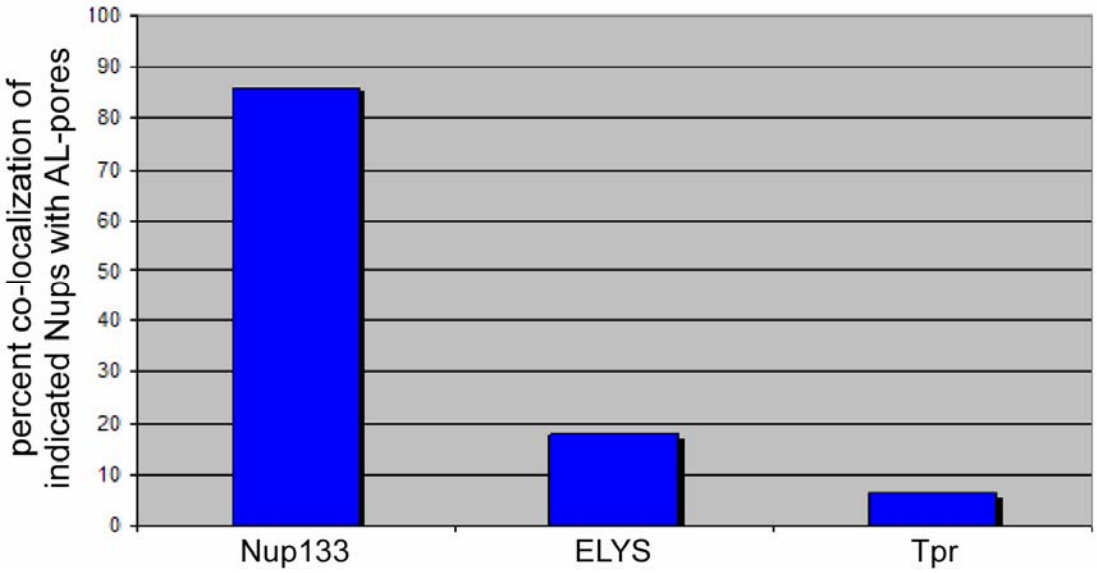

Figure A.3. Quantitation of co-localization of the indicated Nups with AL-pores. Z-stack projections through HeLa cells were used to count cytoplasmic AL-pores, as visualized by anti-FG-Nup antibody, mAb414. Percent co-localization of the indicated nucleoporins was determined by dividing the number of AL-pores co-staining with the indicated Nups, by total number of AL-pores.

References

Belgareh, N., Rabut, G., Bai, S.W., van Overbeek, M., Beaudouin, J., Daigle, N., Zatsepina, O.V., Pasteau, F., Labas, V., Fromont-Racine, M., Ellenberg, J., and Doye, V. (2001). An evolutionarily conserved NPC subcomplex, which redistributes in part to kinetochores in mammalian cells. J Cell Biol *154*, 1147-1160.

Cordes, V.C., Reidenbach, S., Rackwitz, H.R., and Franke, W.W. (1997). Identification of protein p270/Tpr as a constitutive component of the nuclear pore complex-attached intranuclear filaments. J Cell Biol *136*, 515-529.

Dabauvalle, M.C., Loos, K., Merkert, H., and Scheer, U. (1991). Spontaneous assembly of pore complex-containing membranes ("annulate lamellae") in Xenopus egg extract in the absence of chromatin. J Cell Biol *112*, 1073-1082.

Kessel, R.G. (1992). Annulate lamellae: a last frontier in cellular organelles. Int Rev Cytol *133*, 43-120.

Krull, S., Thyberg, J., Bjorkroth, B., Rackwitz, H.R., and Cordes, V.C. (2004). Nucleoporins as components of the nuclear pore complex core structure and Tpr as the architectural element of the nuclear basket. Mol Biol Cell *15*, 4261-4277.

Rasala, B.A., Orjalo, A.V., Shen, Z., Briggs, S., and Forbes, D.J. (2006). ELYS is a dual nucleoporin/kinetochore protein required for nuclear pore assembly and proper cell division. Proc Natl Acad Sci U S A *103*, 17801-17806.

APPENDIX B

xNup160 C-terminus binding partners

Introduction

Throughout this thesis, I describe the progress I have made into understanding the order and regulation of nuclear pore assembly. I have demonstrated that ELYS and the Nup107-160 complex are fundamental in initiating nuclear pore *assembly*. However, our lab is also interested in understanding nuclear pore *structure* and *function*. The nuclear pore is the only known gateway between the nucleus and cytoplasm. Nuclear pore complexes (NPCs) span the nuclear envelope and function in the facilitated transport of large proteins and RNAs, and the diffusion of small proteins and chemicals, across the nuclear envelope. Components of the nuclear pore also play a role in the formation of proper mitotic spindles and kinetochores, intranuclear bodies, and chromatin organization and transcriptional silencing (Suntharalingam and Wente, 2003). Thus, the pore is crucial for many aspects of normal eukaryotic cell physiology.

As described previously, the Nup107-160 complex functions to initiate nuclear pore assembly and is a vital structural component of the pore. Our laboratory identified Nup133 and Nup160, two members of the complex in 2001 (Vasu *et al.*, 2001), simultaneously with another group (Belgareth *et al.,*

2001. Our lab showed that Nup133 and Nup160 were stably associated with Nup96 and Nup107, and that these four proteins interact physically with the non-complex proteins, Nup98 and Nup153. In the same work, we showed that Nup133 and Nup160 were important for mRNA export. Later work from the lab also demonstrated that the complex is absolutely essential for post-mitotic nuclear pore assembly and/or structure in *Xenopus* extracts (Harel *et al.*, 2003b). Eventually, all nine members of this complex were identified (Radu *et al.*, 1994; Fontoura *et al.*, 1999; Belgareh *et al.*, 2001; Vasu *et al.*, 2001; Harel *et al.*, 2003b; Loiodice *et al.*, 2004). Strikingly, the Nup107-160 complex makes up about 1/3 of the nuclear pore.

Surprisingly, the Nup107-160 complex may have additional functions. The complex localizes to kinetochores from prophase to anaphase of mitosis (Belgareh *et al.*, 2001; Harel *et al.*, 2003b; Walther *et al.*, 2003a; Loiodice *et al.*, 2004) and contributes to proper kinetochore function (Zuccolo *et al.*, 2007). The Nup107-160 complex also binds to the spindle apparatus and is required for correct bipolar spindle assembly (Enninga *et al.*, 2003; Orjalo *et al.*, 2006). The complex may have additional functions as well, considering the nuclear pore seems to be participating in more aspects of nuclear biology than just nuclear-cytoplasmic transport.

Results

The first project I undertook in the lab was to identify and characterize novel functions for the Nup107-160 complex. My approach was to identify structural differences between the yeast and vertebrate complexes, then investigate the function(s) of said differences. The yeast homologue of the Nup107-160 complex is the Nup84 complex. Similar to the vertebrate homologue, the yeast Nup84 complex is important for mRNA export (Doye *et al.*, 1994; Aitchison *et al.*, 1995; Li *et al.*, 1995; Goldstein *et al.*, 1996; Siniossoglou *et al.*, 1996; Siniossoglou *et al.*, 2000; Bai *et al.*, 2004). However, the yeast Nup84 complex differs from the Nup107-160 complex in a number of ways. Yeast undergo closed mitosis, thus the Nup84 complex does not disassociate from the pore during mitosis. As a result, it does not localize to kinetochores and it does not play a role in post-mitotic NPC assembly as the vertebrate homologue does (Belgareh *et al.*, 2001; Harel *et al.*, 2003b; Walther *et al.*, 2003a; Loiodice *et al.*, 2004). The vNup107-160 complex also contains two additional members, WD repeat proteins Nup37 and Nup43 that are not found in yeast (Loiodice *et al.*, 2004). Finally, BLAST two protein alignments of *S.pombe* vs. human complex members reveal that, of the seven proteins shared in common, five are highly conserved (Figure B.1). The two proteins that are not well conserved are Nup133 and vNup160/yNup120. Even though according to this alignment tool, yeast and vertebrate Nup133 only share a small region of homology, both are about the same size (Figure

B.1, Nup133, blue shaded region). vNup160 and its yeast homologue yNup120 also only share a small region of homology according to the BLAST two protein alignment program (Figure B.1, Nup160, blue shaded regions). Strikingly, vNup160 is about 300 amino acids longer in length than yNup120 (Figure B.1, Nup160; Figure B.2A). Of note, while these initial alignments did not indicate any homology between the C terminus of vNup160 and spNup120, later BLAST searches with Nup160 C-terminus was able to reveal regions of homology in some lower eukaryotes, including fungi (data not shown).

I began my investigation into the function of the C terminal extension of Nup160, which I will refer to as "Beyond the Box" or BB (Figure B.2), by analyzing the effects of addition of excess recombinantly expressed GST-xNup160-BB to *Xenopus* reconstitution reactions. Functional nuclei can be formed in vitro by combining a purified *Xenupos* egg membrane fraction and soluble egg cytosol together with an energy regenerating system and a source of chromatin (Forbes *et al.*, 1983; Lohka and Masui, 1983; Newport, 1987). This nuclear reconstitution system can be used as a tool to study biochemically 'mutant' nuclei, often either by the removal of a critical protein by immunodepletion or by the addition of dominant negative protein fragments. Analysis of the 'mutant' phenotype then provides valuable clues about the function of the protein of interest. However, 5-12 μM GST-xNup160-BB did not affect nuclear assembly, including nuclear membrane fusion and nuclear

pore assembly, or nuclear envelope breakdown (data not shown). These preliminary results suggest that xNup160-BB does not function in the above processes. However, previously identified dominant-negative proteins, like importin β aa 45–462, require higher concentrations to inducce nuclear assembly defects (Harel *et al.*, 2003a). Thus, we feel these results are not conclusive.

GST-xNup160-BB interacts with proteins involved in a variety of cellular functions.

To learn more about the function of the C terminus of xNup160, I set out to identify proteins that interact with xNup160-BB. I performed GST pulldowns with GST-xNup160-BB from *Xenopus* egg extracts. Pulldowns were performed with GST or GST-xNup160-BB, both in the presence and absence of the nuclear pore assembly factor, RanQ69L-GTP. It is believed that RanGTP may induce interactions between multiple pore subunits, and has been shown to do so between Nup107-160 complex and Nup153 (Walther *et al.*, 2003b). Silver stain analysis revealed that GST-xNup160-BB specifically pulls down several proteins, compared to GST alone and GST-xNup160-BB incubated with buffer instead of egg cytosol (Figure B.3). In collaboration with Steve Briggs and Zhouxin Shen, we identified the xNup160-BB interacting proteins via liquid chromatography tandem mass spectrophotometry (LC-MS/MS). Interestingly, I was able to categorize most of the identified

interacting proteins into three classes: nuclear pore-associated proteins, kinetochore- and microtubule-associated proteins, and proteins involved in chromatin remodeling and gene expression (Table 1). A second GST-xNup160-BB pulldown-MS experiment verified most of these potential binding partners (data not shown).

MS analysis identified the nucleoporins Nup107, Nup133, and Nup153, and nuclear transport factors importin α and importin β as potential xNup160-BB binding partners (Table 1). According to the MS results, Nup107 and Nup133 bound xNup160-BB both in the presence and absence of RanQ69L-GTP. Nup153 only pulled down with BB in the presence of RanQ69L-GTP, while importin α and importin β interacted with BB only in the absence of Ran (data not shown). These results were verified by immunoblot analysis. Nup133, a member of the Nup107-160 complex, binds BB both in the presence and absence of RanQ69L-GTP (Figure B.4). Nup107 is also a member of this complex and has been shown to directly bind to Nup133 in yeast (Lutzmann *et al.*, 2002). Unfortunately, we could not probe the pulldowns for Nup107, due to a lack of antibody. Immunoblot analysis also verified an interaction between Nup153 and xNup160-BB in the presence of RanQ69L-GTP (Figure B.4). This result is consistent with the known interaction between Nup153 and the Nup107-160 complex: Nup153 can co-immunoprecipitate with the entire Nup107-160 complex only in the presence on RanGTP (Walther *et al.*, 2003b). Importin β, a transport factor and the

negative regulator of nuclear pore assembly, binds to xNup160-BB, but only in the absence of RanGTP (Figure B.4).

Interestingly, centrin was identified to interact with the C-terminal extension of Nup160 (Table 1). In yeast, the centrin homologue Cdc31p has been shown to associate with nuclear pores and function in mRNA export (Rout *et al.*, 2000; Fischer *et al.*, 2004). However, there has been no experimental evidence to date linking centrin to the nuclear pore in vertebrates (Cronshaw *et al.*, 2002; Matunis, 2006). Indeed, I was able to verify the interaction between centrin and xNup160-BB by immunoblot (Figure B.4). Based on these pulldown experiments, a colleague was able to show, for the first time, that vertebrate centrin localizes to nuclear pore complexes and functions in mRNA and protein export (Resendes *et al.*, 2008).

The other two classes of proteins found to interact with xNup160-BB in the pulldown experiments were kinetochore- and microtubule-associated proteins, and proteins involved in chromatin remodeling and gene expression (Table 1). Future experiments are needed to verify these interactions and to understand how Nup160 potentially functions in kinetochore/spindle biology and/or chromatin structure and function.

Discussion

The Nup107-160 complex is the largest and, arguably, the most critical subunit of the nuclear pore. In order to determine novel functions of the

vertebrate Nup107-160 complex, I set out to investigate the function of the C-terminus of Nup160. The addition of excess GST-xNup160-BB to *Xenopus* reconstitution reactions revealed that the protein fragment did not affect nuclear assembly, nuclear pore assembly, protein import, or nuclear envelope breakdown (data not shown). These data suggest that Nup160-BB does not function in any of these processes; however a more conclusive analysis is required to verify this conclusion.

Interestingly, LC-MS/MS analysis of GST-pulldown precipitates revealed that xNup160-BB potentially binds to a variety of proteins which can be categorized into three classes: nucleoporins, kinetochore- and microtubule-associated proteins, and proteins involved in chromatin remodeling and gene expression (Table 1). Although very interesting, these three classes were not unexpected. We know Nup160 binds nucleoporins at the pore. We know that Nup160 goes to kinetochores and spindle poles at mitosis. And we know that the yeast nuclear pore plays a role in chromatin organization and gene expression (Marshall *et al.*, 1997; Feuerbach *et al.*, 2002; Ishii *et al.*, 2002; Casolari *et al.*, 2004; Casolari *et al.*, 2005; Brown and Silver, 2007).

LC-MS/MS analysis also revealed that nucleoporins Nup107, Nup133, and Nup153 also interact with xNup160-BB. The nucleoporin interacting data provides clues about the orientation of the Nup107-160 complex within the pore. The structure of the homologous complex in yeast, the Nup84 complex, has been determined. The Nup84 complex is Y-shaped, with Nup120 on one

end of the Y and Nup133 and Nup107 on the other (Siniossoglou *et al.*, 2000; Lutzmann *et al.*, 2002). If the structure of this complex is conserved in vertebrates, as is believed, then Nup160 and Nup133/Nup107 would reside on opposite ends of the Y structure. Thus, the most likely way the C-terminal extension of Nup160 could interact with Nup133 is if they are associated with separate complexes (Figure B.5). As the concentration of RanGTP increases around the chromatin periphery during nuclear pore assembly, Nup153 would bind to Nup160/Nup133/Nup107 on the nuclear face of the pore to form the nuclear basket.

Importantly, LC-MS/MS analysis of xNup160-BB binding partners led to the discovery that vertebrate centrin localizes the nuclear pores and functions in protein and mRNA export (Resendes *et al.*, 2008).

LC-MS/MS analysis of xNup160-BB binding partners also suggests that BB interacts with proteins of the kinetochore and spindle as well as proteins involved in chromatin remodeling and gene expression. There is no doubt that future experiments delving into these interactions will lead to new insights into the role of Nup160 in a variety of cellular processes.

Figures

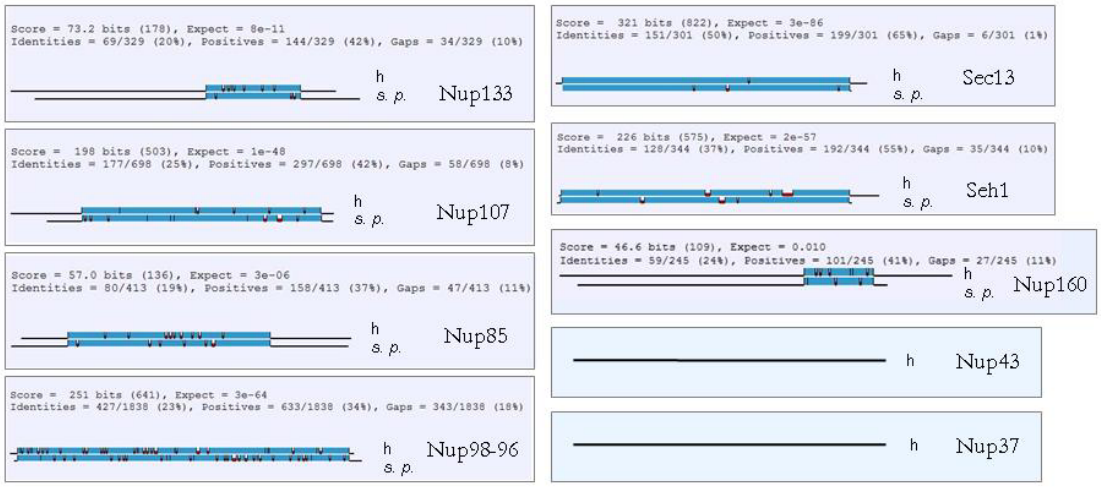

Figure B.1. Alignments of human (top) and *S. pombe* (bottom) Nup107-160/Nup84p complex proteins. BLAST two protein alignments were performed on human and *S. pombe* homologues of the hNup107-160 complex and spNup84 complex members. The Nup107-160 complex contains nine members, most of which are comparable in size to the yeast homologues. Blue boxes denote regions of homology. Yeast do not have homologues for vNup43 and vNup37. hNup160 contains a C-terminal extension not found in the yeast Nup120 homologue.

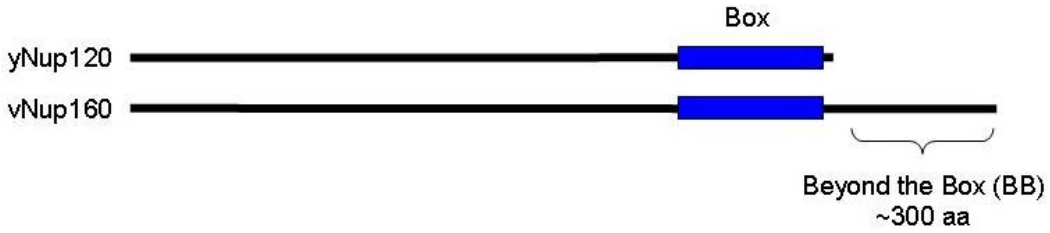

Figure B.2. Vertebrate Nup160 has a unique C-terminal extension. A cartoon representing an alignment between *S. pombe* Nup120 and the vertebrate homologue, Nup160. The blue box represents a region of homology. The vertebrate homolog has a C terminal extension of 300 amino acids in length, referred to as Beyond the Box or BB. xNup160-BB was GST-tagged and expressed.

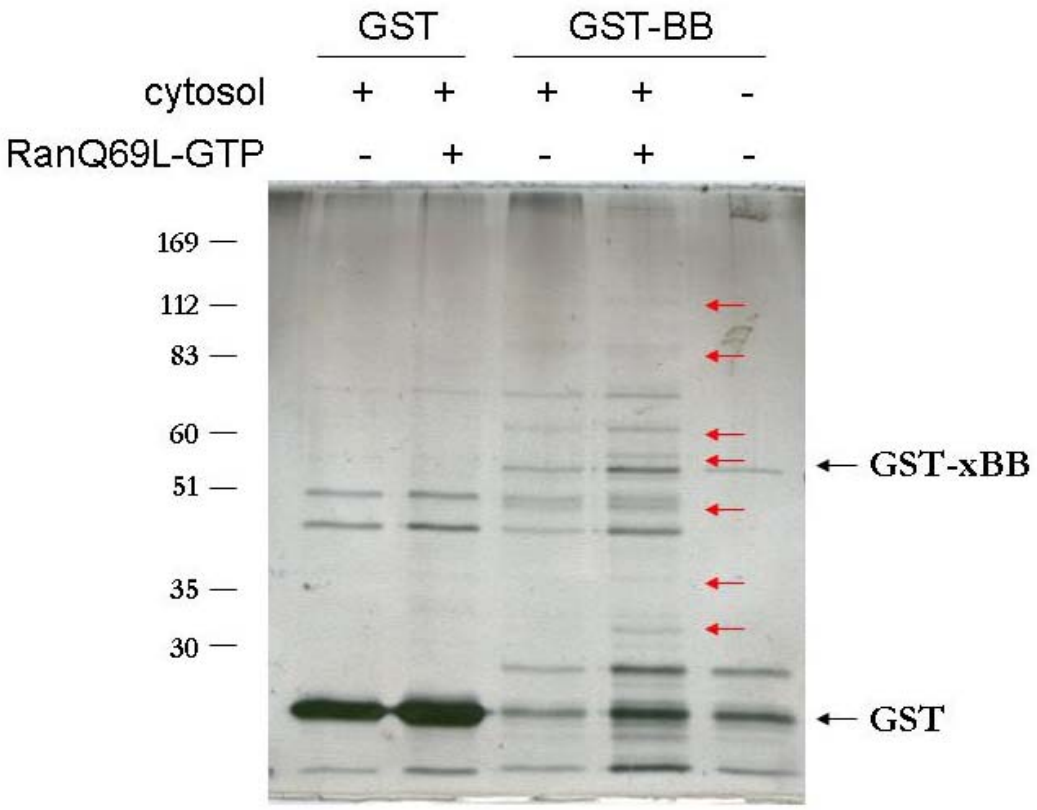

Figure B.3. xNup160-BB interacts with several distinct proteins. Silver stain analysis of a GST pulldown experiment reveals that GST-xNup160-BB interacts with several proteins (red arrows), both in the presence and absence of the nuclear pore assembly factor, RanGTP.

Table 1. Selected proteins identified by LC-MS/MS in Nup160 C terminus pulldowns.

Potential interactors	# Distinct peptides	Function
Nuclear pore proteins		
Importin β	17	transport factor
Importin α	7	transport factor
Centrin	3	nuclear pore-associated (yeast)
Nup107	3	nucleoporin
RanGAP1	2	Ran GTPase activating protein
Nup153	2	nucleoporin
Nup133	1	nucleoporin
Kinetochore/microtubule related-proteins		
β tubulin	19	microtubule subunit
α tubulin	15	microtubule subunit
PP2, regulatory subunit	8	protein phosphatase
PP2, catalytic subunit	4	protein phosphatase
APACD	4	microtubule architecture
Cdc2	3	cell cycle kinase
Gene silencing/ activating proteins		
HDAC3 complex subunit	8	histone deacetylase
RuvB-like 1/Tip49b	7	DNA helicase
RuvB-like2/Tip49a	7	DNA helicase
histone deacetylase 1	5	histone deacetylase
histone deacetylase 3	4	histone deacetylase
Rbbp7	4	chromatin remodeling
Other		
Facl2	26	palmitoyl-CoA ligase
p97	4	ATPase involved in membrane fusion

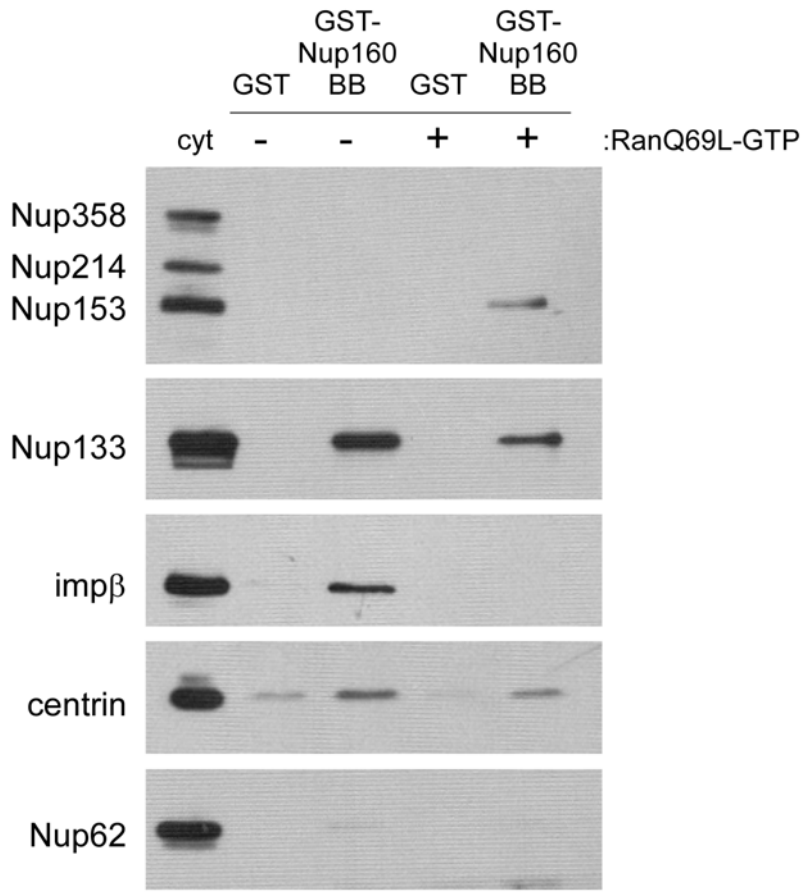

Figure B.4. xNup160-BB interacts with Nup133, Nup153, importin β and centrin. GST and GST-xNup160-BB pulldowns were performed from *Xenopus* interphase egg extract, either in the presence or absence of a nonhydrolyzable form of the nuclear pore assembly factor, RanGTP. Immunoblot analysis reveals that BB interacts with importin β only in the absence of RanGTP. Nup153 interacts with BB only in the presence of RanGTP. BB specifically pulls down Nup133 and centrin under both conditions. BB does not interact with Nup62, Nup214, or Nup358. Egg cytosol, 'cyt' was loaded for comparison.

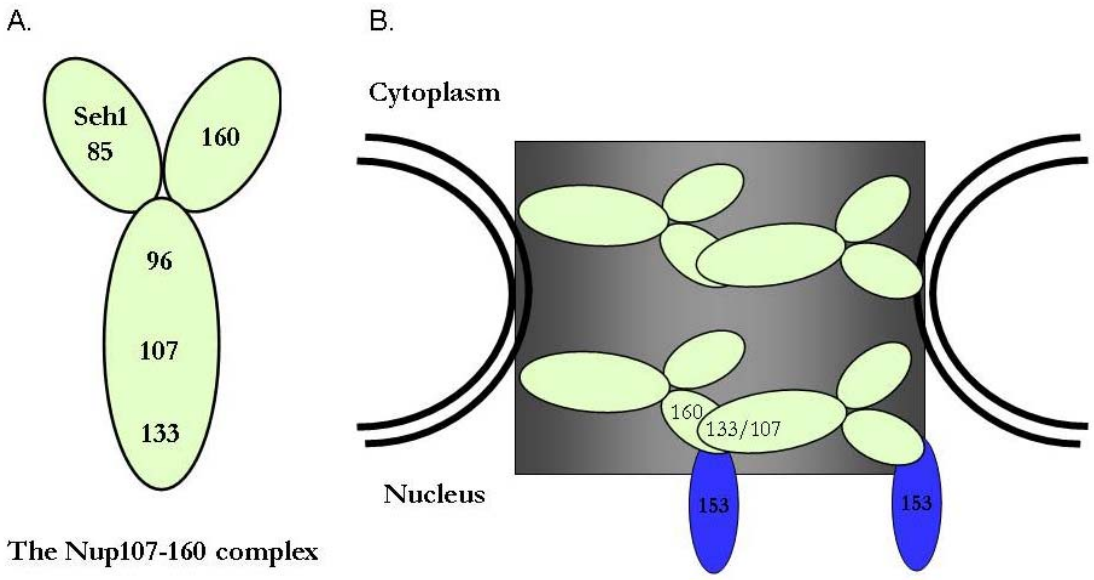

Figure B.5. A model for the orientation of the Nup107-160 complex within the nuclear pore. (A) A cartoon representing the structure of the Nup107-160 complex, based on that of the homologous yeast Nup84 complex (Siniossoglou *et al.*, 2000; Lutzmann *et al.*, 2002). (B) Nup160 binds to Nup133 and Nup107 of the adjacent Nup107-160 complex molecule within the nuclear pore (grey box). They also bind to Nup153 of the nuclear basket.

References

Aitchison, J.D., Blobel, G., and Rout, M.P. (1995). Nup120p: a yeast nucleoporin required for NPC distribution and mRNA transport. J Cell Biol *131*, 1659-1675.

Bai, S.W., Rouquette, J., Umeda, M., Faigle, W., Loew, D., Sazer, S., and Doye, V. (2004). The fission yeast Nup107-120 complex functionally interacts with the small GTPase Ran/Spi1 and is required for mRNA export, nuclear pore distribution, and proper cell division. Mol Cell Biol *24*, 6379-6392.

Belgareh, N., Rabut, G., Bai, S.W., van Overbeek, M., Beaudouin, J., Daigle, N., Zatsepina, O.V., Pasteau, F., Labas, V., Fromont-Racine, M., Ellenberg, J., and Doye, V. (2001). An evolutionarily conserved NPC subcomplex, which redistributes in part to kinetochores in mammalian cells. J Cell Biol *154*, 1147-1160.

Brown, C.R., and Silver, P.A. (2007). Transcriptional regulation at the nuclear pore complex. Curr Opin Genet Dev *17*, 100-106.

Casolari, J.M., Brown, C.R., Drubin, D.A., Rando, O.J., and Silver, P.A. (2005). Developmentally induced changes in transcriptional program alter spatial organization across chromosomes. Genes Dev *19*, 1188-1198.

Casolari, J.M., Brown, C.R., Komili, S., West, J., Hieronymus, H., and Silver, P.A. (2004). Genome-wide localization of the nuclear transport machinery couples transcriptional status and nuclear organization. Cell *117*, 427-439.

Cronshaw, J.M., Krutchinsky, A.N., Zhang, W., Chait, B.T., and Matunis, M.J. (2002). Proteomic analysis of the mammalian nuclear pore complex. J Cell Biol *158*, 915-927.

Doye, V., Wepf, R., and Hurt, E.C. (1994). A novel nuclear pore protein Nup133p with distinct roles in poly(A)+ RNA transport and nuclear pore distribution. Embo J *13*, 6062-6075.

Enninga, J., Levay, A., and Fontoura, B.M. (2003). Sec13 shuttles between the nucleus and the cytoplasm and stably interacts with Nup96 at the nuclear pore complex. Mol Cell Biol *23*, 7271-7284.

Feuerbach, F., Galy, V., Trelles-Sticken, E., Fromont-Racine, M., Jacquier, A., Gilson, E., Olivo-Marin, J.C., Scherthan, H., and Nehrbass, U. (2002).

Nuclear architecture and spatial positioning help establish transcriptional states of telomeres in yeast. Nat Cell Biol *4*, 214-221.

Fischer, T., Rodriguez-Navarro, S., Pereira, G., Racz, A., Schiebel, E., and Hurt, E. (2004). Yeast centrin Cdc31 is linked to the nuclear mRNA export machinery. Nat Cell Biol *6*, 840-848.

Fontoura, B.M., Blobel, G., and Matunis, M.J. (1999). A conserved biogenesis pathway for nucleoporins: proteolytic processing of a 186-kilodalton precursor generates Nup98 and the novel nucleoporin, Nup96. J Cell Biol *144*, 1097-1112.

Forbes, D.J., Kirschner, M.W., and Newport, J.W. (1983). Spontaneous formation of nucleus-like structures around bacteriophage DNA microinjected into Xenopus eggs. Cell *34*, 13-23.

Goldstein, A.L., Snay, C.A., Heath, C.V., and Cole, C.N. (1996). Pleiotropic nuclear defects associated with a conditional allele of the novel nucleoporin Rat9p/Nup85p. Mol Biol Cell *7*, 917-934.

Harel, A., Chan, R.C., Lachish-Zalait, A., Zimmerman, E., Elbaum, M., and Forbes, D.J. (2003a). Importin beta negatively regulates nuclear membrane fusion and nuclear pore complex assembly. Mol Biol Cell *14*, 4387-4396.

Harel, A., Orjalo, A.V., Vincent, T., Lachish-Zalait, A., Vasu, S., Shah, S., Zimmerman, E., Elbaum, M., and Forbes, D.J. (2003b). Removal of a single pore subcomplex results in vertebrate nuclei devoid of nuclear pores. Mol Cell *11*, 853-864.

Ishii, K., Arib, G., Lin, C., Van Houwe, G., and Laemmli, U.K. (2002). Chromatin boundaries in budding yeast: the nuclear pore connection. Cell *109*, 551-562.

Li, O., Heath, C.V., Amberg, D.C., Dockendorff, T.C., Copeland, C.S., Snyder, M., and Cole, C.N. (1995). Mutation or deletion of the Saccharomyces cerevisiae RAT3/NUP133 gene causes temperature-dependent nuclear accumulation of poly(A)+ RNA and constitutive clustering of nuclear pore complexes. Mol Biol Cell *6*, 401-417.

Lohka, M.J., and Masui, Y. (1983). Formation in vitro of sperm pronuclei and mitotic chromosomes induced by amphibian ooplasmic components. Science *220*, 719-721.

Loiodice, I., Alves, A., Rabut, G., Van Overbeek, M., Ellenberg, J., Sibarita, J.B., and Doye, V. (2004). The entire Nup107-160 complex, including three new members, is targeted as one entity to kinetochores in mitosis. Mol Biol Cell *15*, 3333-3344.

Lutzmann, M., Kunze, R., Buerer, A., Aebi, U., and Hurt, E. (2002). Modular self-assembly of a Y-shaped multiprotein complex from seven nucleoporins. Embo J *21*, 387-397.

Marshall, I.C., Gant, T.M., and Wilson, K.L. (1997). Ionophore-releasable lumenal Ca2+ stores are not required for nuclear envelope assembly or nuclear protein import in Xenopus egg extracts. Cell Calcium *21*, 151-161.

Matunis, M.J. (2006). Isolation and fractionation of rat liver nuclear envelopes and nuclear pore complexes. Methods *39*, 277-283.

Newport, J. (1987). Nuclear reconstitution in vitro: stages of assembly around protein-free DNA. Cell *48*, 205-217.

Orjalo, A.V., Arnaoutov, A., Shen, Z., Boyarchuk, Y., Zeitlin, S.G., Fontoura, B., Briggs, S., Dasso, M., and Forbes, D.J. (2006). The Nup107-160 nucleoporin complex is required for correct bipolar spindle assembly. Mol Biol Cell *17*, 3806-3818.

Radu, A., Blobel, G., and Wozniak, R.W. (1994). Nup107 is a novel nuclear pore complex protein that contains a leucine zipper. J Biol Chem *269*, 17600-17605.

Resendes, K.K., Rasala, B.A., and Forbes, D.J. (2008). Centrin 2 localizes to the vertebrate nuclear pore and plays a role in mRNA and protein export. Mol Cell Biol.

Rout, M.P., Aitchison, J.D., Suprapto, A., Hjertaas, K., Zhao, Y., and Chait, B.T. (2000). The yeast nuclear pore complex: composition, architecture, and transport mechanism. J Cell Biol *148*, 635-651.

Siniossoglou, S., Lutzmann, M., Santos-Rosa, H., Leonard, K., Mueller, S., Aebi, U., and Hurt, E. (2000). Structure and assembly of the Nup84p complex. J Cell Biol *149*, 41-54.

Siniossoglou, S., Wimmer, C., Rieger, M., Doye, V., Tekotte, H., Weise, C., Emig, S., Segref, A., and Hurt, E.C. (1996). A novel complex of nucleoporins, which includes Sec13p and a Sec13p homolog, is essential for normal nuclear pores. Cell *84*, 265-275.

Suntharalingam, M., and Wente, S.R. (2003). Peering through the pore: nuclear pore complex structure, assembly, and function. Dev Cell *4*, 775-789.

Vasu, S., Shah, S., Orjalo, A., Park, M., Fischer, W.H., and Forbes, D.J. (2001). Novel vertebrate nucleoporins Nup133 and Nup160 play a role in mRNA export. J Cell Biol *155*, 339-354.

Walther, T.C., Alves, A., Pickersgill, H., Loiodice, I., Hetzer, M., Galy, V., Hulsmann, B.B., Kocher, T., Wilm, M., Allen, T., Mattaj, I.W., and Doye, V. (2003a). The conserved Nup107-160 complex is critical for nuclear pore complex assembly. Cell *113*, 195-206.

Walther, T.C., Askjaer, P., Gentzel, M., Habermann, A., Griffiths, G., Wilm, M., Mattaj, I.W., and Hetzer, M. (2003b). RanGTP mediates nuclear pore complex assembly. Nature *424*, 689-694.

Zuccolo, M., Alves, A., Galy, V., Bolhy, S., Formstecher, E., Racine, V., Sibarita, J.B., Fukagawa, T., Shiekhattar, R., Yen, T., and Doye, V. (2007). The human Nup107-160 nuclear pore subcomplex contributes to proper kinetochore functions. Embo J *26*, 1853-1864.